Understanding the processes governing the origin of clay coated sand grains and sediment heterogeneity in petroleum reservoirs: insights from a modern marginal marine system

UNIVERSITY OF LIVERPOOL

Thesis submitted in accordance with the requirements of the University of Liverpool for the degree in Doctor of Philosophy by

Luke J. Wooldridge

December 2017

Table of contents

List of Figures

List of tables

Understanding the processes governing the origin of clay coated sand grains and sediment heterogeneity in petroleum reservoirs: insights from a modern marginal marine system

Luke J. Wooldridge

The main cause of porosity-and permeability-loss in sandstone reservoirs undergoing diagenetic cementation during prolonged burial and heating is the growth of authigenic quartz. Clay minerals attached as coats to grain surfaces have been reported to inhibit this damaging quartz cementation. How clay minerals form as clay coats at the site of deposition remains uncertain despite clay-coated sand grains being of paramount importance for subsequent sandstone reservoir properties and the economic worth of a given prospect or discovery. Being able to predict the distribution of clay-coated sand grains in petroleum reservoirs is thus important in helping to find and exploit anomalously good reservoir quality deep in sedimentary basins.

This study adopted a high-resolution modern analogue approach focused on surface and near-surface sediment from the Ravenglass Estuary, UK. The bio-sedimentary study utilised a combination of fieldwork, core logging, a range of scanning electron microscopy techniques, and quantified sediment characteristics, biofilm abundance, clay coat compositional analysis, and clay-coat coverage. The study involved the development of novel clay-coat classification techniques that are capable of being used to quantify clay-coat characteristics and differentiating clay-coat mineralogy from that of the whole sediment.

The work has produced a novel, fully quantitative biological and sedimentological understanding of the marginal-marine sediments at Ravenglass. For the first time, biofilms have been shown to play a fundamental role in the formation of clay coated sand grains and in governing the diagenetic characteristics of marginal marine sediments. Clay coated sand grains were shown to be heterogeneously distributed and compositionally variable across marginal-marine sediments. The distribution of clay-coated grains across the Ravenglass Estuary is principally controlled by the interplay between an inner estuarine biologically-mediated clay coat factory origin, and the transport of clay-coated grains into higher energy depositional environments resulting in a degree of clay coat abrasion and the reduction of clay-coat coverage. Clay-coat mineralogy is, principally, controlled by the deposited clay minerals with relative enrichment of clay-coating chlorite in the inner-estuarine sand-tidal-flat and tidal-bar depositional environments.

The identification of the origin, mineralogy, and distribution of modern detrital-clay coats revolutionizes the understanding of clay-coated sand grains and offers a first step towards a credible predictive capability in ancient and deeply-buried sandstones since these depositional clay coats will transform to diagenetic clay mineral coats upon burial and heating.

“I finished my education as I started it, playing in a sand pit”

Dedicated to Wilfred and Catherine Wooldridge

Acknowledgments

Firstly, I want to acknowledge the support and motivation given and sacrifices endured by my parents in providing me with very best possible education. I can honestly say I would not be where I am today if not for you both and for that I will be eternally grateful and privileged.

Secondly, I would like to thank my girlfriend Katy-Beth for suffering without complaint the many hours of "boring" geology talk and isolation caused by the writing of this thesis. Your help in teaching me statistical analysis has been invaluable and I thank you for being a constant source of motivation and unwavering support for me to complete this PhD.

Thirdly, my main supervisor Richard Worden for his support and guidance in facilitating my ideas no matter how seemingly abstract, which has enabled a very enjoyable 4 years. His patience and guidance in paper corrections has been invaluable and I leave a much better scientist and communicator. I want to thank my second supervisor Rob Duller for constructive discussions which stimulated several ideas included in this work.

Special mention is due to Joshua Griffiths, I could not have asked for a better research and field partner. The ability to discuss ideas has been invaluable and went a long way to shaping the results of this research.

Thanks are owed to James Utley and Anu Patel, for their support in fieldwork and data analysis. Special thanks are owed to Anu, for persevering in making me a "geo-biologist", training me in lab techniques and for putting up with the many breakages of lab equipment.

I would also like to thanks all the companies involved in the Chlorite Consortium (BP, BG, Shell, Statoil, Cheveron, Eni, Woodside, and Petrobas). In particular I would like to thank

James Churchill, Nigel Clark, and Peter Armitage, whose contribution in facilitating training, opportunities, and feedback went beyond what their role required.

Thank you all, it has been a fantastic and rewarding few years.

1. Introduction

The main cause of porosity- and permeability-loss in sandstone reservoirs during prolonged burial and heating, after compaction, is the growth of authigenic quartz cement (Walderhaug 1996; Worden and Morad 2000). Much research has been focussed on factors that inhibit quartz cement since they may lead to anomalously high porosity sandstones deep in sedimentary basins (Bloch et al. 2002). Clay-coated sand-grains are the principal reported cause of the inhibition of the porosity-occluding quartz cements and thus preservation of anomalously high porosity in ancient, deeply-buried sandstone reservoirs (Ajdukiewicz and Larese 2012; Bloch et al. 2002; Dowey et al. 2012; Ehrenberg 1993; Heald and Larese 1974; Storvoll et al. 2002). Despite the potential fundamental importance of clay-coated sand-grains in governing the economic viability of many deeply-buried sandstone reservoirs and almost five decades of research, there remains no credible capability for making predictions about grain coat coverage in ancient and deeply-buried reservoir rocks (Dowey et al. 2012; Pittman and Lumsden 1968; Wooldridge et al. 2017b).

The research reported in this thesis can be summarised as series of related studies focused on answering the following three fundamental questions;

1. What processes govern the origin, distribution, and mineralogy of clay-coated sand grains?
2. How can the presence of clay-coated sand-grains be predicted?
3. How do sediment biofilms influence the reservoir quality of marginal marine sediments?

The principal aim of this research was to constrain the origin and distribution of clay-coated sand-grains in a modern marginal marine system which can, by analogy, be applied to help prediction of anomalously high porosity in ancient, deeply-buried sandstones. The second aim was to assess the role of biological activity on sediment heterogeneity. A summary of

the research questions that are addressed in this study and the collected data sets is given in Figure 1.1. This study addressed the above stated research questions by focussing on the Ravenglass Estuary, Cumbria, UK.

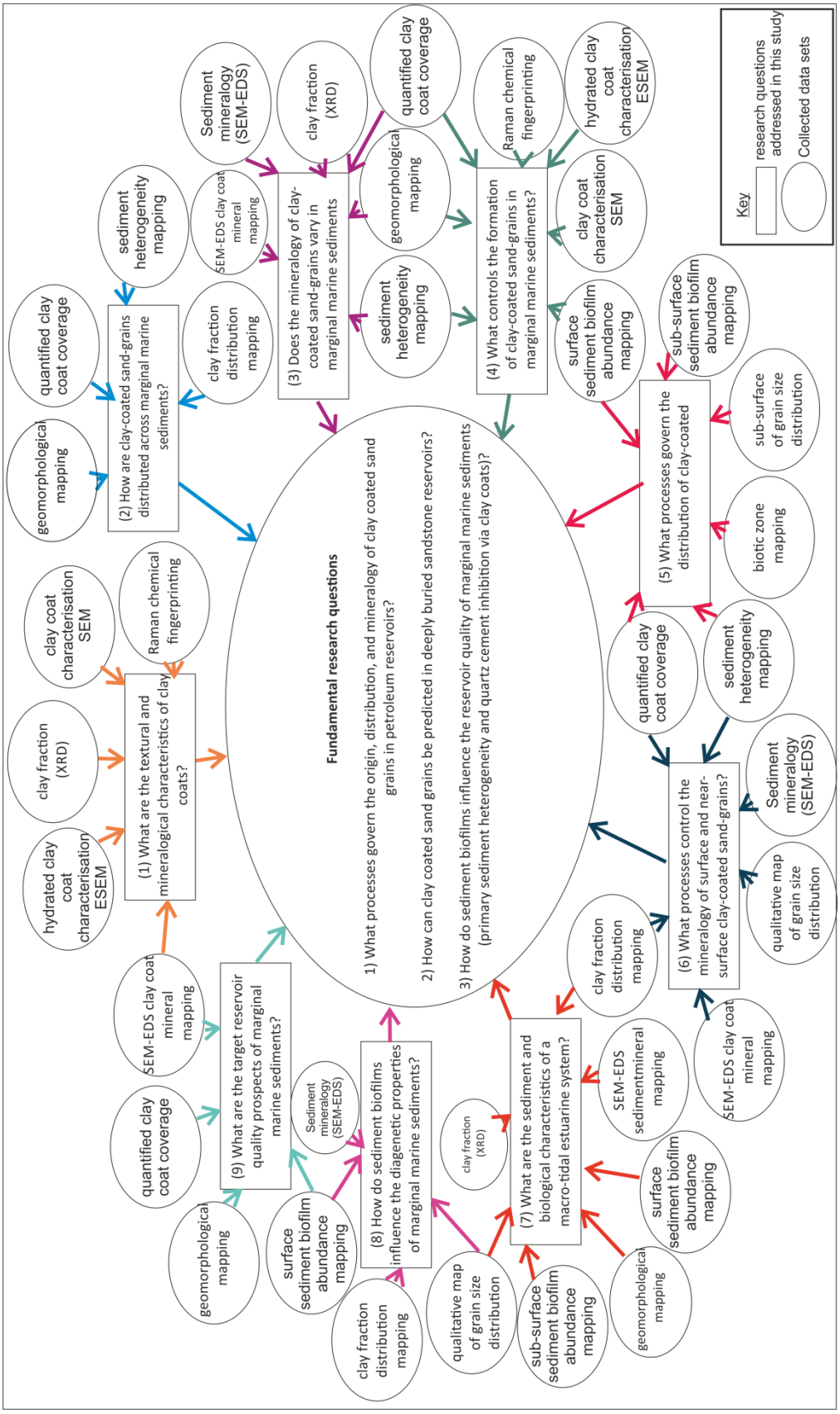

Figure 1-1 Summary figure outlining the key research questions and complied data sets of the study.

1.1. Research questions

This thesis reports a series of studies focused on addressing the following questions in order to answer the principal research questions of the study (Fig. 1.1)

1. What are the textural and mineralogical characteristics of clay coats? (concluded: 8.1.1)
2. How are clay-coated sand-grains distributed across marginal marine sediments? (concluded: 8.1.2)
3. Does the mineralogy of clay-coated sand-grains vary in marginal marine sediments? (concluded: 8.1.3)
4. What controls the formation of clay-coated sand-grains in marginal marine sediments? (concluded: 8.2.1)
5. What processes govern the distribution of clay-coated sand-grains? (concluded: 8.2.2)
6. What processes control the mineralogy of surface and near-surface clay-coated sand-grains? (concluded: 8.2.3)
7. What are the sediment and biological characteristics of a macro-tidal estuarine system? (concluded: 8.3.1)
8. How do sediment biofilms influence the diagenetic properties of marginal marine sediments? (concluded: 8.4.1)
9. What are the target reservoir quality prospects of marginal marine sediments? (concluded: 8.5.1)

1.2. A modern analogue methodology

The principal aim of the research is to constrain the origin and distribution of clay-coated sand-grains across a fluvial to marginal marine transect of depositional environments.

There are four potential approaches to develop a fundamental understanding on the formation and distribution of clay-coated sand-grains: (i) core based analysis, (ii) outcrop-based studies, (iii) experimental studies, and (iv) modern analogue studies (Wooldridge et al. 2017b).

Core-based studies allow the incorporation of petrography, mineralogy, and supporting petrophysical data to understand the distribution of clay coats. However, such studies typically suffer from: (i) a limited spatial resolution of samples (lack of abundant cores in most fields with small or clustered datasets), and (ii) the abiding uncertainty about both the primary mineralogy, and exact environment of deposition, owing to the challenges of diagenetic modifications (Wooldridge et al. 2017b).

Outcrop-based studies overcome the problem of limited spatial resolution, particularly with the inclusion of cores to create a three-dimensional context. However, outcrops typically suffer from weathering-related recent changes to clay mineralogy which hinders the characterisation of clay-coat mineralogy (Wooldridge et al. 2017b).

Experimental studies such as Ajdukiewicz and Larese (2012) and Aagaard et al. (2000) are crucial in constraining the link between detrital-and diagenetic-clay coats (Table 1.1, Fig. 1.2). However, an experimental approach would be incapable of fully replicating the complexities of a marginal marine system.

This study attempts to fulfil the aims by applying a high resolution surface analogue methodology, combined with core analysis (< 1 metre) to reveal the heterogeneity in clay coat characteristics across the Ravenglass Estuary. The high resolution surface data set offered the opportunity to constrain both the distribution of clay-coated sand-grains and the origin (i.e. the attachment mechanism of clay minerals to grain surfaces), results that may not be evident in ancient sediments. The advantages of this method are: (i) it allows a

high-resolution investigation into the distribution of detrital-clay-coated grains, (ii) un-cemented sediment enable a wide range of sediment and biological characterisation techniques, and (iii) it removes the ambiguous depositional-environment and weathering clay mineral overprint of core-and outcrop-based analysis. One issue related with a modern analogue methodology, is the uncertainty in knowing the applicability of surface distribution trends to that of the subsurface. To overcome such limitations, focus was placed on testing the surface identified controls and distribution trends against a shallow (< 1 metre) core data set (Chapter 4).

1.3. Background: Placing this study into the field of reservoir quality research

The following section introduces pertinent information, which constrains how the research data chapters integrate into, and develops, the discipline of clastic reservoir quality.

The introduction is structured around the around the following themes.

1. The research in the context of sandstone reservoir quality.
2. Clay-coat derived anomalous high deeply-buried porosity sandstones,
    a. Clay coat terminology,
    b. Quartz cementation in sandstones,
    c. Clay coat derived inhibition of quartz cementation.
3. Reported mechanisms of clay coat formation.
4. The biological control on clastic sedimentary systems and reservoir quality.

1.3.1.. Sandstone reservoir quality and the context of the research

Reservoir quality (i.e. porosity and permeability) in deeply-buried sandstones is mainly controlled by three factors; (1) the primary depositional characteristics of the sediment (e.g. grain size, sorting, clay content, clay mineralogy, and bulk assemblage mineralogy), (2)

the extent of mechanical and chemical compaction, and (3) the volume and type of pore-filling cement (Worden and Morad 2000).

This research is focused on factor (3) by understanding the origin and distribution of modern clay-coated sand-grains, which have been established, on burial, to inhibit the growth (volume) of authigenic quartz cement in sandstones (Aagaard et al. 2000; Billault et al. 2003; Ehrenberg 1993). In order to establish, firstly, the distribution and, secondly, the origin of clay-coated sand-grains across a modern marginal marine system, it has been necessary to generate a unique, high resolution data set of sediment and biological heterogeneity to constrain the mechanisms which control factor (1) (depositional sediment characteristics).

Primary sediment heterogeneity (i.e. grain size variability) controls the initial porosity and permeability of the sediment and typically provides the fundamental control on the diagenetic alteration and resulting reservoir quality of the sandstone upon burial (Morad et al. 2010). Growth of the porosity-occluding quartz cement in sandstones is reported to be the dominant control on post-compositional porosity in many deeply-buried sandstones (Worden and Morad 2000). The presence of clay-coated sand-grains (chlorite, illite, and mixed clay mineralogy coats) have been reported to be the origin of elevated reservoir-quality in numerous deeply-buried sandstone reservoirs, via the inhibition of the typical porosity-occluding quartz cement (Bloch et al. 2002; Dowey et al. 2012; Ehrenberg 1993; Storvoll et al. 2002; Stricker and Jones 2016).

1.3.2.. Importance of clay coat derived anomalous high porosity sandstones

The occurrence of deeply-buried (> 3 km) anomalously high porosity sandstones have been associated with the presence of clay-coated sand-grains (e.g. chlorite and illite) (Bloch et al. 2002; Ehrenberg 1993). Namely, that the net volume of quartz cement is reported to be

inversely correlated to the extent (completeness) of clay-coat coverage in the Jurassic sandstones of the Norwegian continental shelf (Bloch et al. 2002), the Jurassic and Triassic sandstones of the Ordos Basin, China (Luo et al. 2009), the Lower Miocene sandstones from the Matagorda Island well, Gulf of Mexico (Dutton et al. 2012), and the Triassic Judy Sandstone Member in the Heron Cluster, UK (Stricker and Jones 2016).

1.5.3. Summary of clay coat terminology and diagenetic evolution:

The term clay coat encompasses both detrital (pre-diagenesis) and diagenetic-clay coats (post- diagenesis) (Ajdukiewicz and Larese 2012; Dowey et al. 2017) (Table 1.1). Detrital-clay coats form at or near the surface of the sediment via the physical attachment of clay minerals (diverse mixture of phyllosilicates) to sand-grain surfaces (Dowey et al. 2017; Wooldridge et al. 2017b; Worden and Morad 2003). Diagenetic (occurring in sandstones) clay-coated sand-grains are reported to form via two processes; (i) the thermally-driven recrystallization of attached detrital-clay coat material (known as diagenetic-recrystallized coats), and (ii) the *in-situ* authigenic growth, through mineral interactions with the pore fluids (known as diagenetic-authigenic coats) (i.e. dissolution of grains and re-precipitation of the dissolved material), most commonly, reported to occur on an existing root structure (i.e. nucleation on a diagenetic-recrystallized coat) (Ajdukiewicz and Larese 2012; Bloch et al. 2002; Gould et al. 2010; Skarpeid et al. 2017; Worden and Morad 2003). In well-illustrated examples of diagenetic-clay coats from the Triassic, Judy Sandstone Member in the Heron Cluster, UK (Stricker and Jones 2016), the Cretaceous reservoirs in the Scotian Basin, Canada (Gould et al. 2010), and in the Jurassic sandstones of the Haltenbanken area, Norway (Bloch et al. 2002), a stratigraphy can be defined. Diagenetic clay coats typically consist of: (i) an inner unstructured, and tangentially-oriented (to grain surface) “root structure”, and (ii) an outer layer perpendicularly oriented (to the grain surface) composed

of euhedral clay minerals (e.g. plates of chlorite) that project from the sand-grain surface into the pore (Bloch et al. 2002; Gould et al. 2010; Stricker and Jones 2016) (Fig. 1.2).

Diagenetic-recrystallized coats have been reported to form the inner tangentially orientated (parallel to grain surface), densely packed mass of platey-anhedral, mineralogical heterogeneous, clay minerals of diagenetic-clay coats (Fig. 1.2 B, C, D). Diagenetic-clay coats with an authigenic component are reported to grow out of detrital coats (Bloch et al. 2002; Gould et al. 2010; Pittman et al. 1992) and consist of euhedral typically spaced particles, oriented perpendicular (radial) to the grain surface (Ajdukiewicz and Larese 2012; Billault et al. 2003) (Figs. 1.2B, C, D).

The presence of a detrital-clay coat (clay material) is reported as a necessary requirement for extensive diagenetic-clay coats in shallow marine sandstones (Aagaard et al. 2000; Ajdukiewicz and Larese 2012; Ehrenberg 1993). Ehrenberg (1993) reported that detrital-clay coats transformed through diagenesis into radially orientated chlorite crystals prior to quartz cementation and feldspar dissolution. Aagaard et al. (2000) in experiments replicating diagenesis showed the transformation (neoformation) of an iron-rich, discontinuous, detrital-clay coat (berthierine-dominated mixed-layer clay), into a complete chlorite clay coat, with textures comparable to naturally-occurring samples. For example, detrital-clay material attached to sand-grains can transform on burial (temperature around 90 °C), depending on the initial mineralogy of the phyllosilicates into either chlorite, illite, kaolinite, or mixed mineralogy diagenetic coats (Worden and Morad 2003).

Billault et al. (2003) introduced a three stage development for diagenetic-clay coats in deeply-buried sandstones: (1) initial development of detrital-clay coats on sand-grains (i.e. attachment of clay minerals to grain surfaces), (2) thermally-driven transformation of the detrital-clay coat material (diagenetic-recrystallized coats), and (3) growth of authigenic clay coat components directly from pore fluid precipitation (diagenetic-authigenic coats),

governed by geometrical selection from the underlying detrital root material and the availability of an *in-situ* source of required ions (e.g. lithic-volcanic rock fragments) (Bloch et al. 2002) (Fig. 1.1E).

This research is focused on establishing a predictive capability for the distribution of diagenetic-clay coats in deeply-buried sandstones, based on an understanding of the principal, controlling mechanisms, which govern the origin and distribution of detrital-clay coats which represent the precursor material to clay coats in sandstones.

The relative timing of transformation from a detrital-clay coat to a diagenetic-clay coat (Fig. 1.2) remains relatively poorly constrained in the literature. The reported occurrence of chlorite clay coats underlying and inhibiting quartz cements suggests that transformation (thermally driven neoformation from discontinuous detrital-clay coats to continuous diagenetic coats) occurs early in the paragenetic sequence at temperatures lower than 80 ^{o}C (the typical onset temperature of quartz cement precipitation) (Ajdukiewicz and Larese 2012; Worden and Morad 2000). Diagenetic clay coats are reported to encase hollow structures, representative of dissolved feldspars, again suggesting early transformation (Billault et al. 2003; Ehrenberg 1993; Gier et al. 2008). Billault et al. (2003) further reported the development of clay coats prior to the onset of pronounced mechanical compaction for the M'Bya reservoir, Gabon, the Malih X1 reservoir, Oman, the Kahar reservoirs, Syria, and the Haltenbanken reservoirs, Norway.

From various sources in the literature (Ajdukiewicz and Larese 2012; Billault et al. 2003; Ehrenberg 1993), it has been possible to produce a new summary synthesis of the relative timing and morphological changes of clay coat evolution (Fig. 1.2A, E);

(i) The early attachment of detrital-clay coats to grain surfaces at or near the sediment surface prior to the onset of compaction (focus of this research).

(ii) The transformation from a discontinuous detrital-clay coat to a continuous diagenetic grain coverage (if sufficient attached detrital-clay material is available for neoformation) prior to the onset of extensive quartz cementation and feldspar dissolution.

(iii) The precipitation of authigenic clay coat components via the dissolution of grains and re-precipitation of the dissolved material.

In this research, unless specifically stated, clay coats and clay-coated sand-grains refer to the detrital-clay coat phase (Table. 1.1).

	Terminology	Suggested definitions		Distinguishing morphology
surface-shallow burial	Detrital-clay coats	A clay mineral-dominated coat on a sand-grain that formed before, during, or immediately after deposition via the physical attachment of clay minerals (diverse mixture of phyllosilicates) (i.e. low temperature and while still in the depositional environment).		Discontinuous, micron scale, accumulations of clay- to silt-sized material (clay particles, organics, and lithics) typically presenting as either clumps, tangentially attached coats, or bridging strands of clay material between grains, creating a diverse mixture of phyllosilicates.
Deep burial	Diagenetic-clay coats	A clay mineral-dominated coat (of undefined mineralogy) on a sand-grain that formed during burial and diagenesis (typically > 2,000 m and/or > 70°C).		
	Diagenetic-recrystallized clay coats	Depositional controlled (i.e. attachment of the clay mineral assemblage to form detrital-clay coats in depositional environments).	A detrital clay mineral-dominated coat that formed before, during, or immediately after deposition, that has been mineralogically and texturally modified via thermally-driven (burial) recrystallization, as the sediment entered a different geochemical and textural regime.	Tangentially orientated (parallel to grain surface), densely packed mass of platey-anhedral mineralogical heterogeneous clay minerals.
	Diagenetic-authigenic clay coats	Provenance controlled (i.e. lithic and mineralogy of the sediment assemblage controlling the availability and mineralogy of the dissolved material necessary for authigenic coat formation).	*In-situ* authigenic growth (somewhat deeper burial), through mineral interactions with the pore fluids and direct re-precipitation of the dissolved material, most commonly, reported to occur on an existing recrystallized detrital root structure (nucleation site).	Euhedral typically spaced particles, perpendicular (radial) to grain surface (i.e. extending pore ward).

Table 1-1 Defining clay coat terminology, after Dowey et al. (2017).

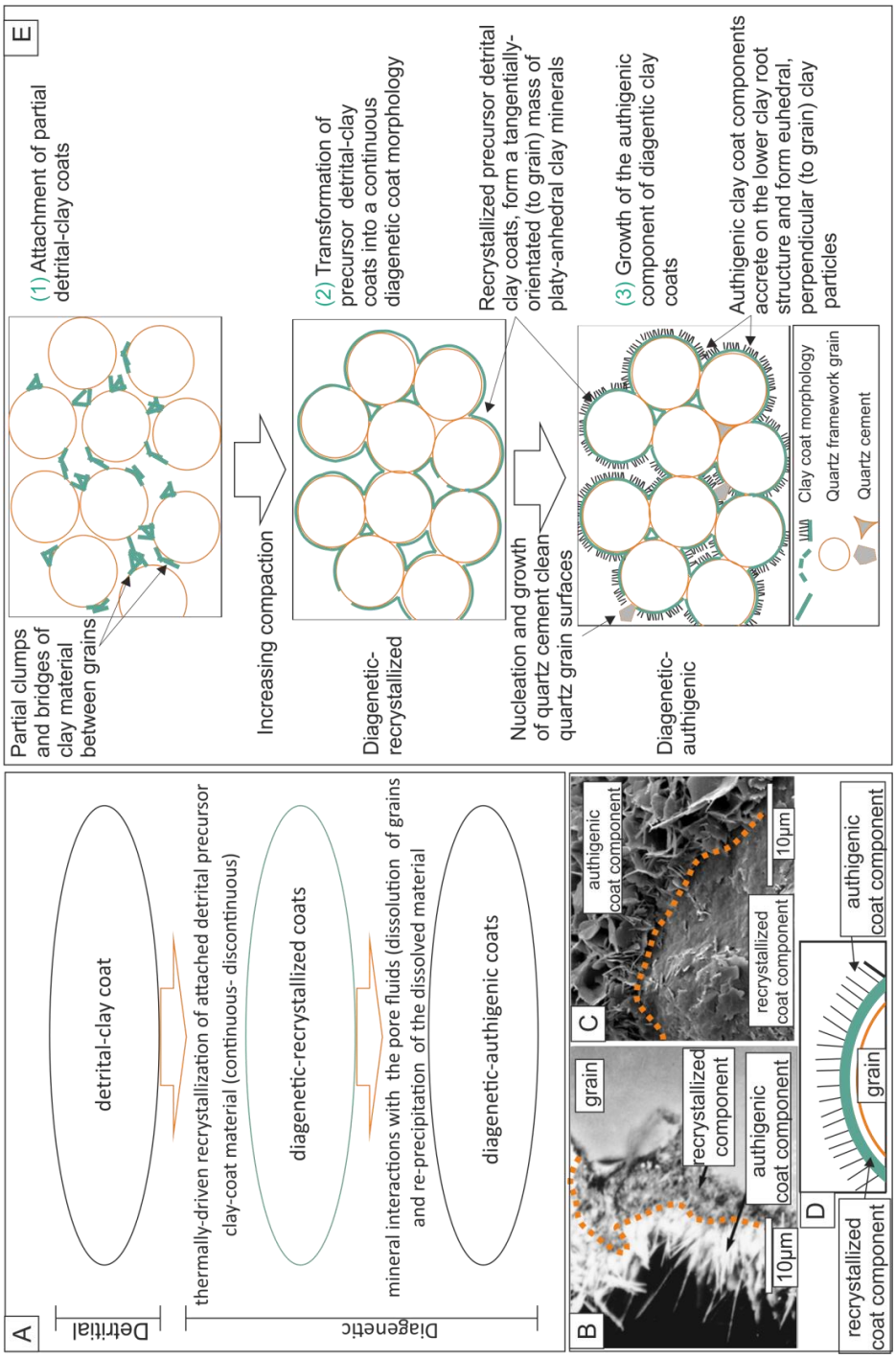

Figure 1-2 Synthesis figure illustrating the diagenetic evolution of clay coats. (A) Flow chart outlining the terminology and diagenetic stages of clay coat evolution. (B) Annotated cross sectional, scanning electron microscope image (SEM) through a diagenetic clay coat from the Haltenbanken Area, North Sea, UK, modified from Bloch et al. (2002). (C) SEM image of a diagenetic clay coat from the Judy Sandstone Member in the Heron Cluster, UK, modified from Stricker and Jones (2016). (D) Schematic illustration of the diagenetic clay coat stratigraphy as illustrated in B and C. (E) Schematic illustrations documenting the diagenetic evolution in clay coat morphology from detrital- to diagenetic-clay coat phases.

1.3.4. A summary of quartz cementation in sandstones

In order to identify how the presence of clay minerals stuck onto sand-grain surfaces can inhibit quartz cementation it is worth reviewing the processes of quartz cementation in sandstones. Clay coats do not affect the precipitation or occurrence of other pore-filling cements such as carbonates, sulphates, or zeolites that occur in sandstones (Bloch et al. 2002; Pittman et al. 1992).

For quartz cementation to occur in sandstones it is necessary to have: (i) a thermodynamic driving force overcoming the kinetic barrier to quartz nucleation, and (ii) a silica source or supply. The geochemical control on the nucleation and formation of quartz cements have been discussed at length in the following papers by Ajdukiewicz and Larese (2012); Lander et al. (2008); Worden and Morad (2000).

The silica-bearing fluid sources for quartz cementation in clastic sediments have been reported to derive from: (i) the breakdown of feldspars into the clay minerals (feldspar has a higher Si/Al ratios than the replacing illite and kaolinite clay minerals), (ii) the diagenetic transformation of smectitie into illite or chlorite (relatively high Si/Al ratio of smectite compared to illite/ chlorite), (iii) pressure dissolution of quartz grains (grain dissolution with local re-precipitation driven by concentration gradients), (iv) sand body-scale re-distribution of silica, and (v) amorphous silica (e.g. volcanic glass and *Rhaxella perforate* sponge spines) (Worden and Morad 2000).

Quartz cement in sandstones has been shown to form as scattered overgrowths which nucleate on quartz grain surfaces at sites between grain-surface discontinuities (i.e. attached non-quartz materials such as clay minerals and damaged grain regions resulting from surface abrasions) (Lander et al. 2008). The initial quartz cements nucleate as "blob-like" anhedral

crystallites on isolated sites across a quartz grain surface (Ajdukiewicz and Larese 2012; Lander et al. 2008; Pittman 1972). Epitaxial growth of the anhedral quartz crystallites causes the lateral spreading of the cement across the grain surface until they mutually contact and so coalesce with other originally isolated overgrowths (Ajdukiewicz and Larese 2012; Lander et al. 2008). Continued growth of the coalesced crystallites produces euhedral terminations associated with authigenic quartz cements (Lander et al. 2008).

At moderate temperatures the presence of clay coats (clay minerals adhered to grain surface) and other discontinuities (i.e. damaged grain regions) produce isolated quartz crystals, resulting in a reduced growth rate and isolated nanocrystals of quartz cement opposed to euhedral overgrowths (Lander et al. 2008).

1.3.5. The origin of clay coat derived inhibition of quartz cement

Clay coats are reported to inhibit quartz cement via a two-step process: (i) Clay coats, if complete, physically isolate quartz grain surfaces from silica saturated pore fluids, retarding initial quartz cement nucleation (known as nucleation inhibition) which occurs at moderate temperatures (approximately < 115 °C) (Ajdukiewicz and Larese 2012). (ii) At high temperature (115 °C to > 160 °C), isolated nanocrystals of quartz cement begin to nucleate between the clay mineral particles of the coat. At these temperatures clay particles in the coat act as barriers (kinetic or diffusion barrier) inhibiting the epitaxial growth (lateral spreading across the grain surface) and subsequent coalescence of quartz cements (growth inhibition). Clay coats thus result in a reduced cement growth rate and volume with quartz cements occurring as isolated quartz nanocrystals between clay mineral constituents of the coat instead of large euhedral overgrowths (Ajdukiewicz and Larese 2012; Billault et al. 2003). Isolated quartz nanocrystals have been reported in the clay mineral coats of the Jurassic, Haltenbanken reservoirs, Norway

(Billault et al. 2003) and the Triassic Skagerrak reservoirs, North Sea, UK (Stricker and Jones 2016).

Clay coat discontinuities inhibit quartz cement (volume) until the isolated (by clay minerals in the coats) quartz crystallites, grow around the clay coats and form euhedral terminations (Lander et al. 2008), typically at elevated temperatures e.g. > 160 °C (Ajdukiewicz and Larese 2012). The result is that the principal factor controlling the effectiveness of clay coats to inhibit the typical porosity-occluding quartz cement and thus preserve elevated primary porosity in deeply-buried sandstones, is the completeness of grain coverage (i.e. nucleation inhibition) (Ajdukiewicz and Larese 2012; Bloch et al. 2002; Skarpeid et al. 2017).

An important secondary control on the inhibition of quartz cement growth is the ability of the attached clay coats to inhibit epitaxial cement growth (i.e. growth inhibition) which is controlled by morphology, which is a function of mineralogy (e.g. chlorite or illite). The difference in morphology between the predominant clay mineral coats; (i) chlorite (platy crystals) and illite (fibrous hair like crystals) in deeply-buried sandstones has been the proposed origin of the common association of the predominant chlorite-opposed to illite clay mineralogy coats, with quartz cement inhibition in deeply-buried sandstones (Ajdukiewicz and Larese 2012).

Chlorite clay coats have been reported to be the most common mineral coat that can preserve elevated primary porosity values (Billault et al. 2003; Bloch et al. 2002; Dowey et al. 2012; Ehrenberg 1993). However, illite (Dutton et al. 2012; Parry et al. 2009; Storvoll et al. 2002) and mixed mineralogy (Ozkan et al. 2011; Pay et al. 2000; Stricker and Jones 2016) clay coats are also observed. The prerequisites for chlorite clays coats has been subject to review by Dowey

et al. (2012), with a comprehensive list of quartz cement inhibiting illite and mixed mineralogy clay coat examples complied in Chapter 7.

The heterogeneous mineralogy of diagenetic-clay coats has been reported (Gier et al. 2008; Luo et al. 2009; Martinius et al. 2005; Storvoll et al. 2002; Stricker and Jones 2016) with mixed chlorite-and illite-coats, potentially, more common than complete monomineralic coats (Chapter 7). Kaolinite is seldom reported as a component of coats but is present in the Devonian, Jauf Formation, Saudi Arabia (Al-Ramadan et al. 2004).

The result is that clay coats on grain surfaces (discontinuities) inhibit: (i) the initial quartz cement nucleation and (ii) the epitaxial growth and coalescence, resulting in a net reduced volume of quartz cement (i.e. isolated quartz crystals compared to large euhedral overgrowths). The ability to predict both the distribution and grain coverage of clay coats (i.e. nucleation inhibition) is necessary in order to make a robust prediction. The potential, influence of clay-coat mineralogy (morphology) in controlling quartz cement volume (i.e. inhibition of epitaxial cement growth) required this research to establish both the distribution of clay-coat coverage and the mineralogy of clay coats across the marginal marine system.

1.4. Reported mechanisms of clay-coated sand-grains formation

Clay-coated sand-grains have been a focus of research for near five decades (Dowey et al. 2017; Matlack et al. 1989; Pittman and Lumsden 1968; Wilson 1992; Wooldridge et al. 2017b), yet, despite the potential importance, the controlling mechanisms of detrital-clay coat formation (i.e. attachment of clay minerals to grain surfaces) (Fig. 1.2) remain only hypothesised and not constrained to level that will permit an accurate predictive model. To addresses this, a multifaceted characterisation approach was applied collecting data sets to evaluate the relative merits of reported mechanisms of detrital-clay coat formation. Each of

the principal reported mechanisms is surmised below, with a relative time line of concept development, supporting evidence, and detailed descriptions of each processes presented in Chapter 5.

Prior to this research detrital-clay-coated sand-grains in sand-dominated assemblages, have been reported to derive from the sedimentological processes of inheritance, infiltration, and drying adhesion (Moraes and De Ros 1992; Wilson 1992) and biologically via macro-organism produced biofilms (McIlroy et al. 2003; Needham et al. 2005; Worden et al. 2006). The ability to constrain the principal mechanism of clay coat formation would revolutionise current understanding and facilitate the construction of robust predictive models, which are applicable to other estuarine systems and, potentially, wider marginal marine depositional environments (e.g. deltas).

1.4.1. Sedimentological processes of clay coat formation

Inherited clay-coats are defined as clay-coats that form on sand-grains in specific depositional environments, prior to reworking and eventual deposition (Wilson 1992). The research, thus, places emphasis on establishing quantified surface data sets to observe systematic trends in clay-coat coverage (i.e. reduction in coating-extent from fluvial in-put) which would be indicative of inheritance.

Infiltration as processes of clay coat formation occurs when clay minerals and clay- to silt-sized material, previously suspended in water, enter a sand body during water percolation (Matlack et al. 1989). A reduction of flow velocity at sand-grain contacts and above impermeable layers causes the deposition of suspended clay-silt sized material onto grain surfaces (Crone 1975; Dowey 2013; Matlack et al. 1989). Infiltration have been reported to occur prevalently in course grained, arid to semi-arid environments which accommodate extensive infiltration

through the episodic surface run-off and lowered water tables (Matlack et al. 1989). However, limited work has been undertaken on the potential importance of infiltration in the post-depositional accumulation of clay coats in marginal marine sediments.

Drying adhesion attachment of clay material to sand-grain surfaces is reported to occur in estuarine sediments (Dowey 2013; Wilson 1992) via the evaporative drying during tidal exposure. However, the preservation potential of dehydration attached clay material on rehydration (tidal inundation) remains unconstrained in the literature.

1.4.2. Biological processes of clay coat formation

In a series of experiments by Needham et al. (2005) and Worden et al. (2006) the faecal casts of the lugworm *Arenicola marina* (a dominant macro-faunal organism in clastic intertidal environments) was imaged to consist of partial clay coats. Clay material was attached the sand-grain surfaces via the adhesive properties of a biofilm mucus (see next section), added to the sand-grains in the gut of the worm during digestion. Although experimentally proven, the ability of the macro-organism, lugworm *Arenicola marina,* to explain the spatial distribution of detrital-clay-coated sand-grains remains un-constrained. This research thus focused on characterising the biotic zone of the Ravenglass Estuary, in order to evaluate if this mechanism could explain the distribution of clay-coated sand-grains.

The link between clay coats (in particular chlorite) and marginal marine settings (e.g. estuarine, deltaic, and coastal shelf environments) that experience a fluvial influence is well established (Bloch et al. 2002; Ehrenberg 1993), with a potential 54 % of all current reported chlorite clay-coated sandstones, originally, deposited in such environmental conditions (Dowey et al. 2012). This work is thus focused on an estuarine system, collecting surface and near-surface trends in clay-coat coverage in unison with sedimentological and biological data sets in order to

constrain the processes which control the origin and geographically constrained distribution of clay-coated sand-grains.

1.5. The biological control on clastic marginal marine systems

Recent publications investigating biological (biofilm)-sediment interactions have demonstrated the profound influence of biological cohesion (biostabilization) on sedimentary systems (Decho 2000; Garwood et al. 2015; Jones 2017; Malarkey et al. 2015; Schindler et al. 2015). Biofilms (extracellular polymeric substances), also colloquially known as “bio-glue and mucus” (Agogué et al. 2014; Higgins et al. 2003; Hoagland et al. 1993) excerpt a fundamental control on the sediment dynamics (Jones 2017; Stal 2003). Biofilms excerpts a cohesive force (binding agent) on sand-grains and have been shown to influence sediment stability (Vignaga et al. 2013), sediment transport, bedform stability (Malarkey et al. 2015; Schindler et al. 2015), grain-size heterogeneity, and to exacerbate the entrapment of fine (clay to silt) sized material (Garwood et al. 2015).

Intertidal sediments of western Europe are extensively colonized by silicate phototrophic epipelic (motile) diatoms which represent the dominant biofilm producing microphytobenthic (MPB) organism (Stal 2003; Underwood and Paterson 1993). Diatoms produce biofilms (EPS) for a variety of functions (Decho 1990). One function is to facilitate the adhesion to grain surface, reorientation, and cell movement of the diatom in response to tidal and daylight cycles to maintain optimum environmental conditions (Stal 2003; Underwood and Paterson 1993). The EPS “mucus” strands on movement detach from the diatom but remain attached to sand-grain surfaces thus accumulating as biofilms (Higgins et al. 2003; Stal 2003), producing a sticky mucus matrix (Jones 2017) on grain surfaces in intertidal sediment.

Biological-sediment interactions are well known in carbonate systems (O'reilly et al. 2017; Riding 2000). The potential influence of biofilms in clastic sediments has been largely overlooked (Jones 2017). Thus, emphasis was placed on constraining the potential, fundamental role played by biofilms "bio-glue" and biological organisms in controlling sediment characteristics (e.g. grain size, sorting, and clay content) in clastic marginal marine systems. Detailed reviews on the sedimentological aspects of biofilms are given in Chapters 3 and 4.

1.6. Organisation of thesis:

The thesis is presented in a series of chapters written in a paper format including those that are published or ready for submission. The result is that some location descriptions, methodologies, and ideas reoccur. A summary of the publication status and contributions made by co-authors for each chapter is given below.

1.6.1. Chapter 2

Title: Clay-coated sand-grains in petroleum reservoirs: understanding their distribution via a modern analogue

Citation: Wooldridge, L.J., Worden, R.H., Griffiths, J., and Utley, J.E., 2017, Clay-coated sand-grains in petroleum reservoirs: understanding their distribution via a modern analogue: Journal of Sedimentary Research, v. 87, p. 338-352, doi:10.2110/jsr.2017.20.

Aim: To establish the presence, distribution, textural characteristics, and mineralogy of clay coated sand-grains across the Ravenglass Estuary.

The chapter documents the distribution, textural, and mineralogical characteristics of clay coated sand-grains across a fluvial to marine transect of depositional environments. The novel

data set is incorporated with a high resolution framework of sediment heterogeneity (grain size, sorting, clay fraction content, and clay mineralogy) in order to constrain potential controls.

Author contributions:

- Wooldridge, L.J: Main author. Conceived the research, designed the paper, undertook sample collection, and performed analysis.
- Worden, R.H: Responsible for project funding and undertook manuscript review.
- Griffiths, J: Performed field work, undertook sample collection, and aided in field analysis.
- Utley, J.E.P: Undertook sediment clay fraction and XRD analysis
- The comments of Iris Verhagen, Sally Sutton, Rikki Weibel, and an anonymous reviewer were incorporated during the review of this paper.
- In addition thanks goes to Joanne Jeffreys and Robert Wilcox for their assistance in collecting lugworm population density and qualitative grain size data sets.

1.6.2. Chapter 3

Title: Biofilm origin of clay-coated sand-grains

Citation: Wooldridge, L., Worden, R., Griffiths, J., Thompson, A., and Chung, P., 2017, Biofilm origin of clay-coated sand-grains: Geology, v. 45, p. 875–878, doi:10.1130/G39161.1

Aim: To establish the principal origin of clay-coated sand-grains (i.e. mechanism of clay mineral attachment to sand-grain surfaces) in marginal marine sediments by exploring the potential role of micro-organism produced biofilms.

This work applied SEM petrography, biological (organic bio-marker analysis), chemical (Raman spectroscopy), and statistical approaches to establish the origin of clay-coated sand-grains and sediment heterogeneity in a marginal-marine estuarine system.

Author contributions:

- Wooldridge, L.J: Main author. Conceived the research, designed the paper, undertook sample collection, and performed analysis.
- Worden, R.H: Responsible for project funding and undertook manuscript review.
- Griffiths, J: Performed field work and undertook sample collection.
- Thompson, A: Aided in the construction of the biofilm method and analyses.
- Chung, P: Gave guidance and aided in Raman spectroscopy analysis and environment scanning electron imaging.
- The comments of Stuart Jones, Joann E. Welton, and Marsha W.French were incorporated during the review of this paper.

1.6.3. Chapter 4

Title: The origin and of clay-coated sand-grains and sediment heterogeneity in tidal-flats
Citation: *In preparation* for submission to Journal of Sedimentary Research

Aim: To evaluate the principal controls on the distribution of clay-coated sand-grains in the near-surface.

This bio-sedimentary study of tidal-flats involved quantifying clay-coat coverage, sediment heterogeneity (grain size, sorting, and clay fraction content), and biological characteristics (biofilm abundance and the intensity of bioturbation) of surface and near-surface (core) samples. The results were collected to constrain the principal controls on the generation, distribution, and mineralogy of clay-coated sand-grains in near-surface sediment.

Author contributions:

- Wooldridge, L.J: Main author. Conceived the research idea, designed the paper, undertook sample collection, and performed analysis.
- Worden, R.H: Responsible for project funding and undertook manuscript review.

- Griffiths, J: Performed field work and undertook sample collection.
- Duller, R: In depth discussions and figure review.
- Utley, J.E.P: Performed field work and undertook sediment clay fraction analysis
- Thompson, A: Aided in the construction of the biofilm quantification method and was heavily involved in the analyses.

1.6.4. Chapter 5

Title: The origin of clay-coated grains in marginal marine sandstones: insights from a modern analogue

Citation: *In preparation* for submission to Journal of Sedimentology

Aim: To identify the controlling mechanisms that govern the origin and distribution of clay coated sand-grains

The chapter applies a range of SEM petrography techniques (SEM, ESEM, SEM-EDS) and collects data sets of clay-coat coverage, sediment biofilm abundance, grain size, sorting, and clay fraction content. The results evaluate in light of the data from the Ravenglass Estuary the principle controls on the distribution of clay coats across marine depositional environments.

Author contributions:

- Wooldridge, L.J: Main author. Conceived the research idea, designed the paper, undertook sample collection, and performed analysis.
- Worden, R.H: Responsible for project funding and undertook manuscript review.
- Griffiths, J: Performed field work, undertook sample collection and aided in grain size and sorting quantification.
- Duller, R: In depth discussions and figure review.
- Utley, J.E.P: Undertook sediment clay fraction analysis
- Thompson, A: Aided in the construction of the biofilm quantification method and was heavily involved in the analyses.
- Chung, P: Aided in ESEM imaging of clay coated sand-grains.

- In addition thanks goes to Joanne Jeffreys and Robert Wilcox for their assistance in collecting lugworm population density data sets.

1.6.5. Chapter 6

Title: How to quantify clay-coat grain coverage in modern and ancient sediments

Citation: *In preparation* for submission to Journal of Sedimentary Research

Aim: To detail the methods available for the quantification of the degree of grain coat coverage in modern and ancient sediment

The study presents a qualitative method which uses categorical bin classes based on SEM images of whole sediment and two quantitative methods which measured both the fraction of the perimeter of a grain that is covered by attached clay and the volume of clay present as clay coats, both from SEM analysis of polished sections. The data sets were collected to establish if qualitative and quantitative clay coat classification methodologies produce comparable data.

Author contributions:

- Wooldridge, L.J: Main author. Conceived the research idea, designed the paper, designed and organised the creation of the Petrog (clay-coat coverage) quantification technique, conceived the concept and developed the method for SEM-EDS (clay coat volume quantification), undertook sample collection, and performed analysis.
- Worden, R.H: Responsible for project funding and undertook manuscript review.
- Utley, J.E.P: Aided heavily in the construction of the SEM-EDS quantification method and was involved in the analyses.
- Griffiths, J: Performed field work and undertook sample collection.

1.6.6. Chapter 7

Title: The origin and distribution of clay-coat mineralogy

Citation: *In preparation* for submission to AAPG Bulletin

Aim: To document clay-coat mineralogy across a marginal marine system

The study applied a novel automated scanning electron microscope-energy dispersive spectrometry (SEM-EDS) methodology which allowed the ability to differentiate clay-coat mineralogy from that of the whole sediment. The study thus offered the ability to: (i) explore the spatial distribution of clay-coat mineralogy and (ii) constrain the controlling mechanisms which clay-coat mineralogy.

Author contributions:

- Wooldridge, L.J: Main author. Conceived the research idea, designed the paper, designed quantification technique, undertook sample collection, and performed analysis.
- Worden, R.H: Responsible for project funding and undertook manuscript review.
- Griffiths, J: Performed field work and undertook sample collection.
- Utley, J.E.P: Aided heavily in the construction of the quantification method and was involved in the analyses.

2. Clay-coated sand-grains in petroleum reservoirs: understanding their distribution via a modern analogue

2.1. Abstract

Clay-coated grains can inhibit ubiquitous, porosity-occluding quartz cement in deeply-buried sandstones and thus lead to anomalously high porosity. A moderate amount of clay that is distributed in sandstones as grain coats is good for reservoir quality in deeply-buried sandstones. Being able to predict the distribution of clay-coated sand-grains in petroleum reservoirs is thus important to help find and exploit such anomalously good reservoir quality.

The study adopted a high-resolution, analogue approach, using the Ravenglass Estuary marginal-shallow marine system, in NW England, UK. Extensive geomorphic mapping, grain-size analysis, and bioturbation-intensity counts were linked to a range of scanning electron microscopy techniques to characterize the distribution and origin of clay-coated sand-grains in surface sediment.

Our work shows that grain coats are common in this marginal-shallow marine system, but they are heterogeneously distributed as a function of grain size, clay fraction, and depositional facies. The distribution and characteristics of detrital-clay-coated grains can be predicted with knowledge of specific depositional environment, clay fraction percentage, and grain size. The most extensive detrital-clay-coated grains are found in sediment composed of fine-grained sand containing 3.5 to 13.0 % clay fraction, associated with inner-estuary tidal-flat facies. Thus, against common convention, the work presented here suggests that, in deeply-buried prospects, the best porosity might be found in fine-grained, clay-bearing inner-tidal-flat-facies sands and not in coarse, clean channel-fill and bar facies.

2.2. Introduction

Porosity and permeability generally decrease with increasing depth of burial in sandstones, although a significant number of deeply-buried sandstone reservoirs have unusually high porosity and permeability (Bloch et al. 2002). Such anomalously high porosity and permeability have most commonly been linked to the presence of chlorite-clay-coated grains that inhibit the growth of porosity-occluding quartz cement (Ajdukiewicz and Larese 2012; Ehrenberg 1993; Worden and Morad 2000).

The term clay coat encompasses both detrital and diagenetic origins (Ajdukiewicz and Larese 2012). Detrital-clay-coated grains occur at or near the surface of the sediment, and are principally the focus of this study.

Diagenetic clay coats either develop from the thermally driven recrystallization of low-temperature, detrital precursor clay coats or they grow *in situ* due to the authigenic alteration of detrital or early diagenetic minerals interacting with the pore fluids during burial (Ajdukiewicz and Larese 2012; Wise et al. 2001; Worden and Morad 2003).

Chlorite and illite clay coatings are considered to preserve reservoir quality by reducing the nucleation area on detrital quartz grains that is available for authigenic quartz cementation (Ehrenberg 1993; Pittman et al. 1992). Porosity can be at least 10 % higher than expected where grain-coating clays are abundant (Ehrenberg 1993). Experiments undertaken by Ajdukiewicz and Larese (2012) and Lander et al. (2008) along with observations by Billault et al. (2003) led to the conclusion that clay crystals in the clay coat act as barriers, inhibiting epitaxial quartz cement growth and subsequent coalescence to form thick quartz overgrowths. The main factors controlling the effectiveness of clay-coated grains for the inhibition of authigenic,

porosity-occluding quartz cement are the extent, completeness, and distribution of the detrital precursor clay-coated grains (Billault et al. 2003).

Oil-field-based studies which collectively show that clay coats are most common in fluvial to marginal marine sediments, including Jurassic sandstones on the Norwegian continental shelf (Bloch et al. 2002),the Jurassic and Triassic fluvial, lacustrine to deltaic sandstones of the Ordos basin, China (Luo et al. 2009), the marginal marine Jauf Formation, eastern Saudi Arabia (Al-Ramadan et al. 2004), the Upper Cretaceous Tuscaloosa Formation, USA (Pittman et al. 1992), and see review by Dowey et al. (2012). However, there is no model capable of predicting the occurrence of clay-coated grains or the degree of completeness of grain coats in fluvial to marginal marine sediments.

The positive influence of chlorite- and illite-clay-coated grains on reservoir quality in deeply-buried sandstone has resulted in extensive reservoir core-based research (Billault et al. 2003; Ehrenberg 1993; Gould et al. 2010; Skarpeid et al. 2017) and laboratory experiments (Aagaard et al. 2000; Ajdukiewicz and Larese 2012; Pittman et al. 1992). Chlorite-coated grains have been observed to inhibit quartz cement, and the need to understand the origin of chlorite-coated grains was the driving force that led to the current study. Notable chlorite-clay-coated reservoir units include the Tilje Formation, Norwegian continental shelf (Ehrenberg 1993), the Tuscaloosa Formation, U.S. Gulf Coast (Ajdukiewicz and Larese 2012), and the Rotliegend Sandstone, northern Netherland (Gaupp and Okkerman 2011). Sandstones which contain illite and mixed-layer illite smectite clay-coated grains have been less commonly advocated but include the Garn Formation, Mid-Norway (Storvoll et al. 2002), the Williams Fork Formation, Colorado (Ozkan et al. 2011) and the Jauf Formation, Eastern Saudi Arabia (Al-Ramadan et al. 2004; Cocker et al. 2003).

Aagaard et al. (2000) showed that low-temperature, discontinuous, detrital-clay-coated grains recrystallized during experiments at 90 °C to form thick, continuous, diagenetic clay coats that are morphologically consistent with naturally occurring reservoir examples. In some examples, euhedral clay minerals grow out into the pore from an underlying, unstructured clay coat (Bloch et al. 2002; Gould et al. 2010). Such clay-coat stratigraphy could be the result of a detrital, or very early diagenetic, clay coat acting as a seed for deep-burial neoformation of diagenetic-clay coats.

Despite the importance of being able to predict the occurrence and distribution of detrital-clay-coated grains, there is no all-encompassing model that is useful for ranking prospects or populating reservoir models with the completeness of clay coats in marginal marine sandstones. Relatively little fundamental work has been undertaken on the controls on clay-coat growth in sediments, although Wilson (1992) and Matlack et al. (1989) undertook early studies focused upon environments (aeolian, marine-shelf, marginal marine, fluvial) in which clay-coated sand-grains occur and potential mechanisms of formation (bioturbation, infiltration, inheritance). In order to predict anomalously high porosity in the subsurface, there is a need to focus on the origin and spatial distribution of detrital-clay-coated grains since clay coats inhibit quartz cement in deeply-buried sandstones (Bloch et al. 2002). Anomalously high porosity has also been shown to derive from other processes such as early oil charge, overpressure, and microquartz coatings (Bloch et al. 2002).

The four main ways to develop a fundamental understanding of primary sedimentary environment and mineral distribution, and thus the processes that lead to clay coats, are: core-based studies, outcrop-based studies, experimental studies, and modern-analogue studies. Core-based studies have problems of limited spatial resolution of samples (wide spacing between wells and the lack of abundant cores in most fields) and the abiding uncertainty about

both the primary mineralogy and exact environment of deposition due to subsequent diagenetic modifications. Outcrop-based studies overcome the spatial resolution problem but typically suffer from weathering-related recent changes to mineralogy, plus outcrop-diagenesis studies routinely have problems in seeing through the long history of burial, heating, and then uplift. The study adopted a modern-analogue approach, linking the distribution of detrital-clay-coated grains to sedimentary processes and characteristics (grain size, percentage clay fraction) and biological processes (bioturbation). The detailed study of sediment from modern environments permits a high-resolution investigation into the distribution of detrital-clay-coated grains, removing the limited spatial distribution, stratigraphic coverage, and ambiguous depositional-environment interpretations of subsurface core-based studies. This study addresses the following questions, focussed on the marginal-shallow marine Ravenglass Estuary system (Fig. 2.1).

1. What are the textural characteristics of detrital-clay-coated grains in a modern marginal-shallow marine setting?
2. What are the mineralogical characteristics of clay-coated sand-grains in a modern marginal-shallow marine setting?
3. How variable is the coverage of detrital-clay-coated grains in a modern marginal-shallow marine system?
4. What controls the formation and distribution of detrital-clay-coated grains?
5. Are the clay coats in this modern, marginal-shallow marine system texturally comparable to other modern or subsurface examples?
6. What is the potential impact of using modern analogues for the prediction of reservoir quality in ancient and deeply-buried sandstones from the same primary environment?

2.3. Geomorphology of the study area

The Ravenglass Estuary is located in Cumbria, NW England. The mid to upper portions of the Ravenglass Estuary are fed by three rivers, the Esk, the Mite and the Irt, with the lower, western part of the estuary connected by a single channel to the Irish Sea (Bousher 1999) (Fig. 2.1). Ravenglass sediment is quartz-dominated (Daneshvar 2011; Daneshvar and Worden 2016) with depositional environments translatable to marginal shallow marine petroleum reservoirs. Ravenglass is a modern analogue equivalent to the environment of deposition for many ancient and deeply-buried, chlorite-coated sandstone reservoirs such as the tidally influenced, shallow marine-deltaic Tilje Formation, Norway (Ehrenberg 1993), the braid-delta margin with foreshore and shoreface deposits of Garn Formation, Norway (Storvoll et al. 2002), and the shallow marine to deltaic Lower Vicksburg Formation, USA (Grigsby 2001).

The 5.6 km² estuary has a maximum tidal range of 7.55 m and is 86 % intertidal (Bousher 1999; Lloyd et al. 2013). The estuary has extensive back-barrier tidal-flats and tidal-bars, fringed by well-established saltmarsh vegetation (Bousher 1999). The estuary is connected to the Irish Sea through a single, 500 m-wide tidal inlet that dissects a fringing coastal barrier which is topped with aeolian dunes. The three fluvial channels, fluvial overbank, foreshore, and ebb-delta complex provide a complete fluvial to marine transect that were investigated in terms of depositional environments, and detrital-clay-coat abundance, with analysis of detrital-clay-coat mineralogy (Fig. 2.1). Despite the high spring tidal range, the estuary contains geomorphological elements consistent with a mixed-energy (wave-tide) regime, following the estuary classification scheme proposed by Ainsworth et al. (2011). This indicates a tidal hydrodynamic dominance in the inner estuary and wave-dominated processes occurring along the foreshore coastal side of the barrier spits.

The marginal-shallow marine Ravenglass system can be divided into fluvial-, estuary-, shallow marine-, and aeolian-dune-dominated regimes, with the results of this study subdivided by sub-environment. The estuary has a clay-mineral sediment assemblage consisting of chlorite, illite, and kaolinite, largely derived from suspended fluvial sediment, originating from incision and weathering of the hinterland geology (Daneshvar 2011; Daneshvar and Worden 2016). The southern River Esk drains the Palaeozoic Eskdale Granite; the northern River Irt drains the Triassic Sherwood Sandstone Group and the Borrowdale Volcanic Group; the central, but minor, River Mite drains a combination of Eskdale Granite, Triassic Sherwood Sandstone Group, and the Borrowdale Volcanic Group (Moseley 1978).

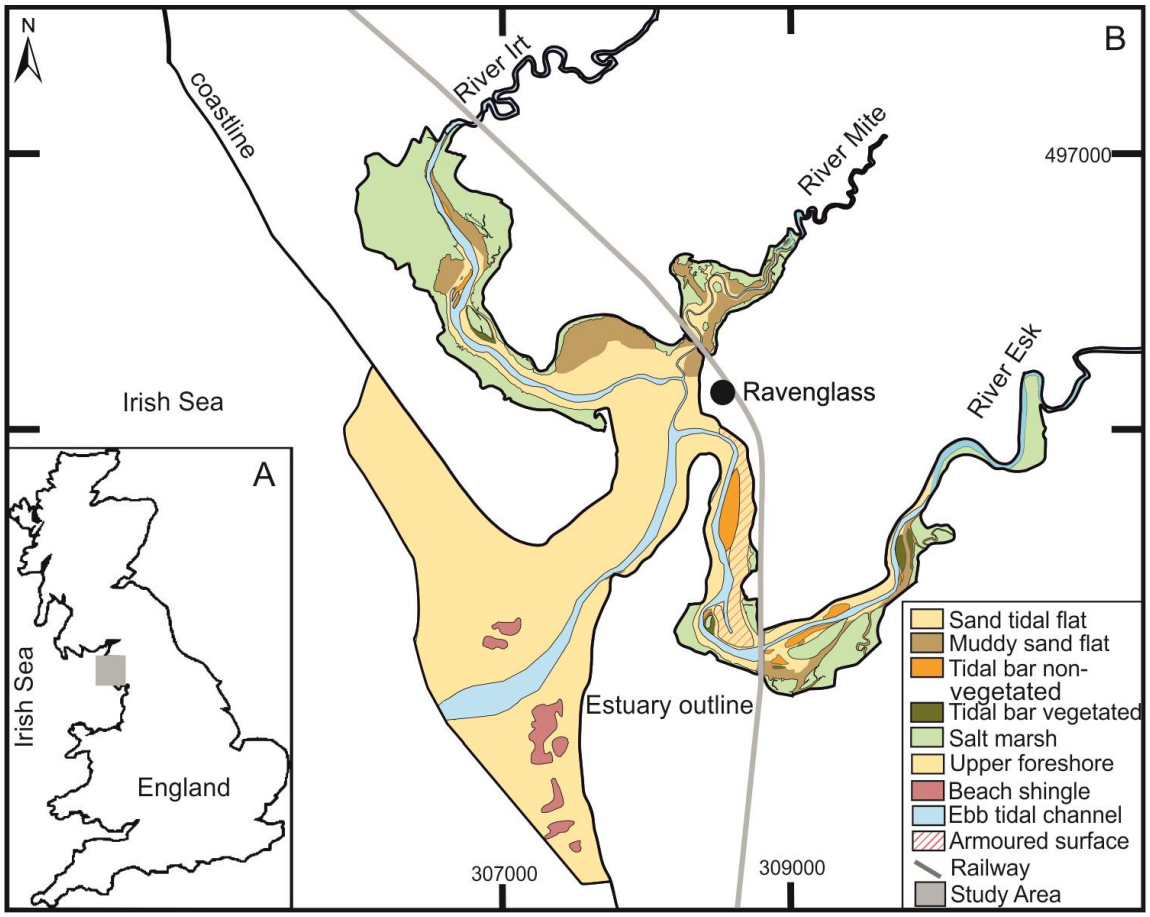

Figure 2-1 Location and depositional environment map of the Ravenglass Estuary. (A) The Ravenglass Estuary, in the UK. (B) Regional map showing the study area and component depositional environments. Tidal flats have been subdivided based upon their component clay fraction (< 2 μm); 0 to 10 % sand flat, 10 to 30 % muddy sand flat, 30 to 80 % sandy mud flat. The classification is modified from the scheme initially proposed by Dyer (1979). The black square indicates the location of the sediment sample from which clay-coat (SEM-EDS) and sediment-clay-fraction (XRD) mineralogical analyses (Figs. 2.4 and 2.5) were undertaken.

2.4. Materials and methods

2.4.1. Field-based mapping of the estuary

The estuary was initially mapped by identifying each depositional environment via world imagery and Google Earth. Extensive field mapping and sampling of all geomorphological elements enabled ground-truthing of mapped depositional elements and interpolation using ArcGIS. Tidal flats were further subdivided using the scheme proposed by Dyer (1979), based upon component volume clay fraction (< 2 μm fraction):

0 to 10 % clay fraction is classed as sand flat,

10 to 30 % is muddy sand flat,

30 to 80 % is sandy mud flat.

Surface sediment grain size (approximately 2 cm depth) was determined at 3151 sites in the field using grain-size cards and mapped using interpolation in ArcGIS (https://www.arcgis.com). Density of lugworm faecal casts (number per square meter) was recorded in the field using a 1 m^2 quadrat, randomly thrown at 3151 sites in the estuary. Lugworm density was mapped across the entire intertidal exposed area, and also mapped using interpolation in ArcGIS. Polished thin sections were constructed from samples across a tidal-flat succession to allow mineralogical quantification via automated scanning electron microscope energy dispersive spectrometry (SEM-EDS). Sediment clay-fraction mineralogy was established through X-ray diffraction analysis (XRD).

2.4.2. Determination of clay-coat coverage

This study is focused principally on a suite of 181 surface sediment samples which were subject to grain-coat petrography. The sample sites were chosen to provide sufficient spatial coverage

and encompass a fluvial to shallow marine transect incorporating all depositional environments. The volume of the clay size fraction (< 2 μm, weight percentage) was established for 95 of the 181 sites.

Approximately 50 cm^3 of surface sediment was collected at each of the 181 sites. The sediment was then subsampled and dried at room temperature. Quantification of detrital-clay-coverage was achieved using scanning electron microscope (SEM) analysis of grain mounts on a 1 cm diameter stub. The grain-mount stubs were examined by SEM petrography in backscattered electron (BSE) imaging.

A complete traverse across each SEM stub was collected by stitching together nine or more BSE images taken for each sample to produce a representative image of approximately 200 grains. In comparison to thin-section-based approaches for the study of grain coats, this approach permitted the investigation of detrital-clay-coated grains in three dimensions. It also allows the detailed classification of each sample (Fig. 2.2). The study adopted a novel approach that initially categorizes the samples in terms of absence (group 1) or presence (groups 2 to 5) of clay coat and then subdivides those with coats into the degree of coat coverage (by surface area). Detrital-clay coats in this study were thus categorized into five principal classes:

1) Complete absence of attached clay coats.

2) Less than half of the grains have a small (~ 1 to 5 %) surface area of attached clay coats.

3) Every grain exhibits at least ~ 5 to 15 % surface area of attached clay coats.

4) Clay coats observed on every grain with the majority exhibiting extensive (~ 15 to 30 %) surface-area grain coverage.

5) Extensive > 30 % surface area covered by clay coats observed on every grain.

To ensure reliability of the method and interpretation, duplicate SEM stub preparation and analysis was undertaken for 38 of the 181 samples to check the consistency of the classification method. Noted all replicates faithfully reproduced the initial classification. Critical-point drying (Jernigan and McAtee 1975) was not applied to the samples, owing to the absence of delicate fibrous clays associated with authigenic growth.

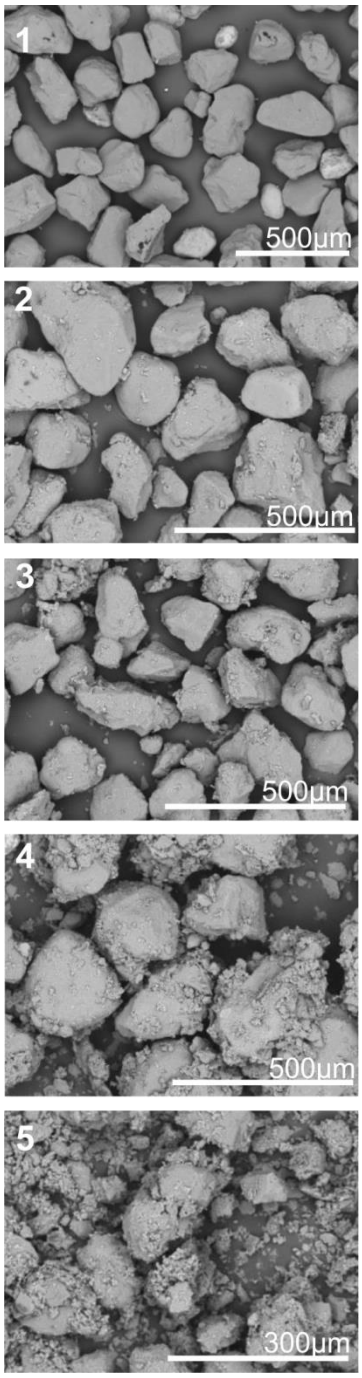

Figure 2-2 SEM electron images showing the variable extent of attached clay coats observed in surface sediment samples, which define the basis of the utilized classification scheme. 1) Complete absence of clay coats. 2) 1 to 5 % attached clays on less than half of the grains. 3) Every grain exhibits 5 to 15 % clay coats coverage. 4) Clay coats observed on every grain, with the majority exhibiting extensive 15 to 30 % coverage. 5) Extensive, > 30 % clay-coats coverage observed upon every grain.

2.4.3. Clay-coat mineralogy

Mineralogical quantification of clay-coated sand-grains from a sand-mud tidal-flat was undertaken via SEM-EDS using an FEI-QEMSCAN® (Armitage et al. 2010; Armitage et al. 2016). This approach was selected to enable *in situ* imaging of clay mineralogy, distribution characteristics and define the link between sediment clay mineralogy and that of clay coats. Three polished thin sections were constructed from surface sediment. The QEMSCAN® system comprises a scanning electron microscope coupled with fast energy dispersive spectrometers (EDS), a microanalyzer, and an electronic processing unit, which integrates the data to provide information about the micron-scale texture and chemical and mineral composition. The step size for the analysis was 1 µm to ensure that the fine fraction in the sediment was analyzed as well as framework grains.

The data are presented as a combination of a backscatter secondary electron image, and fully quantitative mineralogical content image (framework grains) and quantitative clay mineralogy (total clay, illite, chlorite, kaolinite) to represent the sediment assemblage and component clay-coated sand-grains.

2.4.4. Determination of clay fraction content

The percentage of the clay fraction (< 2 µm) was established via homogenized sediment subsamples, dried at 60 °C. A few grams of sample were added to 200 ml of water and then ultrasonicated for 20 minutes with vigorous stirring at five minute intervals. Gravity settling removed sand- and silt-size particles, with the supernatant water (containing the clay-grain-size particles) decanted and settled by centrifugation to obtain the clay fraction. The separated clay fraction was dried at 60 °C, crushed in an agate pestle and mortar, and then weighed, revealing the percentage clay fraction in the sediment sample.

2.4.5. The mineralogy of the bulk-sediment clay fraction

Classification of the clay fraction (< 2 μm) mineralogy was undertaken by X-ray diffraction analysis (XRD). The clay-size fraction was detached from framework grains using an ultrasonic bath and isolated using centrifuge settling, at 5000 rpm for 10 minutes. The separated clay fraction was dried at 60 degrees and scanned as a randomly oriented powder, using a PANalytical X'Pert Pro MPD X-ray diffractometer. XRD analysis was carried out for the same sample that was mineralogy mapped through (SEM-EDS) analysis.

2.5. Results

2.5.1. Surface sedimentary characteristics and distribution of biological activity

Sedimentary environments were identified in the field, with further subdivision of the tidal flats based upon the lab-derived clay fraction data sets into sand-flat, muddy sand-flat, and sandy mud-flat (Fig. 2.1).

High-resolution, spatial distribution maps of sediment grain size reveal a wide range of mean grain sizes, from very fine- to coarse-sand-size sediment (Fig. 2.3A). There is a large-scale trend of decreasing grain size away from the ocean, and smaller-scale patterns of decreasing grain size with increasing distance from the main ebb channel, towards the tidal limit (Fig. 2.3A).

A heterogeneous distribution of lugworms occurs in the estuary, as denoted by the widely varying density of lugworm cast (Fig. 2.3C). The lugworm density at the sediment surface is taken to indicate the intensity of bioturbation in the biotic zone of the sediment (McIlroy et al. 2003; Needham et al. 2005). The highest density of lugworms (31 to > 50 per m^2) was observed in the outer sand tidal flats and non-vegetated-tidal-bar depositional environments (Figs. 2.1 and 2.3C). Comparing the map of sediment grain size (Fig. 2.3A) to the map of

lugworm population (Fig. 2.3B) suggests that well-developed lugworm populations tend to be confined predominantly to the inner estuary, where the sediment grain size tends to be between 88 and 177 μm.

The data on percentage sediment clay fraction were split into eight classes (Fig. 2.3B). Samples that contain > 1.5 % clay fraction are confined to the inner estuary. Samples that contain < 1.5 % clay fraction occur in the seaward portion of the estuary and outer tidal flats (Fig. 2.3B). This pattern suggests that there is an inverse relationship between overall grain size and the amount of co-deposited clay fraction, i.e., the percentage of the clay fraction increases with decreasing grain size.

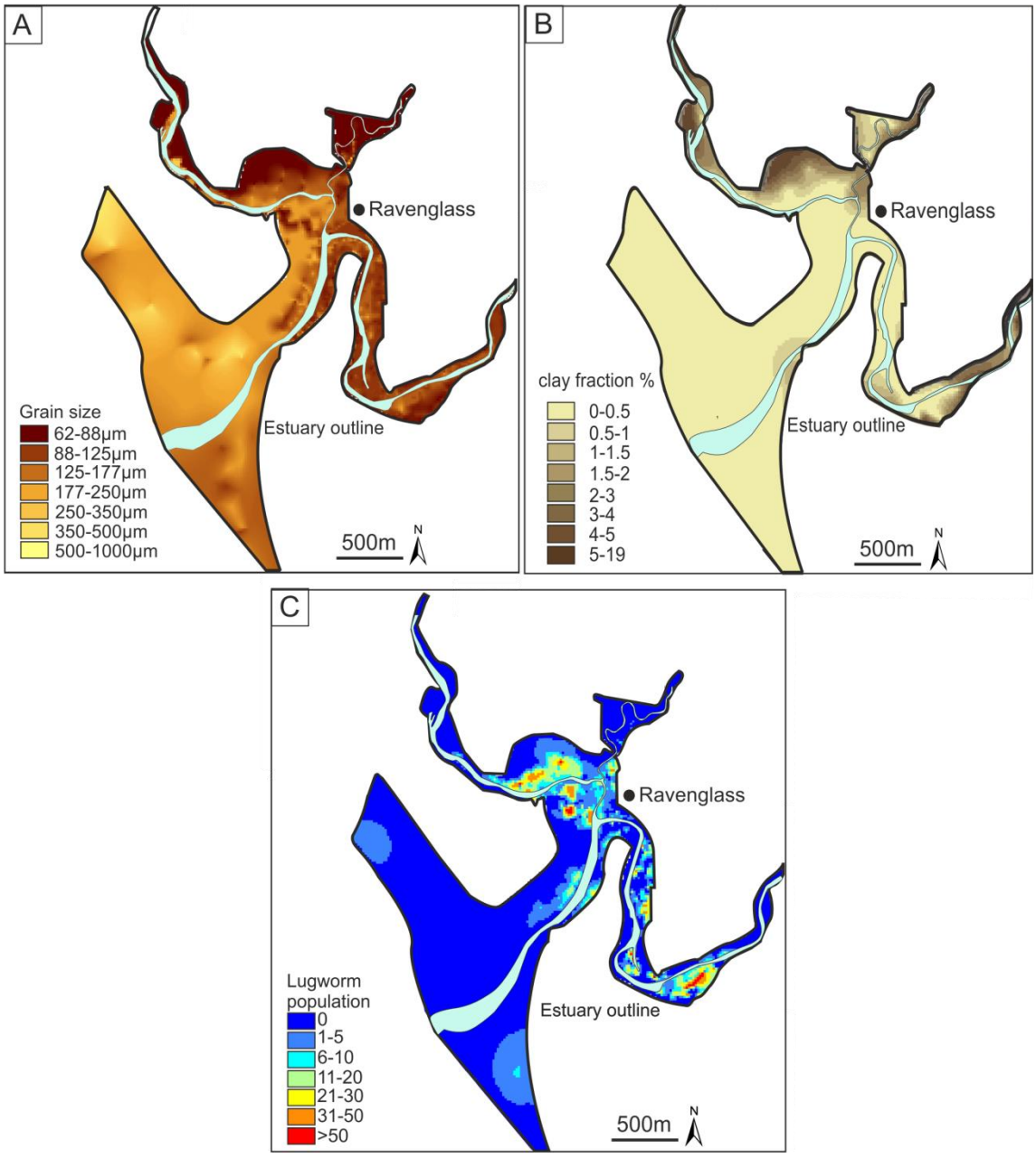

Figure 2-3 Distribution maps of surface sedimentary and biological characteristics. (A) High-resolution map of surface-sediment grain size. (B) Surface distribution of clay-fraction percentage. (C) High-resolution map of lugworm population in surface sediment.

2.5.2. Mineralogy of the clay fraction

The sediment samples have a clay fraction composed of illite, chlorite, and kaolinite, with an average 7.6 % clay fraction in the sediment. X-ray diffraction shows that the clay fraction is dominated by illite (62 % of the clay fraction) with chlorite (17 % of the clay fraction) and kaolinite (21 % of the clay fraction) expressing similar values (Fig. 2.4).

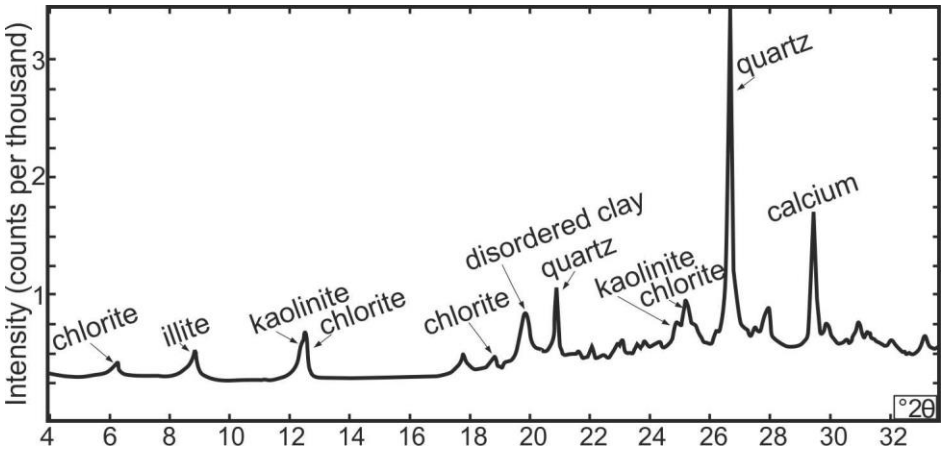

Figure 2-4 X-ray diffractogram used to quantify the bulk-sediment clay-fraction mineralogy of surface sediment in the Ravenglass Estuary (for location, see Fig. 2.1).

2.5.3. Characteristics of detrital-clay coats

The observed detrital-clay-coated grains are generally characterized by thin and discontinuous accumulations of individual but interlocking (overlapping and aligned clay platelets) clay minerals (Fig. 2.5). This study has focussed on the morphology of the coat, and does not rely on a differentiation based on internal structure. Each sample was characterized by the morphology of the coat, the extent (degree) of grain coverage, and abundance (proportion of grains that contain coats) (Figs. 2.2). The clay coats occur on both convex and concave grain faces, but the coats with the greatest thickness occur in grain indentations (Figs. 2.5G, 2.6E, 2.7). Clay coats occupy up to about 60 % of the surface area of individual grains in a given sample.

Detrital-clay coats are composed of individual interlocking clay minerals with a mixed mineralogy even along a singular ridge structure and a range of accessory impurities consisting of silt-size quartz and bioclastic debris. Clay coats have been observed on all component framework grains in the sediment assemblage (quartz, feldspar, dolomite, calcite). The sand-grains in this study are coated with a mixture of clay minerals (Fig. 2.7), dominated by illite (9.1 % image-area), with minor chlorite (1.7 % image-area) and kaolinite (1.1 % image-area). There was no identified variability between clay mineralogy and morphological classes of component clay coats (ridged, bridged, and clumped).

Detrital-clay coats occur with a variety of morphologies (Fig. 2.5). The method grouped the samples into three principal morphological classes: ridged, bridged, and clumped (Fig. 2.6).

Ridged clay coats consist of elongate intergrowths of plate-like clay minerals, oriented at high angles to the grain surface (Fig. 2.6A). Ridged coats have variable lengths (< 200 μm) and are preferentially observed upon relatively flat grain surfaces with minimal (silt) impurities. Ridged clay-coated grains occur predominantly in the coarser, cleaner sediment assemblages that are associated with outer-tidal-flat and non-vegetated-tidal-bar environments.

Bridged-clay-coat textures occur between detrital grains. Bridged clay coats consist of elongate clay-mineral aggregates that connect two grains. Bridged clay coats are relatively uncommon in surface sediment, possibly as a result of the sampling procedure (Fig. 2.6B).

Clumped clay coats are highly variable in both extent and thickness (Figs. 2.5 and 2.6C). Clumped coatings can reach sizes of up to 200 μm and contain silt-size fragments as well as clay-grade material. Clumped clay coats are most abundant in the upper-estuary, intertidal, muddy sand-flats, tidal-bars, and saltmarsh depositional environments.

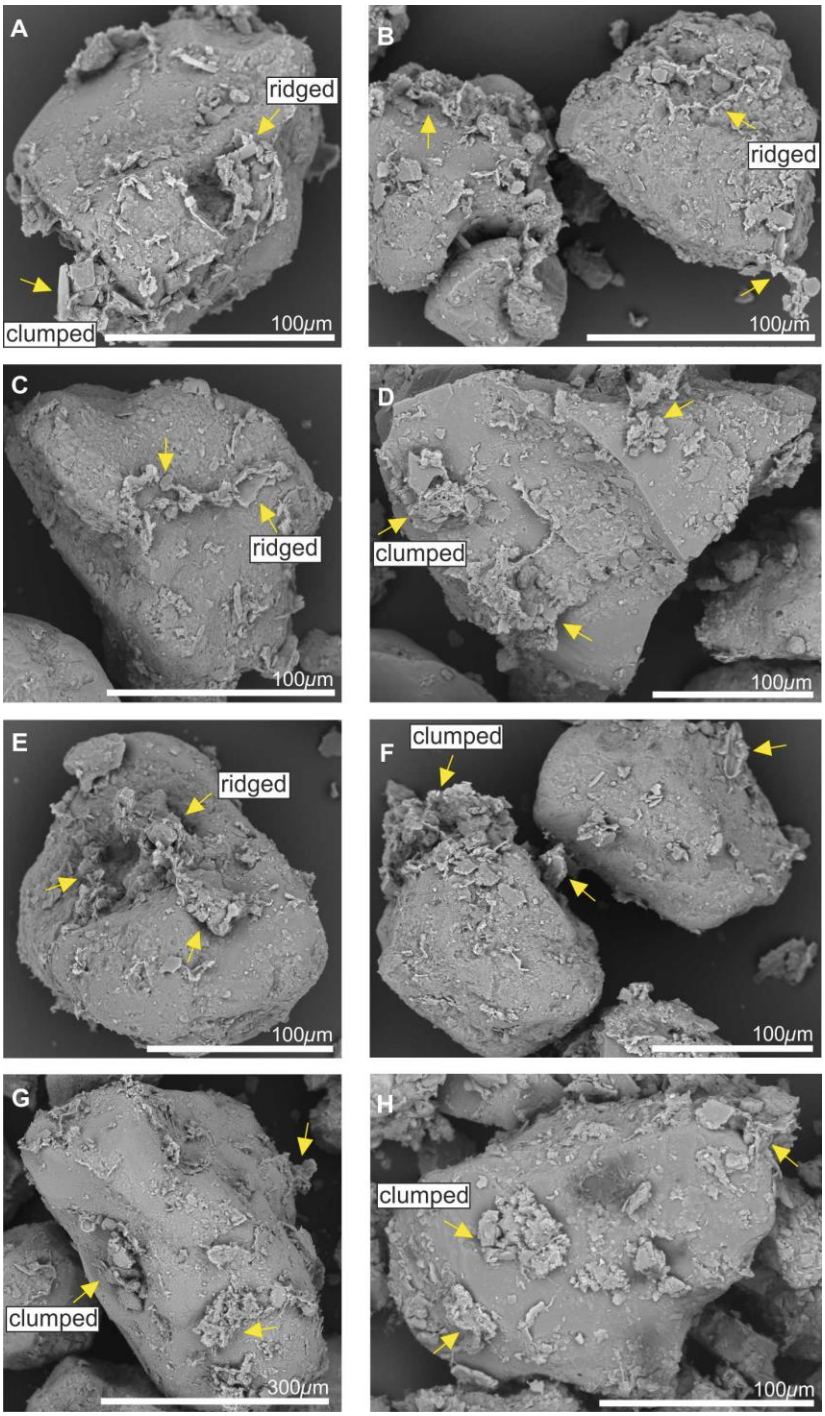

Figure 2-5 Representative SEM electron images of the textural characteristics of surface clay-coated sand-grains. Arrows indicate regions of clay-coat coverage. Note the extent of the ridged clay-coat morphologies composed of interlocking and aligned clay particles A, B, C, and E. The clumped clay-coat aggregates composed of clay minerals, lithics, and organics are illustrated in A, D, G, and F. The textural clay-coat characteristic of extending pore-ward from the sand-grain are observed in A, C, and F and with greatest accumulation (thickness) observed in grain indentations E and G.

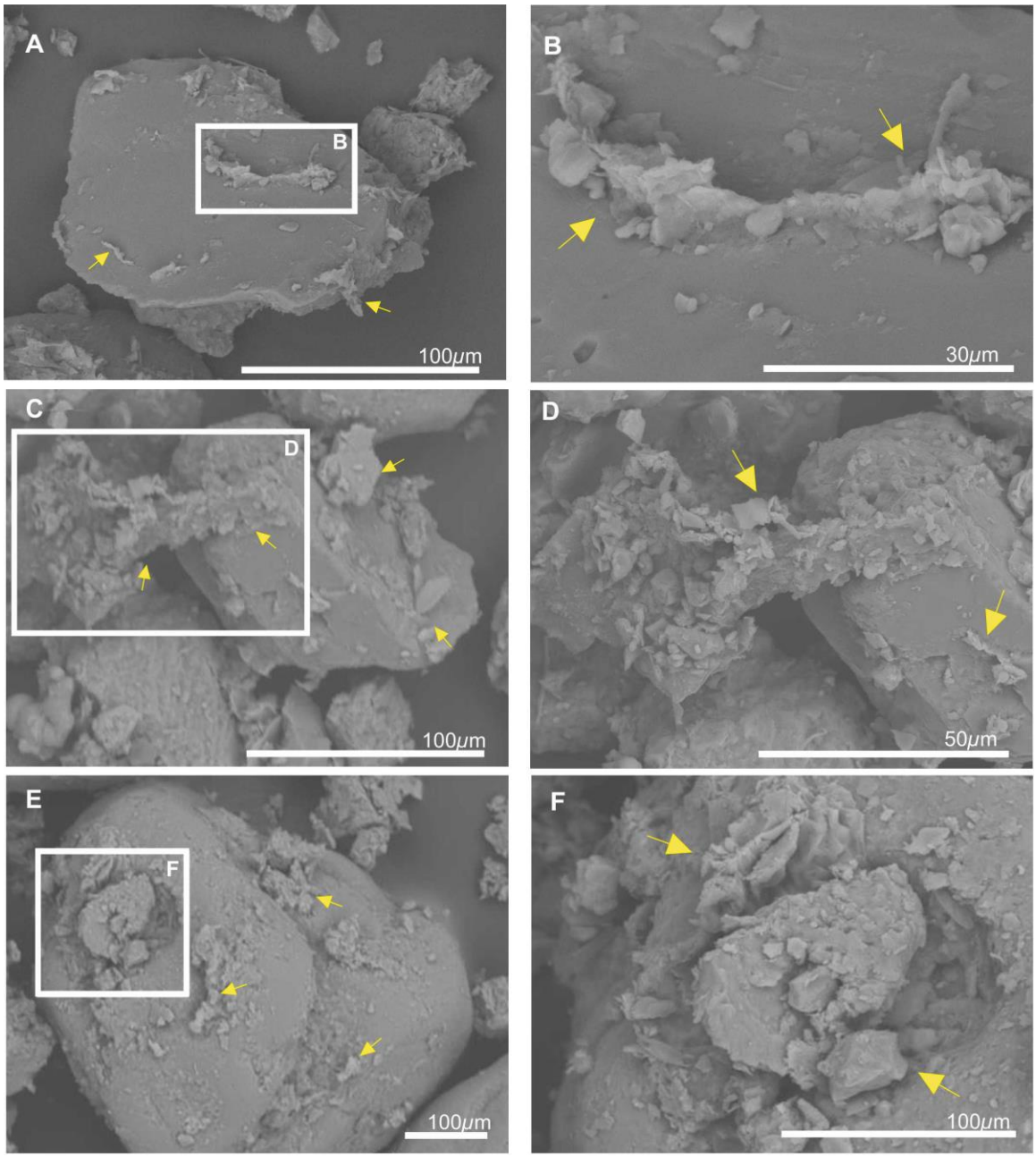

Figure 2-6 Clay-coat textures showing the main morphological feature classification observed in surface sediment samples. (A) Ridged clay coat. (B) Bridged clay-coat structure. (C) Clumped clay coat. Note greatest thickness of attached coating in the grain indentation enlarged in F. Arrows indicate regions of clay-coat coverage.

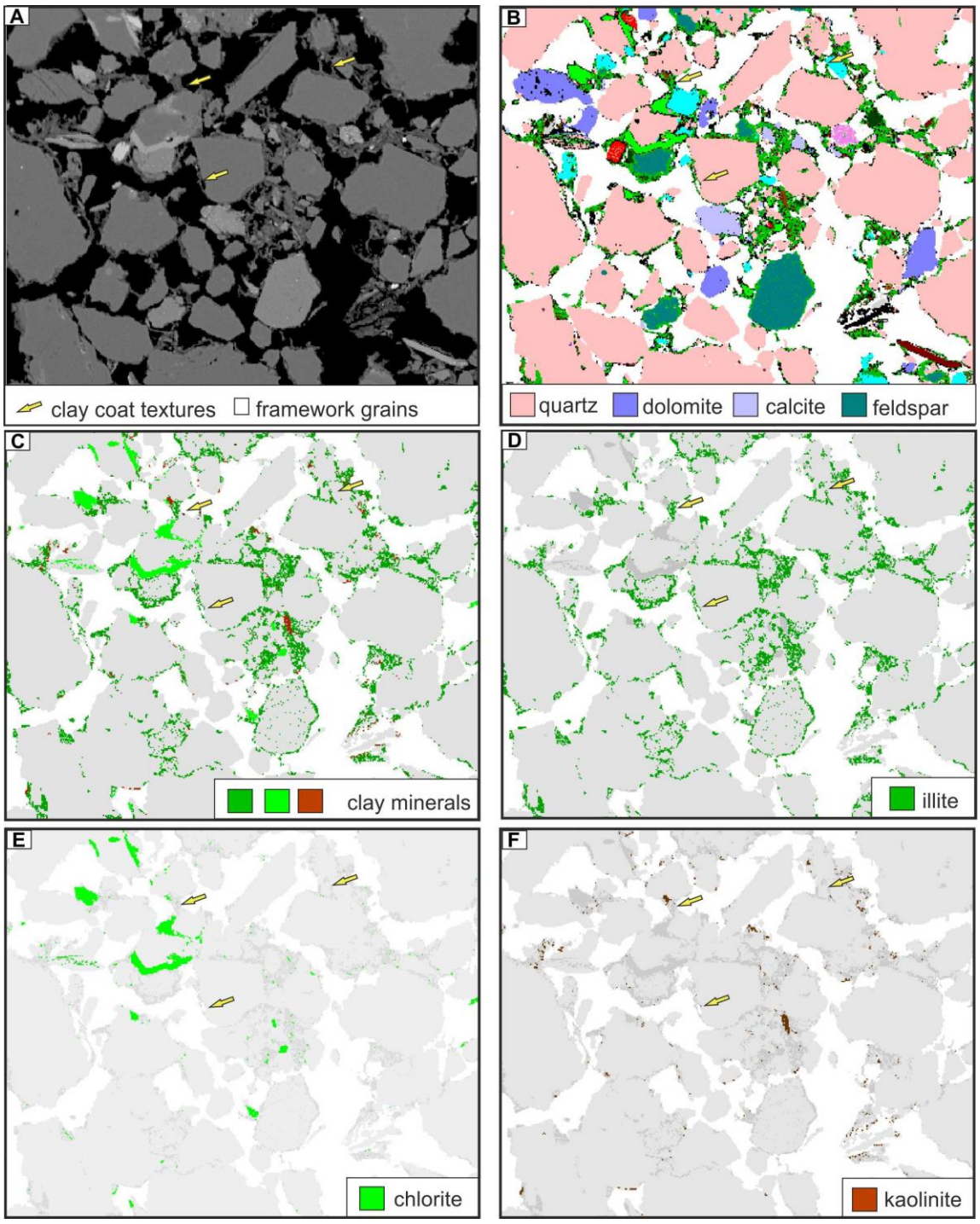

Figure 2-7 Scanning electron microscope energy dispersive spectrometry (SEM-EDS) image, showing clay coat and bulk sediment mineralogy in muddy sand-flat sediment (for location, see Fig. 2.1). (A) Backscattered electron image. (B) SEM-EDS image of framework grain mineralogy. (C) SEM-EDS image of the component clay-fraction mineralogy. (D-F) SEM-EDS images of the distribution of illite, chlorite, and kaolinite. Arrows indicate regions of attached clay coating.

2.5.4. Spatial distribution of detrital-clay-coated grains

There is a high degree of variability in the distribution of detrital-clay-coated grains, although most outer-estuary sediment exhibits no more than minor attached clay coats (Fig. 2.8). The proportion of detrital-clay-coated grains in the estuary tends to increase with distance from the open ocean and with distance from the main ebb channel. Clay coats are most extensive in the upper reaches of the three estuary channels. There is a strongly heterogeneous distribution of clay-coat classes in the southern Esk estuary arm, while the northern Irt and central Mite estuary arms show more homogeneous distributions. In the central and seaward portions of the estuary, clay coats tend to be either absent or present in trace amounts (classes 1 and 2).

The surface sediment samples have here been plotted against depositional environment, with the aim of allowing clay-coat data from modern sediments to be compared to ancient, deeply-buried sediments (Fig. 2.9). Detrital-clay-coated grains are present in the fluvial-channel sediments, ranging from absent (class 1) to extensive (class 4) depending upon the position of the sample relative to the channel axis. Grains from inner-meander and point-bar samples typically have better developed clay coats representative of classes 3 and 4. Grains from fluvial overbank samples tend to have the best developed detrital-clay coats on grains (classes 3 to 5).

Inner-estuary tidal depositional environments have a heterogeneous coverage pattern of detrital-clay coated grains. Clay coats are more extensively developed on detrital grains in vegetated, as opposed to non-vegetated, tidal bars (Fig. 2.9). Tidal flats (sand-flat, muddy sand-flat, sandy mud-flat) are the only inner-estuary depositional environment in which the full spectrum of clay-coat-grain coverage has been observed (classes 1 to 5). Samples that contain > 10 % clay fraction correspond to muddy sand-flats. All grains in all samples from muddy sand flats contain some degree of clay coating. Samples from sandy mud-flat (with > 30 % clay

fraction) contain extensive (classes 4 and 5) detrital-clay-coat-grain coverage. Saltmarsh sediment assemblages have uniformly well-developed detrital-clay coats (class 5). The observed variability in detrital-clay-coat characteristics in tidal environments correlates to grain size; the more extensively developed detrital-clay coats (classes 4 and 5) occur in sediment dominated by very fine-sand-grain size (e.g., compare Fig. 2.8 with Fig 2.3A).

The samples from foreshore, ebb-delta, tidal-inlet, and aeolian-dune depositional environments largely do not contain detrital-clay-coated grains. Most samples from the vegetated, dune-topped spits, and sheltered region in the tidal inlet contained no clay-coat coverage (class 1), and the remainder had minor clay-coat coverage (class 2) (Fig. 2.9).

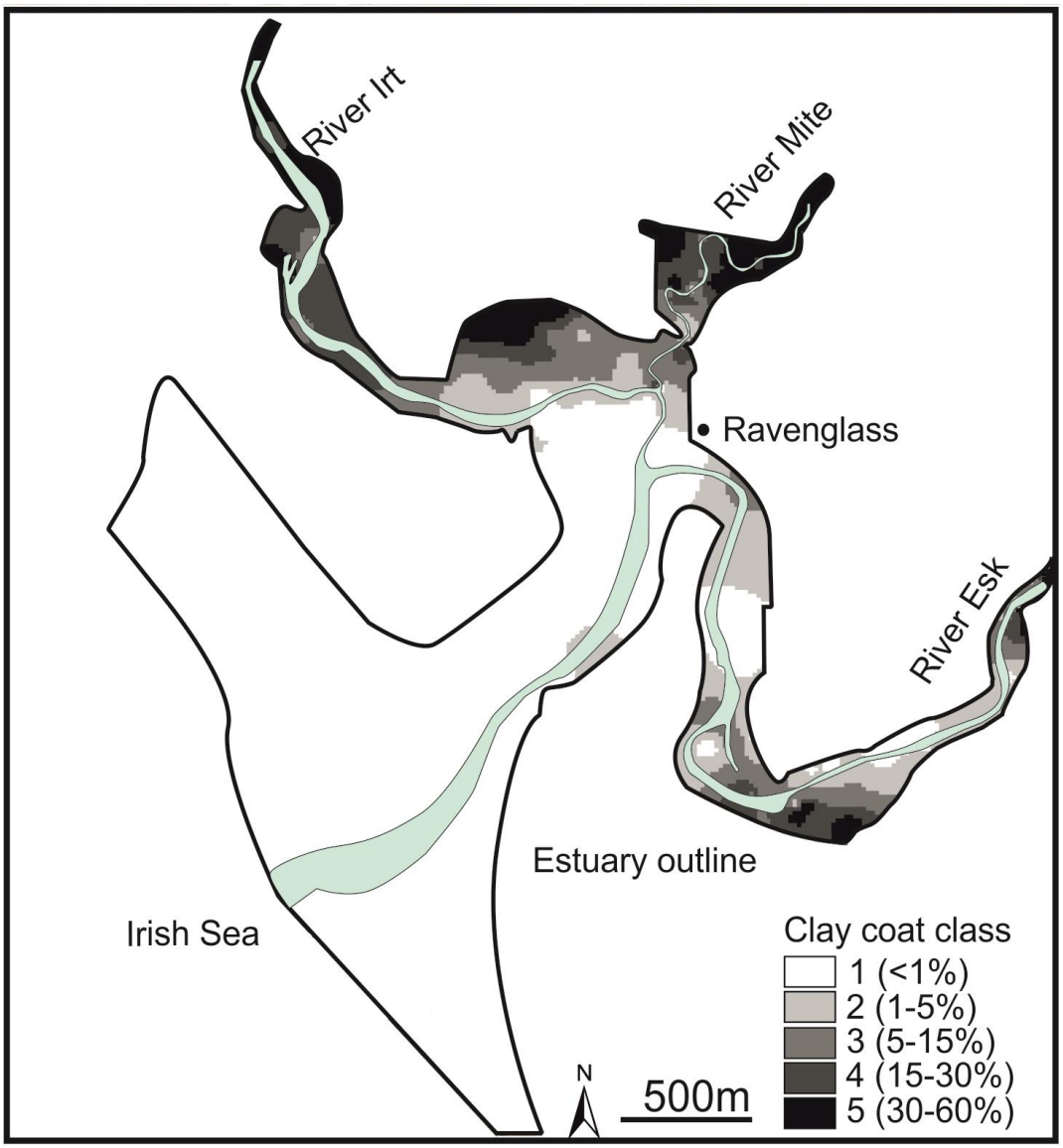

Figure 2-8 Distribution map of surface clay-coated sand-grains in the Ravenglass Estuary (n = 195). The surface distribution of areas in light grey signify at least partial clay-coat coverage, with dark grey to black regions indicating extensive surface clay-coated sand-grains.

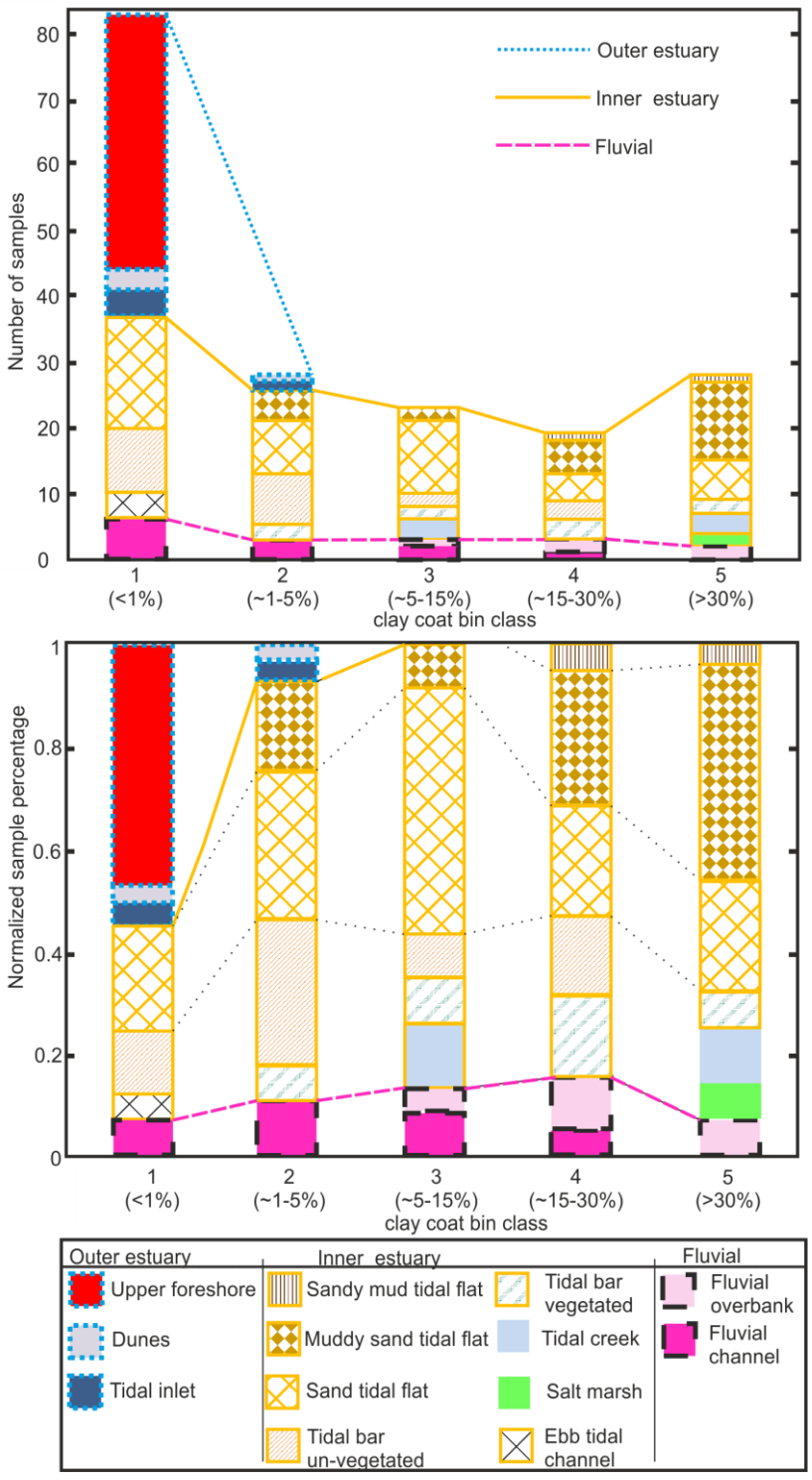

Figure 2-9 Frequency histograms for all sediment samples, divided by depositional-environment and clay-coat bin class. (A) Total number of samples in each clay coat class. (B) Normalized data to reveal relative importance of various environments for optimum clay-coat coverage. Clay-coat classes 1 and 2 have minimal to complete absence of clay coats.

2.5.5. Detrital-clay-coated grains: grain size, clay fraction, and bioturbation

Bin class intervals were plotted against average grain size, percentage clay fraction, and lugworm density (Fig. 2.10). This confirms that there is increasing percentage clay fraction with decreasing grain size. This also shows that increasing the percentage of the clay fraction correlates with increasing clay-coat coverage (class number). Thus, clay-coat class 3 (every grain exhibiting at least 5-15 % attached clay coats) corresponds to sediment with a 2.5 % clay fraction, while clay coat class 5 (extensive, > 30 %, clay coats observed on every grain) corresponds to sediment with 10 % clay fraction (Fig. 2.10). The coverage of clay coats does not seem to simply relate to lugworm density, with the two highest clay-coat classes found in association with low lugworm densities (Fig. 2.10).

Detrital-clay coats vary systematically in a given depositional environment (Fig. 2.9). Extensive detrital-clay-coated grains are observed in the inner-estuary tidal depositional environments, and they increase in extent towards the upper tidal limit (Figs. 2.8 and 2.9). Variations in grain size and clay fraction are secondary controls, with a lower fine-sand-grain size and > 5 % clay fraction required to form uniform-extensive detrital-clay coats upon grains (classes 3 to 5). There are negligible attached clay coats (classes 1 and 2) observed in the high-energy (upper fine to lower medium grain size), clean (< 2 % clay fraction) sand assemblages of the outer sand tidal-flat, foreshore, ebb-delta, and aeolian-dune environments.

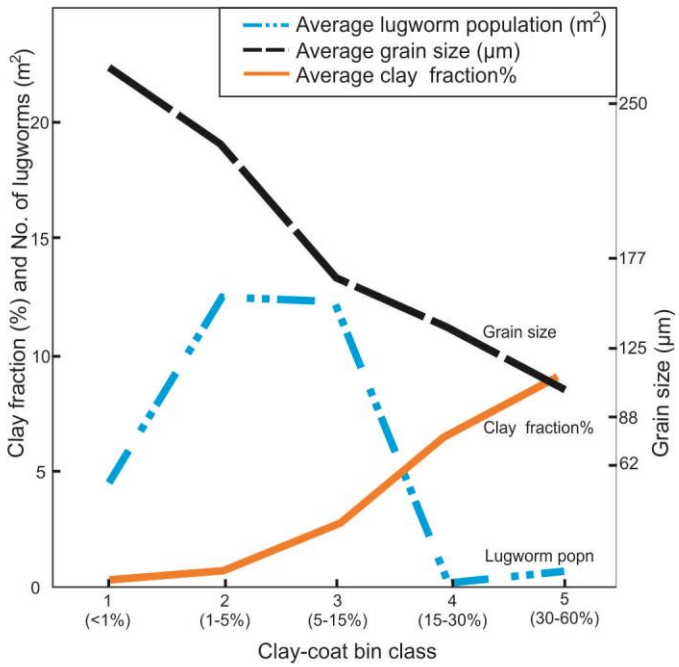

Figure 2-10 Average grain size, lugworm population, and clay-fraction percentage plots for each representative clay-coat bin class.

2.6. Discussion

2.6.1. Origin of detrital-clay-coat textures

The internal fabric and outer morphology of clay coats in deeply-buried reservoirs have been described in a few studies. Clay coats tend to be composed of an inner, densely packed, tangentially oriented, root layer that tends to be overlain by an outer coat composed of perpendicular euhedral flakes that grow into open pore spaces (Ajdukiewicz and Larese 2012; Wise et al. 2001). It has been proposed that the inner layers are the result of thermally driven recrystallization of precursor detrital-clay coats (Aagaard et al. 2000; Billault et al. 2003). The clay coats from the Ravenglass Estuary, described here, are therefore analogues for the inner layer of clay coats reported from deeply-buried reservoirs.

The observed ridged and bridged textures in this study (Figs. 2.6A, B, 2.7) have been reported previously in a range of case studies (Dowey 2013; Houseknecht and Ross Jr 1992; Matlack et al. 1989; Moraes and De Ros 1992; Wilson 1992) and in synthesis experiments (Matlack et al. 1989). Ridged detrital-clay-coat textures have been interpreted to derive from infiltration processes (Wilson 1992); bridge structures have been reported to form where ridges join two adjacent grains; bridged structures develop distinct ridged texture when the sediment is disaggregated (Matlack et al. 1989). The sediment from the Ravenglass Estuary exhibits many of the textural characteristics that have been reported to result from clay infiltration into sand-dominated sediment (Wilson 1992). Infiltrated ridged detrital-clay-coat textures have been reported in the Brazos River and Galveston marginal marine system, Texas (Matlack et al. 1989), as well as in the Anllóns Estuary, Spain, and Leirárvogur Estuary, Iceland (Dowey 2013).

Infiltration occurs when water that contains suspended clay and silt flows into partially water-saturated sandy sediment. In estuarine settings, infiltration is driven by a hydraulic gradient produced by the effect of the tidal range. This gradient drives suspended clay through the sediment at falling tide, towards the low-tide main ebb channel or during times of flooding due to increased rainfall in the hinterland (Santos et al. 2012). Reduction of flow velocity results in the deposition of the suspended clay and silt particles onto the sand-grains (Dowey 2013; Worden and Morad 2003).

Clumped clay coat textures that are comparable to those illustrated in this study (Fig. 2.6C) have been reported in the sediment of the Mandovi Estuary, India (Kessarkar et al. 2010), with similar clump sizes and textures. The subtropical Mandovi Estuary clay coats are composed of clay particles, bioclasts, and organics that produce a heterogeneous mineralogy that is reported to be fluvially derived from weathering products in the hinterland (Kessarkar et al. 2010). Clumped-clay accumulations have also been reported in the fluvial to estuarine

Rappahannock River, Virginia (Pierce and Nichols 1986). In both the Rappahannock and the Mandovi examples, clumped textures were interpreted to originate from the deposition of biogenic (fecal) pellets and flocculated estuarine aggregates (Crone 1975) under conditions of stagnant pore water in the estuary.

A comparison of clay-coat textures found in the Ravenglass Estuary with other modern analogues, as well as experiment-based results, suggests that clay coats derive from a combination of infiltration, resulting in the ridged-bridge textures, and flocculation with the deposition of biogenic fecal pellets resulting in clumped textures.

2.6.2. Origin of detrital-clay-coat mineralogy: internal or external to the estuary?

The illite-dominated, mixed mineralogy of the clay-coated sand-grains, determined by spatially resolved SEM-EDS (Fig. 2.7), is consistent with the clay-fraction mineralogy identified by XRD (Fig. 2.4). Had the clay coats formed in the hinterland, a much more varied clay-coat mineralogy would be expected than revealed by micro-studies using SEM-EDS (Fig. 2.7) and bulk studies using XRD (Fig. 2.4). Therefore, the observation that the clay-coat mineralogy reflects the bulk clay mineralogy of the estuary implies that the clay-coats were formed in the estuary itself rather than in the hinterland.

2.6.3. Distribution and origin of detrital-clay coats

It has been reported that the primary depositional environment of a clastic sediment exerts a strong control on subsequent diagenetic processes, via the sediment texture, primary mineralogy, organic content, and aqueous chemistry (Ehrenberg 1997; Morad et al. 2010; Worden and Morad 2003). The concept of a depositional control on the occurrence, type, and subsequent diagenetic evolution of detrital-clay coats is reasonably well established (Bloch et

al. 2002; Dowey et al. 2012; Ehrenberg 1993; Luo et al. 2009; Matlack et al. 1989). The results of this study confirm a depositional-environment control but reveal, for the first time, systematic variability of the extent and completeness of clay-coat coverage on a scale of marginal marine depositional sub-environments.

2.6.4. Comparison of clay coats in Ravenglass to modern estuary studies

In the Ravenglass marginal-shallow marine system, the most extensive detrital-clay-coated grains are confined to the inner-estuary tidal-flat, tidal-bar, saltmarsh, and fluvial point-bar depositional environments. In contrast, detrital-clay-coated grains are effectively absent in the coarse, clean sand that is associated with outer tidal-flats, foreshore, dune topped spits, fluvial channel axis, and main ebb channels. The distributions that are illustrated in Figures 2.8 to 2.10 have similarities to the distribution of detrital-clay-coated grains along the Texas Gulf Coast, Galveston, and in the Brazos River (Matlack et al. 1989). The Texas study reported clay-coated grains from fluvial point bars, but an absence of detrital-clay-coated grains in beach, delta-beach, flood-tidal-delta, and delta-plain surface sediments. Studies of the Anllóns Estuary, Spain, and Leirárvogur Estuary, Iceland, undertaken by Dowey (2013) support the observed distribution in this study, with detrital-clay-coated grains being best developed in the less marine-influenced, middle and upper estuary reaches related to muddy tidal-flats.

2.6.5. Comparison of Ravenglass clay coats to ancient, deeply-buried clastic sediment

Reservoir studies, based on cored wells and interpretation of primary depositional environments, tend to be hampered by a lack of high-resolution facies interpretation and relatively poor definition of the spatial and stratigraphic distribution of clay-coated grains. To date, there is no published subsurface reservoir dataset that compares to the high spatial

resolution and the complete certainty of the depositional environment used in this modern-analogue study.

Although morphologically dissimilar, occurring as discontinuous clumps and ridges, broad textural and mineralogical similarities are identifiable between the precursor detrital-clay coats of this study and clay coats in diagenetically altered reservoirs. Mixed mineralogy has been reported in several reservoirs, for example the Lower Cretaceous Mississauga Formation (Gould et al. 2010) and the Jurassic Garn formation (Storvoll et al. 2002), in which the inner (tangential) diagenetic clay coats consist of a mixed illite-chlorite mineralogy that is broadly similar to the mixed mineralogy of the detrital-clay coats in Ravenglass (Fig. 2.7).

In the Upper Carboniferous submarine-fan and marine slope facies of the Arkoma Formation, USA, it has been reported that muddy clay-coated-grain facies offer the best reservoir-quality prospects compared to the well-sorted, clean sandstones (with little or no dispersed clays) (Houseknecht and Ross Jr 1992). In the Arkoma Formation, amalgamated sandstone units contain beds with clay-coated grains and no quartz overgrowth and adjacent clean sandstone beds that are devoid of clay-coated grains but with pervasively quartz overgrowth, and therefore have negligible remaining porosity (Houseknecht and Ross Jr 1992). Although the environment of deposition is different, the Arkoma example illustrates that a small quantity of clay that is co-deposited with sand can lead to improved reservoir quality.

2.7. Controls on the formation and distribution of detrital-clay coats

This study has produced a high-resolution, modern-analogue data set and established the distribution patterns of detrital-clay coats relative to surface sedimentary and biological facies. Percentage clay fraction, grain size, and bioturbation have all been advocated as controls on the origin of clay-coated grains in ancient, deeply-buried sandstones.

2.7.1. Role of grain size

From this study, the observed inverse relationship of increasing coverage of detrital-clay coats with decreasing grain size (Fig. 2.10) is consistent with previous observations by Wilson (1992) that clay coats are more extensively developed in finer-grained sandstones in Holocene aeolian dune, and marine-shelf settings. The Permian-Carboniferous Unayzah sandstones, Saudi Arabia, also have a reported relationship between mean grain size and the average percentage coverage of grains, with fine to very fine sandstone exhibiting the greatest degree of clay-coat coverage (Shammari et al. 2010).

2.7.2. Role of percentage-clay-fraction control

The role of percentage clay fraction (< 2 μm) in the formation and distribution of detrital-clay-coated grains is not well established in the literature. However, the Anllóns Estuary, Spain, has a clay-fraction percentage that increases in marginal areas towards the upper tidal limit (Dowey 2013), consistent with the present study. The Anllóns example identified a trend comparable with Ravenglass of increasing clay-coat coverage with increasing co-deposited clay-fraction percentage (Dowey 2013). Furthermore, in the Texas Gulf Coast at Galveston and in the Brazos River, virtually no clay-coated grains occur in environments that are characterized by low suspended-sediment concentrations (assumed here to be proportional to the percentage clay fraction) (Matlack et al. 1989).

2.7.3. Bioturbation control

Sediment bioturbation (specifically ingestion and excretion) has been experimentally shown to lead to the creation of clay coats on detrital sand-grains (McIlroy et al. 2003; Needham et al. 2006; Needham et al. 2004; Needham et al. 2005). This mechanism works through the

production of a mucus membrane on sand-grains, which then adheres finer clay to silt-size sediment onto the sand-grains.

In the present study, the distribution of clay-coated grains does not spatially correlate with the degree of bioturbation observed in the estuary (compare Figs. 2.3, 2.8, and see Fig. 2.10). It is also notable that a similar conclusion can be drawn from the Lower Cretaceous Missisauga Formation, Scotian Basin, where the coverage of clay-coated grains does not positively correlate with the degree of bioturbation (Gould et al. 2010). The lack of correlation between bioturbation and the degree of clay-coated grains in this study may result from the limited environmental grain-size niche of the utilized lugworm biogenic proxy. To address this, a focused study on the abundance distribution of estuarine macro- and micro-organisms would be required.

2.8. Implications for hydrocarbon exploration

2.8.1. Target reservoir-quality prospects

At depths > 3 km (temperatures > 90 °C) pervasive authigenic quartz typically starts to become a dominant cement in sandstones (Bloch et al. 2002). Such sandstones risk becoming extensively quartz cemented if grain coats are absent, or poorly developed, on grain surfaces (Ajdukiewicz and Larese 2012).

Based on the surface distribution patterns of detrital-clay coats presented here (Figs. 2.8, 2.9, 2.10), the best prospects for anomalously high reservoir quality due to the presence of clay-coated grains in deeply-buried sandstones (> 3 km) should be sought in the fine-sand-size sediment which also contains approximately 5 % clay-fraction percentage (i.e. groups 4-5, Fig. 2.10). Specifically targeting clay-bearing sandstones in the hunt for elevated porosity is against

common convention, which would typically target the cleanest, most clay-free sandstones. Our interpreted optimum value of approximately 5 % clay fraction (on the assumption that clay fraction occurs predominantly as clay coatings) is based upon the likelihood of producing extensive clay coats in sandstones. However, the presence of highly elevated clay content would of course produce a detrimental effect on permeability and porosity (see next section). Sites with fine-sand-size sediment that also contain approximately 5 % clay fraction correspond to inner-estuary tidal-bar, tidal-flat and, fluvial-point-bar facies in the Ravenglass system. In contrast, coarse, clean sand from tidal-channel, outer-sand-flat, and foreshore facies would, upon deep burial, potentially experience pervasive quartz cementation due to the lack of inhibiting detrital-clay-coated grains if the sediment reached temperatures sufficient for quartz cementation.

2.8.2. Goldilocks zone of optimum detrital-clay-coat coverage

The high-resolution, marginal to shallow marine model for the distribution of detrital-clay-coated grains presented in this study can be used, by analogy, to help in the prediction of clay-coated sandstones in the deep subsurface. Too much clay is highly detrimental to sandstone reservoir quality (Armitage et al. 2016; Houseknecht and Ross Jr 1992; Worden and Morad 2003) since abundant clay minerals fill pores and block pore throats between sand-grains. The quantity of clay in a sandstone that is sufficient to coat grains (and thus inhibit quartz cement) but not enough to block pore throats, surprisingly, remains poorly resolved, and is addressed below.

Bloch et al. (2002) noted that a minor amount of clay (as little as 1 to 2 % of the rock volume) can coat a relatively large surface area of sandstone grains, but the optimum amount for specific clay minerals has not been precisely defined. Here examples from previous studies

were used to help constrain broad percentages of total clay quantities as clay coats that can lead to the development of diagenetic coats which can successfully inhibit quartz cement. Pittman et al. (1992) suggested an optimum range of 5 to 13 % sediment volume of clays occurring as chlorite grain coats for the Tuscaloosa Formation and 4 to 7 % for the Berea Sandstone. Heald and Baker (1977) reported an optimum range of 3.5 to 6.5 % volume of illite clay coats for reservoir quality in the Rose Run sandstone.

It is thus possible to tentatively propose (from the observed association of clay fraction occurring predominantly as clay coatings) lower and upper threshold values of 3.5 and 13.0 % total volume of clay minerals (chlorite, illite, and mixed) as the optimum range for the eventual development of clay coats that can form continuous barriers that prevent quartz cementation and so preserve reservoir quality. Using the 3.5 to 13.0 % range of total volume of clays, it was possible to map out regions in the Ravenglass Estuary that would lead to the best reservoir quality, were this sedimentary system to be deeply-buried (Fig. 2.11). These optimum regions, termed “Goldilocks zones”, encompass the central tidal-flat region, non-vegetated, and upper-estuary tidal-bar depositional environments.

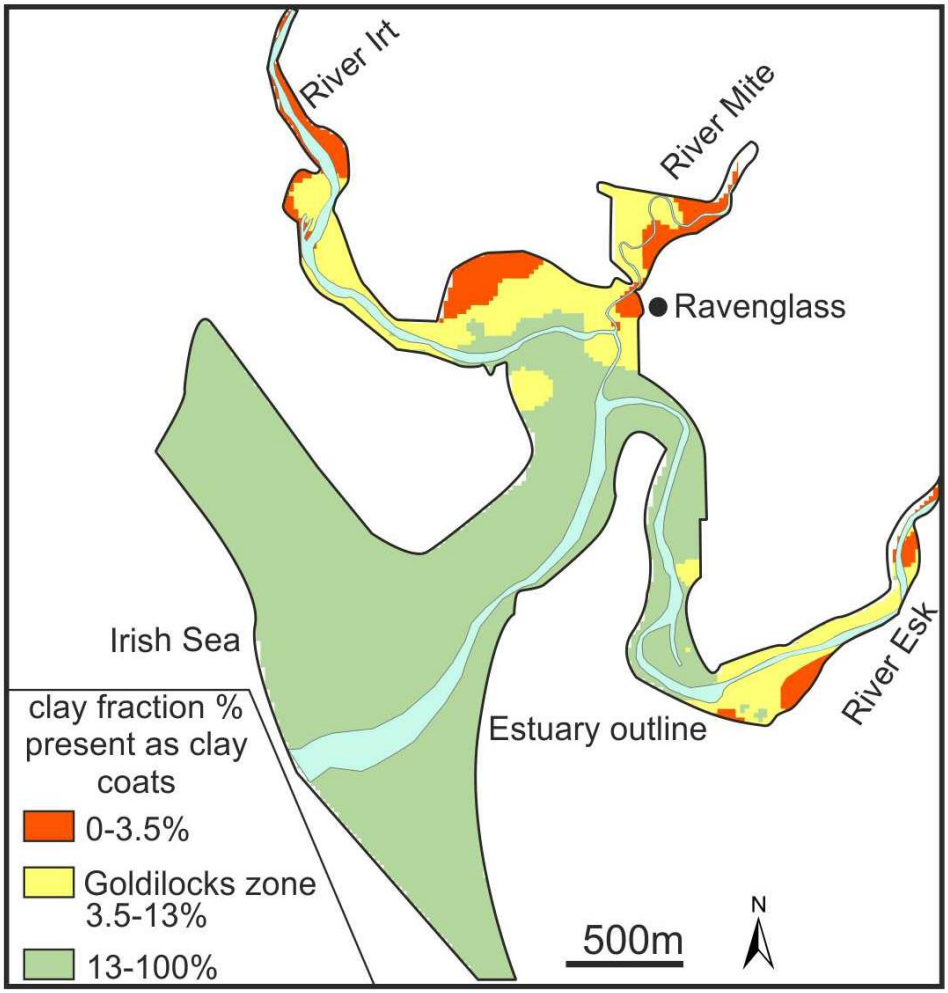

Figure 2-11 Distribution map indicating the literature-constrained Goldilocks zone of the optimum reservoir quantity, based on the total clay content present as clay coats (i.e., detrital-clay-coated sand-grains inhibiting quartz cement but not blocking pore throats).

2.9. Conclusions

1. The work presented here, from the Ravenglass Estuary, UK, is the first high-resolution study of the distribution of detrital-clay-coated grains in a modern marginal to shallow marine setting.
2. Sedimentary environment is the main control on the absolute quantity of clay mineral coverage of detrital-clay-coated sand-grains in these sand-dominated sediments.
3. Detrital-clay coats in recent sediments have discontinuous ridged, bridged, and clumped textures. The coats on sand-grains are formed of individual interlocking clay minerals with silt-size lithic and bioclastic accessory components and were probably derived from a combination of infiltration (of clay-bearing water into sand-dominated sediment), flocculation, and biogenic processes. Clay coats range from being absent to covering > 30 % of sand-grain surfaces.
4. The observation that the illite, chlorite, and kaolinite clay-coat mineralogy reflects the bulk clay mineralogy of the estuary implies that the clay coats were formed *in situ* in the estuary rather than in the hinterland.
5. The distribution of detrital-clay-coated grains is principally a function of sediment grain size and clay-fraction percentage. In the Ravenglass case study, a sediment assemblage composed of fine-grained sand containing > 5 % clay fraction percentage is necessary for the development of uniformly well-developed clay coats on detrital grains.
6. The best prospects for anomalously high reservoir quality in deeply-buried marginal marine sandstones (i.e., with inhibited growth of quartz cement) should most likely be sought in clay-rich inner-estuary tidal facies.

3. Biofilm origin of clay-coated sand-grains

3.1. Abstract

The presence of clay sized particles and clay minerals in modern sands and ancient sandstones has long presented an interesting problem, because primary depositional processes tend to lead to physical separation of fine- and coarse-grained materials. Numerous processes have been invoked to explain the common presence of clay minerals in sandstones, including infiltration, the codeposition of flocculated muds, and bioturbation-induced sediment mixing. How and why clay minerals form as grain coats at the site of deposition remains uncertain, despite clay-coated sand-grains being of paramount importance for subsequent diagenetic sandstone properties. This study has identified a new biofilm mechanism that explains clay material attachment to sand-grain surfaces and that leads to the production of detrital-clay-coats. This study focuses on a modern estuary using a combination of fieldwork, scanning electron microscopy, biomarker analysis, and Raman spectroscopy to provide evidence of the pivotal role that biofilms play in the formation of clay-coated sand-grains. This study shows that within modern marginal marine systems, clay-coats primarily result from adhesive biofilms. This bio-mineral interaction potentially revolutionizes the understanding of clay-coated sand-grains and offers a first step to enhanced reservoir quality prediction in ancient and deeply-buried sandstones.

3.2. Introduction

Bio-sediment interactions (microbially induced sedimentary structures) have been recognized in rocks from almost all geological time periods (Noffke et al. 2006). Biofilms have been shown to play a fundamental role in sediment dynamics and the subsequent diagenesis of marginal marine sedimentary systems (Stal 2003), affecting grain-size heterogeneity (Garwood et al. 2015), sediment stability (Vignaga et al. 2013), sediment transport and bedform stability (Malarkey et al. 2015; Schindler et al. 2015). Intertidal biofilms typically result from the secretion of extracellular polymeric substances (EPS) (adhesive mucilage) by microphytobenthic (MPB) communities that are composed of algae (diatoms, euglenids, crysophyceans, dinoflagelates), cyanobacteria, and other photosynthetic bacteria (Jesus et al. 2009). This study focused primarily on the role of silicate phototrophic epipelic (motile) diatoms, which represent the dominant micro-organism within intertidal sediments of western Europe (Stal, 2003; Underwood and Paterson, 1993).

EPS (colloquially known as bio-glue and mucilage) is produced, within intertidal siliciclastic estuarine settings, by epipelic diatoms for a variety of functions (Agogué et al. 2014; Decho 1990; Higgins et al. 2003). One function of EPS is to facilitate the vertical movement of diatoms, which colonize the sediment in response to tidal and daylight cycles, for photosynthetic purposes and to maintain optimum environmental conditions (Hoagland et al. 1993; Stal 2003). Excreted EPS strands allow diatom movement in near-surface sediment, but they also anchor diatoms to sand-grain surfaces. The strands detach from the diatom on movement and remain on mineral grain surfaces; this produces a web of bridging and coating mucus (biofilm) strands on grain mineral surfaces (Garwood et al. 2015; Higgins et al. 2003).

Biofilms in intertidal sediments have been reported to result in an adhesive coat on sand-grains that acts as a binding agent capable of forming aggregates of diatoms, organics, and clay

minerals (Kessarkar et al. 2010) and that is also responsible for fine particle entrapment in sand-dominated estuarine tidal-flats (Garwood et al. 2015). In the presence of common divalent cations, such as Mg^{2+} and Ca^{2+}, that are present in estuarine waters, EPS biofilm fractions become water insoluble, tightly bound to sand-grain surfaces and resistant to degradation increasing with depth in the top few millimeters of the sediment column (De Winder et al. 1999; Stal 2003).

The goal of this study was to establish the mechanism by which clay-grade particles overcome hydrodynamic segregation and are physically bound in a sand-rich deposit. Specifically the study sought to determine how clay minerals adhere to sand-grain surfaces. Our main hypotheses were that biofilms control the formation of clay grain coats, and that the amount of biofilm present directly affects the degree to which sand-grains are coated with clay minerals.

3.3. Data sets and methods

Surface sediment samples were collected from the Ravenglass Estuary in northwest England (Wooldridge et al. 2017b). This estuary is a modern analogue that is equivalent to the environment of deposition for an estimated 54 % of all chlorite clay-coated sandstones (Dowey et al. 2012).

Textural and chemical classification included a range of scanning electron microscopy (SEM), environmental scanning electron microscopy (ESEM) and Raman spectroscopy on a suite of 112 polished thin sections; 112 dried, loose sediment, grain mounts; and 5 un-dried (hydrated) sediment samples. The samples were analyzed for biofilm abundance using the established biomarker proxy chlorophyll-a (Stal 2003; Underwood and Paterson 1993), as well as clay-coat

textural characterization, clay-coat chemical analysis, and percentage of clay coat grain coverage.

Grain clay-coat coverage was quantified using polished thin sections of grain mounts. The method used involved point counting 50 sand-grains per sample and measuring the total perimeter of each sand-grain and the length that is covered by attached clay-coats using Petrog statistical software (Pantopoulos and Zelilidis 2012). Repeat analyses of the same sample indicated an average ±1.7 % error for mean clay-coat coverage quantification.

Ninety seven surface sediment samples were collected on the 19 and 20 May 2016, within 4 hours of low tide. The material was collected within sterilized foil, stored on ice during collection, placed in a freezer at -18 °C for transport, and then -80 °C within four hours. Standards and samples were handled in subdued light during analysis. Chlorophyll-a samples and calibration standards were prepared in 90 % acetone. Sediment samples (200 mg) were weighed and 2 mL of 90 % acetone added and mixed. Method blanks (no sediment) were treated in the same manner as the samples. The extracts were transferred and filtered through a 0.4 µm Phenex RC membrane. A Trilogy fluorometer (model 7200–000) measured the fluorescence of the 90 % acetone, blanks, standards and samples. A standard curve was generated to calculate chlorophyll-a concentration using the formula: chlorophyll-a concentration (µg/g) = [fluorescence units/slope] × [dilution (µl)/weight extracted (g)].

3.4. Results

3.4.1. Textural and chemical characterization of clay coated sand-grains

Clay-coated sand-grains were observed to contain a network of fine fibrous filaments that link sand-grains in the modern Ravenglass marginal-marine environment (Fig. 3.1B). The filaments produce a framework that binds together fine grained detrital material, such as clay minerals,

organics, and silt-grade lithic clasts. This thin film of extraneous material was found to partially coat sand-grains, leaving other parts of sand-grains with clean, uncoated surfaces (Fig. 3.1C). The film appears to have adhesive properties, because fine-grained clay- to silt-size materials are stuck on the part of the grain covered with the film but not on the film-free parts of sand-grains. Thus the film appears to act as an adhesive, creating aggregates composed of clay- to silt-sized detritus stuck to sand-grain surfaces. It is also noteworthy that diatoms can be observed anchored to sand-grains in the vicinity of adhesive films (Fig. 3.1C). In hydrated (natural) form, clay-coats are discontinuous, tangentially-orientated clay flakes on the parts of sand-grain surfaces that are covered with the adhesive film, with no observed supporting clay matrix. Clay in the sediment is exclusively observed as discontinuous clay coatings or bridging structures (Figs. 3.1A, 3.1B, and 3.1C).

Raman spectroscopy was employed to generate a spatially resolved chemical signature of the film, specifically to determine whether the film on the sand-grain surfaces was organic. The Raman spectrum (Fig. 3.2), generated from a film on a representative clay-coated sand-grain, contains molecular bands that are fully consistent with organic-rich complex mixtures that are typical of EPS mucilage and biofilm-specific polysaccharides (Ivleva et al. 2009). Diatoms are directly anchored to sand-grain surfaces by excreted EPS (Figs. 3.1C).

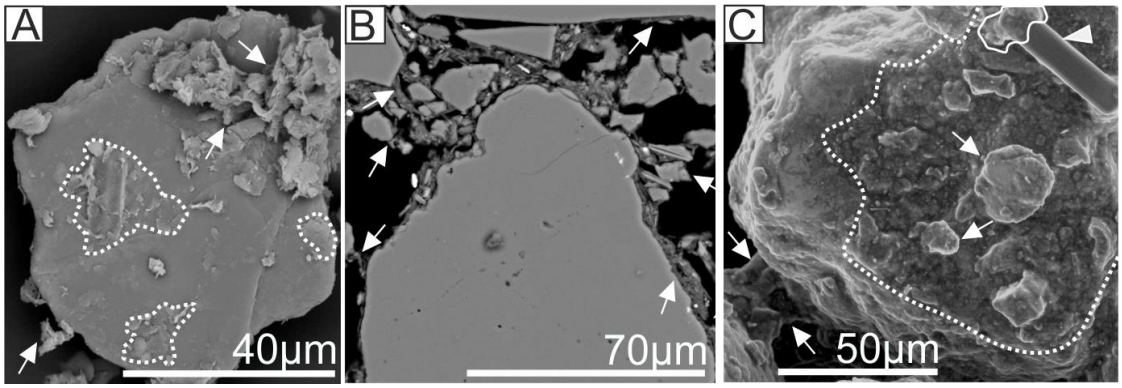

Figure 3-1 Backscattered electron and environmental scanning electron microscope (SEM) images of clay-coated grains. Arrows indicate clay coatings. Dashed lines outline the extent of the biofilm coats on the grain surface. (A) SEM image of loose sediment. (B) Thin section of clay-coated sand-grains from an intertidal estuarine setting. (C) Environmental SEM image of hydrated sediment. Triangle in top right points to a diatom with excreted extracellular polymeric substance grain attachment outlined.

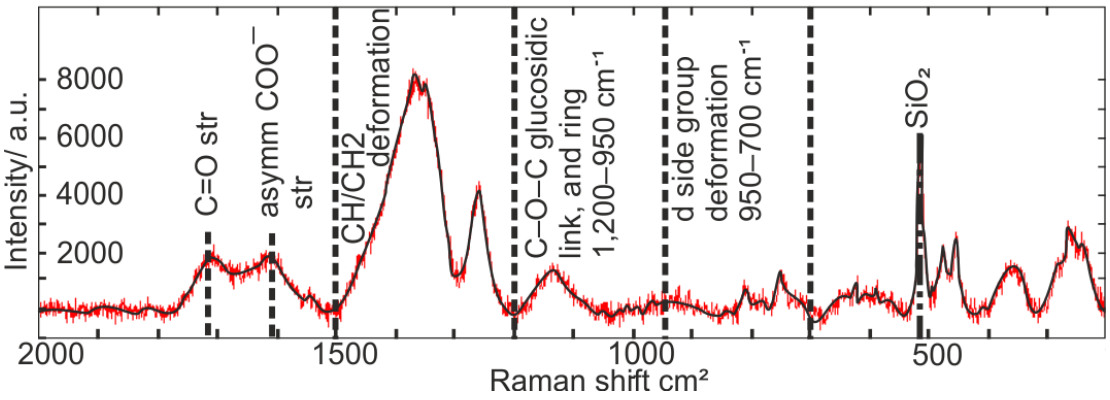

Figure 3-2 Laser Raman fingerprint of a clay-coated grain. The Raman spectrum is of the tidal-flat sediment, imaged in Figure 3.1. The chemical signature is representative of an organic-rich mixture that is typical of a biofilm (Ivleva et al. 2009). Abbreviations: asymm—asymmetrical; str—stretching.

3.4.2. Distribution of sediment clay coated grains and biofilm abundance

The degree of sand-grain clay-coat coverage ranges from 0.5 to 87 % within sediment at the surface of the Ravenglass Estuary (Fig. 3.3A). The distribution of clay-coat coverage has been mapped for the estuary using interpolation in ArcGIS (https://www.arcgis.com). This revealed a highly heterogeneous pattern (Fig. 3.3A). Clay-coat coverage in the estuarine sediment increases in a landward direction, and is most extensive within the mid- to upper estuary, in deposits representing tidal-flat and tidal-bar depositional environments (Wooldridge et al. 2017b).

Chlorophyll-a concentration in the estuarine sediment varies from 0.4 to 45 μg/g. Chlorophyll-a concentration has been shown to be a proxy for diatom-produced biofilm abundance within sediments (Stal 2003), indicating that biofilms are not homogeneously distributed across the estuary. The study used ArcGIS to map chlorophyll-a abundance within the estuary, thus revealing the heterogeneous distribution of biofilms by proxy (Fig. 3.3B). Chlorophyll-a increases in concentration in a landward direction, and is most extensive within the mid- to upper estuarine tidal-flats. The chlorophyll-a distribution is supported by other, significantly less detailed, studies of tidal flats (Stal 2003; Underwood and Paterson 1993).

A Pearson's correlation coefficient was used to test the statistical significance between chlorophyll-a (biofilm) abundance and clay-coat coverage. This approach revealed a Pearson's correlation of 0.745 with a P value of < 0.001, confirming a statistical link between the degree of clay-coat coverage and sediment biofilm abundance (Fig. 3.4).

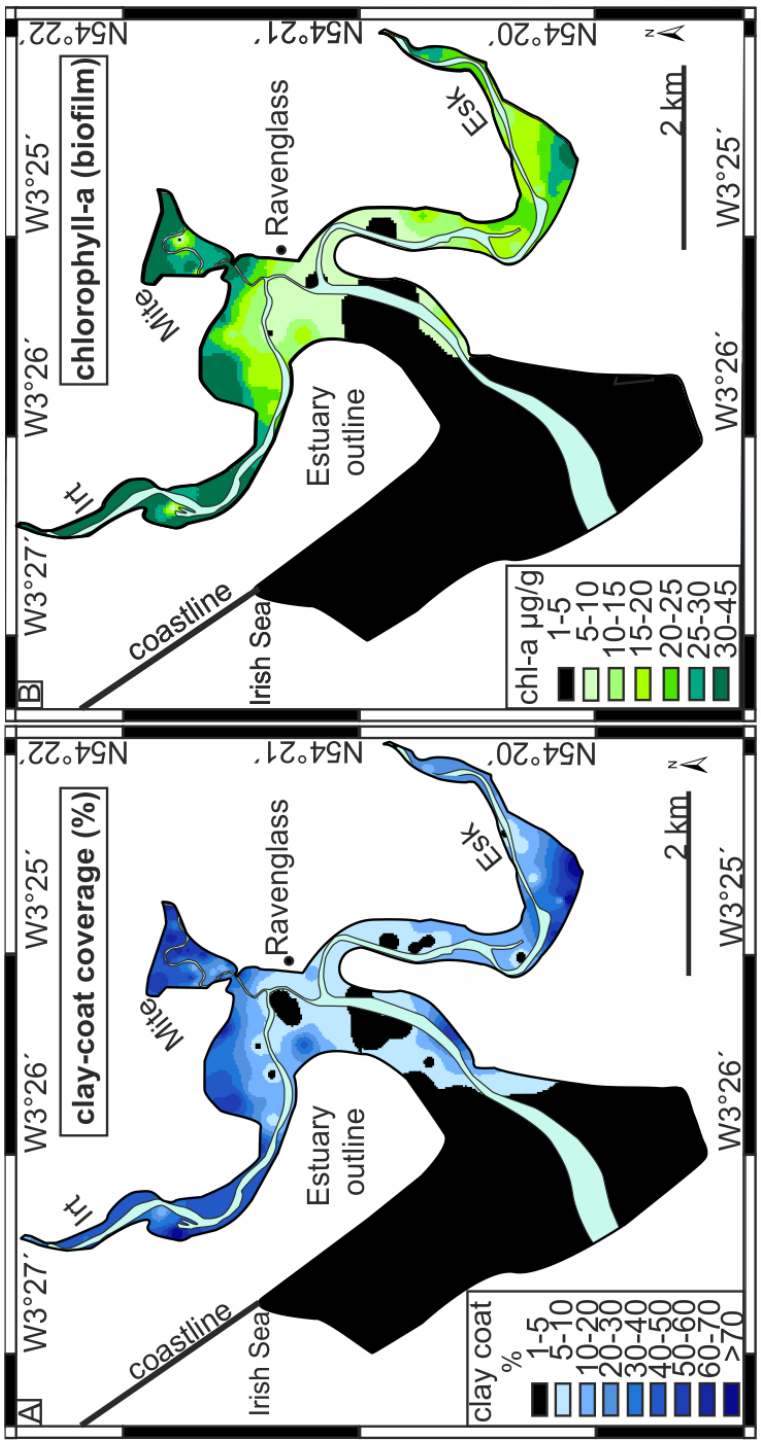

Figure 3-3 Distribution maps of clay-coated sand-grains and sediment biofilm abundance. (A): Clay-coat coverage of sand-grains established from quantitative petrography. Rivers Irt, Mite, and Esk are indicated. (B): Chlorophyll-a concentrations. Darker shades in (A) and (B) represent greater extent of clay-coat coverage and greater abundance of sediment biofilm (chl-a—chlorophyll-a).

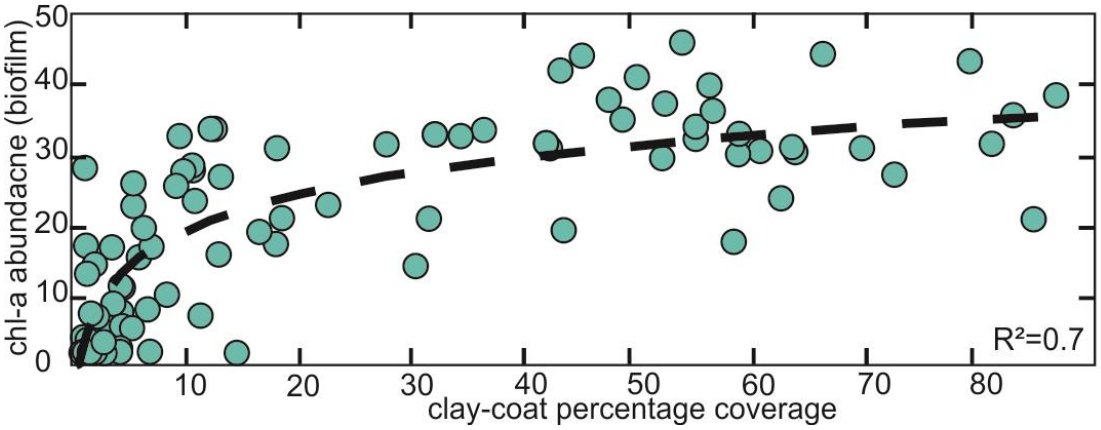

Figure 3-4 Cross plot of percentage clay-coat coverage and biofilm biomarker (chl-a—chlorophyll-a) indicating a positive correlation between increased sediment biofilm abundance and clay-coat coverage.

3.5. Discussion: Origin of clay material attachment

The textural characteristics of the sediments are consistent with biofilms produced by diatoms (Higgins et al. 2003), as reported in studies of both modern (natural) estuaries (Kessarkar et al. 2010; Tolhurst et al. 2003) and laboratory-based experiments (Malarkey et al. 2015; Paterson 1989). This study found textures that are consistent with reported diatom trails and linkages (Fig. 3.1), upon and between grains, that form due to the movement-related production of EPS secretions (Higgins et al. 2003).

The adhesive properties of biofilms (Higgins et al. 2003) are apparent because they attach clay material to sand-grain surfaces, and can form a linked sediment-clay string between grains (Figs. 3.1C and 3.1D). Raman spectroscopy further confirms that the texturally identified films have a biological origin and can be correctly identified as biofilms (Fig. 3.4).

Chlorophyll-a abundance is controlled by the environmental niche of MPB communities. Diatoms of this type become stressed in sediments that undergo turbulent conditions (such as those typically found in lower estuary locations), and therefore they become less abundant (Stal 2003). They also become stressed at sites that have relatively short periods

of exposure to light, for example, in outer tidal-flats where there is limited exposure to full daylight at low tide (Stal 2003; Underwood and Paterson 1993).

The identified heterogeneous distribution of diatoms (environmental niche) and their EPS secretions result in some grains being coated with adhesive EPS and others remaining uncoated, thus resulting in different degrees of clay material adhesion to grain surfaces across an estuarine system (Fig. 3.3). The spatial distributions of clay coat abundance and chlorophyll-a are remarkably similar (Figs. 3.3A and 3.3B).

The results thus suggest that the origin and distribution of clay-coated sand-grains is primarily controlled by biofilms, based on (1) the similarities of the textures of the clay coats in our samples to those reported to be due to biofilms (Fig. 3.1) (Malarkey et al. 2015; Vos et al. 1988), (2) the compositional identification of organic biofilm compounds within the adhesive film on which clay material is attached (Fig. 3.2), and (3) the close correspondence of the distribution of clay-coat coverage and sediment biofilm abundance (chlorophyll-a) (Figs 3.3A and 3.3B) and the positive statistical correlation (Fig. 3.4).

This newly proposed biofilm origin of clay-coated sand-grains, involving a central role for marginal marine, epipelic diatoms, does not entirely contradict previously-reported explanations for clay-coats. Instead, our work has revealed a bio-glue mechanism of clay particle attachment during which clay material, introduced via bioturbation by macro faunal organisms (Worden et al. 2006), codeposition, or infiltration (Matlack et al. 1989; Wilson 1992; Wooldridge et al. 2017b), could be attached to sand-grain surfaces. Our proposal is that diatoms (MPB) produce a biofilm that acts as a bio-glue that coats and bridges sand-grains, producing a sticky web (EPS) that binds and traps codeposited and later-infiltrated clay particles.

There is a reduction in both biofilm abundance (Fig. 3.3B) and clay-coat coverage from the inner to outer estuary (Fig. 3.3A). Note that clay coats are found, albeit at low abundance (5-10 % coat coverage) at sites where biofilms are at their lowest concentration (1-5 μg/g;

e.g. in parts of the main channel). This may represent transportation of clay-coated grains from the site of greatest biofilm concentration in the inner estuary (i.e. the clay-coat "factory") out of the estuary via the main channel, accompanied by a degree of abrasive clay-coat degradation due to grain collisions (Wilson 1992). As a consequence, with transport, inner estuary biofilm-mediated clay coatings persist as partial attached coats, potentially explaining the weaker spatial correlation in the main channel (Fig. 3.3).

3.6. Implication for clay-coated sand-grains in sandstones

The clay-coated sand-grains reported in this study potentially represent precursor coats to those found in numerous deeply-buried sandstones (Aagaard et al. 2000; Ajdukiewicz and Larese 2012; Dowey et al. 2012). Clay-coated grains in sandstones are of interest because they affect petroleum reservoir quality; they inhibit quartz cement growth during prolonged burial and heating (Bloch et al. 2002; Worden and Morad 2000). If, as reported by Bloch et al. (2002), burial diagenetic clay-coats result from recrystallization of clay-coats formed during deposition, then developing a robust understanding of the origin of the primary coats will lead to models capable of predicting reservoir quality in sandstones (Wooldridge et al. 2017b). It should be noted that diatom (MPB) biofilm-producing organisms have been reported previously from other modern estuarine environments (Paterson et al. 2000) and deltaic sediments (Delgado 1989). This has implications for a possible consistent biofilm-mediated origin for the reported similar clay-coated sand-grain textures within such marginal marine sedimentary systems (Dowey et al. 2017).

Clay coated sand-grains are not limited to marginal marine sediments but the link between biofilms and coats remain unconstrained. However, biofilms have been reported to attach dust particles to sand-grain surfaces in desert environments (Belnap and Weber 2013). Clay coats have been reported in meander fluvial point bar environments (Wooldridge et

al. 2017b), in which biofilm abundance is comparable to estuarine sediments (Gerbersdorf et al. 2008).

Biofilm (EPS) bound aggregates of clay particles and freshwater diatoms on sand-grains have been reported in marine sediment 27 km from the nearest river mouth, implying that biofilm attachments remain effective during transport from the inner estuary clay-coat factory into the marine realm (Kessarkar et al. 2010). A marginal marine, primary origin of clay coated grains has been suggested within the continental slope (sediment gravity-flows) and basin plain sediments of the Atoka Formation, Arkoma basin, USA (Bloch et al. 2002; Houseknecht and Ross Jr 1992) and West of Shetland, UK (Sullivan et al. 1999). These reports suggest that biofilm-bound clay-coated sand-grains that develop within estuarine setting may be resistant to sediment reworking and transport. The biofilm origin of clay-coated sand-grains reported here may also explain the origin of clay-coated grains within continental shelf and slope and basin plain sediments (Dowey et al. 2012).

3.7. Conclusion

This paper documents a novel biological mechanism that explains the origin of clay-coated sand-grains in modern marginal marine sediments. The results show that clay particle attachment is mediated by a biofilm. The discovery of a biological-biofilm mechanism of clay-coat formation in sediment at or near the Earth's surface is of great significance and achieves a crucial step in understanding and predicting the distribution of clay-coats in deeply-buried sandstone reservoirs.

4. The origin and of clay-coated sand-grains and sediment heterogeneity in tidal-flats

4.1. Abstract

The presence and distribution of clay minerals attached to grain surfaces as coats (also known as rims) are of great interest because they affect petroleum reservoir quality via the inhibition of the porosity-occluding quartz cement during prolonged burial and heating. Being able to predict the distribution of clay-coated sand-grains in petroleum reservoirs is thus important to help find and exploit anomalously high porosity sandstones deep in sedimentary basins.

Current predictive schemes for the distribution of clay coats in marginal marine sediments derive from surface-based data sets, with limited emphasis placed on the preservation of trends into the subsurface. The post-depositional processes of bioturbation (sediment homogenisation) and infiltration of clay into sand-grade sediment have been widely invoked as potential, post-depositional processes that produce clay coats in modern sands and ancient sandstones. However, the potential for such processes to alter surface trends and govern clay coat distribution in the subsurface remains unconstrained.

The study developed a novel fully quantitative model of clay-coat coverage in order to identify the controlling mechanisms that govern clay coat distribution. This study has focused on surface and near-surface sediments in the Saltcoats tidal-flat deposits of the Ravenglass Estuary, UK. This bio-sedimentary study involved geomorphic mapping, core logging, a range of scanning electron microscopy (SEM) techniques, and quantification of grain-size, clay fraction content, biofilm abundance (total carbohydrate and biomarker analysis), clay-coat coverage, and clay-coat mineralogy.

This study has shown that infiltration and bioturbation have not significantly affected the extent of clay-coat grain coverage in the near-surface sediment. Instead, the extent,

distribution, and mineralogy of clay coats in the near-surface are governed by the surface-based hydrological segregation of the clay mineral assemblage and biological clay coat formation. This study thus supports the use of modern analogue surface-based predictive models for clay-coat derived reservoir quality in ancient and deeply-buried sandstones.

4.2. Introduction

One of the most widely reported origins for the preservation of anomalously high porosity deep in sedimentary basins is the presence of clay-coats (rims) on sand-grain surfaces (Ajdukiewicz and Larese 2012; Bloch et al. 2002; Ehrenberg 1993; Worden and Morad 2000). Chlorite, illite, and mixed mineralogy clay-coated sand-grains have been shown to inhibit the growth of the otherwise ubiquitous, porosity occluding, quartz cement at depth (Ajdukiewicz and Larese 2012; Billault et al. 2003; Lander et al. 2008).

Diagenetic processes (compaction, cementation, and mineral dissolution) experienced by deeply-buried sandstones (> 3 km) typically prevent the preservation of economically viable porosity (Worden and Burley 2003; Worden and Morad 2000). The need to understand the origin of anomalously high porosity in deeply-buried sandstones has driven significant research into the prediction of clay-coated grains (Bloch et al. 2002; Dowey et al. 2012; Saïag et al. 2016; Wilson 1992). Many recent attempts to constrain a predictive capability have focused on producing modern analogue models, from surface based analyses (Dowey 2013; Dowey et al. 2017; Wooldridge et al. 2017b), but with limited focus placed on the preservation of identified trends into the near-surface.

There has been only a small amount of research reported on the potential role of infiltration and bioturbation in controlling the formation and distribution of clay-coated sand-grains in the near-surface (Matlack et al. 1989; Wilson 1992), but yet, these process remain widely cited in both modern (Dowey 2013; Dowey et al. 2017; Matlack et al. 1989) and ancient marginal marine sediments (Bloch et al. 2002; Gier et al. 2008; Moraes and De Ros 1992). This paper aims to address this gap in understanding and constrain the role played by post-depositional processes on the characteristics of clay-coated sand-grains, via a modern analogue methodology.

Tidal-flats occur on a wide range of coastlines (with tidal ranges from less than 1 to 15 m) and represent an important depositional component of both estuarine and deltaic systems (Flemming 2012; Martinius and Van den Berg 2011; Semeniuk 2005). Sandstones that were originally deposited in tidal-flat environments are a component that is widely reported in marginal-marine petroleum reservoir systems (Martinius and Van den Berg 2011) and form notable reservoir facies from a number of well-characterised systems: e.g. the Cretaceous, Sacha Field, Oriente Basin, Ecuador (Higgs et al. 2002), the Lower Jurassic, Beatrice Field, North Sea, (Stevens 1991), and the Jurassic, Heather Field, North Sea (Glasmann et al. 1989).

The multi-scale heterogeneity of tidal sandstones represents a challenge for reservoir characterisation in terms of constraining modelling parameters, and in planning oil and gas field developments (Martinius et al. 2005). Previous work on the characterisation of tidal-flat sediments has focused on classifying: morphology (Flemming 2012; Yang et al. 2005), sedimentary textures (Chakrabarti 2005; Chang and Choi 2001; Flemming 2012), the effect of hydrological dynamics on grain size distribution (Brockamp and Zuther 2004; Chang and Choi 2001; Yang et al. 2005), sediment mineralogy, and sediment clay fraction distribution (< 2 μm) (Brockamp and Clauer 2012). However, the biological aspect of tidal-flat sedimentary environments remains relatively poorly defined and largely un-quantified (Jones 2017).

Tidal-flat sediments are composed of non-cohesive sand, cohesive mud, and the excretions of sticky, cohesive extracellular polymeric substances (EPS) by colonizing biological organisms (Jones 2017; Malarkey et al. 2015). Biological organisms, in particular those that develop biofilms (molecular networks of sticky EPS) among sediment grains (Garwood et al. 2015; Hoagland et al. 1993; Stal 2003), have been shown to play a fundamental role on the

dynamics and characteristics of estuarine tidal-flat sediments (Garwood et al. 2015; Schindler et al. 2015; Stal 2003; Wooldridge et al. 2017a).

Biofilms are produced via the secretion of EPS (adhesive mucilage) by sediment-inhabiting microphytobenthic (MPB) biological communities that are composed of diatoms, euglenids, crysophyceans, dinoflagelates, cyanobacteria, and photosynthetic bacteria (Jesus et al. 2009). Sediment colonising benthic diatoms account for > 95 % of all benthic organisms in the tidal-flat settings of western Europe (Underwood and Paterson 1993) and therefore are the principal focus of this work. Marginal marine biofilms in sediments have been shown to increase the sediment cohesion which in turn influences: (i) tidal-flat erosion rates (Hoagland et al. 1993; Vos et al. 1988), (ii) grain size heterogeneity (Garwood et al. 2015), (iii) tidal-flat geomorphology (Stal 2010), and (iv) bedform stability (Malarkey et al. 2015; Schindler et al. 2015).

This work documents the heterogeneity of a tidal-flat by characterising the surface and near-surface distribution trends in grain size, grain sorting, clay fraction percentage (< 2 μm), biological populations (macro- and micro-organism), biofilm abundance, and clay-coat coverage. Since sampling was undertaken at high resolution, the study permitted the quantification of post-depositional processes, such as infiltration and bioturbation on the formation of clay-coated sand-grains. By focussing on the Saltcoats tidal-flat in the Ravenglass Estuary, UK (Fig. 4.1), this study addresses the following questions:

1. What are the sedimentological and biological characteristics of a tidal-flat sedimentary package?
2. What are the textural characteristics of detrital-clay-coated sand-grains in a tidal-flat sedimentary package?
3. How are detrital-clay-coated sand-grains distributed in a tidal-flat sedimentary package?

4. Is there a post-depositional increase in detrital-clay-coated sand-grain coverage?
5. What controls the distribution of clay-coated sand-grains in the near-surface?
6. Do surface distribution trends of clay-coated grains reflect those in the near-surface?

4.3. The origin and significance of sedimentary biofilms

Biological-sediment interactions are an emerging area of investigation for geologists with recent publications demonstrating the profound influence of biological cohesion (biostabilization) on sedimentary systems (Decho 2000; Garwood et al. 2015; Jones 2017; Malarkey et al. 2015; Schindler et al. 2015; Wooldridge et al. 2017a). Biofilms account for up to 50 % of the organic production in estuarine tidal-flat sediments (Smith and Underwood 2000). EPS, colloquially referred to as "bio-glue and mucus" (Agogué et al. 2014; Hoagland et al. 1993), forms a sticky coat on and between sand-grains, and is associated with exacerbated entrapment of fine (clay to silt) particles (Garwood et al. 2015; Wooldridge et al. 2017a). EPS is composed principally of carbohydrate compounds (95 % polysaccharides) (Stal and De Brouwer 2003; Stal 2003).

Biofilms are characterised as sheets composed of numerous, small, overlapping strands of mucilage which bind sand-grains in a mucus matrix, consequently preventing the independent movement of grains due to their 'stickiness' (Higgins et al. 2003; Hoagland et al. 1993; Jones 2017). A brief summary of the sedimentological aspects of biofilms is provided here although characterisation and an assessment of their origin has been the subject of earlier detailed reviews (Hoagland et al. 1993; Jones 2017; Stal 2003).

EPS is produced by diatoms for a variety of functions (Decho 1990). One function is to enable cell adhesion, reorientation, and cell movement in response to tidal fluctuations in order to: (i) maintain optimum environmental conditions for photosynthesis (avoiding low light and anaerobic conditions), (ii) prevent damage during evaporative desiccation of the

sediment, and (iii) minimise dispersal during tidal inundation (Higgins et al. 2003; Hoagland et al. 1993; Paterson 1989; Stal and De Brouwer 2003). Epipelic diatoms move by a process termed "gliding" (Higgins et al. 2003) which involves the secretion of mucus strands (EPS). The EPS strands on movement detach from the diatom but remain attached to sand-grain surfaces thus accumulating as a biofilms (Higgins et al. 2003; Stal 2003).

Diatoms inhabit the top few cm's of the sediment (typically < 2 mm) (i.e. where light can still penetrate the sediment); in this zone, they mediate the accumulation of clay- to silt-sized particles and mud floccules during slack water conditions (Garwood et al. 2015; Stal 2003; Vos et al. 1988). Biofilms in the water-column that become detached from the sediment surface during rising tides have been reported to enhance the flocculation and deposition of suspended clay particles (Garwood et al. 2015; Vos et al. 1988). Biofilm-induced sediment stabilisation derived from diatoms is not limited to estuarine tidal environments (Herlory et al. 2004; Paterson et al. 2000; Underwood and Paterson 1993); they have been reported to occur in the deltaic, marginal marine habitats of the Ebro Delta (Spain) (Delgado 1989) and in freshwater streams that experience heavy sedimentation loads (Rosowski et al. 1986). Low concentrations of biofilms (EPS) has previously been reported to be pervasively present in estuarine tidal-flat (De Winder et al. 1999; Malarkey et al. 2015) and fluvial sediments (Gerbersdorf et al. 2008).

The preservation of diatom-excreted biofilms is dependent on the specific type of biofilm material; some are water-soluble (colloidal) and some are water-insoluble (EDTA-extractable, bulk, bound, or capsular) (Stal 2003; Underwood et al. 1995). The water-insoluble EPS fraction develops in the presence of divalent cations, such as Mg^{2+}, Ca^{2+}, and electrically-charged silts and clay minerals that are common in estuarine waters (Stal and De Brouwer 2003; Stal 2003). Water insoluble EPS fractions can be tightly bound to sand-grain surfaces and are resistant to degradation (De Winder et al. 1999; Stal 2003). Water

insoluble EPS biofilms that are bound to grain surfaces have been reported to survive tidal inundation and accumulate in the sediment column (De Winder et al. 1999; Taylor and Paterson 1998).

There is no single analytical method capable of detecting all components of EPS (biofilm) in sediments (Underwood et al. 1995). A phenol-sulphuric acid analytical method can detect a wide range of carbohydrates that represent the majority of the EPS components (Decho 1990). The phenol-sulphuric acid analytical method is an established, and widely-used, method for biofilm quantification in subsurface estuarine sediments (De Winder et al. 1999; Underwood et al. 1995; Underwood and Paterson 1993). Determining the biofilm fraction in terms of total carbohydrate in sediments is not trivial (Stal and De Brouwer 2003). For surface sediments, biofilm abundance is, typically, measured via the biomarker chlorophyll-a, which is the main photosynthetic pigment of diatoms (Herlory et al. 2004; Jiménez et al. 2015; Underwood and Paterson 1993).

4.4. Clay coat derived anomalously high porosity sandstones

Diagenetic-clay-coats in sandstones derive from: (i) the thermally-driven recrystallization of a precursor detrital-clay-coat and (ii) in situ precipitation of clay (accretion) directly from pore fluids, typically on a precursor clay "root structure" (Ajdukiewicz and Larese 2012; Wise et al. 2001; Worden and Morad 2003). The clay-coated sand-grains, reported in this study of a modern estuary, represent the precursor, detrital-clay coat (root structure) component previously illustrated in diagenetic-clay coats (Bloch et al. 2002; Gould et al. 2010; Stricker and Jones 2016).

Experiments by Aagaard et al. (2000) showed that discontinuous detrital-clay coats recrystallized at 90 °C to form a continuous, coat morphology consistent with that of diagenetic-clay-coats in naturally occurring reservoir sandstones. Billault et al. (2003) and

Ajdukiewicz and Larese (2012) suggested that the extent, completeness, mineralogy, and distribution of the detrital-clay coat material are the principal controls on the ability of clay-coats to inhibit quartz cementation during burial and heating.

Detrital-clay-coated sand-grains have been previously reported to form at, or near, the surface of the sediment column by the sedimentological and biological processes of inheritance, infiltration, drying-adhesion, bioturbation, and biofilms produced by both macro- and micro-organisms (Matlack et al. 1989; Needham et al. 2004; Needham et al. 2005; Wilson 1992; Wooldridge et al. 2017a; Worden et al. 2006).

The post-depositional processes of infiltration (e.g. described in arid desert environments) and bioturbation (sediment mixing) have been reported to produce clay coats in arid and marginal-marine sediments (Matlack et al. 1989; Wilson 1992). Bioturbation and infiltration have been experimentally shown to produce clay-coated sand-grains (Matlack et al. 1989; Needham et al. 2005; Worden et al. 2006). Although there is somewhat limited evidence of the magnitude of the effects, in marginal-marine sediments, these processes are considered to be important controls on clay mineral distribution in such settings (Bloch et al. 2002; Dowey 2013; Dowey et al. 2017; Matlack et al. 1989).

Infiltration occurs when clay minerals and clay- to silt-sized material, previously suspended in water, enter a sand body during water percolation. Velocity reduction of the water flow occurs at sand-grain contacts and above impermeable layers, thus causing deposition of the suspended solids onto grain surfaces (Dowey 2013; Matlack et al. 1989). Infiltration has been reported to occur most commonly in coarse-grained, arid to semi-arid environments which permit extensive infiltration through the vadose zone (Matlack et al. 1989; Wilson 1992). Santos et al. (2012) reported that infiltration and pore water movement can occur on a cm- to meter-scale in marginal marine sediments via the

processes of tidal pumping and wave setup, driven by a hydraulic gradient produced by tidal asymmetry and wave amplitude.

Sediment mixing due to bioturbation was documented by McIlroy et al. (2003) in which non-selective, filter-feeding, burrowing lugworms (*Arenicola marina*) destroyed the original sedimentary layered fabric over a period of 20 weeks, and, in doing so, introduced clay material into previously clean, sand-dominated sediment.

4.5. Study site

This study is focused on the Saltcoats siliciclastic tidal-flat, in the Ravenglass Estuary, northwest England (SD 07608 96767) (Wooldridge et al. 2017b). The 5.6 km^2 area, Ravenglass Estuary is a shallow, macro-tidal, mixed-energy system that is dominated by tidal-flats (Bousher 1999; Lloyd et al. 2013; Wooldridge et al. 2017b). Saltcoats represents the largest tidal-flat located at the confluence of the River Irt and River Mite arms of the estuary (Fig. 4.1). Topographically the tidal-flat consists of a 3.5 m elevation sloping into the main ebb tidal-channel and fringed on the landward side by established saltmarsh vegetation. The estuary experiences a maximum 7.55 metre tidal range (Lloyd et al. 2013).

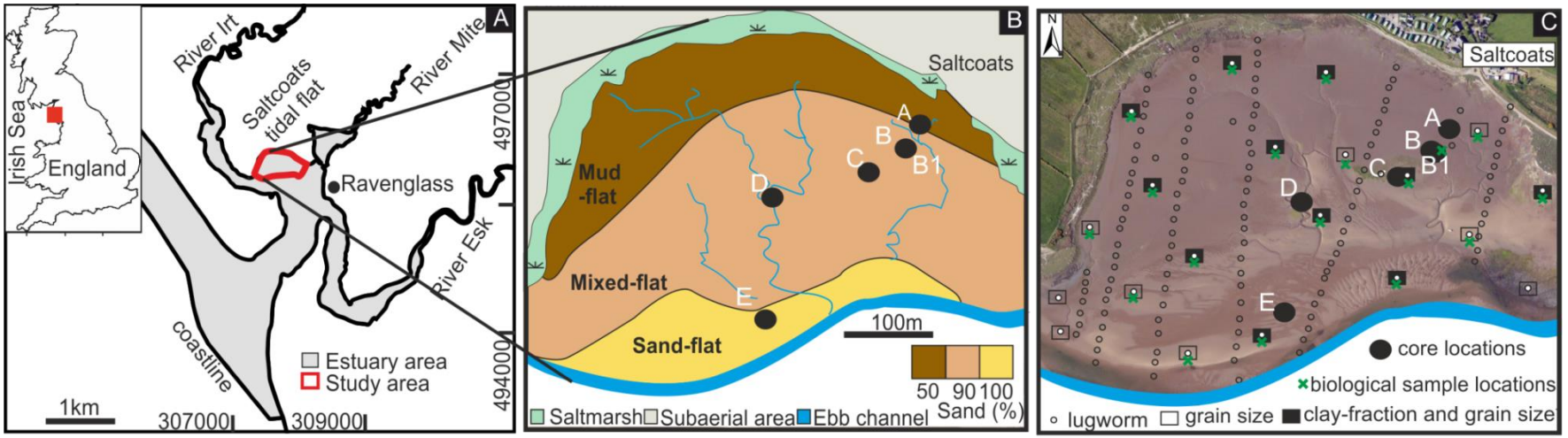

Figure 4-1 Location and depositional environment maps of the Saltcoats tidal-flat. (A) Location of Saltcoats in relation to the Ravenglass Estuary and the UK. (B) Map showing the study area and component depositional environments subdivided by sand percentage; mud-flat (15-50 % sand), mixed-flat (50-90 % sand), and sand-flat (> 90 % sand) as defined by laser particle size analysis. (C) Arial image of the Saltcoats tidal-flat showing sample locations.

4.6. Materials and Methods

The work focused on both surface and near-surface sediments with results initially reported separately for both. To allow comparison of this modern data set to ancient sandstones originally deposited in the same environmental conditions, trends in sedimentological and biological distributions have been segregated into tidal-flat depositional environments and corresponding core (near-surface) sedimentary facies. Surface depositional environments and bedforms were mapped in the field with samples collected in a grid system and plotted using the interpolation function in ArcGIS (https://www.arcgis.com). A Pearson's correlation coefficient was used to test the statistical significance between all sedimentary and biological variables. Elevation data was obtained from the UK Environment Agency.

4.6.1. Surface data sets

Surface sedimentary data sets consisted of 22 samples from which quantitative clay fraction (< 2 μm), grain size, and sorting values were established, and 8 polished thin sections constructed (Fig. 4.1C).

Quantitative sediment grain size and sorting analysis was undertaken via laser granulometry using a Beckman Coulter LS200, with values presented in the modified geometric graphical measures (Folk and Ward 1957). The clay-fraction (< 2 μm) of the sediment was calculated from representative homogenised sediment sub-samples following the methodology outlined in Wooldridge et al. (2017b).

The intensity of bioturbation by macro-organisms was quantified by counting lugworm (*Arenicola marina*) faecal cast density, recorded in the field in 1 m^2 quadrants at 140 sites on the tidal-flat (Fig. 4.1C).

4.6.2. Near-surface data sets

The cored transect (spanning about 500 m) encompasses the range of depositional environments from mud-flat (core A), upper mixed-flat (core B), lower mixed-flat (core C), tidal creek point-bar (core D), and sand-flat (core E) (Fig. 4.1B). Images of surface environmental conditions through which the cores were drilled are presented in Figure 4.2.

Five 1-m cores (50 mm diameter) were collected, from a transect across the Saltcoats tidal-flat, via a jack-hammer window sampler. Core B (mixed tidal-flat, Fig. 4.1B) was collected in duplicate (core B1) with the second core used for biological analyses. In total, 46 sediment subsamples were taken from these five cores, ensuring approximate uniform distribution but also allowing collection of each sediment facies. All cores were logged for grain size (measured in the laboratory using a hand-lens), sorting, primary sedimentary structures, and bioturbation intensity (Taylor and Goldring 1993). Thin sections of polished, impregnated grain-mounts were constructed with quantified grain size, sorting, and clay fraction content analysis (see above) undertaken at thin sectioned intervals.

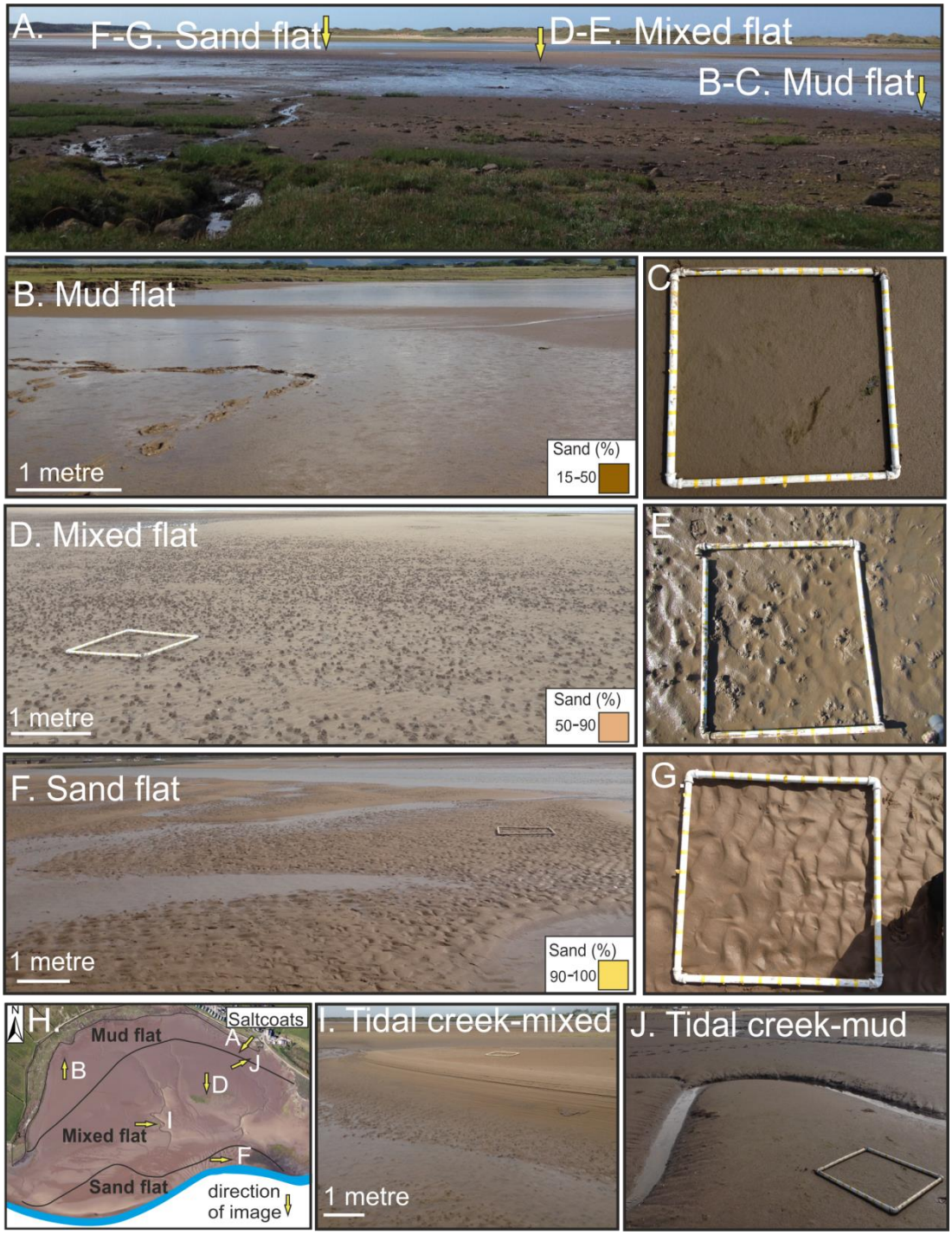

Figure 4-2 Photographs of geomorphic and sedimentary features of the Saltcoats tidal-flat. (A) Overview of the study area; arrows mark the boundary between tidal-flat environments. (B, C) Mud-flat. (D, E) Mixed-flat. (F, G) Sand-flat. (H) Aerial image of the study area. Arrows indicate the location and direction of the photographs (A, B, D, F, I, and J). (I) Channelized tidal creek network dissecting the lower mixed tidal-flat. Note the rippled and bioturbated channel axis. (J) Tidal creek channel draining the mud-flat and upper mixed tidal-flat.

4.6.3. Classification of samples: depositional environments, facies, and mineralogy

Samples were classified by lab-derived sand percentages into: sand-flat (> 90 % sand), mixed-(sand-mud) flat (50-90 % sand), and mud-flat (15-50 % sand) (Brockamp and Zuther 2004). The tidal-flat classification (sand-mud ratio) was applied to define surface environments (accompanied by geomorphological mapping of the tidal-flats) and the near-surface deposits (accompanied by lithofacies identification).

The sedimentary facies identified from core have also been grouped into characteristic facies associations (e.g.by texture, sedimentary structures, bioturbation intensity, and diagnostic features) which are diagnostic of specific depositional units (i.e. mud-, mixed-, and sand-flats) in tidal-flat environments. The lithofacies scheme was used to cross-check the validity of the sand-mud ratio classification in assigning near-surface samples into the correct tidal-flat depositional environment. The use of sand-mud ratios, instead of descriptive facies classifications, allowed direct quantitative comparison of the surface and near-surface datasets. The tidal-flat classification (sand-mud ratio) permitted enhanced classification compared to lithofacies schemes of near-surface samples (i.e. mixed-tidal-flats represent a continuum between mud- and sand-flats and such will have facies comparable to both environments).

Sediment mineralogy was quantified using automated scanning electron microscope-energy dispersive spectrometry (SEM-EDS) techniques with an FEI-QEMSCAN® (Armitage et al. 2010; Wooldridge et al. 2017b). The approach enabled *in situ* imaging of thin sections as well as quantification of sediment mineralogy. The SEM-EDS analysis step-size was 1 µm to ensure that the fine fraction was analysed in unison with the framework grains, thus enabling identification of both the micron-scale morphology and mineralogical composition of sediment samples. Data are here presented as a combination of a backscatter secondary

electron image, and fully quantitative mineralogical content images of bulk-sediment and clay fraction components with values reported in image-area percentages.

4.6.4. Clay-coat coverage and mineralogy

Polished thin sections were prepared from both surface (approximately 2 cm depth) and near-surface sediment. Thin sections were analysed by scanning electron microscopy (SEM) in backscattered electron mode with SEM-EDS undertaken to quantify clay-coat morphology and mineralogy. Grain-mount stubs of loose sediment were also analysed for clay coat morphology via SEM.

A longitudinal transect of 15 SEM images were obtained for each thin sectioned sample, to create a micron-scale representative image of the sediment. Clay-coat quantification was undertaken using the integrated micron-scale SEM images in the Petrog statistical software (Wooldridge et al. 2017a). The method involved calculating the total perimeter of a grain and the length that is covered by attached clay-coats (i.e. independent of clay-coat thickness) for 50 sand-grains per sample, which produced a dataset of > 2,600 analysed clay-coated sand-grains. The method carries ± 1.7 % error with average percentage clay-coat values reported (Wooldridge et al. 2017a).

The mineralogical quantification of the clay-coated sand-grains (clay-coats and framework grains) was undertaken in SEM-EDS (see previous) on surface and near-surface samples to permit the *in situ* micron-scale mineralogical characterisation of the clay-coated sand-grains.

4.6.5. Determination of biofilm sediment abundance (surface sediments)

The distribution of surface sediment biofilm abundance was mapped by measuring the abundance of the biomarker chlorophyll-a (Jiménez et al. 2015; Stal 2003). Eighteen surface sediment samples were collected on a single day within 1 hour of low tide (Fig.

4.1C). The surface material was collected in sterilized foil, initially stored over ice during collection, and then stored at -18 °C during transport and then preserved at -80 °C when back at Liverpool University within 4 hours of collection. Chlorophyll-a analyses were undertaken following the methodology previously outlined in Wooldridge et al. (2017a).

4.6.6. Determination of biofilm sediment abundance (near-surface)

The chlorophyll-a biomarker approach to determine the amount of sediment biofilm material only works for the top approximately 4 mm of sediment, reflecting the present-day environmental niche of the diatoms (MPB) that produce biofilms (Stal 2003). To assess whether surface trends of biofilm abundance are preserved into the near-surface, the total carbohydrate (biofilm) sediment component was calculated via the phenol-sulphuric assay (Underwood et al. 1995). The phenol–sulphuric assay is a colorimetric method widely used to determine the total sediment carbohydrate concentration (including mono-, di-, oligo-, and polysaccharide) (De Winder et al. 1999; Underwood et al. 1995; Underwood and Paterson 1993).

Samples were collected from the duplicate (< 0.5 m distance apart) core of B, B1 (Fig. 4.1B), with samples collected from each encountered facies, which encompassed sediment deposited originally in mud-, mixed-, and sand- tidal-flat depositional environments. Sample collection was undertaken immediately upon extraction of the core. Samples were collected in sterilized foil, stored on ice during collection, placed in a freezer at -18°C for transport (4 hours) back to Liverpool University and then preserved at -80 °C.

Analytical-grade glucose standard was purchased from Sigma-Aldrich. Calibration standards in the range of 5 to 100 µg /mL (in the range 30-550 µM glucose) were prepared from a stock solution of glucose (0.1 mg/mL in water) in 25ml volumetric flasks. 400 µl of each glucose standard and pure distilled water (performing as a blank) were added to a

series of vials and 400 µl volumes of 5 % phenol (w/v), were then added to each of the vials followed by vortex mixing. 2 ml of concentrated, analytical grade sulphuric acid was added rapidly to each vial, vortex-mixed and the resulting vials incubated for 35 minutes at room temperature. The absorbance of each calibration standard solution was then measured on a Jenway 7315 UV/VIS spectrophotometer at 490 nm and 570 nm against the blank.

Samples collected in the field were treated identically to the standards. Typically, 0.2 mg of freeze-dried sediment from each sample was weighed, with 400 µl of distilled milli-q water and 400 µl of 5 % phenol (w/v) added to each sample-extract and incubated at room temperature for 1 hour. 2 ml volumes of concentrated sulphuric acid were added rapidly in a direct stream of acid against the liquid surface. The extracts were transferred and centrifuged at 10000 r.p.m for 1min. The absorbance was measured at 490 nm and 570 nm via a Jenway 7315 UV/VIS spectrophotometer. Method blanks (no sediment added) were treated in the same manner as the samples.

A standard curve (absorption against glucose concentration) was generated to allow the calculation of the concentration of carbohydrate in each sample. The concentration of carbohydrate in the sample is calculated using the following formula: Concentration of glucose in samples (µg/g) = [concentration in µg/ml] /slope x weight of dried sediment extracted x dilution (ml).

4.7. Results

The results are presented in the four themes of the study: (i) sediment heterogeneity, (ii) biological content (macro-and micro-organism distribution and sediment biofilm abundance), (iii) clay-coat coverage variability, and (iv) clay-coat mineralogy. The results of each theme are further separated into surface and near-surface data sets.

4.7.1. Sediment heterogeneity: depositional environment, grain size, grain sorting, clay fraction content, and sediment mineralogy

4.7.1.1 Surface sediment characteristics

The Saltcoats tidal-flat consists of three depositional environments that are arranged broadly parallel to shoreline, consisting of a mud-flat (3 to 3.5 m elevation), mixed (sand and mud)-flat (0.6 to 3 m elevation), and sand-flat (< 0.6 m elevation) (Figs. 4.1B and 4.2A). These three depositional environments represent an evolution from the saltmarsh-fringed landward margin of the tidal-flat to the ebb channel.

The mud-flat has a surface composed of fluidized mud, algal mats, bird tracks, and a pimpled surface (Fig. 4.2B, C). The sand-flat contains extensive low amplitude (approximately < 1 m) 2D dunes (Fig. 4.2F) with surface bedforms dominated by straight-to-lingoid current ripples. The mixed tidal-flat, has a distinct biotic zonation dominated by lugworms (*Arenicola marina*). Tube like faecal mounds (Fig. 4.2D, E) overprint the gradational transition from an upper, structureless muddy surface to a lower current ripple dominated texture.

The whole tidal-flat is drained by a network of dendritic tidal creeks. There is a morphological evolution from approximately 50 cm wide channels (Fig. 4.2I, J) in the mud-flat, with lower channel axes composed of bioclasts and granule to pebble lag deposits, to meter-wide meandering, channelized systems that erode down to depths of ~ 2 m in the mixed-flat, with a current rippled and bioturbated base (Fig. 4.2I).

The spatial distribution of surface sediment properties in terms of grain size, clay fraction, and sorting is presented in Figure 4.3 with values summarised in Table 4.1. There is a broad trend of reducing grain size (from upper medium sand- to silt dominated-assemblages), increasing clay fraction content (from 0.3 to 10.5 %), and reduced sorting (from well sorted

to very poorly sorted) towards the tidal limit (Fig. 4.3B, C, D). The surface sediment type is illustrated via SEM (texture) and SEM-EDS (mineralogy) images (Figs. 4. 4 and 4.5).

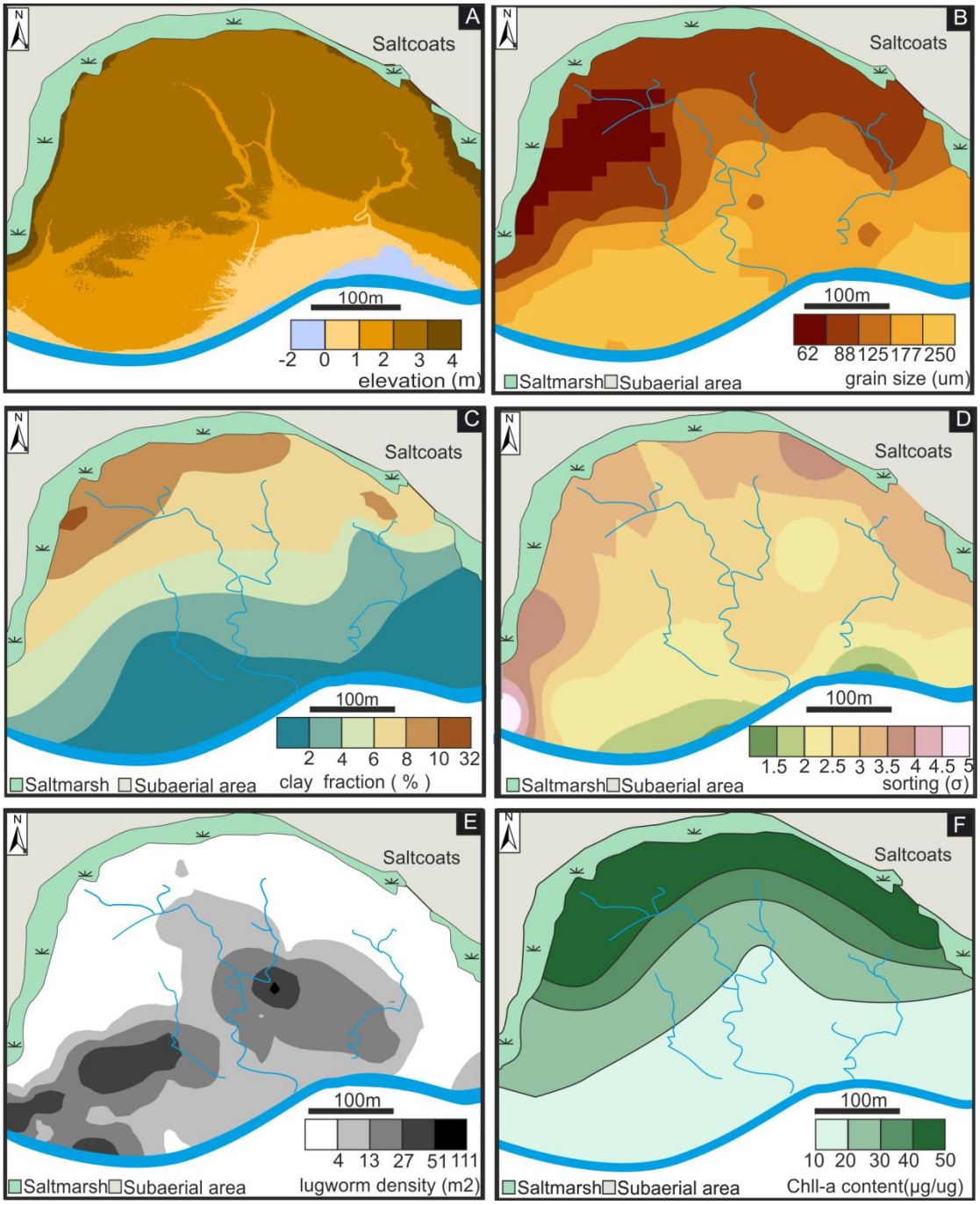

Figure 4-3 Distribution maps of surface sedimentary and biological characteristics. (A) Map of tidal-flat elevation. (B) Map of surface-sediment grain size. (C) Surface distribution of sediment clay fraction percentage. (D) Map of surface-sediment sorting. (E) Map of lugworm population (faecal mound density). (F) Surface distribution of sediment biofilm abundance (chlorophyll-a).

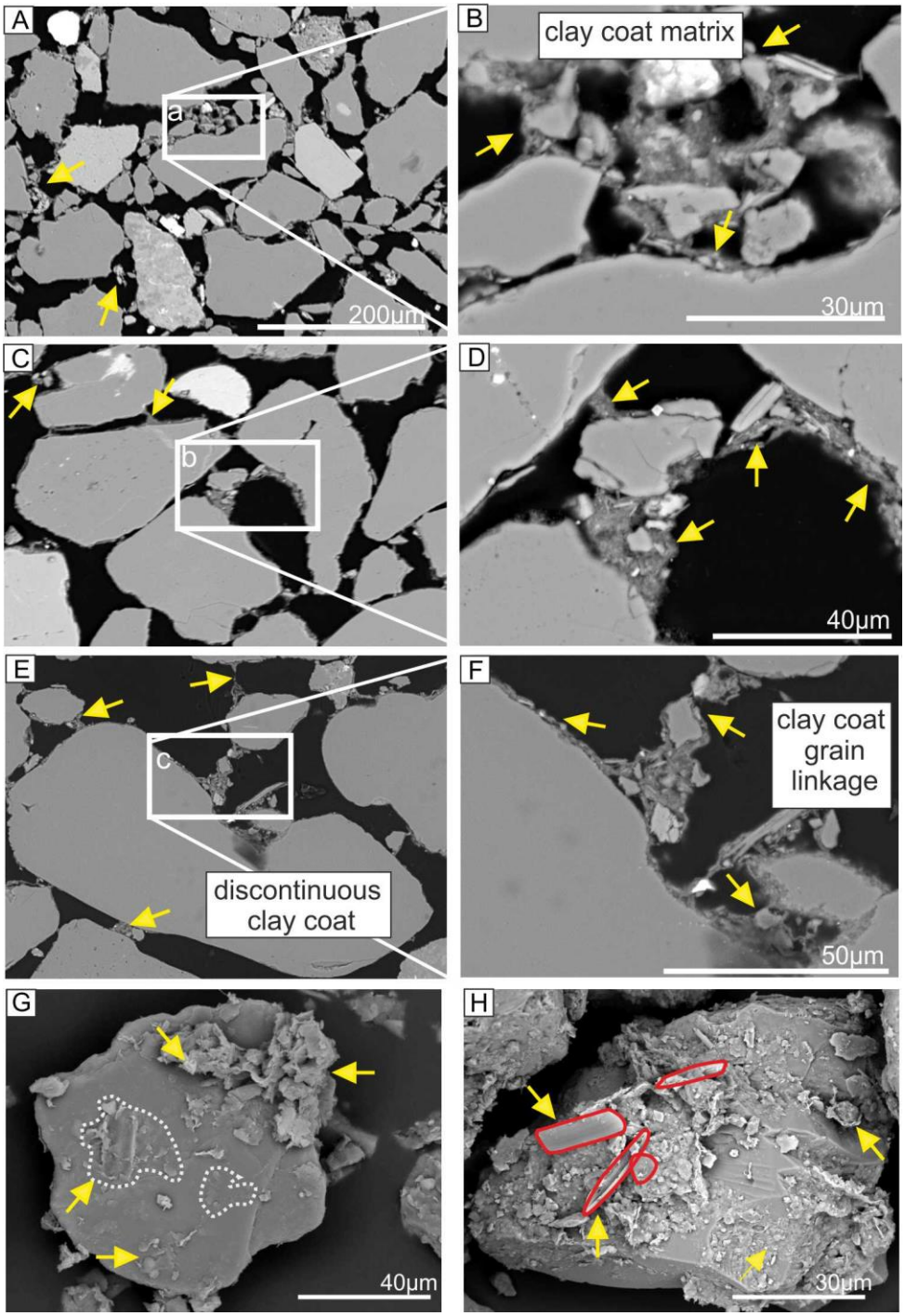

Figure 4-4 Scanning electron microscopy (SEM) images of surface clay-coated sand-grains. Arrows indicate regions and key textural characteristics of clay-coats. SEM images of clay-coats from mud-flat (A, B), and mixed-flat (C- F) sediments. (G and H) are SEM images of loose sediment grain stubs. The representative images illustrate (i) the intricate textural characteristics of clay coats (A, B, C, D, E, and F), (ii) dehydrated biofilm coats on sand-grains surfaces (G), and (iii) the presence of biofilm excreting diatoms in clay-coats (H).

The sediment has a grain assemblage dominated by quartz, feldspar, dolomite, and calcite (Fig. 4.5 and Table 4.2). The clay-fraction is dominated by illite, with lower, broadly equal values of chlorite and kaolinite (Table 4.2). The clay mineral assemblage is distributed, principally as clay coats on, or between grains (approximately 80-90 %) (Fig. 4.5), as clay-rich rock fragments, or as, clumps of clay material that potentially resulted from flocculation. In the sand-flat samples, the clay-fraction component occurs almost exclusively as discontinuous coats on sand-grain surfaces, with the greatest thickness occurring at grain indentations and embayments (Figs. 4.4 and 4.5). In the tidal-flat sediments, illite, chlorite, and kaolinite are all mainly present as grain-coats and bridging-structures. Chlorite is also associated with clay-rich lithic grains (Fig. 4.5). Illite and kaolinite also occur within, and on, feldspar grains (Fig. 4.5). The carbonate content of the sediments is highest in the mud-flat samples (Table 4.2).

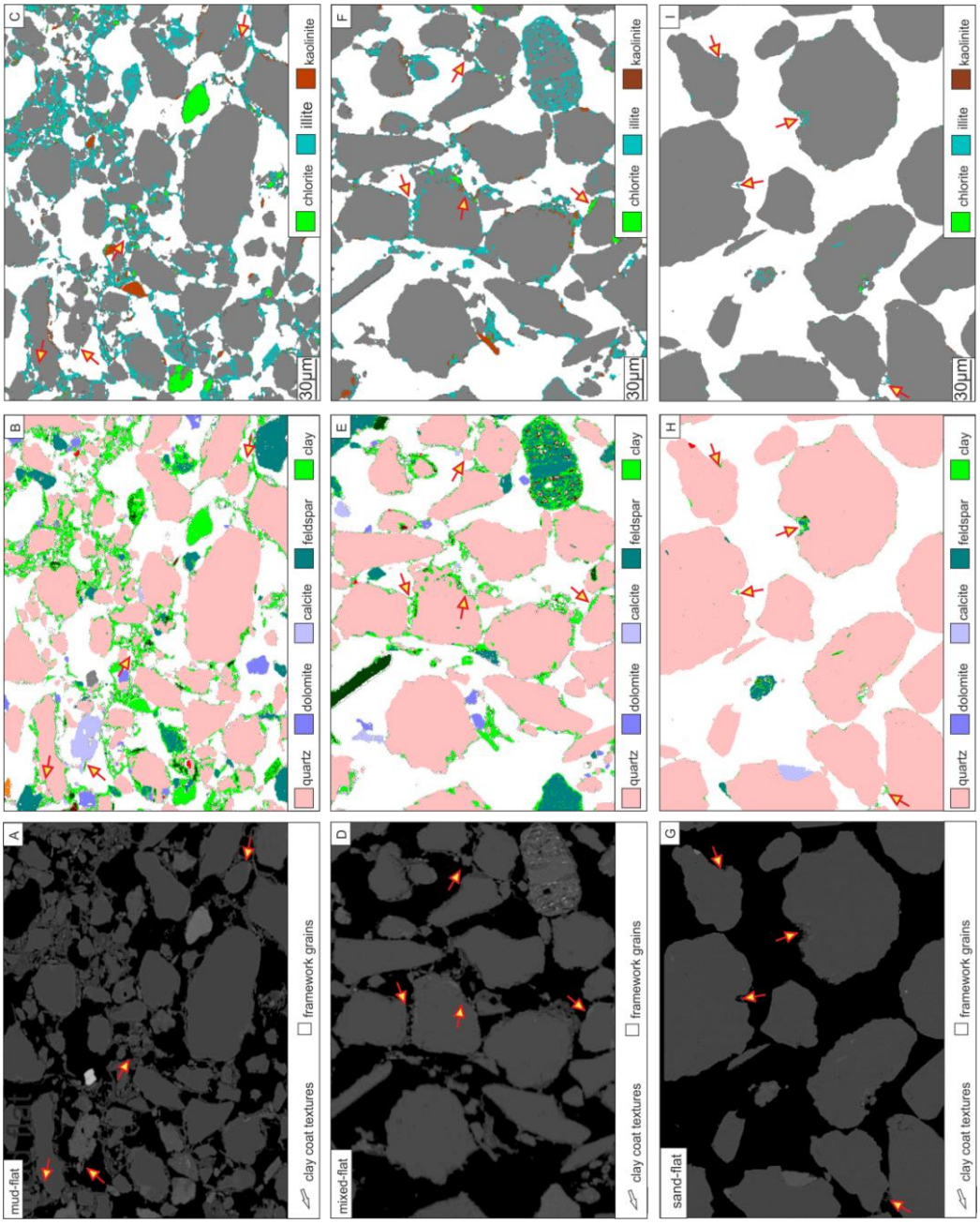

Figure 4-5 Scanning electron microscope energy dispersive spectrometry (SEM-EDS) images of clay-coat mineralogy: mud-flat (A, B, C), mixed-flat (D, E, F), and sand-flat (G, H ,I) depositional environments. Arrows indicate regions and key textural characteristics of clay-coats.

	surface									near-surface								
	MUD			MIXED			SAND			MUD			MIXED			SAND		
		range			range			range			range			range			range	
	average	max	min	average	max	min	average	max	min	average	max	min	average	max	min	average	max	min
Clay-coat coverage (%)	61.7	69.4	57.1	28.7	43.0	13.0	3.9	4.3	3.4	61.9	76.0	50.0	42.8	74.6	13.4	15.7	24.2	2.5
Mean grain size (µm)	37.1	43.7	27.9	102.7	159.7	47.2	213.3	337.8	143.7	37.8	45.6	30.1	104.3	276.3	48.3	187.6	311.4	136.8
Grain size sorting	3.7	4.2	3.2	2.8	4.3	1.9	1.5	1.6	1.3	4.1	5.1	3.3	3.1	4.6	1.9	1.6	1.8	1.4
Clay-fraction (%)	8.6	10.5	7.6	3.3	7.2	0.5	1.2	2.0	0.3	10.0	12.2	6.0	5.8	12.3	2.3	1.7	3.4	0.2
Chl-a (µg/g)	38.4	46.8	25.0	17.7	27.5	10.0	13.4	14.7	11.8	_	_	_	_	_	_	_	_	_
Total carbohydrate	_	_	_	_	_	_	_	_	_	767.8	956.0	579.6	759.0	957.5	461.9	192.6	256.6	128.5

Table 4-1 Sediment, biological, and clay coat heterogeneity of the Saltcoats tidal-flat

		Clay index			Quartz	Feldspars carbonates			Mica	
		Illite	Kaolinite	Chlorite	_	_	Calcite	Dolomite	Muscovite	Biotite
surface	mud	0.80	0.08	0.12	65.55	13.26	2.74	1.90	1.15	1.02
	mixed	0.78	0.09	0.14	75.00	11.49	2.51	1.16	0.67	0.77
	sst	0.75	0.06	0.19	82.18	9.47	1.14	0.60	0.61	0.40
Near-surface	mud	0.73	0.08	0.19	69.81	14.53	4.67	1.86	1.36	0.82
	mixed	0.67	0.14	0.19	69.18	14.02	3.28	1.52	1.25	1.06
	sand	0.62	0.05	0.33	82.52	9.96	1.63	0.80	0.90	0.68

Table 4-2 Scanning electron microscope-energy dispersive spectrometry derived mineralogy of the Saltcoats tidal-flat (values present as image area percentages).

4.7.1.2. Near-surface depositional architecture and sediment characteristics

Detailed facies descriptions used to cross-check the validity of utilised the sand-mud ratio classification scheme are given in Table 4.3; sediment characteristics from the near-surface are presented in Table 4.1. Sedimentary logs summarising grain size, sedimentary structure, bioturbation index, clay fraction percetnage, and clay coat abundance are presented in Figure 4.6.

Both the landward decrease in surface sediment grain size and increase in clay fraction content (Fig. 4.3 C) are broadly replicated in the sediment cores that range from medium sand to silt, hosting a 0.2 to 12 % clay fraction percentage. It is not possible to correlate beds between the five cores even though they occur within 500 m (Fig. 4.6). There is no systematic increase in the proportion of sediment clay fraction with depth (Fig. 4.6). Also, there is no systematic variation of clay-coat coverage with increasing depth for each individual sediment facies or each core (Table 4.4 and Fig. 4.6).

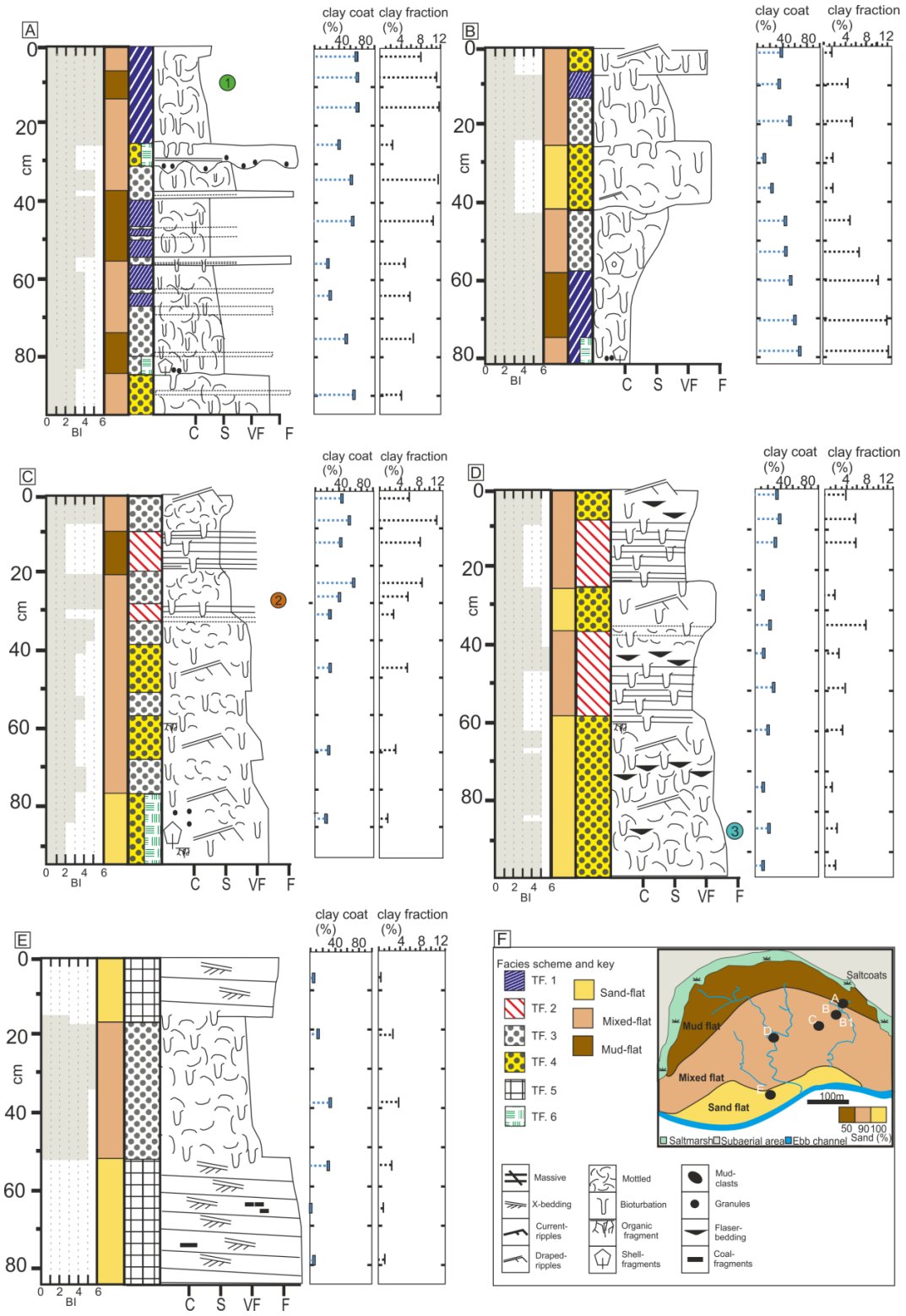

Figure 4-6 Sedimentological, clay-coat coverage, and clay fraction percentage logs of core from the Saltcoats tidal-flat. Graphic logs of bioturbation intensity, clay-coat overage, and clay fraction illustrate the near-surface distribution characteristics. See (F) for an explanation of the symbols and location of cores.

Dominant textures and sedimentary structures for each tidal-flat environments		Depositional processes and environment		Diagnostic textures and sedimentary structures of tidal-flat facies	Core geometry
Mud-flat (15-50 % sand): Sedimentary signature is characterised as intensely bioturbated to mottled texture, with a sparse to poorly preserved, silt dominated, and parallel laminated assemblage hosting granule sized mud interclast, lithics, and minor fragmented bioclasts. **Mixed-tidal flat (50-90 % sand): Intervals consist of heavily bioturbated, parallel and ripple laminated silt-lower medium sand sized sediment. The laminated intervals present a decrease in thickness and density of sand layers with distance landward, cumulating in a heavily bioturbated to mottled texture. Ripple cross lamination is confined to coarse and clean intervals (i.e. > 78 % sand) representing the lower geographic extent of mixed-tidal-flats (Fig. 4.3.).** **Sand-flat (> 90 % sand): Intervals are characterised as alternating massive to ripple cross laminated, bioturbated fine to upper medium sand, hosting granule sized mud clasts, and pebble sized lithic.**	**Mud-flat (TF. 1.2.3)**	Mud-flat	Formed via the principal suspension settling of fine grained predominantly mud to silt size sediment during slack water with post-depositional intensive bioturbation.	**(TF.1)** Mottled (intensely bioturbated) clay- to silt-sized sediment.	Undulating upper contacts depicted predominantly by colour and grain size.
		Mud-mixed flat	Alternating laminations of sand and silt represent "tidal bundle/ couplets' deposition, where each sand- to mud-lamination is produced by variations in tidal-current speed or by waves over a single tidal cycle (Dalrymple et al. 1992; Martinius and Van den Berg 2011). The difference between sand and silt layers derive from varying energy conditions during deposition. Laminations presents as horizontal, wavy, or discontinuous depending on the relative intensity of bioturbation.	**(TF.2)** Parallel laminated sand and silts	Commonly gradational contacts (owing to bioturbation intensity)
	Mixed-flat (TF 1.2.3.4)	Mud-mixed flat	The relative abundance of sand vs silt is dependent upon original surface geographic position (see Figs. 4.2, and 4.3), with variable intensities of bioturbation up to sediment homogenization. These two facies thus form a continuum governed by the pro-gradation and retro-gradation of the tidal-flats determined by the landward extent of sand deposition and ripple formation. Ripple mud drapes deposits during periods of slack-water.	**(TF.3)** Bioturbated, laminated silt- to very fine-grained sand. Silt dominated, often intensely bioturbated (progressing to mottled texture in places) consisting of subordinate sand laminations and ripple laminations, hosting minor bioclastic debris and organics (rootlets).	Contacts are typically bioturbated or gradational
		Mud-mixed – sand flat		**(TF.4)** Bioturbated, rippled-laminated (sand-dominated), v.fine- to fine-sand. Sand-dominated, often intensely bioturbated (approaching mottled), with minor silt laminations, mud drapes (flaser bedding), and current ripples	Contacts are typically bioturbated or sharp-undulating
	Sand-flat (TF 4.5.)	Sand-flat	Low-amplitude tidal-dunes and ripple migration, proximal to the ebb-channel. The observed sparse mud drapes would have been deposited during low-tide.	**(TF.5)** Very fine- to medium-grained, cross-bedded and current-rippled sand. Mud-drapes and mud-intraclasts are rare.	Common erosive-undulating lower contact.
		Tidal creek	Represent lag deposits observed in the base of tidal creek channels (Fig. 4.2).	**(TF.6)** Lithic and bioclastic rich sand. Massive upper fine sand grade sediment hosting lithic and disarticulate bioclastic debris.	Sharp grain size defined contacts.

Table 4-3 Characteristic features and interpretations of core encountered near-surface lithofacies of the Saltcoats tidal-flat. The distribution of lithofacies is shown in Figure 4.6.

4.7.2. Biological activity and indicators

4.7.2.1 Surface biological activity

Lugworm faecal cast density displays clear biogenic zonation across the tidal-flat (Figs. 4.2D, E, and 4.3E) with the greatest cast density found in the intermediate, mixed tidal-flat environments (> 50 faecal casts per m^2). Lugworms are largely absent in the mud-flat as shown by the lack of faecal casts (compare Fig. 4.1B to 4.3E). Lugworms showed a decreasing abundance with proximately to the ebb channel in the sand-flat (compare Fig. 4.1B to 4.3E).

The surface distribution of chlorophyll-a abundance (proxy for biofilm abundance) reveals the presence of biofilm-producing diatoms (MPB) in all tidal-flat environments, with chlorophyll-a varying from 11.8 to 46.8 μg/g (Fig. 4.3F). There is local heterogeneity of chlorophyll-a depicted in Figure 4.3F, but an overarching trend of increasing abundance towards the tidal limit. There is a clear difference in biofilm abundance between depositional environments with an average 38.4 μg/g in mud-flats, 17.7 μg/g in mixed-flats, and 13.4 μg/g in sand-flats (Table 4.1). This indicates that the greatest abundance of sediment-colonising, biofilm-producing diatoms (MPB) and such biofilm material occurs in the mud-flat, with much less in mixed-tidal-flats, and least in sand-flat sediments (compare Fig. 4.1B to Fig. 4.3F).

Diatoms and biofilms are present in surface sediments as aggregates in association with clay-grade material, typically attached to sand-grain surfaces (Fig. 4.4H). Biofilms are present in dehydrated form (an artefact of sample preparation) as thin, wrinkled films coating sand-grain surfaces (Fig. 4.4G). A network of fine, fibrous filaments occur in surface sediments (Figs. 4.4, 4.5) to create linkages between sand-grains; a textural characteristic previously shown to be derived from clay mineral attachment on a biofilm (EPS) root structure (De Winder et al. 1999; Higgins et al. 2003; Hoagland et al. 1993; Malarkey et al.

2015; Vos et al. 1988; Wooldridge et al. 2017a). As a result of sample preparation of near-surface sediment (i.e. thin section construction) diatoms and biofilm film coatings are not identifiable, although the biologically-mediated clay coat textures (i.e. clay linkages between grains) are present (Fig. 4.7) (Wooldridge et al. 2017a).

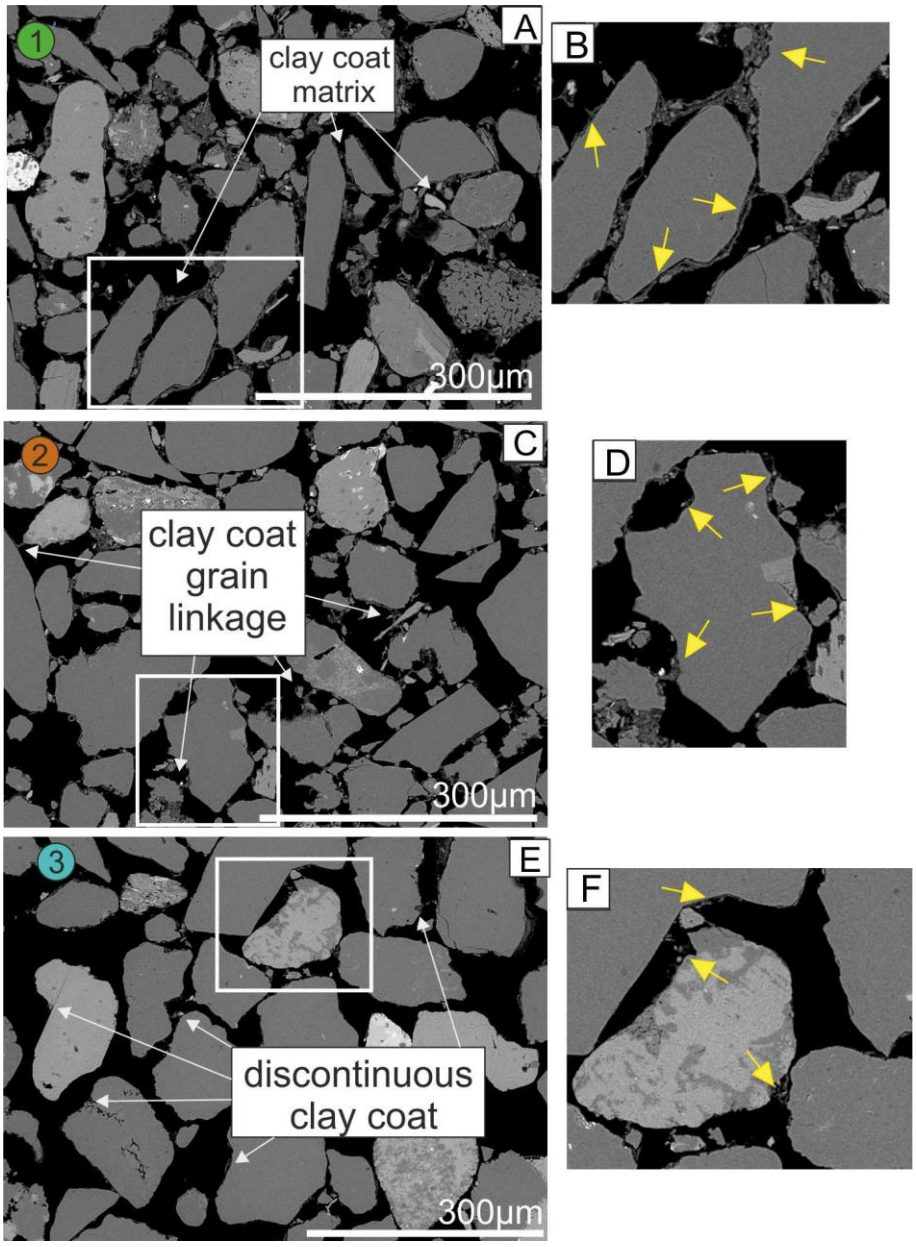

Figure 4-7 Scanning electron microscopy (SEM) images of near-surface clay-coated sand-grains: mud-flat (A, B), mixed-flat (C, D), and sand-flat (E, F) intervals. The position of the imaged sediment is illustrated in Figure 4.6 and correlated by circles 1, 2, and 3. Arrows indicate regions and key textural characteristics of clay-coats.

4.7.2.2 Near-surface biological activity

Using the qualitative bioturbation intensity scale proposed by Taylor and Goldring (1993), showed that bioturbation intensity in near-surface, tidal-flat, sediment varied from 0 (absent) to 6 (complete obliteration of original textures , Fig. 4.6). Extensive bioturbation occurs in the mixed- and mud-tidal-flat environments while relatively reduced amounts of bioturbation occurred in the sand-flats.

Total carbohydrate sampling commenced at 5 cm depth, which is well below the depth reported for typical, active diatom biofilm production (4 to 5 mm) (Hoagland et al. 1993; Stal 2003). This strategy was implemented to avoid active (present day) biofilm growth masking patterns of palaeo-biofilm abundance (Fig. 4.3F). The data indicate that carbohydrate is pervasively present in tidal-flat sediment but with a heterogeneous abundance distribution (Fig. 4.8). Sand-flat sediments have an average carbohydrate content of 192.6 μg/g, mixed-flats have 759.0 μg/g, and mud-flats have 767.8 μg/g (Table 4.1). The pattern of increased sediment biofilm abundance in mud- and mixed- tidal-flat environments is comparable to surface sediments (compare Fig. 4.3F to Fig. 4.8). The total carbohydrate fraction has a positive correlation with increasing clay fraction percentage, and a negative correlation with increasing mean sediment grain size (Table 4.4). There is no statistical correlation between total sediment carbohydrate and depth (Fig. 4.8 and Table 4.4).

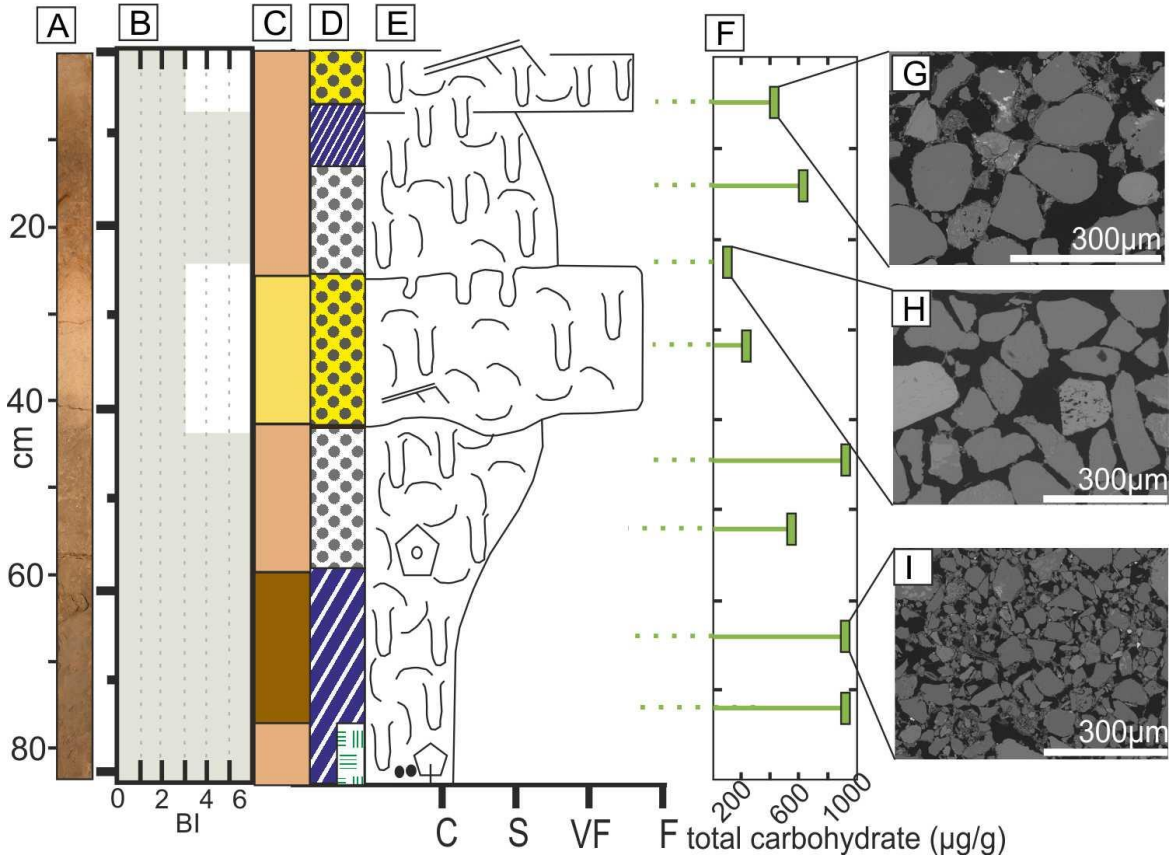

Figure 4-8 Sedimentary log illustrating biofilm abundance in the near-surface tidal-flat sediment: the appearance of dried core material (A), bioturbation intensity (B), the environment of deposition (C), lithofacies (D), sedimentary characteristics (E), the near-surface variability in total carbohydrate content (F), and scanning electron microscopy (SEM) images of the analysed intervals (G, H, and I). For an explanation of the symbols and location of the core see Figure 4.6F.

	Clay-coat coverage (%)	Mean grain size (µm)	Grain size sorting (σg)	Clay-fraction (%)	Sand abundance (%)	Chlorophyll-a	Total carbohydrate	Depth (cm)
Clay-coat coverage (%)		0.000***	0.000***	0.000***	0.000***	0.002*	0.006*	0.134
Mean grain size (µm)	-0.75		0.000***	0.000***	0.000***	0.002*	0.003*	0.175
Grain size sorting (σg)	0.84	-0.76		0.000***	0.000***	0.005*	0.001*	0.542
Clay-fraction (%)	0.87	-0.70	0.76		0.000***	0.000***	0.013**	0.215
Sand abundance (%)	-0.86	0.83	-0.87	-0.85		0.000***	0.011**	0.425
Chlorophyll-a	0.90	-0.70	0.65	0.95	-0.83		N/A	N/A
Total carbohydrate	0.86	-0.89	0.93	0.82	-0.83	N/A		0.069
Depth (cm)	-0.23	0.21	-0.09	-0.19	0.12	N/A	0.67	

Table 4-4 Pearson's Correlation Coefficient matrix calculated from sedimentological and biological data. For P=-values < 0.05 (*), the correlation is statistically significant. P values of (P < 0.01) (**) and (p< 0.001) (***) represent very and extremely significant correlations, respectively.

4.7.3. Characteristics of detrital-clay-coated sand-grains: morphology and mineralogy

The textural characteristics of surface and near-surface clay-coated sand-grains are presented in Figures 4.4, 4.5 (surface) and 4.7 (near-surface). Clay coats cover all component grains (Fig. 4.5). Tidal-flat clay coats consist of a network of partial grain coating and grain-linking, fibrous filaments composed of clay minerals and clay- to silt-sized material (organics, lithics, and clay minerals) capable of coating up to 76 % of grain surfaces. Texturally clay-coats are thickest in the mud- and mixed-tidal-flat sediments (Fig. 4.5).

Clay coats in the sand-flat samples occur as discontinuous thin coats, with greatest thickness in grain indentations; there is an absence of fibrous linkages between grains in sand-flat sediments (Fig. 4.5). Figures 4.4 and 4.7 reveal no obvious differences in the textural characteristics of surface and near-surface clay coats. No grain supporting clay matrix material was present in any of the imaged samples.

Detrital-clay-coats are composed of interlocking heterogeneous clay minerals which produce a mixed mineralogy, composed of illite, chlorite, and kaolinite (Figs. 4.5, 4.9, 4.10 and Table 4.2). There was no difference in clay-coat mineralogy between clay coat textural types (e.g. coating- vs bridging-structures) or framework grains (e.g. bioclasts, quartz, or feldspars) (Fig. 4.5). The mineralogy of clay coats is comparable to the whole sediment, clay mineral assemblage (as determined by X-ray diffraction analysis) previously published for the Ravenglass estuary (Daneshvar 2011; Daneshvar and Worden 2016; Wooldridge et al. 2017b). Clay mineralogy is here reported as index values (e.g. illite/(illite + chlorite + kaolinite)) (employing the assumption that the majority of the sediment clay mineral content is present as clay coat) to constrain the relative distribution trends of the grain

coating clay mineral assemblage. Figures 4.9 and 4.10 show that clay-coat mineralogy varies across tidal-flat sediments.

The clay-coat mineralogy of both surface and near-surface sediment (Figs. 4.9 and 4.10, respectively) have a mixed mineralogy with a minimum 60 % of the clay minerals composed of illite. The proportion of clay-coating chlorite is highest in the coarser-grained (higher energy) sand-flat samples. The surface trend of decreasing illite and increasing chlorite values with progression from the mud- to sand-flat is replicated in the near-surface (e.g. compare Figs. 4.9 to 4.10). A key observation is that clay-coat mineralogy is not homogeneous across tidal-flat sediments.

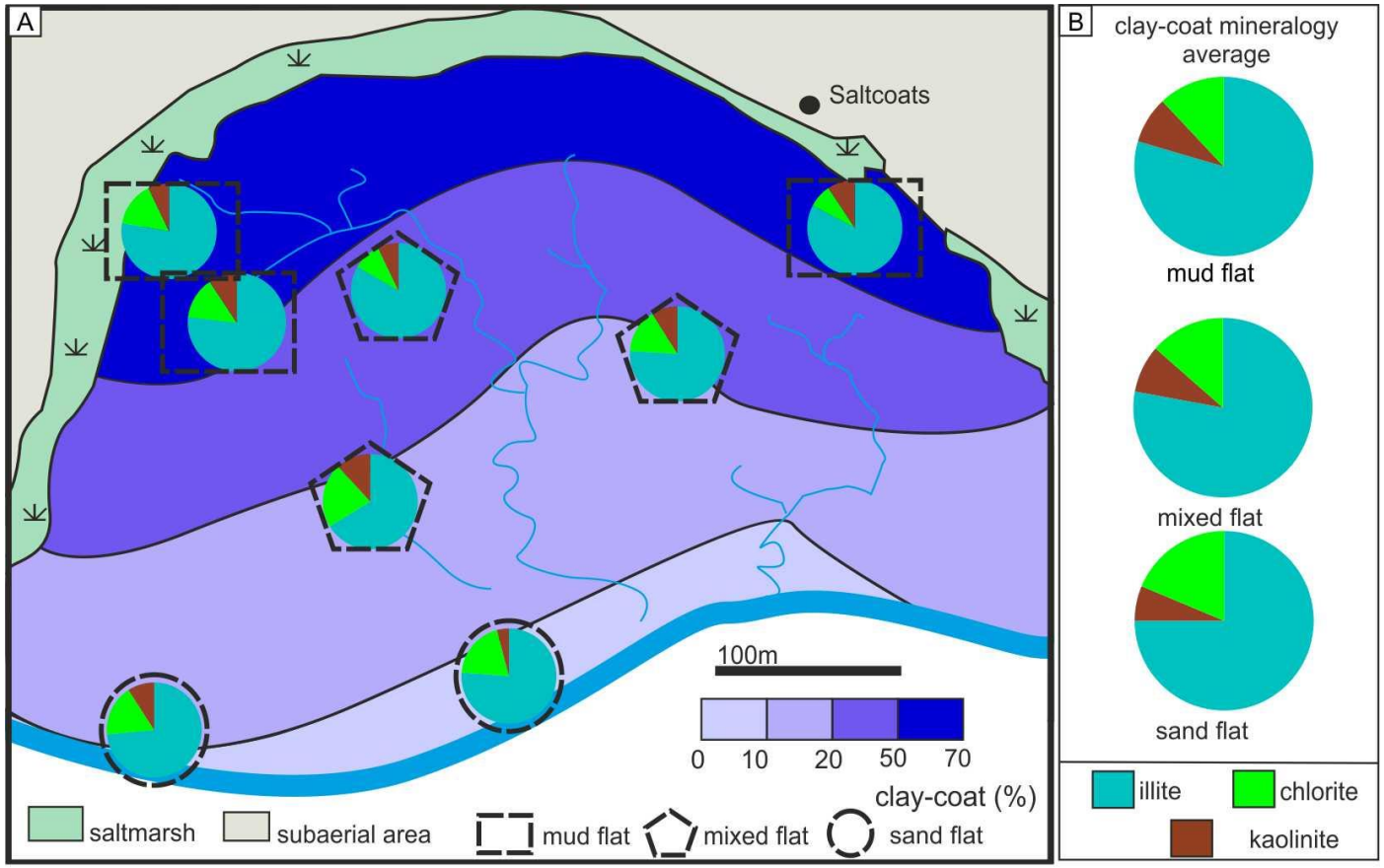

Figure 4-9 Map of surface sediment clay-coat coverage. (A) Areas in light purple signify minimal (< 10 %) partial clay-coat grain coverage, with dark purple to blue regions indicating extensive surface clay-coated sand-grains. Pie charts indicate index values of clay-coat mineralogy. (B) Pie charts illustrating the surface clay-coat mineralogy, grouped by dispositional environment.

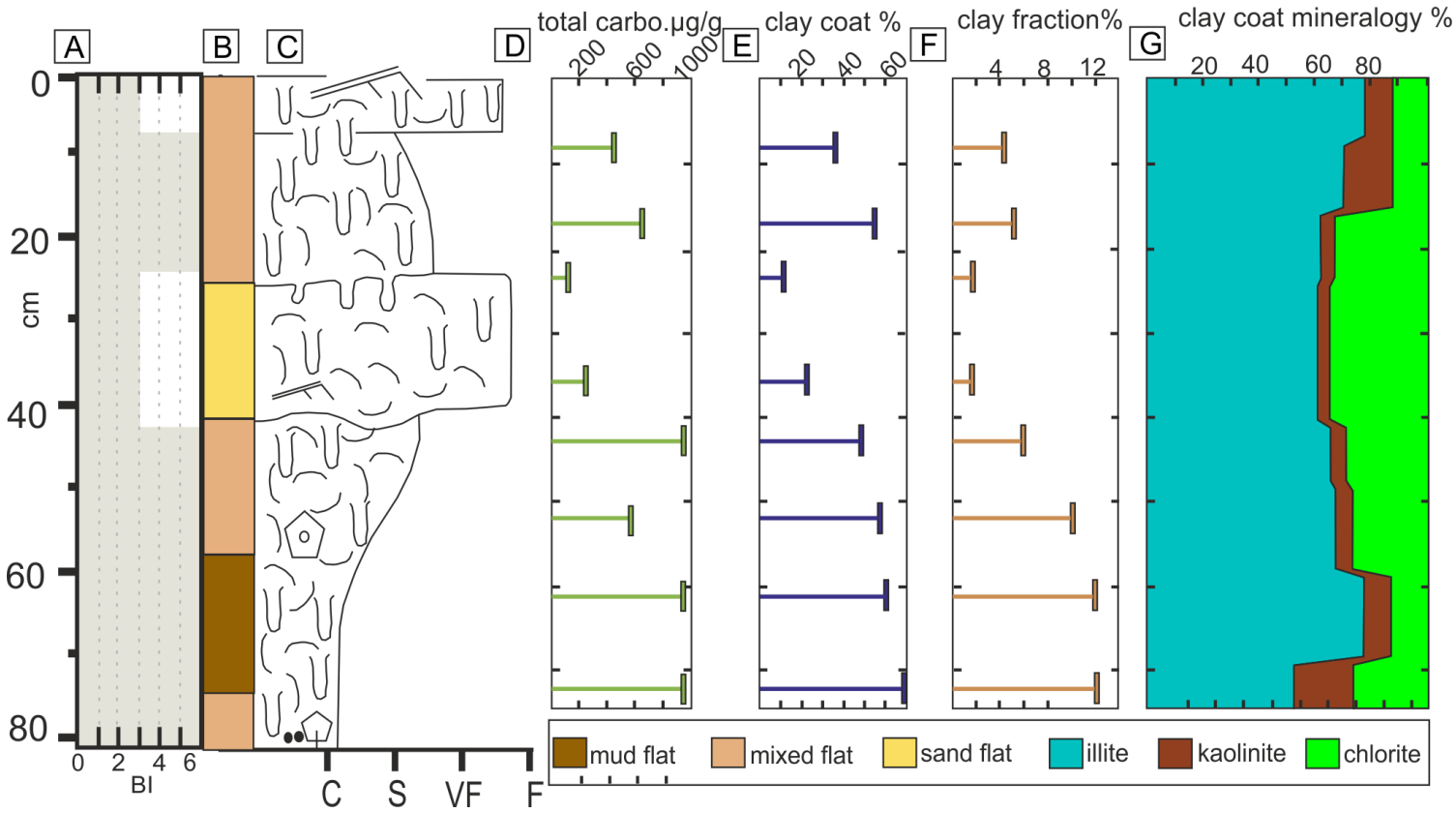

Figure 4-10 Synthesis log of correlated near-surface data sets. Bioturbation intensity(A), the environment of deposition (B), sedimentary log (C), total sediment carbohydrate (D), clay-coat coverage (E), clay fraction percentage (F), and clay-coat mineralogy (G).

4.7.4. Clay coat distribution

4.7.4.1. Clay-coat coverage surface variability

Clay coats are heterogeneously distributed across surface and near-surface tidal-flat sediments (Figs. 4.6 and 4.9). The degree of clay-coat coverage ranged from 3.4 to 69.4 % (Table 4.1). Clay-coat coverage increases towards the tidal limit, revealing a landward increase, with average clay-coat coverage of 3.9 % for sand-flat, 28.7 % for mixed-flat, and 61.7 % for mud-flat sediment assemblages (Fig. 4.9). There is also heterogeneity in the proportion (percentage of measured grains) of grains devoid of clay-coats; sand-flats have 43 %, mixed flats have 6 %, and mud-flats have 1 %, respectively.

4.7.4.2. Clay-coat coverage: near-surface variability

The heterogeneous distribution of clay-coat coverage in the near-surface is illustrated in Figures 4.6 and 4.10. Clay coats from intervals with a high sand percentage (> 90 %), and textural characteristics consistent with a sand-flat environment of deposition (Fig. 6), have the lowest average percentage clay-coat coverage 15.7 % with 24 % of measured grains devoid of coats. Samples from mixed- and mud-flat intervals have average grain coverage values of 42.8 % and 61.9 %, respectively. Clay-coat coverage increases in more heterolithic intervals and those typically characterised by increased bioturbation intensity (Fig. 4.6).

4.7.5. Correlations between clay-coat coverage, depth, sedimentological, and biological data sets

Figures 4. 6, 4.10 and Tables 4.1, 4.4 show that, despite increased clay-coat coverage values for mixed- and sand-flat intervals in the near-surface (compared to surface samples), there is no identifiable, systematic, increase with depth. Pearson's correlation was used to test the statistical significance between: (i) clay-coat coverage and depth, and (ii) the post depositional increase in clay-coat coverage. This approach was, firstly, applied to the

whole data set (Table 4.4) and, secondly, undertaken on samples categorised via sand percentage (sand-mud ratio) into a coherent depositional environment framework (i.e. surface mixed-flat compared to near-surface mixed-flat samples). The second analysis revealed a Pearson's correlation of -0.16 with a P value of 0.71, 0.05 with a P value of 0.81, and 0.28 with a P value of 0.31, for mud-, mixed-, and sand-flat samples, respectively. The data thus show that there is no statistical link between overall clay-coat coverage and depth (illustrated in Fig. 4.6 and Fig. 4.11D), and no statistical post depositional increase in clay-coat coverage with depth per depositional environment.

Textural analysis has identified clear differences between component tidal-flat depositional environments, both in terms of sediment characteristics (Table 4.1 and Figs. 4.2, 4.4, 4.5, 4.8) and biofilm abundance (Figs. 4.3F, 4.7 and Table 4.1). A Pearson's correlation matrix was used to test the statistical significance between data sets of clay-coat coverage, sediment heterogeneity, and biological content (Table 4.4). Figure 4.12 compares clay-coat coverage and sand percentage, which illustrates a strong, linear statistical correlation (Table 4.4), indicating a 25 % difference in clay coating extent between the maximum sand-flat sample and minimum mud-flat sample. There is significant correlation between the extent of clay-coat coverage and sediment heterogeneity in the form of grain size, sorting, and clay fraction percentage (Fig. 4.11, Table 4.4).

Clay-coat coverage has been plotted as a function of sediment heterogeneity for surface and near-surface sediment (Fig.4.11) with the percentage clay-coat coverage increasing in a linear trend with a decreasing grain size and increasing clay fraction percentage. Figure 4.11 shows that, for extensive clay-coat coverage (defined here as > 50 % average grain coverage), a very fine sand with a > 7 % clay fraction component is necessary; these conditions are found in mud- and mixed-tidal-flat environments.

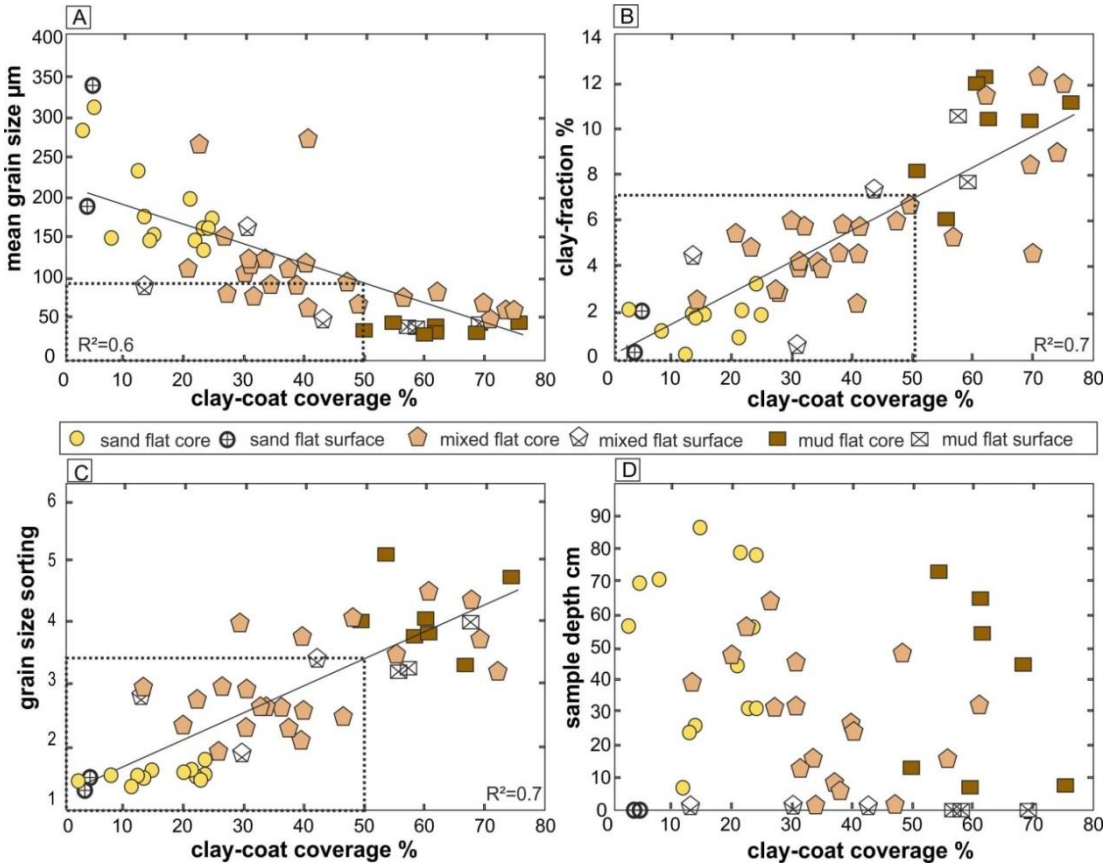

Figure 4-11 Plot of mean grain size, sediment clay-fraction percentage, sorting, and sample depth against clay-coat coverage.

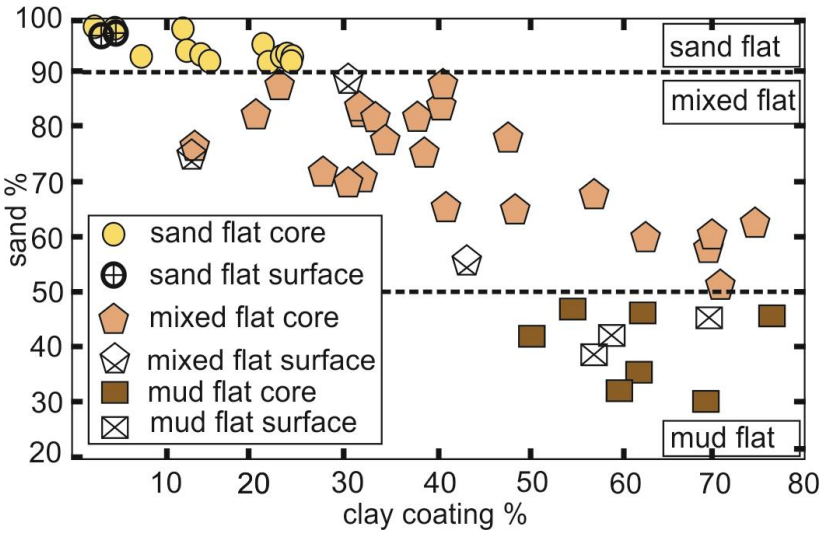

Figure 4-12 Plot of depositional environment (sand mud ratio) against clay-coat coverage.

The surface distribution characteristic of the lugworm population does not spatially correlate to the degree of clay-coat coverage (compare Fig. 4.3E to Fig. 4.9), with mud-flats devoid of an extensive lugworm population. The bioturbation intensity recorded in near-surface sediment (Fig. 4.6) showed no correlation to the extent of clay-coat coverage (Fig. 4.13).

Figure 4.14 and Table 4.4 show a strong, statistical correlation between the degree of clay-coat coverage and sediment biofilm abundance for both surface (chlorophyll-a content) and near-surface (total carbohydrate) sediment. Clay-coat coverage thus increases with an increased abundance of sediment biofilms (Figs. 4.14, and 4.10, and compare Fig. 4.3F to Fig. 4.9).

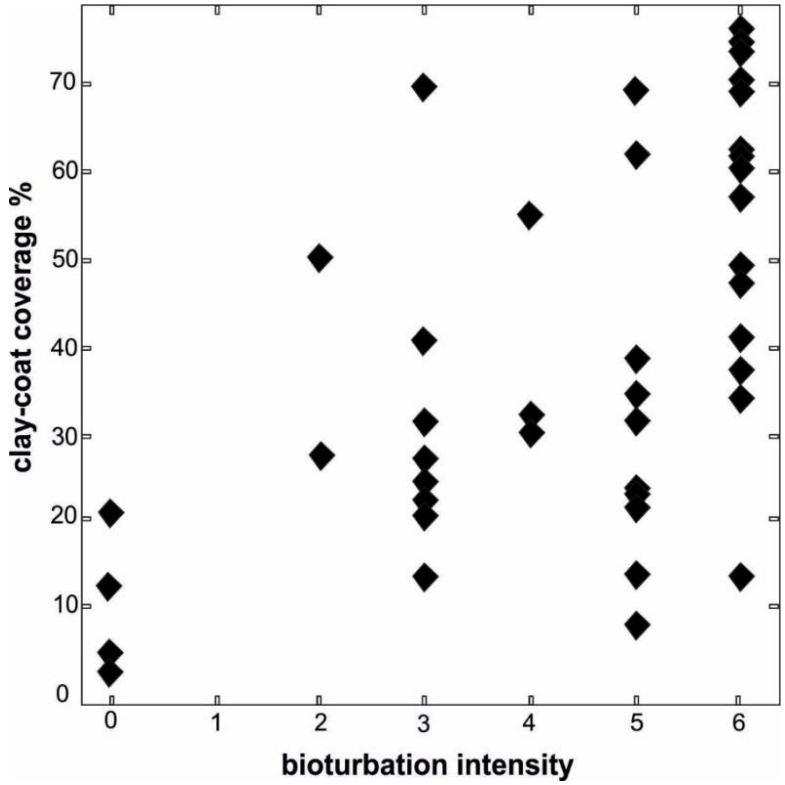

Figure 4-13 Plot of near-surface bioturbation intensity against clay-coat coverage.

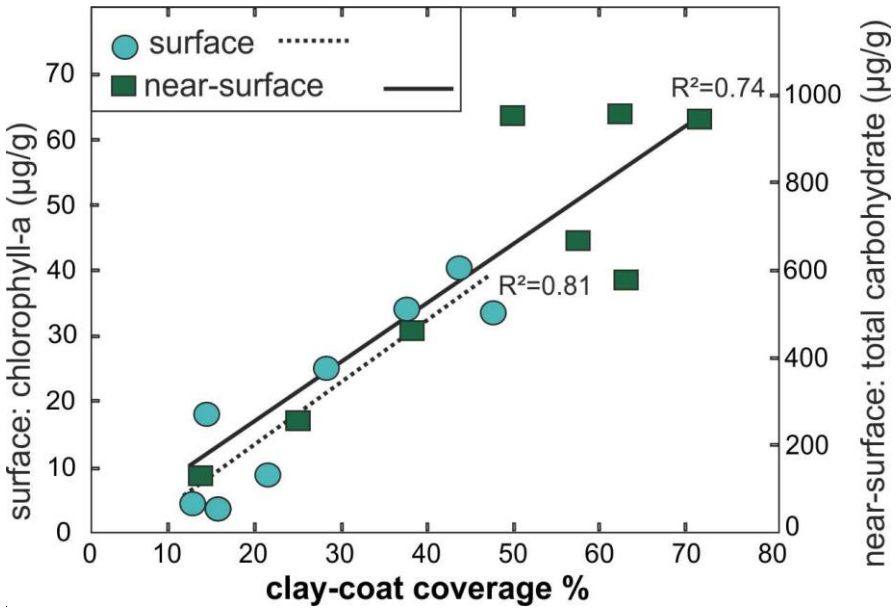

Figure 4-14 Plot of surface (chlorophyll-a) and near-surface (total carbohydrate) sediment biofilm abundance against clay-coat coverage.

4.8. Discussion

4.8.1 Origin of the sedimentological and biological characteristics of the Saltcoats tidal-flat

Tidal-flats typically exhibit zonation in grain size, clay fraction percentage, and surface morphology (Amos 1995), which has been reported to result from the dominant hydrological conditions (i.e. velocity asymmetry between flood and ebb currents) (Amos 1995; Yang et al. 2005). The Saltcoats tidal-flat sediments (surface and near-surface) show a comparable landward decrease in sediment grain size and increased sediment heterogeneity.

The clay fraction occurs principally as clay-coats in the sand-dominated sediment samples (mixed- and sand-flat) of the Saltcoats tidal-flat (Fig. 4.5), explaining the strong correlation between clay-fraction percentage and clay-coat coverage (Table 4.4 and Fig. 4.11B). It is likely that the mechanism that controls the occurrence of clay-coats also strongly influences heterogeneity in tidal-flat sediments. The correlation between clay fraction percentage and the environment of deposition across tidal-flat sediments suggests that sediment heterogeneity is controlled by clay particle entrapment at the site of deposition.

The landward increase in sediment biofilm abundance in surface sediment (chlorophyll-a) indicates that mixed- and mud-tidal-flat environments are extensively colonized by biofilm-producing diatoms. The distribution pattern for the Saltcoats tidal-flat is comparable to that reported for the Severn Estuary, between England and Wales (Underwood and Paterson 1993), in which significantly higher concentrations of chlorophyll-a occurred in sediments towards the tidal limit (landward direction). Similarly, the chlorophyll-a distribution patterns for the Saltcoats tidal-flat are comparable to the Fraser River Estuary, British Columbia, Canada (Jiménez et al. 2015), and the bays in the Ebro delta complex, Spain, (Delgado 1989). The consistent biological trends indicate a common nature and

suggest that diatom and biofilm abundance is broadly predictable in modern estuarine and deltaic tidal-flats.

The negative trend of increasing chlorophyll-a abundance with a decreasing grain size (compare Fig. 4.3F to B and Table 4.4) has also been reported in tidal-flat sediments of the Humber Estuary, UK, the Marennes Estuary, France, and the Dollard Estuary, Netherlands (De Brouwer et al. 2003; Paterson et al. 2000). The positive correlation between biofilm abundance and clay fraction is less well established in the literature (Table 4.4). Koppel et al. (2001) reported that diatoms grow best in high clay fraction rich sediments, so that once EPS is excreted by the diatoms, it has the effect of trapping more clay-silt sized particles, producing more environmentally advantageous conditions and a positive feedback.

The increase in biofilm abundance in the lower energy environments (i.e. mixed- and mud-flats), composed of a finer grain size and correlating to a more clay fraction rich and poorly sorted sediment assemblage, is consistent with the reported hydrological control on diatom (MPB) abundance (Stal 2003; Underwood and Paterson 1993). The higher energy, more turbulent, conditions in sand-flat environments inhibit the establishment of dense diatom (MPB) communities through the constant remobilisation of the sediment substrate (i.e. ripples and dunes, Fig. 4.2G) that disperse diatoms and causes grain to grain collisions and destruction of the fragile silicate diatom frustules (Stal 2003; Underwood and Paterson 1993). The reduced light exposure (tidal period) of sediments close to the low water mark has also been reported as the potential origin for the distribution characteristics of diatom (MPB) abundance (Underwood and Paterson 1993). To assess the dominant control on the abundance of sediment biofilms a focussed study mapping out the abundance of chlorophyll-a against of all geomorphological, hydrological, and biological (macro- and micro-organism populations) conditions would be required.

The near-surface pattern of elevated sediment biofilm abundance in finer grained sediment resulting from mud- and mixed-tidal-flats and the lack of a systematic pattern with depth suggests that biofilm abundance is directly inherited from surface processes and is preserved in the accumulated sediment. Furthermore water insoluble carbohydrate fractions are probably tightly bound to sand-grain surfaces as biofilm (De Winder et al. 1999) and could serve to bind clay and other minerals to grains.

The heterogeneous distribution and range in the concentrations of total carbohydrate with depth are broadly consistent with other near-surface studies (10 mm depth) (De Winder et al. 1999) and (20 mm depth) (Taylor and Paterson 1998). However, it must be noted that such a study on the scale of our work on the Saltcoats tidal-flat has not previously been published.

4.8.2. Biological control on sediment heterogeneity

Tidal-flat clay fraction, mean grain size, and grain sorting values have been illustrated to derive at least in part from the preferential entrapment of clay- and silt- sized particles by biofilms (Garwood et al. 2015; Jones 2017). Tidal-flats consist of non-cohesive, unconsolidated sand, physically cohesive muds, and sticky, cohesive biofilms (Jones 2017). The influence of biofilms in tidal-flat sediment was illustrated by Faas et al. (1993) in the Bay of Fundy, Canada, in which a structureless mud-flat, that had the natural biofilm artificially removed, by a biocide was transformed into a non-cohesive, rippled silt-flat in four tidal cycles.

The influence of sediment-colonising organisms on clastic sediment heterogeneity remains poorly-constrained (Garwood et al. 2015; Jones 2017). The spatial distribution of clay fraction and biofilm abundance is remarkably similar (compare Fig. 4.3C to F). The reported biological entrapment of silt-to clay-sized material (Garwood et al. 2015; Vos et al.

1988) has resulted in a reduced mean grain size (Fig. 4.3B) and produced the statistical correlation between clay fraction percentage and chlorophyll-a abundance (Table 4.4).

The correlation between grain size (and clay fraction) and biofilm abundance at Saltcoats is consistent with a study of the Minas Basin, Bay of Fundy, Canada (Garwood et al. 2015). Biofilm production is restricted to the top few centimetres of the sediment (where light penetrates) so that active, biofilm-mediated entrapment of clay minerals as clay coats is restricted to the sediment surface. The implication is that near-surface trends in biofilm abundance and clay fraction percentage (principally present as clay coats) directly results from the surface abundance of biofilm-excreting diatoms.

4.8.3. Textural characteristics of detrital-clay-coated sand-grains in a tidal-flat sedimentary package

A key conclusion is that clay-coat morphology is heterogeneous across the Saltcoats tidal-flat (Fig. 4.5). The morphology of the clay-coated sand-grains in this study are comparable with those reported from the tidal-flats of the Anllóns Estuary, northwest Spain, and the Leirárvogur Estuary, Iceland (Dowey 2013; Dowey et al. 2017). The evolution in clay-coat morphology between mud- and sand-flat sediments could derive from; (i) the increased hydraulic energy in the sand-flat leading to reduced colonisation by benthic diatoms, and commensurately less biofilm creation to bind clays to grain surfaces (Delgado et al. 1991; Stal 2003), or (ii) the partial abrasive removal of primary clay coat projections and bridging structures on grain mobilisation (Wilson 1992).

In establishing the likely origin of clay coats and their distribution patterns it is worth comparing our interpretations to previously reported mechanisms of clay mineral attachment to sand-grain surfaces. Detrital-clay-coats from intertidal sediments have been cited to derive via the sedimentological processes of inheritance, mechanical infiltration, and drying adhesion (Dowey et al. 2017; Moraes and De Ros 1992; Wilson 1992) and

biologically via macro-and micro-organism produced biofilms (McIlroy et al. 2003; Needham et al. 2005; Wooldridge et al. 2017a; Worden et al. 2006).

The textural morphology of clay coats reported in this study (Figs. 4.4, 4.5, and 4.7) are consistent with previously reported biologically-mediated, clay coat textural components (Wooldridge et al. 2017a) and comparable to the textures of biofilm (EPS) coatings in sediment (Kessarkar et al. 2010; Malarkey et al. 2015; Vos et al. 1988). The identification of intricate bridging structural components in clay coats presents an advancement in the understanding of clay-coat morphology from the traditional ridged, bridged, and clumped textural classification schemes (Wilson 1992; Wooldridge et al. 2017b). It has been noted that biofilm-producing diatoms are associated with detrital-clay-coated grains of the Anllóns Estuary, Spain (Dowey 2013), the Mandovi Estuary, India (Kessarkar et al. 2010), and reported in association with the Gironde Estuary, France (Virolle et al. 2016).

The textural characteristics of clay-coated sand-grains, the positive statistical and spatial correlation between clay-coat coverage and biofilm abundance in both surface (chlorophyll-a) and near-surface (total carbohydrate fraction) sediment, and the observation of diatoms and biofilms on sand-grain surfaces and as components of clay-coats, all strongly suggest a biological control on clay mineral attachment to grain surfaces (Wooldridge et al. 2017a).

4.8.4. Controls on the distribution of clay-coated sand-grains in the near-surface

Trends in clay-coat coverage in the three sedimentary environments (mud-, mixed-, and sand-flat) are broadly reflected in the clay-coat coverage in the near-surface (Table 4.1). Mud-flats have the highest clay-coat coverage (surface, 61.7 %; near subsurface, 61.9 %), while sand-flats have the least coverage (surface, 3.9 %; near subsurface, 15.7 %).

Table 4.1 shows that clay-coat coverage appears to be somewhat higher in the near-surface than the surface for the mud-, mixed-, and sand-flat samples with a 0.2 %, 13 %, and 11.8 % increase, respectively. It is perhaps noteworthy that the clay-coat coverage of surface sand-flat samples increases on average by a factor of 4 in the near-surface (Table 4.1); whereas, clay-coat coverage of surface mixed-flat samples increases on average by a factor of 1.5. Mud-flats do not show any significant variation in clay-coat coverage. There seems to be at least two possible explanations for the variation in clay-coat coverage between surface and near-surface mixed- and sand-flat environments:

1. The variation in clay-coat coverage in sand-flat samples between surface and the near-surface falls within the realm of that is observed (Fig. 4.9) or previously published for surface tidal-flat (sand and mixed) sediments of the Ravenglass Estuary (Wooldridge et al., 2017a).
2. Infiltration may have occurred especially in near-surface sand-flats.

Any sand-flat package that is overlain by mud- or mixed-tidal-flat sediments is unlikely to encounter infiltration at the present day, but, it may have experienced infiltration when exposed at the surface. In addition, clay content may be incorporated into the sediment through bioturbation, from overlying clay-rich facies (Needham et al. 2005). At the surface, mud-flats act as a largely impermeable barrier to pore-waters laden with clay, thus, creating fluidised-mud (Fig. 4.2B); consequently, any underlying 'clean sands' are unlikely to experience infiltration that will lead to any substantial, post-depositional increase in clay-coat coverage.

The lack of a systematic increase in clay-coat coverage with depth, or even in a bed (corresponding to a single sedimentary environment, Fig. 4.6) seems to suggest that metre-scale infiltration is not occurring at the present day. The absence of a statistically-significant, metre-scale trend in the extent of clay-coat coverage between surface and

near-surface sediment (Figs. 4.6 and 4.11D), suggests that the possible post-depositional processes of infiltration and bioturbation have not significantly affected primary depositional (top few centimetres) trends in clay coat characteristics.

The implication from Figure 4.6 is that the trend and distribution of clay-coated sand-grains in the near-surface are principally controlled by surface-based processes. This observation is in accordance to the study by Buurman et al. (1998) in which they argued that due to the typical flocculation of clays and suspended clay- to silt-sized material, the upper pores of the sediment will become clogged and thus extensive infiltration derived penetration of clay material into course sediment (e.g. sand-flats) is unlikely.

Depositional environment thus exerts a dominant control on the characteristics of clay coats in tidal-flat sediment (Table 4.4), this is reasonably well established (Bloch et al. 2002; Dowey 2013; Ehrenberg 1993; Luo et al. 2009; Wooldridge et al. 2017b). Dowey et al. (2017) presented a 1 meter core transects from the Anllóns Estuary, Spain, in which the heterogeneous subsurface distribution in the extent of clay-coated sand-grains was reported to vary depending on the original environment of deposition and there was no systematic overprinting of trends with depth below the surface. The similar trends in clay-coat coverage between the Saltcoats tidal-flat and the tidal-flats of the Anllóns Estuary, Spain, suggest that this is a general feature of many if not all tidal-flats.

The post-depositional process of infiltration has been reported from arid to semi-arid environments due to fluctuating water tables (Matlack et al. 1989; Wilson 1992). However, infiltration of sediment laden waters through the estuarine sediments at the Saltcoats tidal-flat, Ravenglass Estuary, has a possible secondary role in increasing clay-coat coverage but does not alter primary (surface) clay-coat coverage patterns. This is probably because infiltration cannot operate on the metre-scale as a consequence of clay-rich beds acting as baffles.

Animal-sediment interaction-induced sediment mixing, particularly in the highly bioturbated intervals typical of mud and mixed tidal-flats, may have contributed to elevated clay-coat grain coverage, but does not directly explain the distribution patterns of clay coats in the surface or near-surface (compare Fig. 4.3 to 4.9 and Fig. 4.13).

The spatial distribution of surface clay fraction (XRD) mineralogy for Saltcoats was documented by Griffiths (2017) to display a relative increase of illite and decrease in chlorite towards the landward margin (i.e. mixed- and mud-flats). This pattern is commensurate with clay-coat mineralogy of the surface and near-surface sediment, reported here (Figs. 4.9 and 4.10). The relative enrichment of illite in the finer sediment and chlorite in the coarser sediment was interpreted by Griffiths (2017) to result from hydraulically-controlled fractionation as a function of the grain size of different clay minerals in this estuary. Figure 4.5 shows that chlorite in clay coats typically occurs as larger “flakes” compared to illite.

The similarity of bulk clay-coat mineralogy (Fig. 4.9) and fine fraction mineralogy (XRD) previously reported for the estuary (Wooldridge et al. 2017b) suggests that the attachment mechanism does not preferentially adhere, particular clay minerals and instead clay-coat mineralogy reflects the local clay mineral sediment assemblage. The result is clay-coat mineralogy is principally controlled by: (i) provenance patterns and local physicochemical processes (e.g. weathering) that lead different phyllosilicates to have different grain sizes and (ii) by the estuarine hydrologically controlled segregation of the clay mineral assemblage (i.e. chlorite dropped out of suspension closer to the main ebb channel resulting in sand-flats enriched in chlorite).

Surface clay-coat mineralogy is similar to clay-coat mineralogy in the near-surface, with chlorite most enriched in the sand-flat sediments. However noted, the near-surface sand-flat facies have a slightly higher chlorite index than the surface sediments as well as

containing a slightly higher clay fraction (Tables 4.1 and 4.2). Mass balance considerations seem to suggest that the additional 0.5 % clay fraction in the near-surface sediment, over and above the surface sediment clay fraction, was relatively chlorite-enriched with a chlorite index of 0.66. Values used in the equation are given in Tables 4.1 and 4.2 with working shown in the foot note [1].

There seems to be at least two possible explanations; (i) if, local infiltration occurred when sand-flat sediments were at the surface than it is suggestive that the infiltrating clay mineral assemblage was relatively enriched with chlorite, or (ii) the variation in chlorite content in near-surface sand-flats, falls within the realm observed in surface sediment (i.e. sand-flats which are more proximal to mixed-tidal flats are relatively clay fraction and chlorite enriched) (Wooldridge et al. 2017b).

If, large-scale post-depositional infiltration of clay minerals had occurred through the near-surface sediments than a more regular signature (i.e. over-printing the fractionated depositional surface clay assemblage) may be expected. The surface and near-surface clay coats show trends of distribution and mineralogy identical to surface sediments and there is a marked lack of a regular distribution with depth. This strongly suggests that clay-coat mineralogy and distribution trends in the near-surface are principally controlled by the surface based attachment of the locally deposited clay mineral assemblage.

4.8.5. Implication for the origin and prediction of clay-coated sand-grains in tidal-flat sediments

The relationship of clay-coat coverage to grain size and the magnitude of the clay fraction percentage is consistent with other reported surface based distribution models from the Anllóns Estuary, Spain, and Leirárvogur Estuary, Iceland, (Dowey 2013; Dowey et al. 2017).

[1]

$$mineralogy\ of\ additional\ clay\ fraction = \frac{((\text{clay fraction, near surface}) \times (\text{clay ratio, near surface})) - ((\text{clay fraction, surface}) \times (\text{clay ratio, surface}))}{(additional\ clay\ fraction\ betwen\ surface\ and\ near\ surface\ samples)}.$$

The formation of clay-coated sand-grains in sedimentary environments during, or very soon after, deposition can only occur in sediment that contains fine grained material (clay). Hence the correlation between clay coats and fine grain size, high clay fraction, and poorly sorted sediment can be expected since it is characteristic of low energy, tidal-flat hydrological conditions (Flemming 2012). In contrast, sediments deposited in high energy environments that lack means to accumulate clay cannot easily develop clay-coated sand-grains. However, this study has provided a link between microbiological activity, the resulting bio-glue and clay mineral attachment to sand-grain surfaces (Wooldridge et al. 2017a). The abundance of sedimentary biofilms is controlled by the environmental niche of the biofilm excreting organisms (dominated by diatoms) which is primarily a function of hydrodynamic conditions in an estuary (Stal 2003; Underwood and Paterson 1993).

This study has shown that post-depositional bioturbation and infiltration seem to be less important than has been previously suggested. The implication is that distribution, grain coverage extent, and mineralogy of clay-coated sand-grains in near-surface sediments results from surface-controlled processes with a strong influence of the local sedimentary environment. Infiltration and bioturbation have a possible secondary role in increasing clay-coat coverage but do not alter the primary (surface) trends in clay-coat coverage or mineralogy patterns.

The generation of sedimentary and biological proxies for the extent of detrital-clay-coat coverage offers a crucial step towards building a credible capability for making predictions about grain coat coverage in ancient and deeply-buried reservoir rocks. The observation that the principal controls on the occurrence and extent of clay-coated sand-grains in the near-surface are the biological and sedimentological conditions at the site of deposition is fundamental. If specific depositional environments can be predicted using seismic data, wireline logs, core, and cuttings then it may be possible to start predicting where, and to

what extent grain coating clays are present by applying surface based analogue models of clay-coat coverage (Dowey et al. 2017; Wooldridge et al. 2017a; Wooldridge et al. 2017b).

4.9. Conclusions

1. The clay-fraction in tidal-flat sediments occurs principally as clay-coats and bridging structures between sand-grains.
2. Tidal-flat grain size varies from silt to medium sand, the clay fraction varies from 0.2 to 12.2 %, and sorting varies from well sorted to very poorly sorted.
3. Detrital-clay-coated grains consist of discontinuous coats and bridging structures between sand-grains. Clay-coats are composed of clay minerals, silt- to clay-sized lithics, and organics (diatoms). Clay-coat coverage ranges from 2.5 to 76 % with a mixed mineralogy composed of illite, kaolinite, and chlorite.
4. Detrital-clay-coated sand-grains in the near-surface have most extensive grain coverage in samples from mud-flat facies (62 %) with much less in mixed tidal-flat facies (43 %), and least in sand-flat facies (16 %), consistent with patterns in surface clay-coat coverage.
5. In tidal-flat sediments, an assemblage composed of a very fine sand, that contains > 7 % clay-grade material is required to create extensive (> 50 %) clay-coat grain coverage. These conditions are met in the mixed- and mud-flat environments.
6. Biofilm abundance in surface sediments increases from the channel axis to the shore and thus increases from sand-flats to mixed-flats and then to mud-flats adjacent to the shore.
7. Biofilm content is pervasive in all tidal-flat sediments (surface and near-surface). The biofilm abundance of the near-surface shows the same trends as surface sediment with the greatest biofilm content in mud-flat facies and least in sand-flat facies.

8. Clay-coat mineralogy varies across tidal-flat sediments. Sediment in mud-flat environments, are richer in illite and poor in chlorite than sediment in sand-flat environments. The same pattern occurs in samples from the near-surface with sediment from mud-flat facies richer in illite and poor in chlorite than sediment from sand-flat facies.
9. Clay-coat mineralogy is principally governed by the suspension-controlled segregation of the fluvial-derived clay mineral assemblage with chlorite (larger detrital flakes) preferentially deposited in close proximity to the ebb-tidal channel (i.e. sand flats).
10. Clay-coat coverage does not increase with increasing depth below the sediment surface. Therefore the generation, distribution, and mineralogy of clay-coated sand-grains is principally controlled by surface-based processes local to the site of deposition. The post-depositional processes of infiltration and bioturbation have a possible secondary role in increasing clay-coat coverage but do not significantly alter primary depositional (surface) trends in clay-coat coverage.
11. The strong statistical correlation between detrital-clay-coat coverage and biofilm abundance, the consistent biologically-mediated (biofilm) textures of clay-coated sand-grains, and the absence of a pervasive post-depositional increase in the extent of clay-coat coverage, all suggests that clay coats are principally the result of biofilms derived from the normal life activities of diatoms.
12. The similarity in clay-coat coverage, distribution trends, and mineralogy between surface and near-surface sediments supports the use of modern surface-based data sets to develop analogue predictive models for clay-coat-derived reservoir quality in ancient and deeply-buried sandstones.

5. The origin of clay-coated grains in marginal marine sandstones: insights from a modern analogue

5.1. Abstract

Clay mineral coats on sand grain surfaces are reported to inhibit the typical, pervasive, porosity-occluding quartz cement, during prolonged burial and heating. Clay mineral coats are thus a principal cause for elevated primary porosity deep in sedimentary basins. Despite the economic importance in predicting the distribution of clay-coated sand grains in deeply-buried sandstones and near five decades of research, the mechanism controlling the formation of clay coats at the site of deposition remains, only hypothesised and not constrained to level that will permit a credible predictive capability.

This study focused on surface sediment from the Ravenglass Estuary, UK. The study involved geomorphic mapping, a range of scanning electron microscopy (SEM) techniques, and the quantification of biofilm abundance (biomarker analysis), bioturbation-intensity in the biotic zone, grain-size, grain sorting, clay fraction content, and clay-coat coverage.

The work produced a novel, fully quantitative biological and sedimentological framework of the marginal marine sediments at Ravenglass. The data led to the identification of the controlling mechanisms that govern the origin and distribution of clay-coated sand grains across marginal marine sediments. Most complete clay coats are found in sediments associated with inner estuarine tidal-flat and tidal-bar depositional environments. The distribution of clay-coated sand grains across the Ravenglass Estuary can be explained firstly, by an inner estuarine zone of formation (i.e. clay mineral attachment to grain surfaces) and secondly, by the abrasive transport of inner estuarine clay coats into higher energy, outer estuarine, depositional environments. Partial clay-coated sand grains are observed actively exiting the estuarine system. The study revealed that clay coat formation

(i.e. attachment mechanism) is principally the result of biofilms “bio-glue” which coat sand grain surfaces by the normal life activities of diatoms

.

5.2. Introduction:

The occurrence of deeply-buried (> 3 km) anomalously high porosity sandstones has been associated with the presence of clay-coated sand-grains (chlorite, illite, and mixed mineralogy) (Bloch et al. 2002; Ehrenberg 1993; Skarpeid et al. 2017; Storvoll et al. 2002). The net volume of quartz cement has been reported to be inversely correlated to the completeness of clay-coat grain coverage in the Jurassic sandstones of the Norwegian continental shelf (Bloch et al. 2002), the Jurassic and Triassic sandstones of the Ordos Basin, China (Luo et al. 2009), the Miocene sandstones from the Matagorda Island well, western Gulf of Mexico (Dutton et al. 2012), and the Judy Sandstone Member in the Heron Cluster, UK (Stricker and Jones 2016). Clay coats (chlorite, illite, and mixed mineralogy) have been shown to inhibit the growth of the otherwise ubiquitous, porosity-occluding, quartz cement and thus preserve elevated primary porosity (Ajdukiewicz and Larese 2012; Bloch et al. 2002; Skarpeid et al. 2017).

The term clay coat describes clay minerals on sand grains from modern (termed, detrital-clay coats) and ancient deeply-buried (termed, diagenetic-clay coats) sediments. Detrital-clay coats form before, during, or immediately after deposition prior to the onset of diagenesis via the physical attachment of clay minerals and clay- to silt-sized material to sand grain surfaces (Ajdukiewicz and Larese 2012; Dowey et al. 2017). Diagenetic-coats develop, *in-situ*, through the alteration (thermally-driven recrystallization) of the pre-attached detrital-clay coat material or authigenic growth of early diagenetic minerals interacting with pore fluids during burial (i.e. dissolution and re-precipitation of the dissolved material).

Recent publications have focused on constraining the distribution and origin of clay-coated sand grains in both modern and ancient marginal-marine sediments (Dowey 2013; Dowey et al. 2012; Dowey et al. 2017; Saïag et al. 2016; Skarpeid et al. 2017; Wooldridge et al.

2017a). The research was driven by the increasing need to explore and develop deeply-buried sandstone petroleum prospects with one-third of all identified (but undeveloped) reserves (as of 1998) located deeper than 3 km (Appert 1998; Bloch et al. 2002). Diagenetic processes (compaction, cementation, and mineral dissolution) experienced during prolonged burial and heating of sandstones typically degrade reservoir quality (porosity and permeability) and threaten economic viability (Worden and Burley 2003; Worden and Morad 2000; Worden and Morad 2003).

The ability to understand and predict the distribution of clay-coat-derived, anomalously high porosity sandstones (due to quartz cement inhibition) would be indispensable in assessing deeply-buried prospects. Previous clay coat distribution models (Dowey et al. 2017; Wooldridge et al. 2017b) have been hindered by uncertainty about the principal mechanism of clay coat formation (i.e. how clay minerals are attachment to grain surfaces). The aim of this research is thus to constrain the principal origin and distribution of clay-coated sand grains in a modern environment which can, by analogy, be applied to help the prediction of anomalously high porosity in deeply-buried sandstones.

Detrital-clay-coats in surface sand-dominated sediments have been reported to form via the physical-sedimentological processes of inheritance and drying adhesion (Dowey et al. 2017; Moraes and De Ros 1992; Wilson 1992). Detrital-clay-coats have also been reported to form via macro-and micro-organism produced biofilms (McIlroy et al. 2003; Needham et al. 2005; Wooldridge et al. 2017a; Worden et al. 2006). The work here addresses the origin of clay coats in the surface sediment. The post-depositional processes of infiltration (Matlack et al. 1989) and bioturbation (sediment homogenisation) (McIlroy et al. 2003) may also result in clay-coat formation but this happens within a volume of sediment rather than at the surface of the sediment. To assess the influence of post-depositional processes on clay coat formation would require a focused subsurface based investigation.

Matlack et al. (1989) and Wilson (1992) undertook seminal studies into the formation of detrital-clay coats that formed the basis for much research that is summarised below. Wilson (1992) advocated two environments in which detrital-clay coat formation can occur; (1) aeolian sabkha and inter-dune environments via the process of infiltration and adhesive drying and (2) marine shelf-shoreface environments through the processes of bioturbation-induced sediment mixing and the act of sediment passing through the digestive tract of macro-organisms (e.g. lugworms).

5.2.1. Clay coat origin: attachment of clay-coats by sedimentological processes

Inherited clay-coats are defined as clay-coats that form on framework sand grains in specific environments, prior to moderate reworking and eventual deposition (i.e. formation in the hinterland and fluvial transport into estuarine sediments) (Matlack et al. 1989; Wilson 1992).

Drying adhesion, as a process of clay material attachment to sand grain surfaces, was proposed by Dowey (2013) to occur in the estuarine sediments of the Anllóns Estuary, Spain; this environment experiences evaporative drying up to 40 % in the uppermost tidal-flat sediment during tidal exposure (Barrie et al. 2015). However, the preservation potential of dehydration-attached clay minerals and clay- to silt-sized material to grain surfaces on rehydration (tidal inundation) remains unknown.

5.2.2. Clay coat origin: attachment of clay-coats by biological processes

Clay coats have been reported to form biologically via the mediating adhesive properties of biofilm “bio-glue” coatings added to sand grain surfaces by macro-and micro-organisms (Needham et al. 2005; Wooldridge et al. 2017a; Worden et al. 2006). Macro-organism clay coat formation was proven in a series of experiments by Needham et al. (2005) and (Worden et al. 2006). These studies showed that, in the faecal casts of the lugworm

Arenicola marina, clay minerals were attached to grain surfaces via the adhesive properties of a mucus biofilm (Needham et al. 2005; Worden et al. 2006) added to the sand grain in the gut of the worm during digestion. As noted by Dowey et al. (2017), given the variety and range of bioturbating organisms in sedimentary environments, this processes is unlikely to be confined to marginal marine environments or to the lugworm, *Arenicola marina*.

As well as macro-organisms, micro-organisms have also been identified as agents for the attachment of clay minerals to grain surfaces creating clay coats, also involving "bio-glue" (Wooldridge et al. 2017a). Micro-organism-produced biofilms result from diverse microphytobenthic (MPB) communities that are composed of algae (diatoms, euglenids, crysophyceans, dinoflagelates), cyanobacteria and other photosynthetic bacteria (Jesus et al. 2009).

Sediment biofilm characterisation and origin has been the subject of reviews (Hoagland et al. 1993; Stal 2003; Wooldridge et al. 2017a). Extracellular polymeric substances (EPS) colloquially termed as "mucus" (Hoagland et al. 1993) are added to sand grain surfaces by secretion from silicate phototrophic, sediment colonising (benthic), diatoms (algae) which represent the dominant micro-organism in the intertidal sediments of western Europe (Stal 2010; Underwood and Paterson 1993). EPS is produced by diatoms for a variety of functions (Decho 1990). One function of the biofilm is to facilitate movement of algae in the sediment in response to tidal and light cycles in order to maintain optimum environmental conditions for photosynthesis (Stal 2003). Diatoms that excrete EPS (biofilms) form trails on and between sand grain surfaces to facilitate movement through the sediment column (Higgins et al. 2003; Stal 2003).

Biofilms are pervasively present in marginal-shallow marine sediments (Jones 2017; Paterson et al. 2000; Underwood and Paterson 1993; Wooldridge et al. 2017a) and have

been demonstrated to have a profound influence on clastic sedimentary systems, by adding a cohesive force (binding agent) which prevents the independent movement of grains (Jones 2017). This cohesive biofilm ("bio-glue") produced by diatoms and other MPB organisms affect grain size heterogeneity (Garwood et al. 2015), sediment stability (Vignaga et al. 2013), sediment transport, and bedform stability (Jones 2017; Malarkey et al. 2015; Schindler et al. 2015; Wooldridge et al. 2017a).

5.2.3. Clay coat control: hydrodynamic influence on the distribution of clay-coated sand grains

Irrespective of the mechanism of clay mineral attachment to grain surfaces, the development of clay coats can only occur in sediments that contain fine-grained material (clay). A hydrological control on the formation of clay-coated sand grains has been widely reported from the correlation between the extent of clay-coat coverage (e.g. area of a grain surface with clay material attached), grain size, sediment clay fraction content (< 2 μm), and sorting in both modern and ancient sediments (Bloch et al. 2002; Dowey et al. 2017; Shammari et al. 2010; Wilson 1992; Wooldridge et al. 2017b). Despite not offering a mechanism of clay mineral attachment, if hydrodynamic sorting can explain the distribution trends of clay coats (i.e. the distribution of clay is necessary for clay coat formation) then it may be possible to quantify this correlation and so build a credible predictive capability.

This study aims to identify from the reported mechanisms of clay coat formation, the principal origin of clay mineral attachment to sand grain surface (i.e. detrital-clay coat formation) and the distribution of clay-coated sand grains in the surface sediment of the Ravenglass Estuary. Therefore, the following questions are addressed by focussing on the Ravenglass Estuary, Cumbria, UK (Fig. 5.1).

1. What are the sedimentological and biological characteristics of the Ravenglass marginal-shallow marine system?
2. What are the textural characteristics of detrital-clay-coated sand grains in marginal marine sediment?
3. What is the distribution of detrital-clay-coated sand grains in the marginal marine system?
4. What is the principal mechanism of clay coat formation in marginal marine sediments (i.e. attachment of clay minerals to grain surfaces)?

5.3. Study area

The study is focused on the Ravenglass Estuary, located in Cumbria, northwest England (SD 07608 96761) (Bousher 1999; Wooldridge et al. 2017b). The 5.6 km² area, macro-tidal estuary is composed of the rivers- Esk, Mite, and Irt, which merge in a central estuary basin. The estuary is connected by a single (500 m wide) channel to the Irish Sea (Fig. 5.1) and experiences a maximum tidal range of 7.55 m with an asymmetric ebb dominated tidal regime which drains for 10 hours (Kelly et al. 1991; Lloyd et al. 2013).

The estuary offers a complete fluvial to marine transect of depositional environments equivalent to the environment of deposition for many deeply-buried chlorite, illite, and mixed mineralogy clay-coated sandstone reservoirs (Dowey et al. 2012; Ehrenberg 1993; Saïag et al. 2016; Skarpeid et al. 2017). The Ravenglass Estuary has clay minerals composed of illite, chlorite, and kaolinite, derived mainly from a suspended fluvial source (Daneshvar and Worden 2016; Wooldridge et al. 2017b). The clay derives from the incision and weathering of the hinterland Palaeozoic Eskdale Granite, the Triassic Sherwood Sandstone Group, the Borrowdale Volcanic Group, and outcropping glacial units (Griffiths 2017; Moseley 1978).

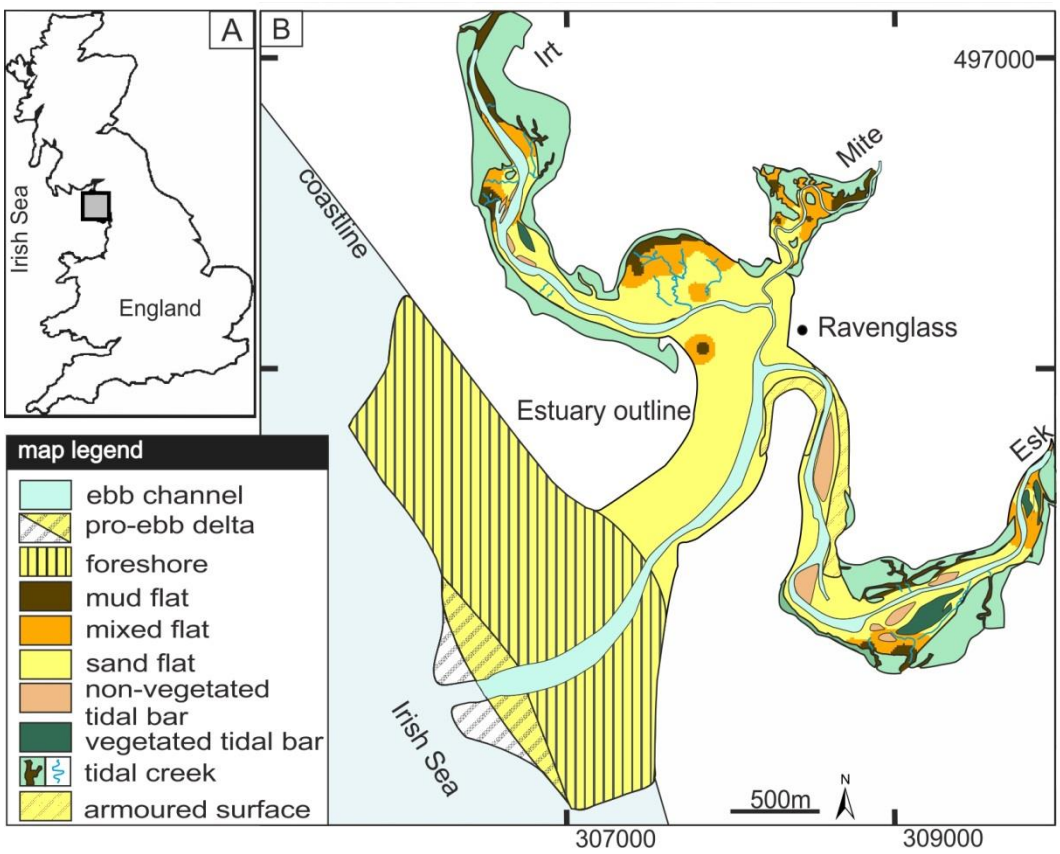

Figure 5-1 Location and depositional maps of the Ravenglass Estuary. (A) The Ravenglass Estuary, in the UK. (B) Map of the study area and component depositional environments.

5.4. Materials and methods:

The study focused on 120 surface sediment samples from which polished thin sections were constructed as grain mounts and grain size, grain sorting, clay fraction (volume of sediment fraction < 2 µm), sediment biofilm abundance, clay-coat coverage, and clay-coat mineralogy were determined. Spatial distribution maps were plotted using the interpolation function in ArcGIS (https://www.arcgis.com). A Pearson's correlation coefficient was used to test the significance of correlations between all clay coat, sedimentary, and biological datasets. Depositional environments were mapped remotely via aerial imagery (world imagery and GoogleEarth) with field mapping and sampling to ground-truth the remotely-mapped depositional environments. Tidal-flats were subdivided

by a sand-mud ratio classification scheme as sand-flat (> 90 % sand), mixed-flat (50-90 % sand), and mud-flat (15-50 % sand) (Brockamp and Zuther 2004).

5.4.1. Sediment heterogeneity

Quantification of grain size and sorting involved laser granulometry on a Beckman Coulter LS200, with values presented in the modified geometric graphical measures (Folk and Ward 1957). The percentage sediment clay fraction (< 2 μm) content was calculated to identify heterogeneity across a macro-tidal estuarine system. Clay fraction measurements were undertaken on representative sediment samples, following the methodology outlined in Wooldridge et al. (2017b).

5.4.2. Clay-coat coverage and mineralogy

Polished thin sections (n = 120) were constructed from surface sediment and imaged via scanning electron microscopy (SEM) and scanning electron microscope-energy dispersive spectrometry (SEM-EDS), to characterise clay-coat morphology (in dried form) and mineralogy.

The textual characterisation of hydrated clay-coats was undertaken via environmental scanning electron microscopy (ESEM) on a FEI Quanta 200F ESEM, run at 3 degrees, 6.5 torr pressure, at 95 % humidity, to remove the surface film of water and reveal the hydrated structure of the clay coats. Samples were imaged within 24 hours of collection.

Quantification of clay coat mineralogy was undertaken via SEM-EDS using an FEI-QEMSCAN® (Armitage et al. 2010; Armitage et al. 2016; Wooldridge et al. 2017b). This approach enabled the *in-situ* imaging of clay-coat mineralogy and the distribution characteristics of the sediment clay fraction. The step size for the analysis was 1 μm to permit the analysis of the fine fraction component.

Clay-coat coverage was quantified using the Petrog statistical software (Pantopoulos and Zelilidis 2012). The method involved point counting 50 sand grains per sediment sample (thin section) and measuring the total perimeter of each sand grain and the length that is covered by attached clay coats (i.e. independent of clay coat thickness). Measurements were undertaken on a longitudinal transect of 15 contiguous SEM images. The reported value of clay-coat coverage is an average of 50 analysed grains per sample, which produced a total dataset of > 6,000 analysed clay-coated sand-grains. The methodology carries an average ± 1.7 % error for clay-coat coverage (Wooldridge et al. 2017a).

5.4.3. Quantification of macro- and micro-organism populations

Bioturbation intensity was quantified by counting lugworm *Arenicola marina* (a dominant macro-faunal organism in clastic intertidal environments) faecal cast density at 3182 sites across the estuary using a 1 m^2 quadrat as described in Wooldridge et al. (2017b) following literature-defined methods for biotic zone characterisation (McIlroy et al. 2003; Needham et al. 2005; Wooldridge et al. 2017b).

Chlorophyll-a is the main photosynthetic pigment for biofilm producing organisms in inter-tidal sediments and an establish biomarker for sediment biofilm abundance (Stal 2010; Underwood and Paterson 1993). A suite of 97 surface samples previously reported in Wooldridge et al. (2017a) encompass the inter-tidal depositional environments. Sample collection and analysis followed the method outlined in Wooldridge et al. (2017a). Being able to directly compare sedimentary, biological, and clay coat data sets is of paramount importance in assessing the principal controlling mechanisms which govern the distribution of clay-coat coverage.

5.5. Results

Data from samples have been grouped into inner and outer estuarine zones and further subdivided by depositional environment to allow comparison of this modern dataset to ancient sandstones that were originally deposited in comparable sedimentary environments. The estuary consists of nine depositional environments: pro-ebb delta, ebb channel, foreshore, mud-mixed-sand tidal-flats, non-vegetated tidal-bars, vegetated tidal-bars, and tidal creeks (Fig. 5.1B).

5.5.1. Sediment textural characteristics across the Ravenglass Estuary

Sediment characteristics across the Ravenglass Estuary are shown in Figure 5.2A and summarised in Table 5.1. The estuary has a grain size range of between 22 to 429 μm and sorting ranging from well sorted to very poorly sorted.

The estuary shows an overall trend of decreasing grain size and sorting away from the ocean (inland, towards the tidal limit) and decreasing grain size and sorting with distance from the main ebb channel in the inner estuary (Fig. 5.2A).

The coarsest sediment (medium sand) is located in deposits from the tidal inlet and foreshore (Fig. 5.2). The outer estuary has broadly homogeneous grain size, dominated by upper fine- to medium-sand (Table 5.1). Inner estuary sediment has heterogeneous grains size and sorting values, ranging from 22 to 429 μm, and well sorted to very poorly sorted sediments. Samples from the southerly Esk arm of the estuary have a higher average grain size and are better sorted than the Irt and Mite arms (compare Fig. 5.1B to 5.2A).

5.5.2. Clay fraction distribution across the Ravenglass Estuary

The clay fraction percentage from Ravenglass shows a heterogeneous distribution (Fig. 5.2C, D and Table 5.1), ranging from 16.3 % to < 0.1 %. Samples which contain < 1 % clay

fraction are principally confined to the outer estuary. Samples containing > 1 % clay fraction occur in inner estuarine depositional environments (compare Figs. 5.1B to 5.2C, D).

Clay fraction content of the sediment increases with proximity to the inner estuary (i.e. tidal inlet for outer estuarine sediments) and towards the tidal limit (Fig. 5.2D). Two un-representative (to the principal trend in clay fraction abundance) sediment samples occur on the southern side of the tidal inlet (Fig. 5.2C) and result from a locally reduced energy regime caused by a man-made spit.

The clay fraction content in the sediment is present mostly as clay coats on sand grains or between sand grains (Fig. 5.3). Sediments from tidal-flat environments are imaged to have a subordinate clay fraction component from clay rich lithics and clumps of clay material potentially resulting from flocculation (Fig. 5.3). In sediment samples from the outer estuarine depositional environments the clay fraction almost exclusively occurs as micron scale accumulation on grain surfaces (Fig. 5.3J, K, L).

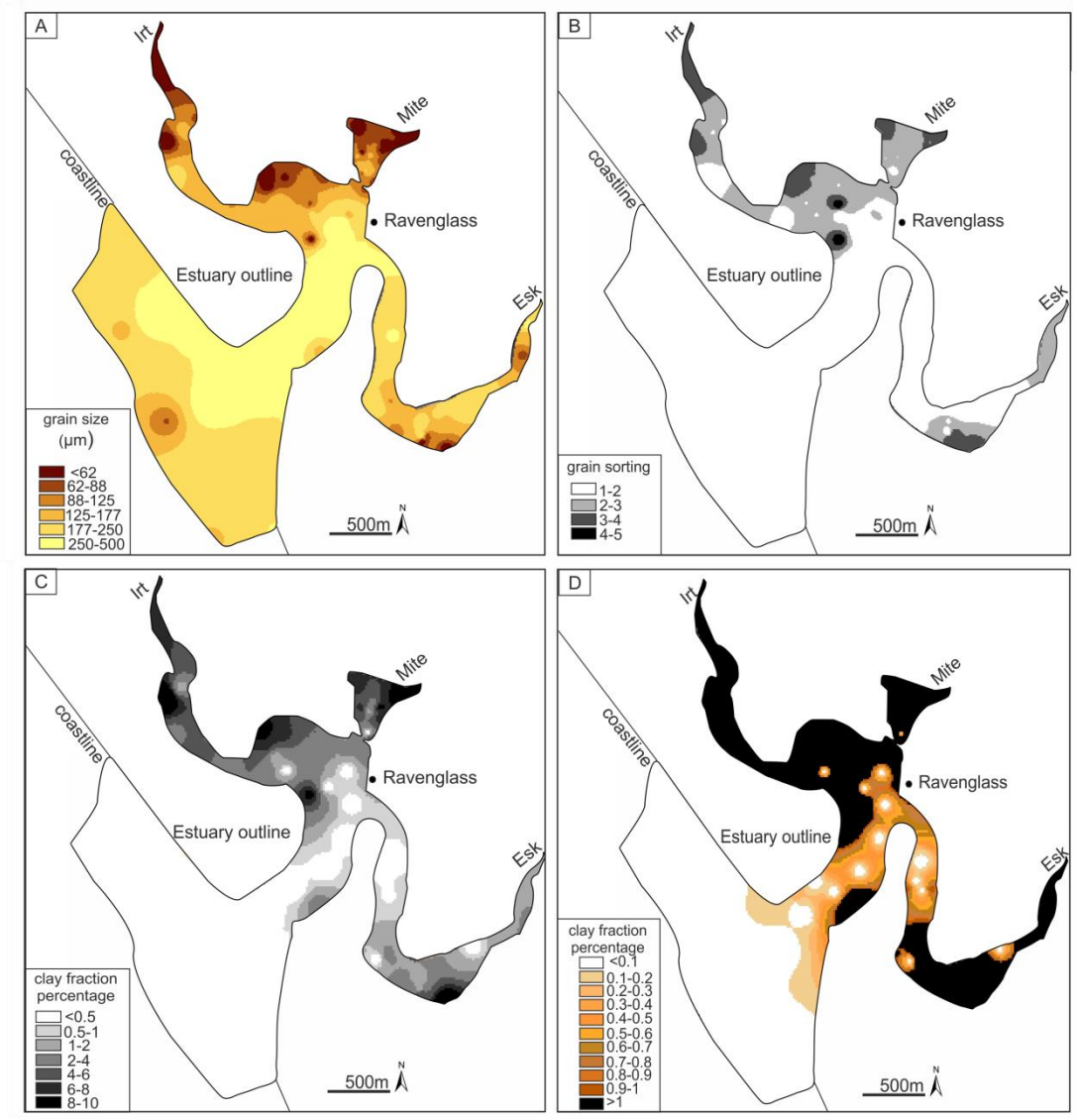

Figure 5-2 Distribution maps of surface sedimentary characteristics. (A) map of sediment mean grain size. (B) Map of sediment sorting using the modified geometric (Folk and Ward 1957) graphical measure. (C) Map of sediment clay fraction percentage. (D) Map showing the distribution trend of samples containing < 1 % clay fraction percentage.

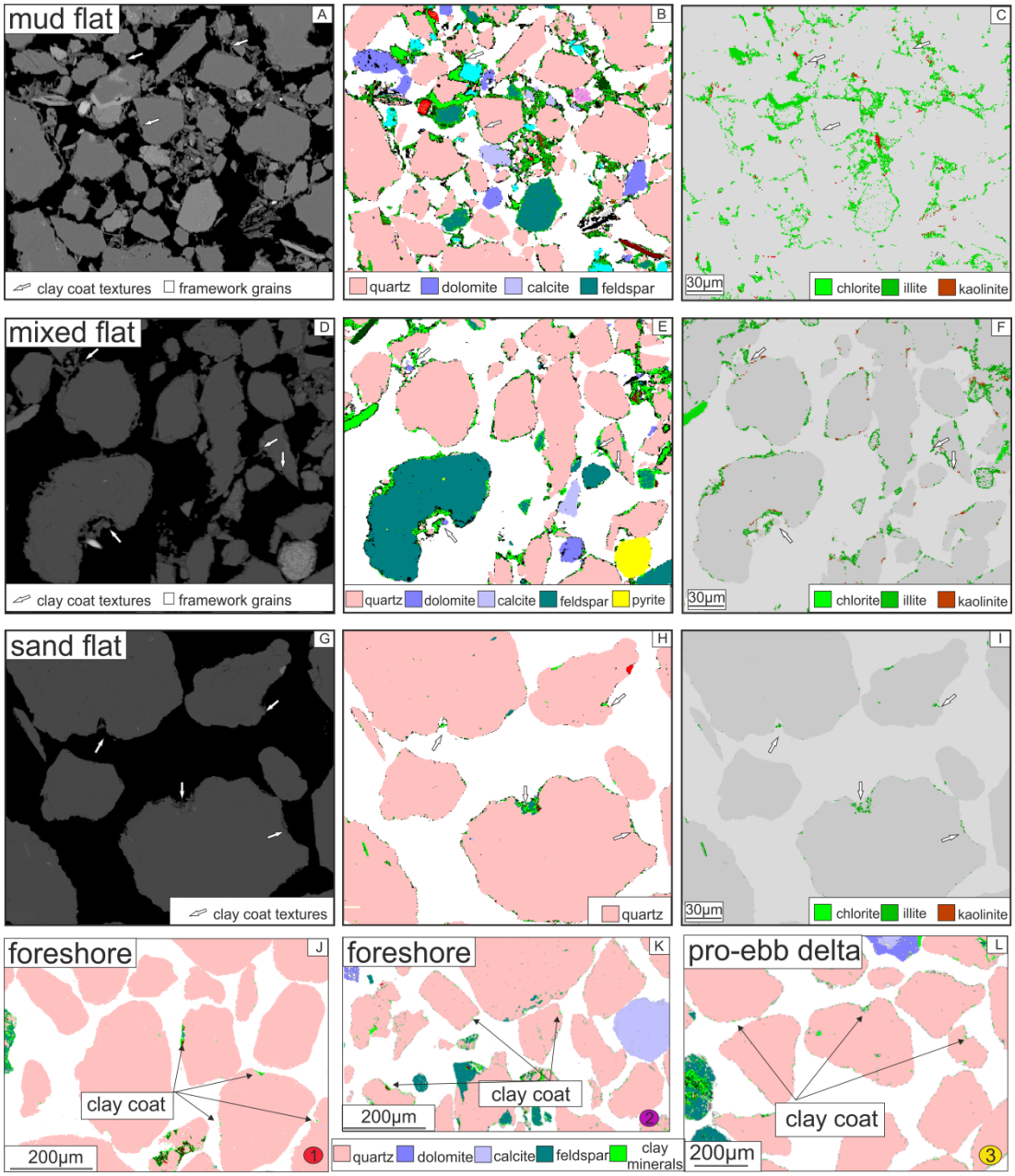

Figure 5-3 Scanning electron microscope–energy dispersive spectrometry (SEM-EDS) image illustrating whole sediment and clay-coat mineralogy. (i) Backscattered electron SEM (A, D, G), (ii) SEM-EDS image of framework grain mineralogy (B, E, H), and (iii) SEM-EDS images of the distribution of illite, chlorite, and kaolinite (C, F, I). Arrows indicate representative regions of attached clay-coats. (J, K, L) are scanning electron microscope–energy dispersive spectrometry (SEM-EDS) image of outer estuarine sediment (for location, see Fig. 5.8).

		Sand (%)	clay-coat coverage (%)	chlorophyll-a (ppb)	clay fraction (%)	Mean grain szie (µm)	Grain size sorting
sand-flat	average	0.98	7.34	12.60	0.46	268.12	1.46
	max	1.00	18.45	34.61	1.03	428.75	2.08
	min	0.92	0.94	0.37	0.07	143.09	1.32
mixed-flat	average	0.73	37.01	26.97	3.95	94.87	2.82
	max	0.88	69.36	43.77	8.16	168.81	4.94
	min	0.55	2.19	6.81	0.11	53.12	2.00
mud-flat	average	0.35	60.45	33.93	9.69	35.55	3.58
	max	0.46	80.75	45.46	16.29	48.88	5.28
	min	0.15	32.08	19.15	3.59	21.76	2.77
vegetated tidal bar	average	0.85	32.52	29.21	2.59	149.92	2.81
	max	1.45	82.57	35.40	3.53	360.69	3.70
	min	0.43	9.60	22.46	1.65	41.19	2.07
non-vegetated tidal bar	average	0.86	16.90	18.44	0.63	194.68	1.98
	max	1.00	58.57	43.63	2.92	352.06	4.25
	min	0.37	1.34	0.92	0.09	36.63	1.30
tidal creek	average	0.43	73.48	33.09	10.62	46.66	3.26
	max	0.74	86.56	40.45	15.12	84.02	3.90
	min	0.21	49.49	20.45	6.12	22.58	2.20
channel	average	0.16	2.11	11.79	0.97	236.88	1.42
	max	0.50	6.23	27.70	0.99	292.51	1.44
	min	0.04	0.46	1.28	0.95	181.24	1.40
pro-ebb delta	average	0.97	1.93	3.44	0.14	202.86	1.71
	max	0.99	2.86	3.44	0.17	314.40	2.43
	min	0.95	0.93	3.44	0.12	85.72	1.30
foreshore	average	0.99	2.35	2.26	0.16	201.27	1.42
	max	1	4.38	5.31	0.50	290.54	1.77
	min	0.94	0.78	0.39	0.04	160.76	1.27

Table 5-1 Sediment and biological heterogeneity of the Ravenglass Estuarine system.

5.5.3. The distribution of macro- and micro-organisms in the Ravenglass Estuary

Density counts of lugworm (*Arenicola marina*) faecal casts (Fig. 5.4) were collected in order to map macro-faunal bioturbation in the biotic zone of the Ravenglass Estuary (McIlroy et al. 2003; Needham et al. 2005). Lugworm faecal counts present a heterogeneous distribution across the estuary (Fig. 5.4A). The lugworm density at the sediment surface is highest (> 30 per m^2) in the mixed-flat and tidal-bar (non-vegetated) depositional environments. Lugworm populations are largely absent in mud-flat and outer estuarine depositional environments (compare Fig. 5.1B to 5.4A).

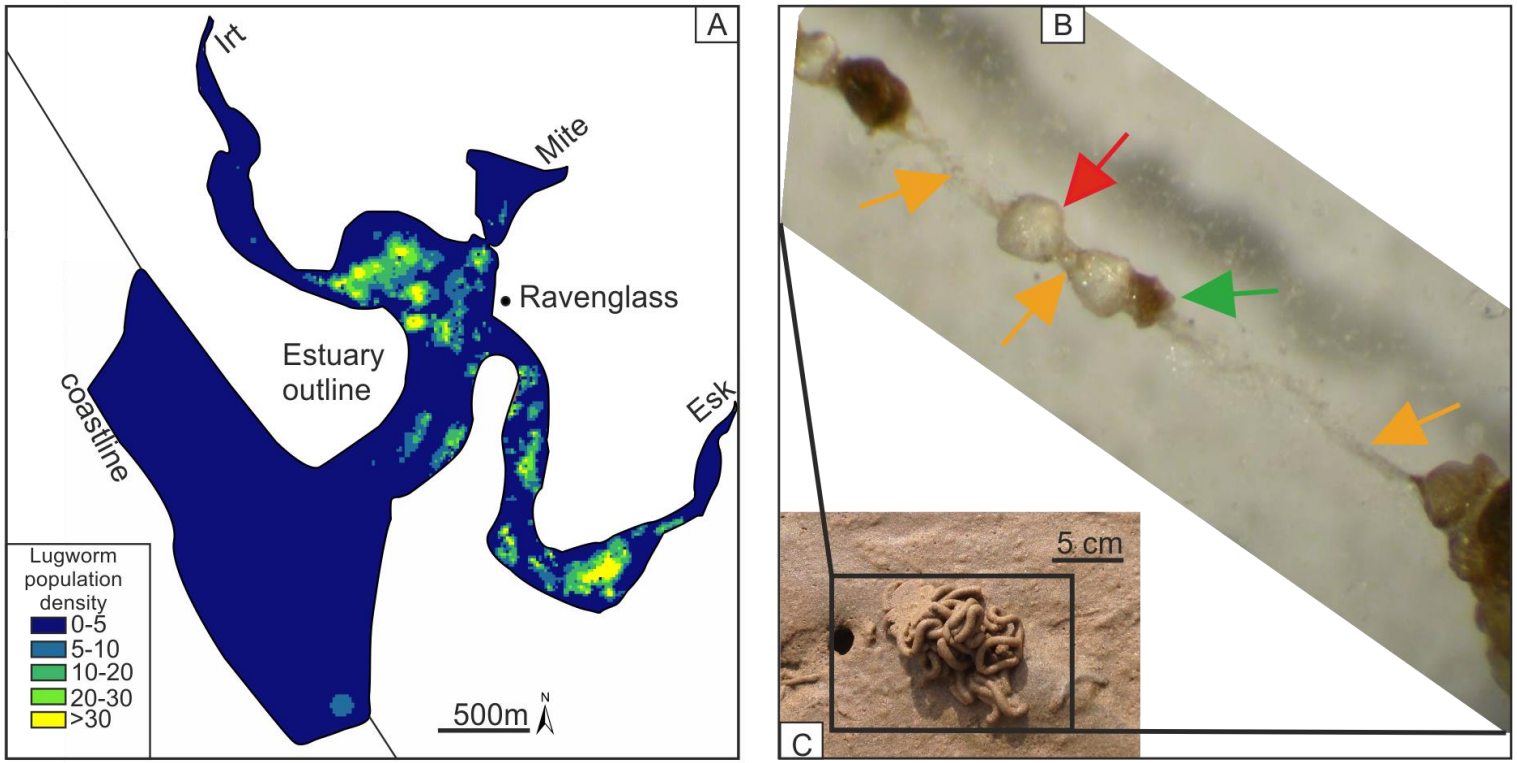

Figure 5-4 Distribution of the macro-faunal, Lugworm, *Arenicola marina*. (B) Image of sand grains from a lugworm faecal cast. Orange arrows indicates EPS (biofilm) coatings attached to the sediment in the gut of the lugworm during digestion (Needham et al. 2006; Worden et al. 2006). Red arrow indicates quartz sand grains. Green arrow indicates clay material bound to quartz sand grain surface via an EPS coating, modified from Needham et al. (2005). (C) A representative surface lugworm faecal cast from the Ravenglass Estuary (mixed tidal-flat).

Textural analysis (SEM and ESEM) of clay-coated sand grains has revealed extensive evidence of a micro-organism, biofilm-producing community that is dominated by diatoms (Figs. 5.5B, D and 5.6A). Diatoms are present as components of clay-coats and attached via EPS excretions to sand grain surfaces. Biofilm material is present as coats on sand grains with textural distinction possible between biofilm-coated and un-coated grain surfaces (Figs. 5.5D and 5.6B, D). Biofilm coats in dehydrated form (an artefact of sample preparation) are present as "wrinkled" surface films on dried sand grain surfaces (Fig. 5.5F) and as intricate linkages between framework grains (Fig. 5.5C, D). Hydrated sediment, samples (ESEM) reveal: biofilm (EPS) that anchor diatoms to grain surfaces, diatom trails (produced via diatom movement), and biofilm grain coats (Figs. 5.5E, G, H and 5.6). Sediment biofilms are thus present as networks of fine, fibrous filaments on and between grains. These are textures previously reported as characteristics of natural (estuarine) and laboratory-grown diatom excreted biofilms (Higgins et al. 2003; Hoagland et al. 1993; Malarkey et al. 2015; Vos et al. 1988; Wooldridge et al. 2017a).

The surface distribution of chlorophyll-a (a biofilm biomarker) has a heterogeneous distribution with biofilm-producing diatoms (MPB) present within all inner-estuarine environments (Fig. 5.7A, B). Chlorophyll-a varies from < 0.5 to 45 ppb (Table 5.1), with sediment samples that contain < 5 ppb confined predominantly to the tidal inlet and outer estuary regions. There is an overarching trend of increasing chlorophyll-a abundance towards the tidal limit (Fig. 5.7A, B). This pattern indicates that the abundance of sediment-colonising, biofilm-producing diatoms (MPB) (Fig. 5.7C) and thus biofilm material is not homogeneously distributed across marginal-marine sediments.

Elevated biofilm material occurs predominantly in lower energy, more heterolithic sediments (compare Figs. 5.2, to 5.7A, B) with relatively little biofilm in the coarse and

clean (low clay fraction) sediments that are characteristic of higher energy depositional environments (i.e. foreshore).

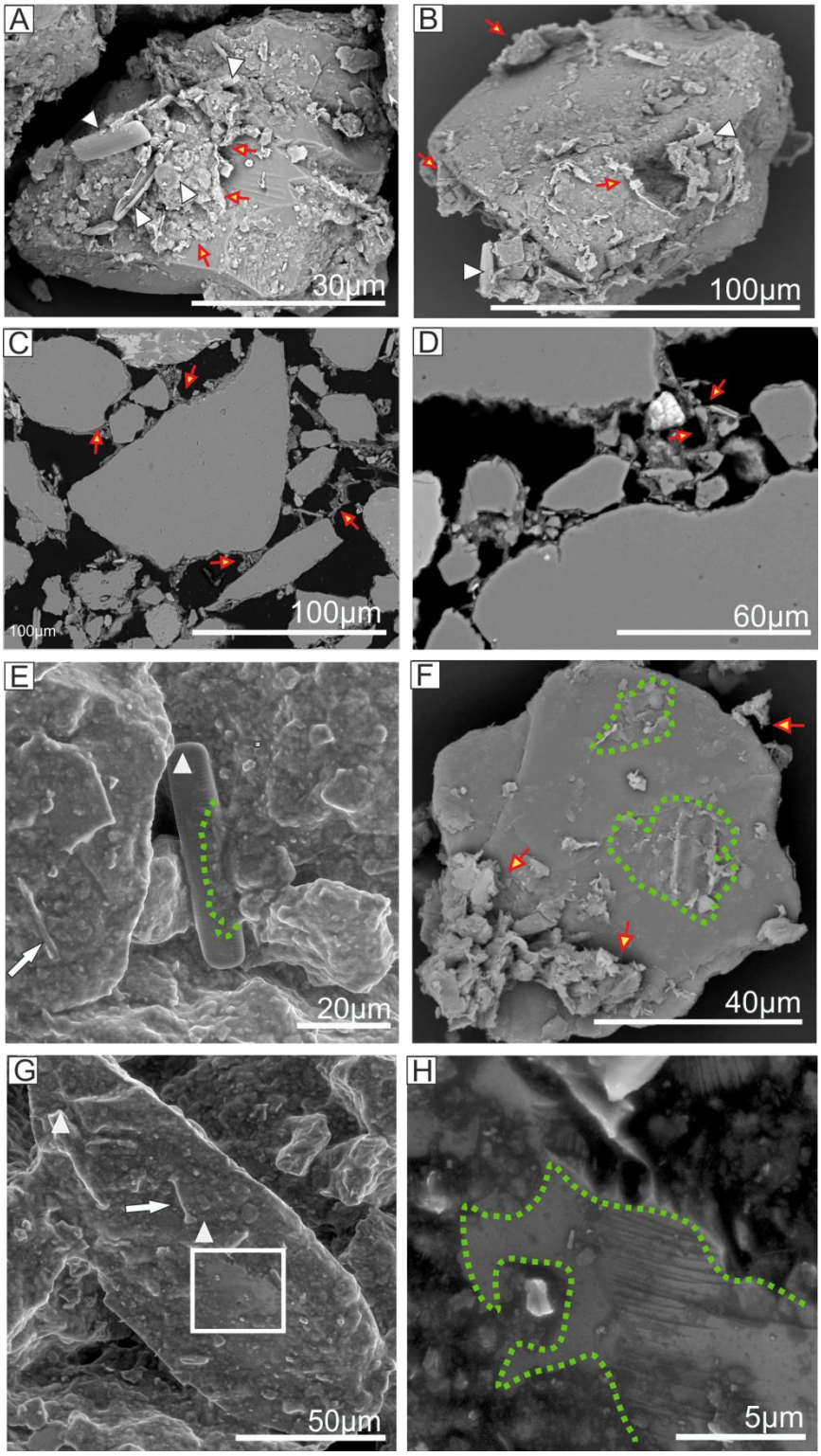

Figure 5-5 Scanning electron microscope (SEM) and environmental scanning electron microscope images (ESEM) of surface estuarine clay-coated grains. (A, B) Backscattered electron SEM image of grain-mount stub. (C, D) Thin sectioned clay-coated sand grains from an intertidal estuarine setting. (E, G, H) Hydrated sediment clay-coated sand grains. (F) Backscattered electron SEM of a loose sediment clay-coated. Arrows (red) indicate the extent of clay coats. Arrow heads point to diatoms. Dashed lines (green) outline the extent of the biofilm coats on the grain surface. White arrows indicate diatom trails.

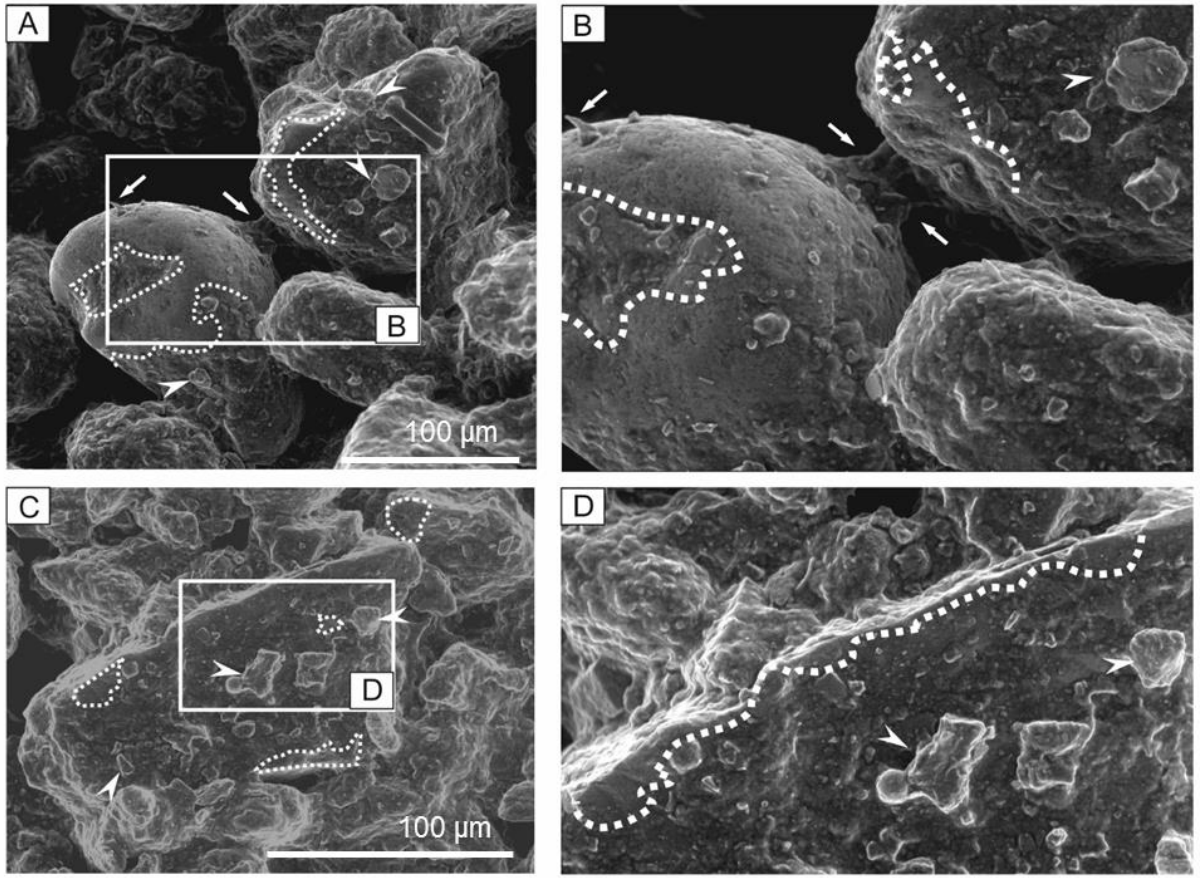

Figure 5-6 Environmental scanning electron microscope images of hydrated clay-coated sand grains. Arrows point to bridging and pore-ward extending (from grain surface) clay coat material. Arrow heads point to examples of tangentially orientated clay mineral particles. Lines define the extent of clay coats on grain surfaces.

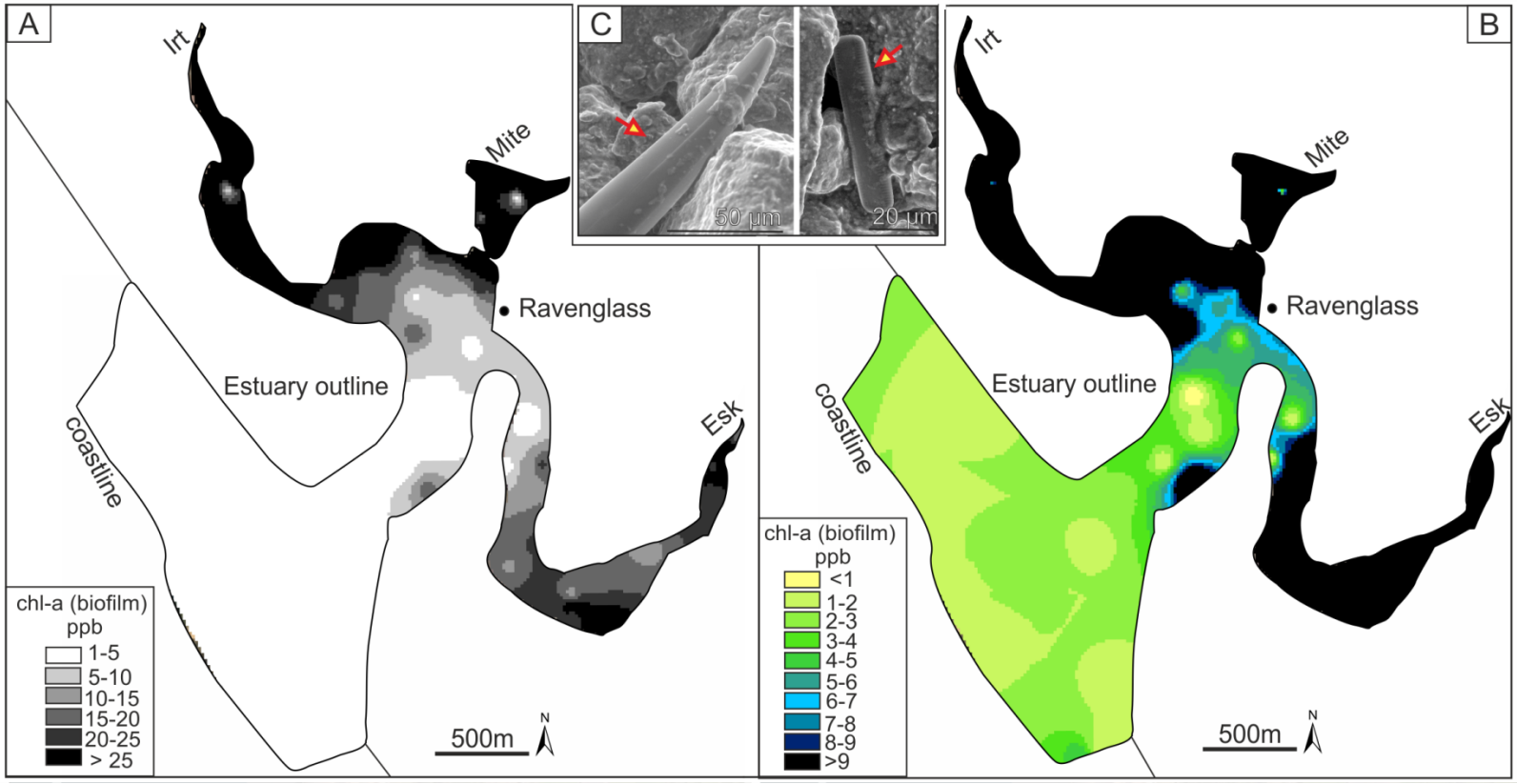

Figure 5-7 Distribution of sediment biofilm abundance. (A) Map of sediment biofilm distribution (chlorophyll-a biomarker). (B) Map showing the distribution of sediment samples which have < 9 ppb chlorophyll-a content. (C) Environmental scanning electron microscope image of the principal diatom biofilm producing micro-organisms.

5.5.4. Textural characteristics of clay-coated sand grains from the Ravenglass Estuary

There are two distinct clay coat morphologies present in the Ravenglass Estuary. Type-1 clay coats occur in sediment samples which contain > 5 % clay-coat coverage (i.e. present in mud-, mixed-, and sand-tidal-flats and tidal-bars), and are present as a network of grain-coating, grain linking, fibrous filaments composed of clay minerals, clay-to silt-sized material (e.g. lithics and clay minerals) and organics (diatoms) to produce partially (up to 86 %) coated sand grains (Figs. 5.3, 5.5, and 5.6). Type-2 clay coats occur in sediment samples which contain < 5 % average clay coat grain coverage (i.e. outer estuarine depositional environments) and display a clay-coat morphology consisting of discontinuous thin coats, with greatest thickness in grain indentations (Fig. 5.3G, H, I, J, K, L). Clay-coats are thickest (greatest volume) in the mud- and mixed-tidal-flat sediments (i.e. type-1) (Fig. 5.3).

In hydrated form, clay-coats from mixed-tidal-flat sediments occur in association with diatoms and the biofilm they created (Figs. 5.5E, G, H and 5.6) (Wooldridge et al. 2017a). Portions of grains that are coated in biofilm have attached clay minerals and clay- to silt-sized aggregates (Fig. 5.5G, H). Hydrated clay coats are characterised as discontinuous coats with minor bridging structures between the framework grains. No clay matrix material was present in any of the imaged samples (Figs. 5.5E, G, H and 5.6).

Clay coats have a mixed mineralogy composed of accumulations of individual interlocking heterogeneous phyllosilicates dominated by illite with minor chlorite and kaolinite constituents (Fig. 5. 3). Clay-coats occur on all component framework grains (e.g. quartz, feldspar, lithic, and bioclastic debris) (Fig. 5.3).

5.5.5. Distribution of clay-coated sand grains in the Ravenglass Estuary

Clay coats are heterogeneously distribution across the Ravenglass Estuary (Fig. 5.8A, B) with the degree of clay-coat coverage ranging from < 1 % to 86.6 % (Table 5.1). Clay-coat coverage increases in a landward direction (i.e. with increasing distance from the open ocean).

There is strong heterogeneity in clay-coat coverage in inner estuarine sediments, with clay-coats most extensively developed towards the tidal limits. Maximum average clay-coat-coverage is present in sediment samples from the mud-tidal-flat (60 %) and tidal creek (73 %) depositional environments. There is a pronounced reduction in the thickness and extent of clay-coat coverage (Fig.5. 3) in tidal-flat sediments and close to ebb-tidal channels. Mud-flats have the highest average clay-coat coverage (60 %) while sand-flats having the least coverage (7 %) in tidal-flat sediments (Table 5.1).

Outer estuarine sediments have a relatively uniform distribution of clay-coat coverage ranging from 4.38 % to < 1 % with most grains exhibiting at least partial attached coats (Fig. 5.3J, K, L). Samples from the pro-ebb delta and foreshore depositional environments have clay-coat coverage values of 1.9 % and 2.35 %, respectively (Table 5.1). The proportion of clay-coat coverage in outer estuarine sediment broadly increases with proximity of the sample to the tidal inlet (Fig. 5.8B).

Clay-coat coverage of the Ravenglass sediments has here been assessed by depositional environment (Fig. 5.9) to facilitate comparison between modern and ancient marginal marine sediments. The degree of clay-coat coverage shows broad differentiation between inner and outer estuarine samples. Inner estuarine samples have between < 1 % and 86 % clay-coat coverage; outer estuarine samples have < 5 % clay-coat coverage. Inner estuarine samples with clay coat coverage of < 5 % are restricted to sediments from sand- and mixed-tidal-flats and non-vegetated tidal-bar depositional environments (compare Figs. 5.1B to

5.9, Table 5.1). Sediment samples containing extensive (> 50 %) grain clay-coat coverage are restricted to mud- and mixed-tidal-flats, tidal-bars, and tidal-creek depositional environments (Fig. 5.9).

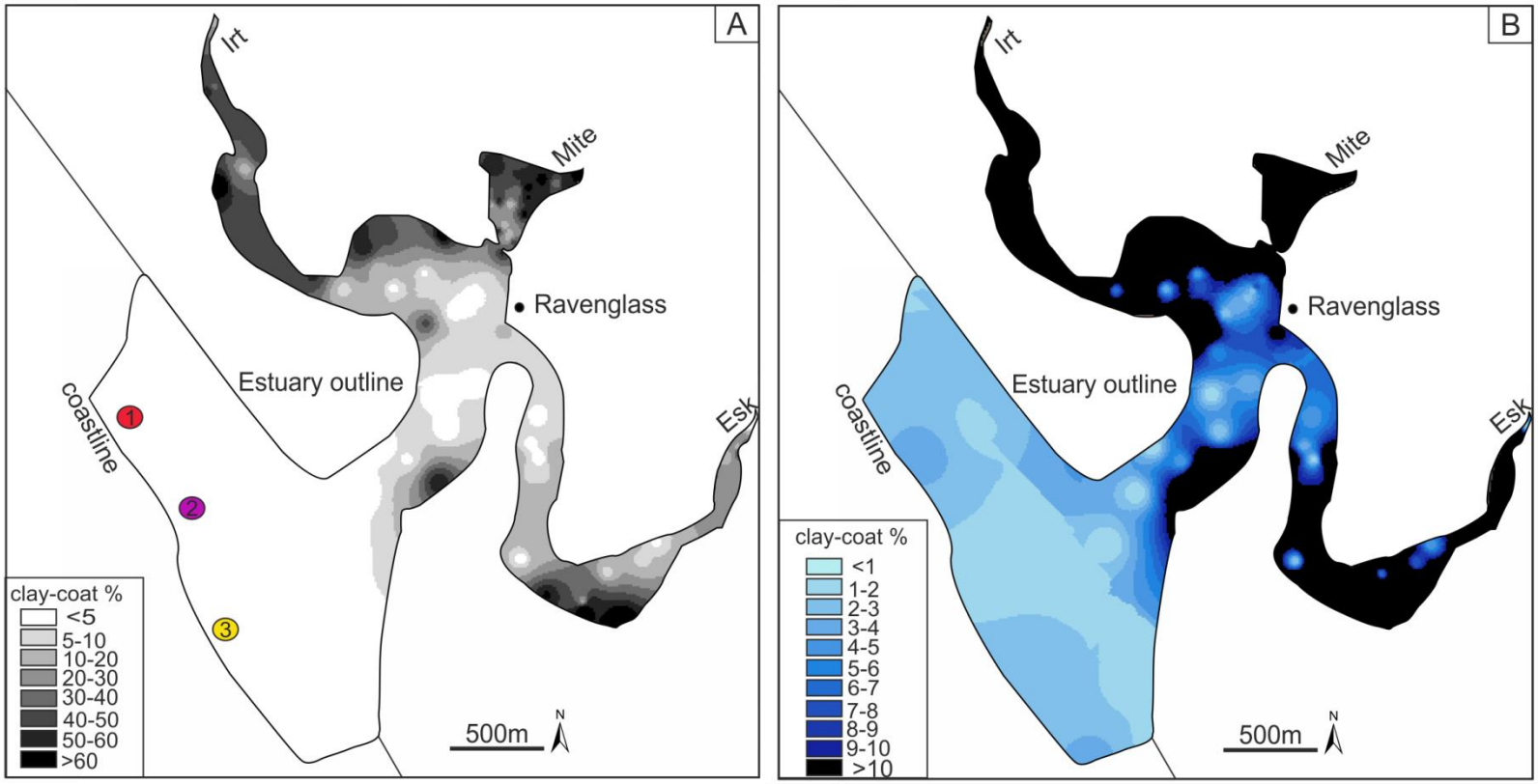

Figure 5-8 Distribution map of clay-coat coverage. (A) Distribution map of clay-coat coverage. (B) Map showing the distribution of samples with < 10 % average clay-coat coverage. Location numbers refer to SEM-EDS images in Fig. 5.3J, K, L.

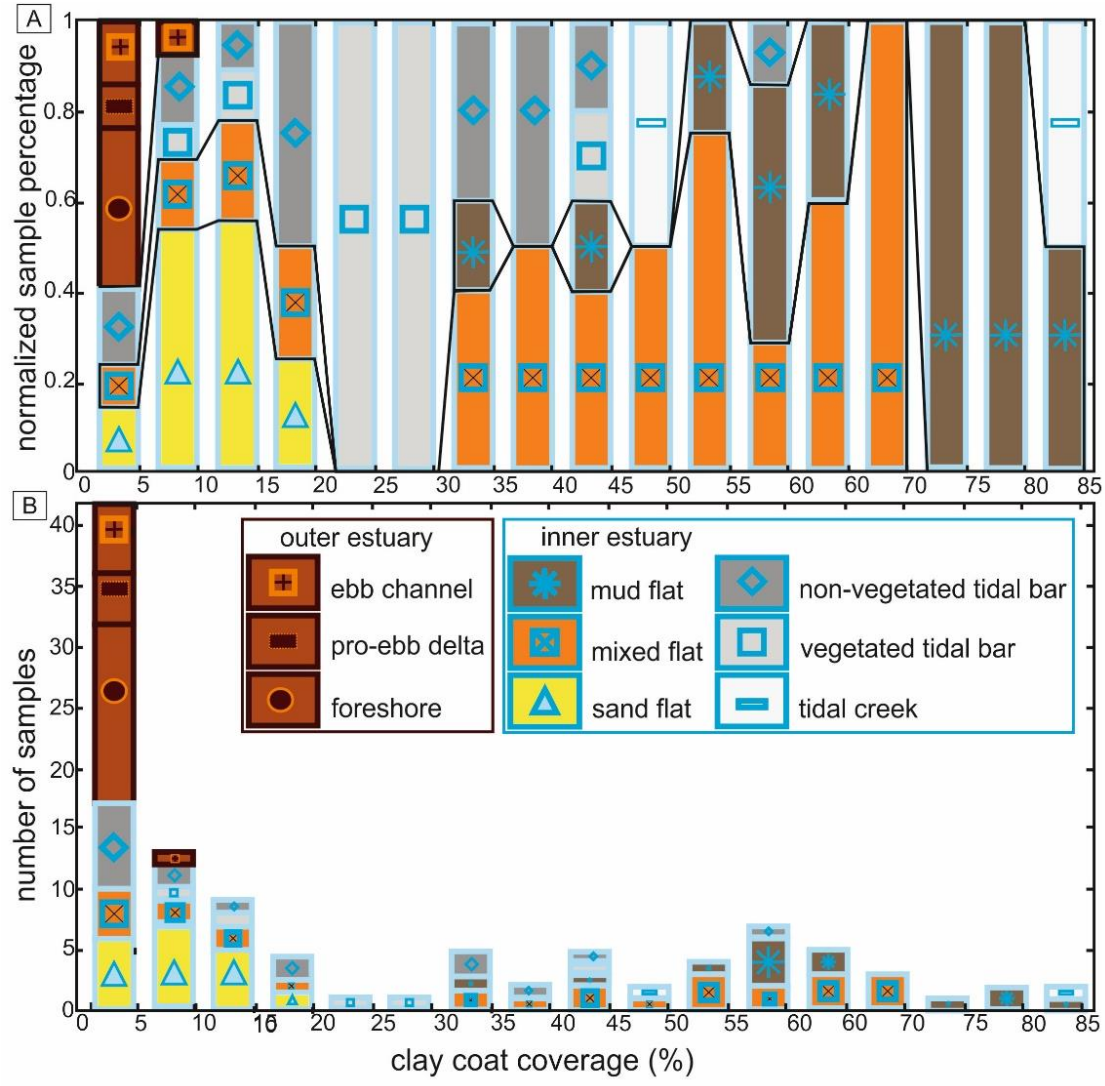

Figure 5-9 Frequency histograms of clay-coat coverage in a depositional environment framework. (A) Normalized data plot to reveal importance of various environments. (B) Total number of samples in each clay-coat coverage class. Correlation lines indicate outer and inner estuarine depositional environments, and inner estuarine tidal-flat samples.

5.5.6. Relationship between sediment characteristics and the degree of clay-coat coverage

There is significant correlation between the extent of clay-coat coverage and sediment characteristics in the form of grain size, sorting, and clay fraction content (Fig. 5.10, Table 5.2). Clay-coat coverage has been plotted as a function of sediment texture (Fig. 5.10) with clay-coat coverage increasing in a linear trend with decreasing grain-size and sorting and increasing clay fraction content.

Very fine sand sediment with > 7 % clay fraction is necessary for extensive clay-coat grain coverage (defined here as > 50 % average grain coverage) (Fig. 5.10); such conditions are met in mud- and mixed tidal-flat and tidal-bar depositional environments. Clay-coat coverage varies as a function of energy regime, with extensive clay-coat coverage occurring in heterolithic sediments (Fig. 5.10) that are characteristic of low energy, inner estuarine environments (Amos 1995).

The spatial distribution of clay-coat coverage with mean grain size and sediment clay fraction content reveals an important geographic discordance between clay-coat coverage and sediment characteristics (i.e. grain size and clay fraction content) (Fig. 5.11). Irrespective of sediment grain size or clay fraction content, samples with > 5 % clay coat grain coverage are confined to inner estuarine depositional environments (e.g. tidal-flats and tidal-bars) (Fig. 5.11).

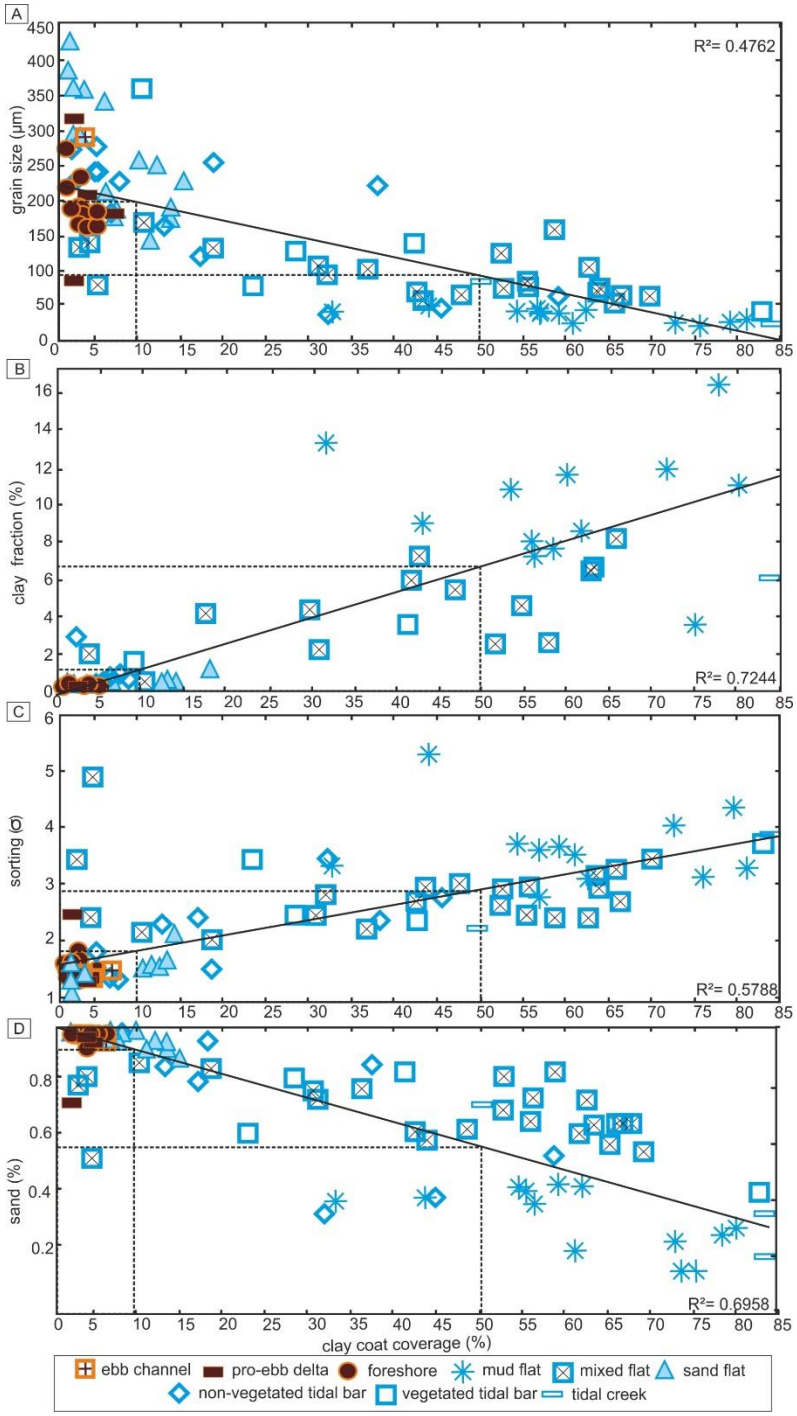

Figure 5-10 Clay-coat coverage plots against sediment heterogeneity. (A) Mean grain size. (B) Clay fraction percentage. (C) Sorting. (D) Sand percentage.

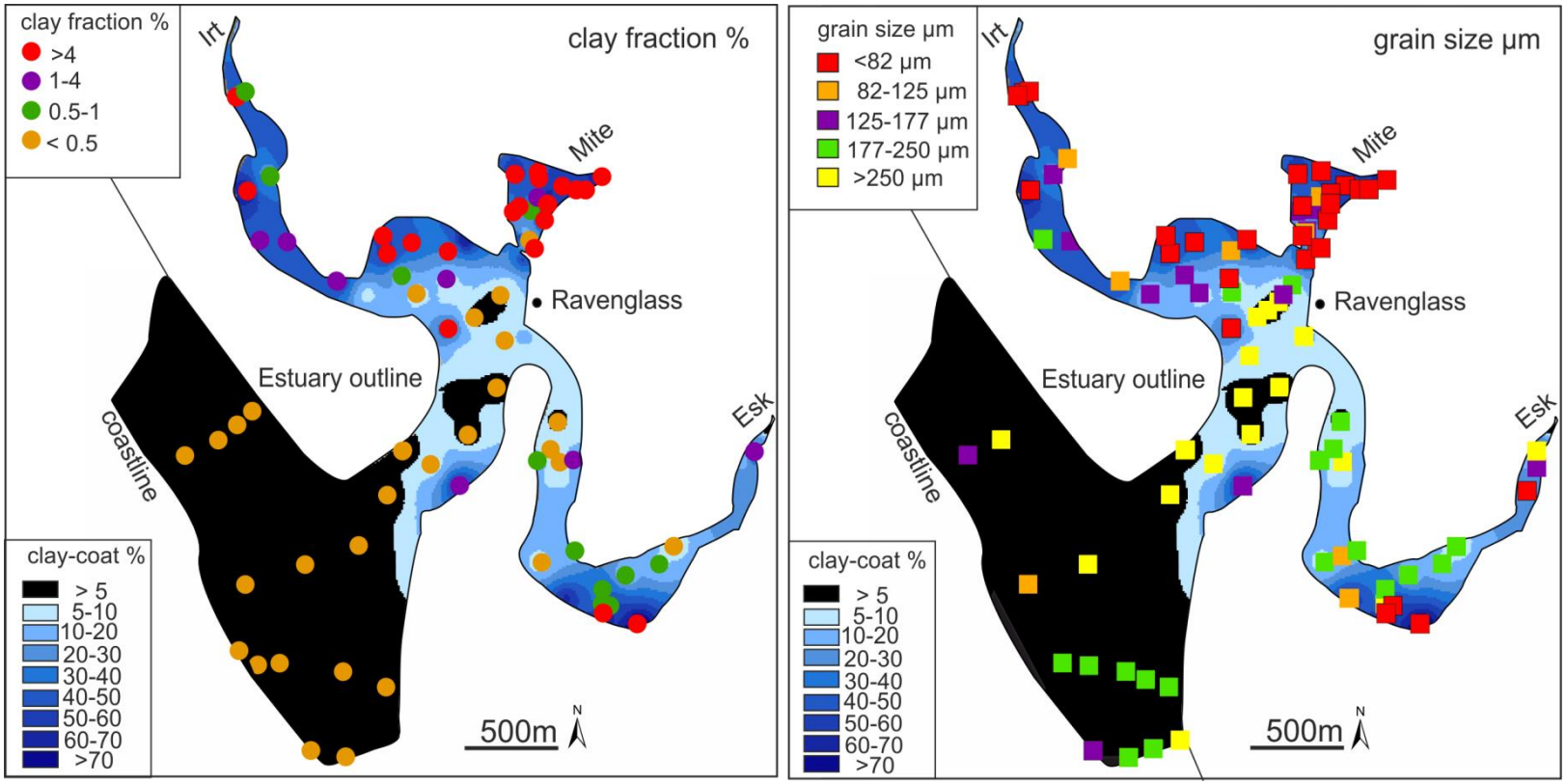

Figure 5-11 Map comparing clay-coat coverage and sediment heterogeneity distribution. (A) Sediment clay fraction percentage and clay-coat coverage. (B) Sediment mean grain size and clay coat coverage.

5.5.7. Statistical analysis: relationships between clay-coat coverage, sediment and biological characteristics

A Pearson's correlation matrix was used to test the statistical relationships between the sedimentological and biological data sets (Table 5.2). The lugworm population (faecal cast density) is not statistically correlated to sediment heterogeneity; grain size, grain sorting, or clay fraction content (Table 5.2). There is a statistical link between chlorophyll-a abundance (sediment biofilm abundance) and grain size, sorting, and clay fraction content. Chlorophyll-a abundance is greatest in finer grained, heterolithic sediments.

The percentage of clay-coat coverage increases with increasing chlorophyll-a abundance (biofilm content) but there is no correlation with lugworm faecal cast density (Fig. 5.12, Table 5.2). The highest clay-coat coverage occurs in sediment (i.e. mud-flat and tidal creek) characterised by low to absent lugworm population (compare Fig. 5.10A to 5.1B).

There is a strong similarity between the spatial distribution of clay-coat coverage and distribution of biofilm (chlorophyll-a) abundance (Fig. 5.13). The extent of clay-coat coverage increases with an increasing presence of adhesive "bio-glue" material.

	sand %	clay coat %	chlorophyll -a (biofilm)	clay fraction	grain size	grain sorting	lugworm popn
sand %		0.256	***0.000	0.332	0.457	0.218	0.856
clay coat %	-0.119		***0.000	***0.000	***0.000	***0.000	0.068
chlorophyll-a (biofilm)	-0.612	0.742		***0.000	***0.000	***0.000	0.106
clay fraction	-0.125	0.843	0.718		***0.000	***0.000	0.067
grain size	0.078	-0.767	-0.692	-0.757		***0.000	0.110
grain sorting	-0.128	0.734	0.572	0.7632	-0.779		0.115
lugworm popn	-0.023	-0.216	-0.205	-0.220	0.2011	-0.198	

Table 5-2 Pearson's Correlation Coefficient matrix calculated from sedimentological and biological data. For P=-values < 0.05*, the correlation is statistically significant. P values of (P < 0.01) and (p< 0.001)*** represent very and extremely significant correlations respectively.**

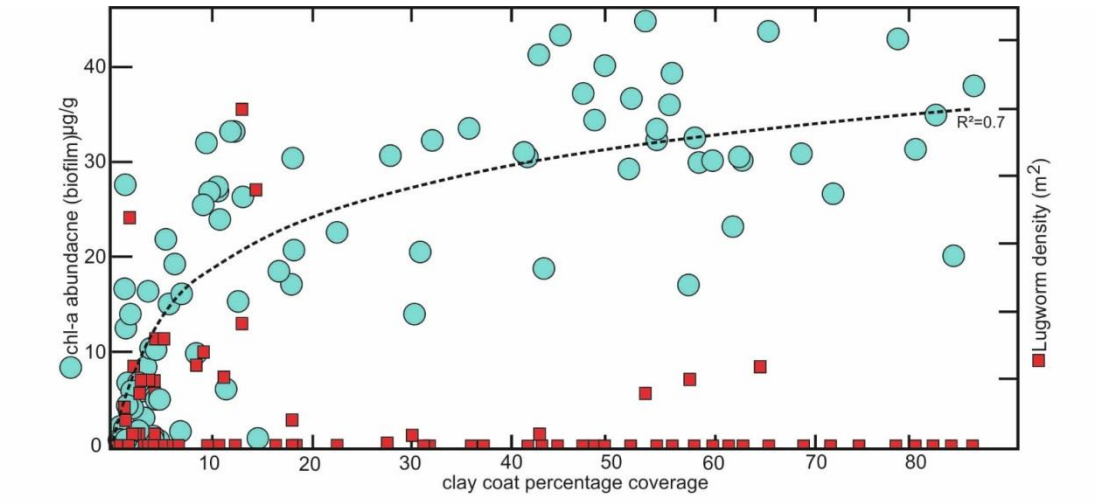

Figure 5-12 Plot of clay-coat coverage against biological heterogeneity. Red squares, indicate lugworm faecal cast density, green circles, indicate sediment biofilm abundance (chlorophyll-a, diatoms population) for each sample.

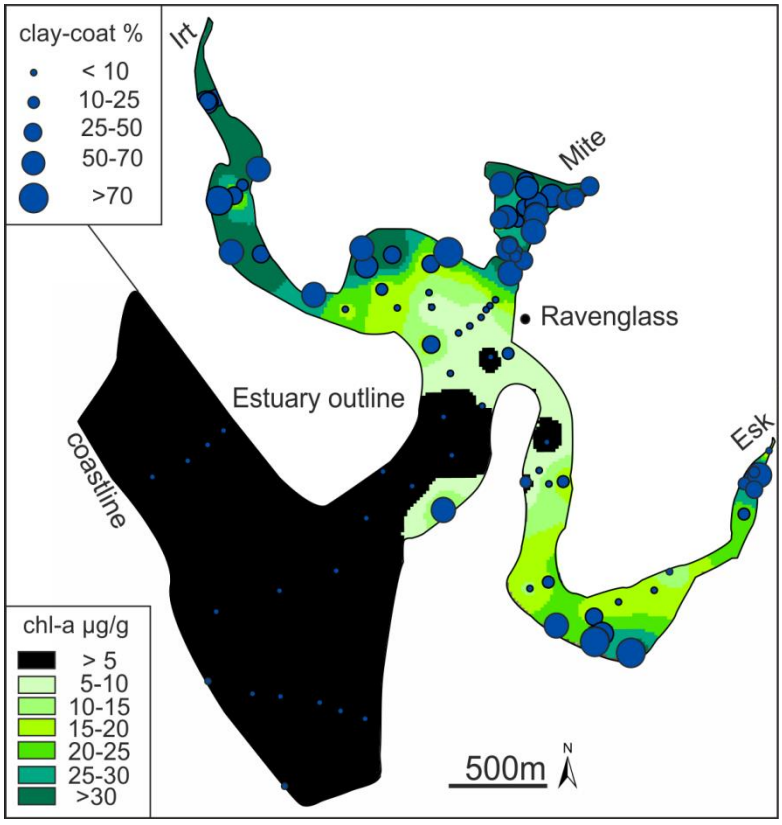

Figure 5-13 Map comparing sediment biofilm abundance and clay-coat coverage distribution.

5.6. Discussion

The relationships between clay-coat coverage, grain size, clay fraction content, and biofilm abundance (biomarker chlorphyll-a) needs to be explained in order to progress the current understanding of the primary origin of detrital grain-coating clay. The results of such an understanding would facilitate a situation where it is possible to use data, maps, and correlations from modern environments to make predictions about grain coating clay in ancient and deeply-buried sandstones.

5.6.1 Interpretation of the origin of clay-coated sand grains

The distribution of the clay-coated sand grains in this study are comparable with those reported from the Anllóns Estuary, northwest Spain, and the Leirávogur Estuary, Iceland (Dowey 2013). The identified clay-coat morphology and the close association with diatoms (biofilms) are replicated in the clay coats from the Anllóns Estuary, Spain (Dowey et al. 2017), the Mandovi Estuary, India (Kessarkar et al. 2010), and the Gironde Estuary, France (Virolle et al. 2016).

Clay-coated sand grains at the surface of modern environments have been reported to result from four main processes: (i) inheritance from the fluvial hinterland, (ii) macro-faunal activity, (iii) microbiological activity, and (iv) hydrodynamic processes in the estuary. These processes will be evaluated in light of the data from the Ravenglass Estuary to discern their relative importance.

5.6.1.1. Clay coat origin: inheritance

It has been proposed that clay coats may form in the fluvial hinterland, or in other parts of the estuary, prior to transport to the site of final deposition (Wilson 1992). These are known as inherited clay-coats. Inherited clay coats could form in subsequently eroded soil

profiles, in the river during quiescent periods or transiently accumulated sediment in the estuary.

If, clay-coats were derived principally from a fluvial source, e.g. in soil profiles, then abrasive degradation during transport (grain-to-grain collision) would be expected to result in a systematic reduction in clay-coat coverage from the source of fluvial input. Although the greatest quantities of clay coats tend to be found in the upper estuary, there is no systematic decrease from the point of fluvial input (Fig. 5.8A). Tidal-flat and tidal creek sediments from the inner-central estuary have the highest degrees of clay-coat coverage (Table 5.1). The presence of clay-coated bioclasts (Fig. 5.3B, E) strongly suggests that clay coats were created in the estuary, discounting a soil-fluvial inherited source.

It is possible that clay coats could be created in one part of the estuary, and then transported, with clay coats then inherited by the new site of deposition. This could explain the occurrence and textural characteristics of clay-coated sand grains in higher energy, estuarine depositional environments (i.e. foreshore and pro-ebb delta; Figs. 5.3J, K, L and 5.8). The transport of clay-coated grains away from inner estuarine tidal-flats and tidal-bars could explain the systematic decrease in clay-coat coverage values from the inner to outer estuarine sediment (Fig. 8B).

5.6.1.2. Clay coat origin: macro-organism-produced biofilms

Clay coats have been experimentally shown to form via attachment of biofilms to grain surfaces through the process of sediment ingestion and excretion by the lugworm, *Arenicola marina* (Fig. 5.10B) (Needham et al. 2005; Worden et al. 2006). The distribution of the lugworm population in the Ravenglass Estuary does not spatially or statistically correlate to the degree of clay-coat coverage (compare Figs. 5.4A to 5.8A, B; Fig. 5.12; Table 5.2). Lugworm bioturbation is thus unlikely to be the principal control on the formation or distribution of clay-coated sand grain across the Ravenglass Estuary.

However, the process of biofilm attachment to sand grain surfaces (Fig. 5.10B) (Needham et al. 2005) may contribute to elevate clay-coat grain coverage, locally, particularly in the highly populated mixed-tidal-flat depositional environments (Fig. 5.4).

5.6.1.3. Clay coat origin: micro-organism produced sediment biofilms

Clay minerals have been reported to adhere to the grain surfaces in the presence of diatom (MPB) produced biofilms ("bio-glue") (Wooldridge et al. 2017a). Evidence that the biofilms produced by micro-organisms (diatoms) are the principal way that clay minerals adhere to sand grains surfaces in the sediment of the Ravenglass Estuary are: (i) the strong resemblance between clay-coated sand grains from Ravenglass (Figs. 5.3, 5.5, 5.6) and biologically-mediated (biofilm) textures (Higgins et al. 2003; Paterson et al. 2000; Underwood et al. 1995; Wooldridge et al. 2017a) and (ii) the strong statistical and geographic correlation between detrital-clay-coat coverage and biofilm abundance (Table 5.2; Figs. 5.12 and 5.13). It is proposed here that the attachment of clay minerals to grain surfaces is principally facilitated by a "bio-glue" mechanism resulting from the normal life activities of diatoms. The distribution of clay coats is thus controlled by the environmental niche of biofilm excreting organisms which is, in turn, governed mainly by hydrodynamic conditions (Stal 2003; Underwood and Paterson 1993).

Diatoms move through the sediment column for photosynthetic purposes responding to light and tidal cyclicity (Stal 2003; Underwood and Paterson 1993). The movement of diatoms is facilitated by the production of EPS strands (Higgins et al. 2003; Stal 2003). On movement through the sediment column in the top few centimetres, EPS strands detach from the diatom and remain attached onto, or bridging between, framework grains. The biofilms thus coat and form adhesive links between grains; this biofilm adhesive matrix is then available to trap deposited or suspended clay or silt sized material and firmly adhere it to either; (i) the grain surface as components of coats, or (ii) trapped as bridging structures

on the biofilm adhesive links between grains (Fig. 5.5). Thus, clay coats in modern sediment can theoretically be classified as microbially-influenced sedimentary structures (Noffke et al. 2001). A summary of the hypothesised origin of biofilm mediated clay coats is presented in Figure 5.14.

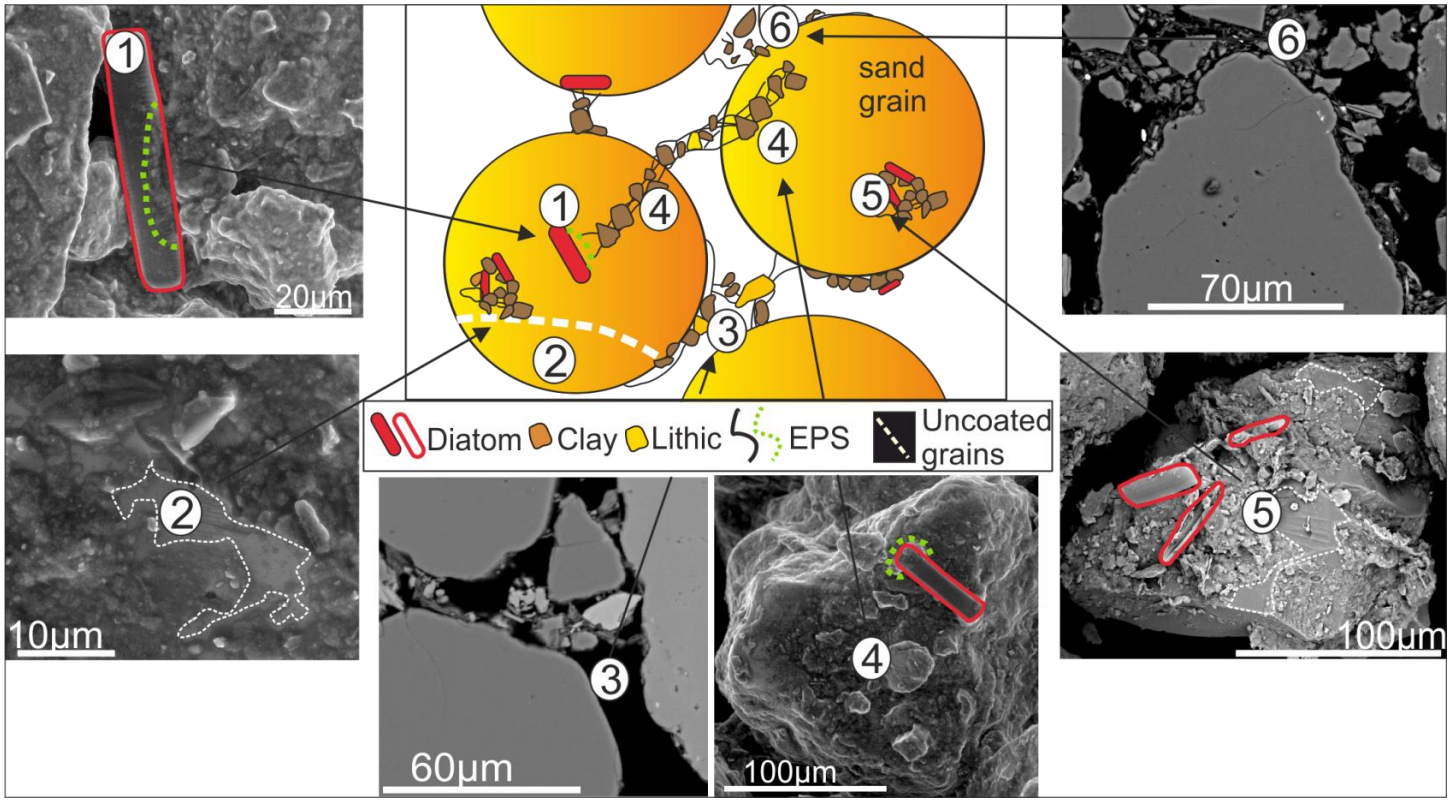

Figure 5-14 Synthesis diagram for the biofilm mediated formation of detrital-clay coats. (1) Excretion of EPS by diatoms. (2) EPS excretions partially coat regions of the sand grain surfaces. (3) During movement diatoms produce EPS bridging structures between grains which act as a root structure for clay mineral bridges. (4) Clay particles are exclusively attached to grain surfaces in the presence of biofilm coats (binding aggregates together). (5) Diatoms are extensively present in clay coats. (6) Where EPS volumes are sufficient matrix bond aggregates encompassing silt sized grains extent into the pore space from the grain.

5.6.1.4. Clay coat control: hydrodynamic influence

It has been reported that estuarine hydrodynamics exerts a fundamental control on the distribution of clay-coated sand grains since clay coats are restricted to sediment with specific grain size, sorting, and clay fraction characteristics (Bloch et al. 2002; Dowey 2013; Wooldridge et al. 2017b). Clay coat abundance correlates with grain size, clay fraction, and sorting (Table 5.2); clay coat formation can only occur in sediment that contains a substantial proportion of fine-grained (clay and silt grade) material.

However, this study has shown that inner estuarine samples with < 0.5 % clay fraction have clay-coat coverage up to 10 %. In comparison, outer estuarine samples with a comparable clay fraction content have clay-coat coverage values exclusively < 5 %. Similarly, upper-fine sand, inner estuarine samples have clay-coat coverage up to 40 %. In comparison, upper-fine sand, outer estuarine samples have clay-coat coverage values exclusively < 5 %.

It is possible to conclude that clay coats only develop in inner-estuarine tidal-flat and tidal-bar depositional environments. Thus sediment characteristics (hydrodynamics) alone cannot explain the distribution of clay-coated sand grains in the Ravenglass Estuary.

5.6.2. Controls on the distribution of clay-coated sand grains across marginal marine systems

The distribution pattern of colonizing, biofilm-producing diatoms in the Ravenglass Estuary (i.e. landward increase, Fig. 5.7) is comparable to that reported in the marginal-marine environments of the Severn Estuary, UK (Underwood and Paterson 1993), the Humber Estuary, UK (Paterson et al. 2000), the Fraser River Estuary, Canada (Jiménez et al. 2015), and the Ebro Delta, Spain (Delgado 1989).

The distribution of clay-coated grains in inner estuarine sediment (Figs. 5.8) is a function of sediment biofilm abundance governed by the hydrologically-controlled environmental niche of the biofilm producing diatoms (MPB) (Fig. 5.13) (Underwood and Paterson 1993).

The abundance of sediment biofilm material (chlorophyll-a) is controlled by the environmental niche of the dominant biofilm-producing organism (i.e. diatoms) (Stal 2010; Underwood and Paterson 1993). Multiple processes occur simultaneously in natural sedimentary systems. For example, the formation clay-coated sand grains by microbiological processes in the inner estuary happens simultaneously with continued transport and deposition. In turbulent environmental conditions, where sediment remobilisation occurs, diatoms undergo dispersal and collision-related damage from grain-to-grain contacts and so become stressed and less abundant (Underwood and Paterson 1993). The reduction in diatom abundance (chlorophyll-a) in the higher energy settings, such as tidal-bars, tidal inlet and foreshore can be explained by increasingly stressed environmental conditions.

Elevated biofilm abundance occurs in low energy environments where there is a lower grain size and a higher clay fraction content (Table 5.2), which is consistent with the reported hydrological control on diatom (MPB) abundance (Stal 2003; Underwood and Paterson 1993).

Evidence for the creation of clay-coated sand grains in the inner Ravenglass Estuary and transport to the outer estuary include: (i) the systematic decrease in the extent of clay-coat coverage from inner to outer estuarine sediments (Fig.5. 8B), (ii) the presence of partial clay coats in samples from the pro-ebb delta (compare Fig. 5.8 to 5.1B and 5.3L), (iii) clay coats from outer estuarine sediments (Figs. 5.3J, K, L) display textural characteristics consistent with abrasive transport (grain-to-grain collision) (i.e. clay coats from foreshore samples display the greatest coat thickness in grain indentations and a lack of clay coat projections) (Wilson 1992).

Biofilm-mediated clay coats (Fig. 5.14), on transport away from zones of active formation in the inner estuary (e.g. tidal-flats and tidal-bars) persist as partial, attached coats in higher

energy settings (prior to abrasive disaggregation of the attached clay coat material). This potentially explains the weaker spatial correlation between clay-coat coverage (Fig. 5.8A, B) and sediment biofilm abundance (Fig. 5.7) in the tidal inlet. The distribution of clay-coat coverage in outer estuarine sediments appears to be a function of distance from the tidal inlet (i.e. inner estuarine "clay coat factory").

The results of this study suggest that the distribution of clay-coated grains across the Ravenglass Estuary is principally controlled by the interplay between: (i) an inner estuarine biologically-mediated clay coat factory, and (ii) the transport of clay-coated grains into higher energy depositional environments resulting in a degree of clay coat abrasion and the reduction of clay-coat coverage (Fig. 5.15).

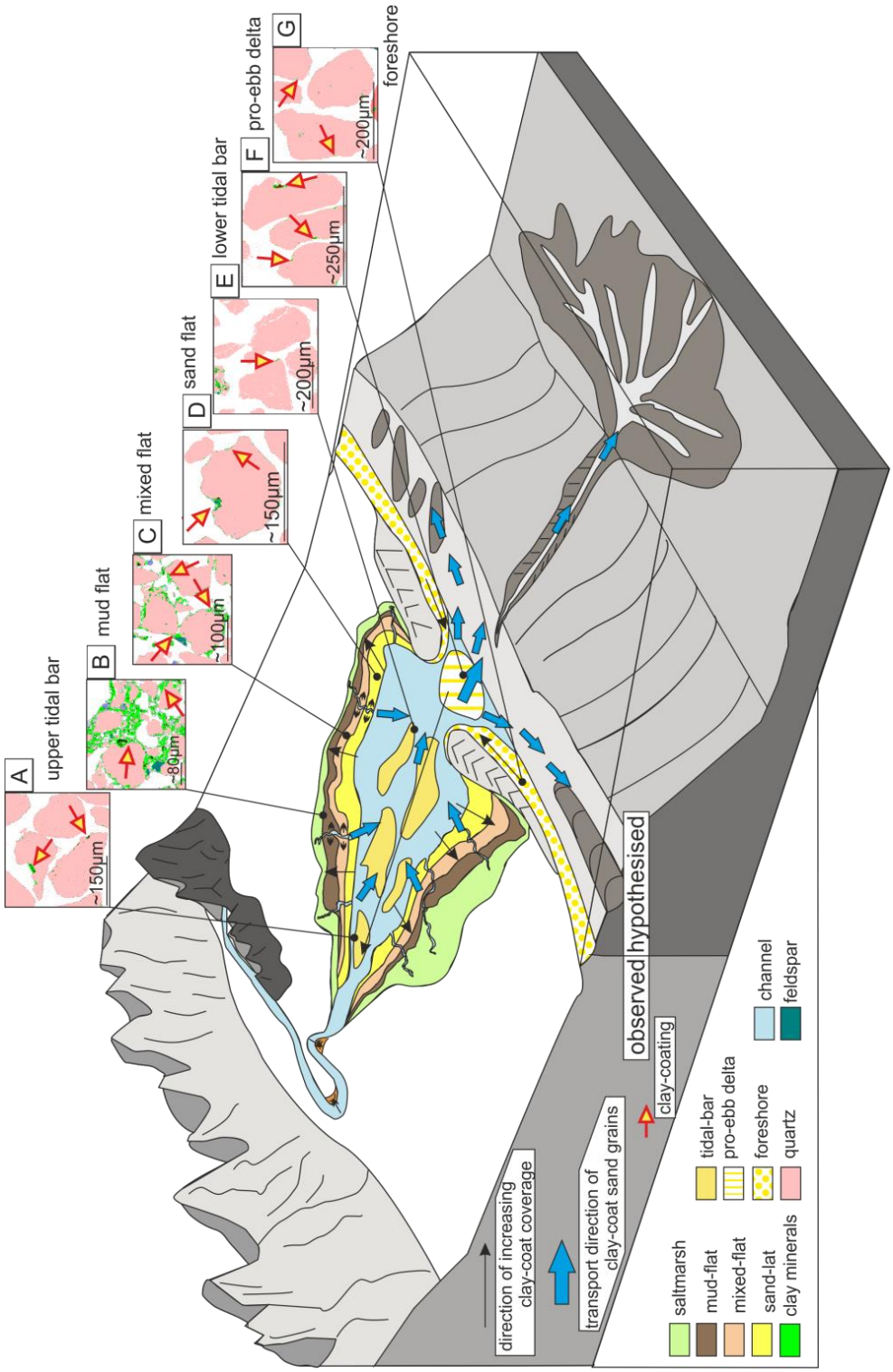

Figure 5-15 Synthesis diagram illustrating the distribution trends of clay-coated sand grains across a typical fluvial to marginal marine transect of depositional environments, after Dalrymple et al. (1992). (A to G) are representative SEM-EDS images of clay-coat coverage and textures from comparable depositional environments in the Ravenglass Estuary. The outer estuary, sub-tidal, offshore environments (greyed region) represent the postulated transport routes of inner estuary clay coats on exit from the estuary.

5.7. Implications for reservoir quality in deeply-buried sandstones

The clay-coated sand-grains reported in this study (detrital-clay coats) potentially represent precursor coats to those found in deeply-buried sandstones (Aagaard et al. 2000; Ajdukiewicz and Larese 2012; Dowey et al. 2017). Using the assumption that increased detrital-clay coat coverage will inhibit quartz cement in deeply-buried sandstones, then the best porosity should be found in mid to upper estuarine sediment in deeply-buried, ancient sandstones. The results thus show that the best prospects for enhanced reservoir quality due to clay-coats should be sought in the tidal-flat and distal tidal-bar depositional environments where the sediment is typically fine-grained and relatively impure (i.e. clay-bearing).

The limited clay-coat coverage in outer estuarine environments (< 4.4 % coat coverage), would potentially produce discontinuous diagenetic-clay coats on burial heating and recrystallization. The completeness of clay coat grain coverage has been reported via experimental (Ajdukiewicz and Larese 2012) and core based (Ehrenberg 1993; Skarpeid et al. 2017) investigations, to be the principal control on the effectiveness of clay coat-derived quartz cement inhibition. The limited extent of primary clay-coat coverage in outer estuarine sandstones would potentially result in discontinuous digenetic coats and thus the sandstone would undergo pervasive quartz cementation and porosity-loss. However, Bloch et al. (2002) noted that coarser-grained sediment has a lower surface area than finer sediment and so a smaller amount of clay (lower clay fraction) is required to coat grains and inhibit quartz cement growth. The quantity (percentage) of detrital-clay coat material in sediment that is needed to form continuous diagenetic clay-coats and thus inhibit quartz cement remains relatively poorly defined (Wooldridge et al. 2017b).

It is possible that the partial clay-coats (< 5 %) that are characteristic of outer estuarine sediment at Ravenglass (Fig. 5.8A, B) could, on heating and recrystallization, and spread out

to form thin continuous diagenetic clay-coats that are capable of inhibiting quartz cementation (Aagaard et al. 2000; Bloch et al. 2002). Such a scenario may explain the occurrence of advantageous clay coats in the tidally-influenced upper shoreface-foreshore sandstones of the Jurassic, Garn Formation, Mid-Norway (Storvoll et al. 2002), and the Jurassic, marginal marine formations (tidal-delta, estuarine shoal, distributary mouth bars) of the Intra-Dunlin Sandstone, Norway (Ehrenberg 1993).

5.8. Clay-coated sand grains: extrapolating to offshore environments

Dowey et al. (2012) concluded that 54 % of all reported chlorite-coated sandstones are found in marginal marine settings. The link between chlorite-coated sandstones and a fluvial source had previously been deduced by Bloch et al. (2002). Ehrenberg (1993) suggested that chlorite-coated sandstones on the Norwegian continental shelf deposited in near-shore marine facies which were probably influenced by nearby fluvial outflow. Clay-coated sand grains (chlorite) in near-shore marine sediments have been postulated to initially form via the interaction (rolling) of grains within a flocculated, fluvially-derived, iron-clay-rich substrate (Bloch et al. 2002; Ehrenberg 1993). An alternative mechanism of clay coat formation is here proposed; one of clay-coated grains formed in the inner estuary and then transported out into the marine realm (Fig. 5.15).

The advantage of the proposed estuarine explanation of clay-coated sand grains in near-shore marine environments are: (i) the pre-attached coats would overcome the issue of hydrological grain size segregation, (ii) offer an increase preservation capacity of the clay material (compared to clay floccules), and (iii) provide a source of clay material pre-bound to sand grain surfaces, which, via diagenetic recrystallization could produce a textural stratigraphy comparable to clay coats in deeply-buried sandstones (diagenetic) (Aagaard et al. 2000; Bloch et al. 2002; Gould et al. 2010). The identified net exodus of clay material,

pre-bound to sand grains, potentially adds insight to the view of Ehrenberg (1993) of a dominant fluvial origin of clay coat material in near-shore marine sediments.

Biofilm-bound clay coats, hosting freshwater diatoms have been found in marine sediment that is at least 27 km from the nearest river mouth (Kessarkar et al. 2010) suggesting that marginal marine processes leave a signal in deep marine sediment. A transient accumulation of near-shore marine sediment, deposited close to the fluvial source, has been proposed as the origin of clay-coated sand grains for some turbidite sandstones (Bloch et al. 2002; Yezerski and Shumaker 2017). Such sediment could accumulate clay-coated grains produced in a marginal marine setting and then be re-transported , potentially partially abraded, but variably preserved in high density flows (Yezerski and Shumaker 2017) (e.g. clay coats in the pro-ebb delta, Fig. 5.3L). It is also possible that clay-coated grains, produced in a marginal marine setting, could be entrained in a hyperpycnal flood event and passed directly into a deep marine setting, with limited abrasion (Mulder et al. 2003). Clay-coated sand grains formed in inner estuarine settings may thus provide a source of clay-coated sand grains in shallow marginal and potentially deeper marine environments (continental shelf-slope and basin floor). This mechanism delivers both sand-grade material, clay minerals, and clay sized particles, all attached as detrital-clay coats, into high energy, sand-dominated sediment deposited in a deep marine setting (Fig. 5.15). This process overcomes the typical physical separation (i.e. hydrological grain size sorting) of fine and coarse-grained materials (Wooldridge et al. 2017a). Further experimental work is needed to constrain the degradation rates of clay-coats in flowing water in order to assess the viability of such mechanisms for producing clay coated turbidite or fan sandstones.

5.9. Conclusions

1. In the Ravenglass Estuary, grain size varies from silt to medium sand, the clay fraction varies from < 1 % to 16 %, and sorting varies from well sorted to very poorly sorted.

2. Biofilms are pervasive but heterogeneously distributed throughout the inner estuary sediments.

3. Sediment biofilm abundance is controlled by the environmental niche of biofilm-excreting organisms, in this case diatoms, which is governed by hydrodynamic conditions in the estuary.

4. Clay coats display a range of morphological types across marginal-marine sediment, from discontinuous thick coats with extensive bridging structures, in mixed- and mud-flats, to discontinuous, thin coats, with the greatest amount of clay coat material in grain concavities, in outer estuarine sediments.

5. Detrital clay-coats are heterogeneously distributed across Ravenglass sediments, ranging from < 1 % to 86 % grain coverage. Clay coat grain coverage is most extensive in inner estuarine tidal-flat and tidal-bar depositional environments.

6. Clay coats are principally the result of biofilm-mediated adhesion of clay minerals to sand grains. The formation of clay coats is geographically confined to inner estuarine sediment; hence known as the “clay coat factory”.

7. The distribution of clay-coated sand grains is principally determined by (i) sediment biofilm abundance and (ii) the variable abrasive reworking and transport of inner estuarine attached clay-coated grains into higher energy

settings. Clay-coated sand grains are actively exiting the estuarine system (i.e. into near-shore marine environments).

8. Sediment composed of very-fine sand with 7 % clay fraction content is necessary for the development of extensive clay coat grain coverage in modern estuarine sands.

9. It is postulated that clay-coated sand grains from the inner estuary may be the source of clay coats in subtidal marginal marine sediments (continental shelf) and even in deep marine sediment deposits.

6. How to quantify clay-coat grain coverage in modern and ancient sediments

6.1. Abstract

A key inhibiting factor in efforts to build a predictive capability for the distribution of clay coat derived reservoir quality in deeply-buried sandstones, has been, the inability to statistically quantify the extent of clay-coat coverage. Clay-coated grains are reported to inhibit quartz cementation during prolonged burial heating and such aid in the preservation of reservoir quality in deeply-buried sandstones. The completeness of clay-coat grain coverage is the principal factor controlling the effectiveness of quartz cement inhibition. Being able to quantitatively constrain the characteristics of clay-coats is thus, of paramount importance in facilitating predictive models for the distribution of clay coat derived enhanced reservoir quality in deeply-buried sandstones.

The study presents two fully quantitative methods capable of quantifying: (i) the extent of the grain covered by attached clay material, and (ii) the volume of clay minerals present as clay coats. This study focused on the surface sediments in the Ravenglass Estuary, UK. This study involved using a combination of scanning electron microscopy (SEM) and scanning electron microscope-energy dispersive spectrometry (SEM-EDS) to characterise clay coat coverage. The study involved documenting the distribution of clay coats across the marginal marine system via qualitative and the two quantitative methodologies to allow assessment of each technique.

This study showed that qualitative classification schemes poorly resolve clay coat variability in sand-dominated sediment (typically with < 10 % average grain coverage) of sand-flats, tidal-bars, and outer estuarine depositional environments. The implication being that current predictive models for the distribution of clay coats in deeply-buried sandstones, based exclusively on qualitative data sets, potentially, underestimate the distribution and

grain coverage in such settings. Quantifying clay coat grain coverage and the volume of grain coating clay minerals, produce comparable spatial distribution trends with volume (thickness) and grain coverage decreasing with distance from the inner estuary. The novel clay coat classification techniques reported in this study are applicable to both modern and ancient sediments and facilitates the means in which to construct a robust predictive capability for clay-coat derived reservoir quality in ancient and deeply-buried sandstones.

6.2. Introduction

The presence of clay minerals arranged as coats (rims) on sand-grain surfaces have been reported to exert a fundamental control on the diagenetic and reservoir quality characteristics of deeply-buried sandstones (Ajdukiewicz and Larese 2012; Bloch et al. 2002; Worden and Morad 2003). Complete clay-coats on sand-grain surfaces (those covering 100 % of grain surfaces) can preserve primary porosity through the inhibition of porosity-occluding authigenic quartz cement (Bloch et al. 2002; Dowey et al. 2012; Ehrenberg 1993).

The need to explore, predict, and develop economically-viable, deeply-buried petroleum prospects (> 3 km) has driven significant research in establishing a predictive capability for the distribution of clay-coated grains, via a range of core based (Gould et al. 2010; Saïag et al. 2016; Skarpeid et al. 2017), modern analogue (Dowey 2013; Dowey et al. 2017; Wooldridge et al. 2017a; Wooldridge et al. 2017b), and experimental (Ajdukiewicz and Larese 2012) investigations. Experimental work and core-based investigations have suggested that the completeness of the coat (here defined as the fraction of surface area of grains covered by attached clay material) is the principal factor governing the effectiveness of quartz cement inhibition and thus the preservation of reservoir quality (Ajdukiewicz and Larese 2012; Billault et al. 2003; Ehrenberg 1993; Houseknecht and Ross Jr 1992; Skarpeid et al. 2017). The processes controlling the origin and distribution of clay-coated sand-grains is not the focus of this work but they have been reviewed previously (Ajdukiewicz and Larese 2012; Dowey et al. 2012; Dowey et al. 2017; Wise et al. 2001; Wooldridge et al. 2017a; Wooldridge et al. 2017b; Worden and Morad 2003). Note that very thin (< 1 μm), but complete, clay coats can inhibit quartz cement so that there is a need to detail the degree of coverage as well as the total amount (volume) of grain-coating clay (Ajdukiewicz and Larese 2012; Bloch et al. 2002). The aim of this work is to detail the methods available

for the quantification of the degree of grain coat coverage in modern and ancient sediment.

6.2.1 Development of clay-coat coverage methods

The protocol for classifying clay-coat coverage has been developed principally over the last 7 years (Ajdukiewicz and Larese 2012; Dowey 2013; Gould et al. 2010; Saïag et al. 2016; Wooldridge et al. 2017a; Wooldridge et al. 2017b) and has involved: (i) the qualitative visual estimation of clay-coat coverage (Dowey et al. 2017) or (ii) the assignment of the sample via morphological characteristics or an estimation of grain surface area coverage into defined bin classes (Gould et al. 2010; Saïag et al. 2016).

Qualitative characterisation has been applied to modern analogue studies (Dowey 2013; Dowey et al. 2017), experimental work (Ajdukiewicz and Larese 2012), and core based analysis (Gould et al. 2010; Saïag et al. 2016). The richest dataset from the qualitative characterisation of clay-coat coverage was by Dowey et al. (2017) on the distribution of clay-coated sand-grains from the Anllóns Estuary, Galicia, northwest Spain. The approach involved estimating the total perimeter length of a grain covered by attached clay-coats (i.e. independent of clay-coat thickness) to constrain clay-coat coverage. The study involved 6,500 coat-coverage measurements with a reported repeatability error of approximately ± 2 %.

Clay-coat classification based exclusively on morphology was undertaken by Gould et al. (2010) on the Lower Cretaceous, Scotian Basin reservoir sandstones, with four classes defined, based on a qualitative 1 to 4 classification scale of attached coats where 1 is no, or trace, coats and 4 is well-developed, thick and continuous coats. Similarly, Saïag et al. (2016) used a three-fold classification for the Permian, tidal-sandstones of the Bonaparte

Basin, Australia, where 1 represents total grain coverage, 0.5 represents partial coat coverage, and 0 represents absence of grain coats.

The development of predictive models for clay-coat derived reservoir quality in ancient and deeply-buried sandstones (Dowey et al. 2017; Saïag et al. 2016; Wooldridge et al. 2017b) has been hindered by the inability to fully quantify the extent of clay-coat coverage on sand-grains. This study has developed a qualitative methodology for clay coat characterisation and two quantitative methods. The qualitative method uses categorical bin classes based on SEM images of whole sediment; the quantitative methods measured both the fraction of the perimeter of a grain that is covered by attached clay and the volume of clay present as clay coats, both from SEM analysis of polished sections. It is envisioned that the development of standard protocols for obtaining quantified, reproducible clay-coat coverage values, will facilitate direct comparisons between studies of both modern and ancient clay-coated sand-grains and thus advance the science and the application of reservoir quality prediction.

The study is focused on the Ravenglass Estuary, UK (Fig. 6.1) and addresses the following questions:

1. Do qualitative and quantitative clay coat classification methodologies produce comparable data?
2. Does quantifying clay coat grain coverage produce comparable data to the quantification of the volume of clay coating material?
3. What is the significance of any differences in distribution pattern for clay coats revealed by the different techniques?

6.3. Materials

This study initially focused on surface samples from the macro-tidal, Ravenglass Estuary, UK (SD 07608 96761) (Lloyd et al. 2013; Wooldridge et al. 2017b). The dataset encompasses fluvial to shallow-marine depositional environments. The sedimentary framework has been documented previously by Wooldridge et al. (2017b) (Fig. 6.1). The mixed-energy Ravenglass Estuary has an inter-tidal area of 5.6 km^2 fed by three rivers, the Esk, the Mite, and the Irt, and is connected to the Irish Sea via a single 500 m-wide tidal inlet that dissects the coastal barrier spits (Fig. 6.1) (Wooldridge et al. 2017b).

This study is principally focused on 38 surface samples that were analysed via scanning electron microscope-energy dispersive spectrometry (SEM-EDS), using a QEMSCAN® system (Wooldridge et al. 2017b). The data set is combined with 112 thin sections of polished impregnated grain-mounts, and 181 loose sediment grain mounts, previously reported in Wooldridge et al. (2017a); Wooldridge et al. (2017b), respectively. Being able to directly compare differences in clay coat distribution derived from qualitative and quantitative methodologies is of paramount importance in assessing the ability of each method to characterise clay-coat heterogeneity across marginal marine depositional environments. Spatial distribution maps were constructed using the interpolated functions in ArcGIS (https://www.arcgis.com).

The study has also employed a small suite of Lower Jurassic, chlorite-cemented, sandstones from the North Sea, in order to test the applicability of grain coat analysis methods developed for the modern sediments of the Ravenglass Estuary.

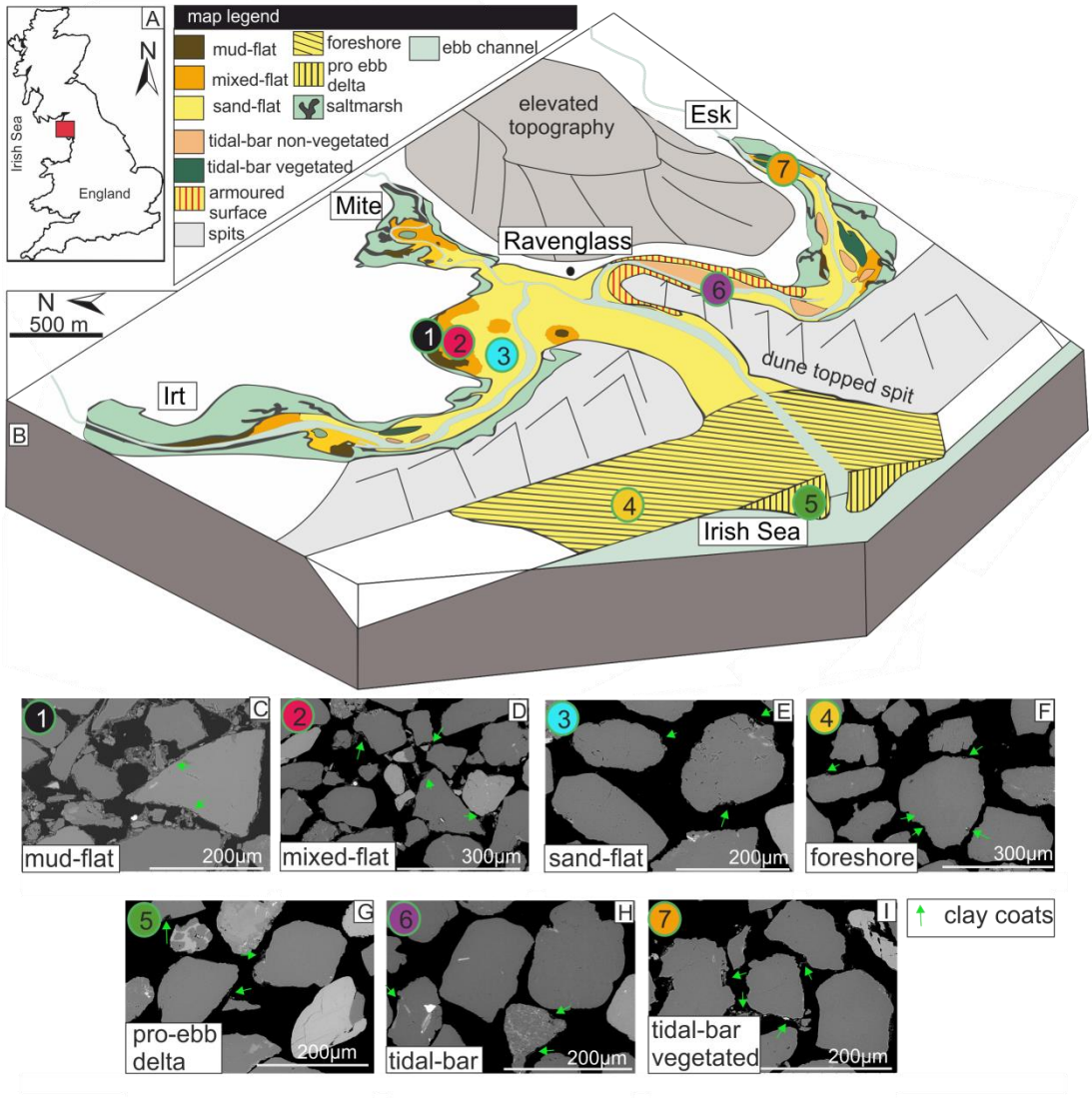

Figure 6-1 Location and depositional environment maps of the Ravenglass Estuary. (A) The Ravenglass Estuary, in the UK. (B) Regional map showing the study area and component depositional environments. Tidal-flats have been subdivided based on the quantified (Laser Granulometry using a Beckman Coulter LS200) sand percentage into; sand-flat (> 90 % sand), mixed sand-mud flat (50-90 % sand) and mud-flat (15-50 % sand) (Brockamp and Zuther 2004). (C, D, E, F, G, H, I) Scanning electron microscopy (SEM) images of surface clay coated sand-grains. Arrows indicate regions of attached clay-coat material. Numbers show sample locations on B.

6.4. Methods

6.4.1. Defining clay-coat coverage by qualitative techniques

Clay-coated grains were categorised, from SEM images of loose sediment grain mounts, from the Ravenglass Estuary into five principal classes, defined by coat morphology and an estimation of clay-coat grain coverage (surface grain area) (Fig. 6.2). As described in Wooldridge et al. (2017b) categorical bin classes were defined as: (1) complete absence of attached clay coats, (2) less than half of the grains have a small (~ 1–5 %) surface area of attached clay coats, (3) every grain exhibits at least ~ 5–15 % surface area of attached clay-coats, (4) clay coats observed on every grain with the majority exhibiting extensive (~ 15–30 %) surface-area grain coverage, and (5) extensive 30 % surface area covered by clay coats observed on every grain.

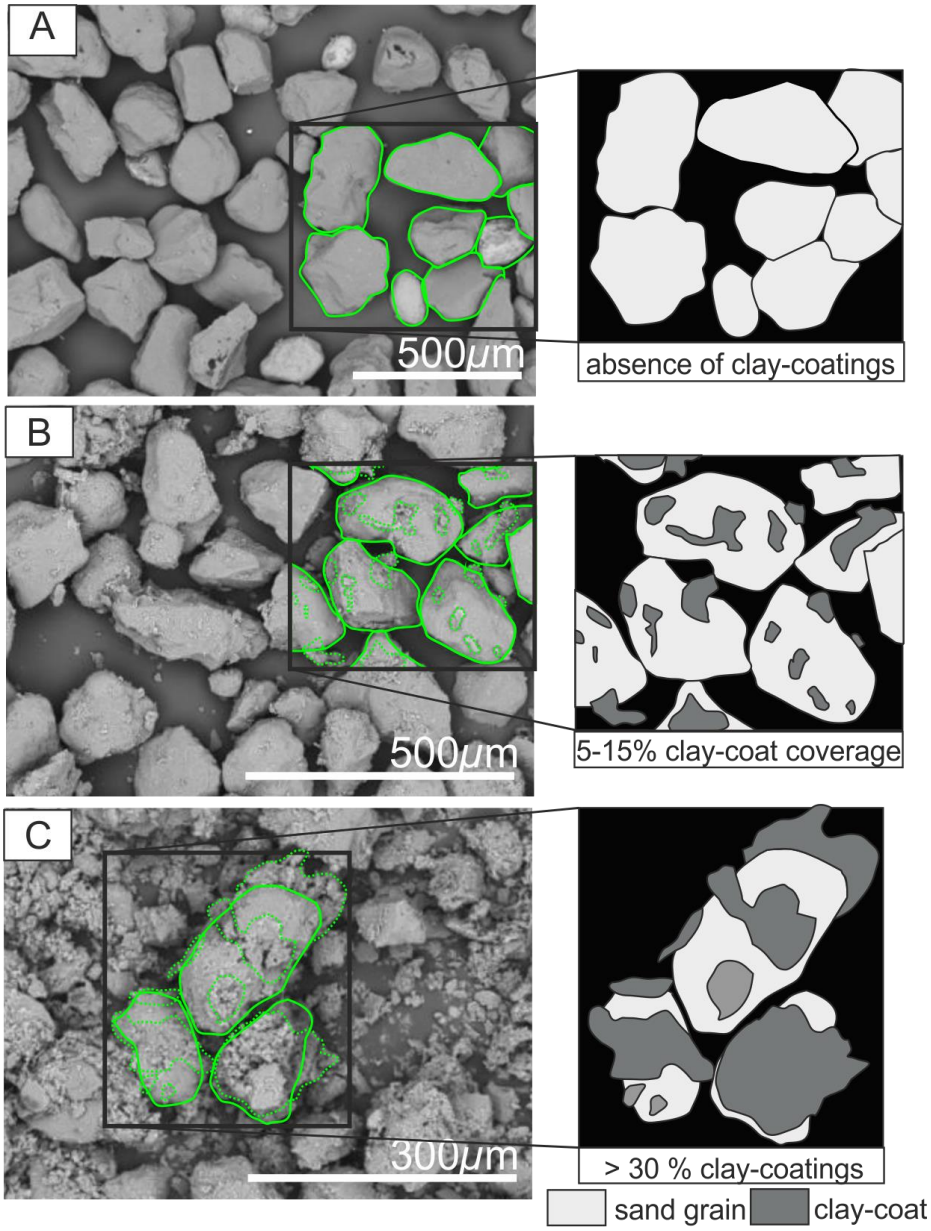

Figure 6-2 Scanning electron microscopy (SEM) images of surface clay coated sand-grains and schematic representation of clay-coating extent. (A to C) illustrate classification of clay-coat extent into classes based on morphology and the visual calculation of the surface area coverage. (A) Complete absence of attached clay coats (group 1). (B) Every grain exhibits at least ~ 5–15 % surface area of attached clay-coats (group 3). (C) Extensive > 30 % surface area covered by clay coats observed on every grain (group 5).

6.4.2. Defining clay-coat coverage by quantitative techniques

6.4.2.1. Measuring clay-coat coverage: the cross sectional perimeter length method: Petrog

Quantifying the length of a grain that is covered by attached clay coats involved using the Petrog statistical system (Pantopoulos and Zelilidis 2012; Wooldridge et al. 2017a). Petrog is commonly used for point counting with its automated, stepping stage and software that stores, collates, and analyses point counted petrographic data (PETROG System, Conwy Valley Systems Ltd (CVS), UK). In conjunction with CVS, the Petrog software was developed to import SEM petrographic images (virtual images) and to quantify clay-coat grain coverage (Fig. 6.3). In order to quantify micron-scale clay-coats (Fig. 6.1C-I), a number of backscattered electron microscope images were collected, at a resolution appropriate to visualise the clay coats on 50 sand-grains per sample, and then analysed with the new Petrog perimeter tool. The method involved defining the total perimeter length of a grain (Fig. 6.3, red line) and then manually selecting the length that is covered by attached clay-coating material (Fig. 6.3, green nodes) (i.e. independent of clay-coat thickness) to calculate the percentage perimeter of the grain covered by clay coat material. Repeat analysis showed an average ± 1.7 % error based on 50 analysed sand-grains per sample (Wooldridge et al. 2017a).

The advantages of this method are: (i) the produced clay coat grain coverage data are comparable to the majority of modern analogue (qualitative) studies (Dowey 2013; Dowey et al. 2017) and (ii) it is possible to import any pre-existing image, of appropriate resolution, of clay-coated sand-grains (e.g. light optical, SEM, or SEM-EDS) and preform the analysis. A limitation of the method is consistency in identifying clay coats which is not trivial owing to SEM resolution and the nature of greyscale images, for thin (< 2 μm) thick coats (i.e. typical of outer estuarine sediments) (Fig. 6.1F, G).

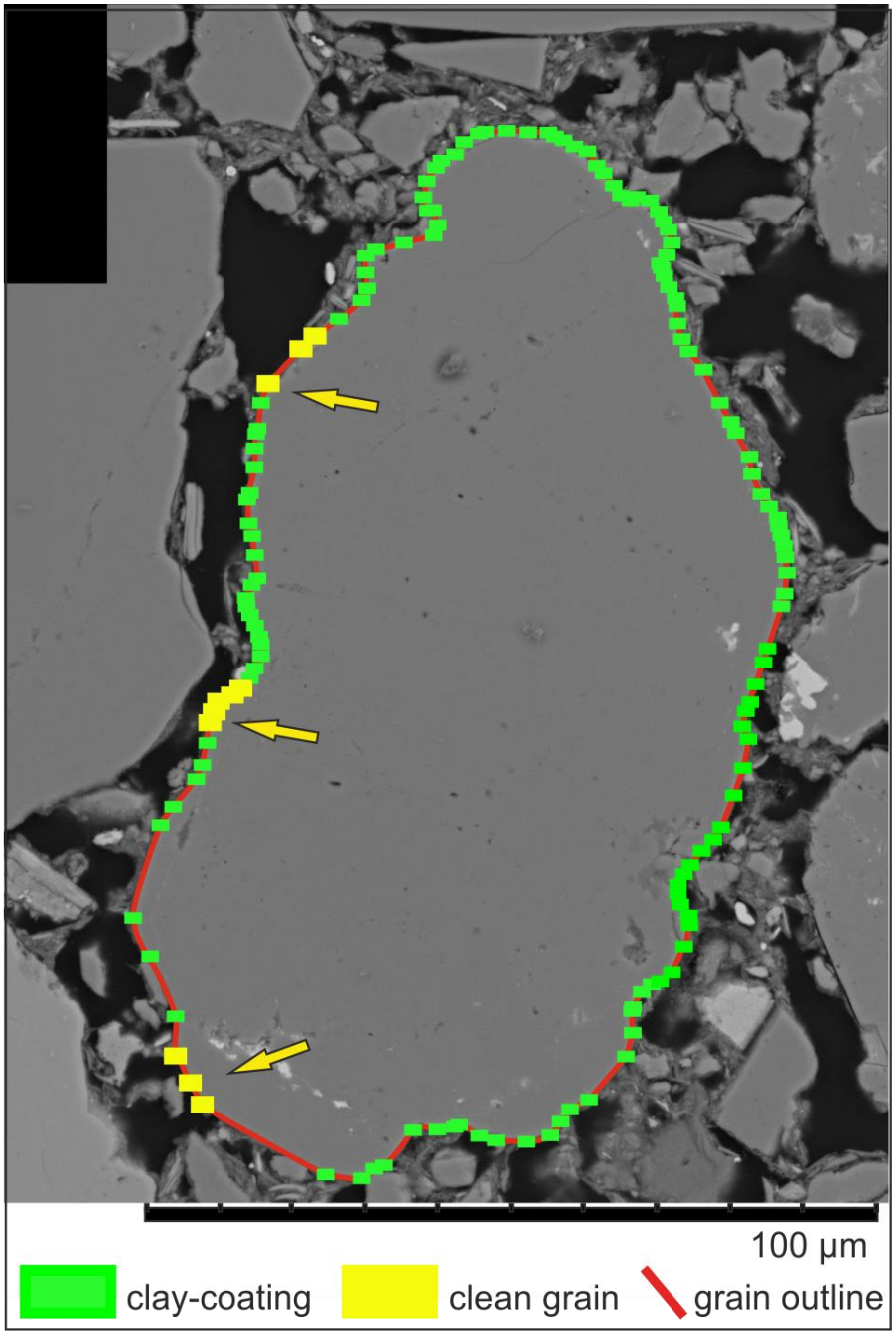

Figure 6-3. Scanning electron microscopy (SEM) image of clay-coated sand-grains (mixed-tidal-flat) from the Ravenglass estuary; showing the cross sectional perimeter length method (Petrog) of clay coat quantification. The red line indicates the user defined perimeter of the sand-grain. Green nodes indicate locations of attached clay coat material. Yellow nodes indicate the locations on the grain devoid of clay-coating.

6.4.2.2. Calculating clay coat coverage: volume of clay minerals present as coats: SEM-EDS

Scanning electron microscope-energy dispersive spectrometry (SEM-EDS) methods enable quantitative, *in-situ*, mineralogical imaging of micron scale textures (e.g. clay mineral coats) to a particle size resolution of 1 μm (Armitage et al. 2010; Wooldridge et al. 2017b). The SEM-EDS system (QEMSCAN®) comprises a scanning electron microscope, fast energy dispersive spectrometers (EDS), a microanalyser and an electronic processing unit (Armitage et al. 2016; Wooldridge et al. 2017b) using the software suite iDiscover. Mineralogical quantification is performed via two EDS detectors with analyses compared to a library of spectra with each analysis point assigned to a specific mineral. The output includes a backscatter electron image (Fig. 6.4A) and a fully quantitative map of mineralogy (framework grains and clay minerals) (Fig. 6.4B) with values presented as image-area percentage and imaged area mass (Fig. 6.4) (Wooldridge et al. 2017b).

The QEMSCAN® granulometry function permits the digital "sieving" of imaged sediment mineral particles by grain size into bin classes, e.g. clay, silt, and sand (Fig. 6.4C), based on the long axis of each particle. It is then possible to digitally sieve by grain size the component clay mineralogy (e.g. chlorite) (Fig. 6.4E).

Some phyllosilicates are present in lithic grains, e.g. chlorite in volcanic rock fragments (Worden and Morad 2003), and are coarse grained (Fig. 6.4C, D). Other phyllosilicates are present as coarse tabular grains (Worden and Morad 2003). Such material cannot form detrital sand-grain coats because it is the same size as the host sand. The spatial resolution limit of the SEM-EDS is slightly less than 1 μm, as defined by the fundamental physics of electron beam-polished section interaction (Emery and Robinson 1993), and so will not be able to detect isolated, sub-micrometre scale clay crystals. Previous studies of clay coats have revealed that they are composed of fine and medium silt-grade material (and finer grained material) (Dowey 2013; Dowey et al. 2017; Wooldridge et al. 2017b) (Fig. 6.5).

Therefore a 32 μm grain size cut-off was initially employed to discriminate material that was incorporated in grain coats. Analysis of samples from the Ravenglass Estuary (Fig. 6.5) revealed that the majority of chlorite and kaolinite crystals in grain coats were 16 μm so that a 32 μm grain size cut-off was used for grain-coating illite and a 16 μm grain size cut-off was used for grain-coating chlorite and kaolinite (Wooldridge et al. 2017b).

The approach adopted is predicated on the assumption that any monomineralic clay particulate clast > 16 μm (for chlorite or kaolinite) or > 32 μm (for illite) in the sediment is present as components of either clay-rich lithic fragments or other aggregates (Figs. 6.4, 6.5) and do not form clay coats. The discrimination of clay minerals based on size produces a quantified value for the total volume (image area) of clay in a sediment assemblage that is present as grain coats.

The advantages of this methodology are that: (i) the method is fully quantitative and automated once the initial size parameters have been established, (ii) the method provides information on clay-coat mineralogy, (iii) the data format (volume of clay present as clay-coats) may be comparable to clay coat volumes derived from point count measurements (format for the majority of ancient clay-coated sandstone studies), (iv) it is possible to extract sedimentological information in the form of grain size, sorting, lithic assemblage, and textural data, to permit direct comparisons between clay coat characteristics and sedimentological heterogeneities, (v) it is possible to import the SEM-EDS images into Petrog (see method above) and calculate exact clay coat grain coverage values for comparison (i.e. by enhanced identification of colour coded clay coats, Fig. 6.5), and (vi) the method gives an indication of the thickness of attached clay coating material and not just the degree of grain coverage.

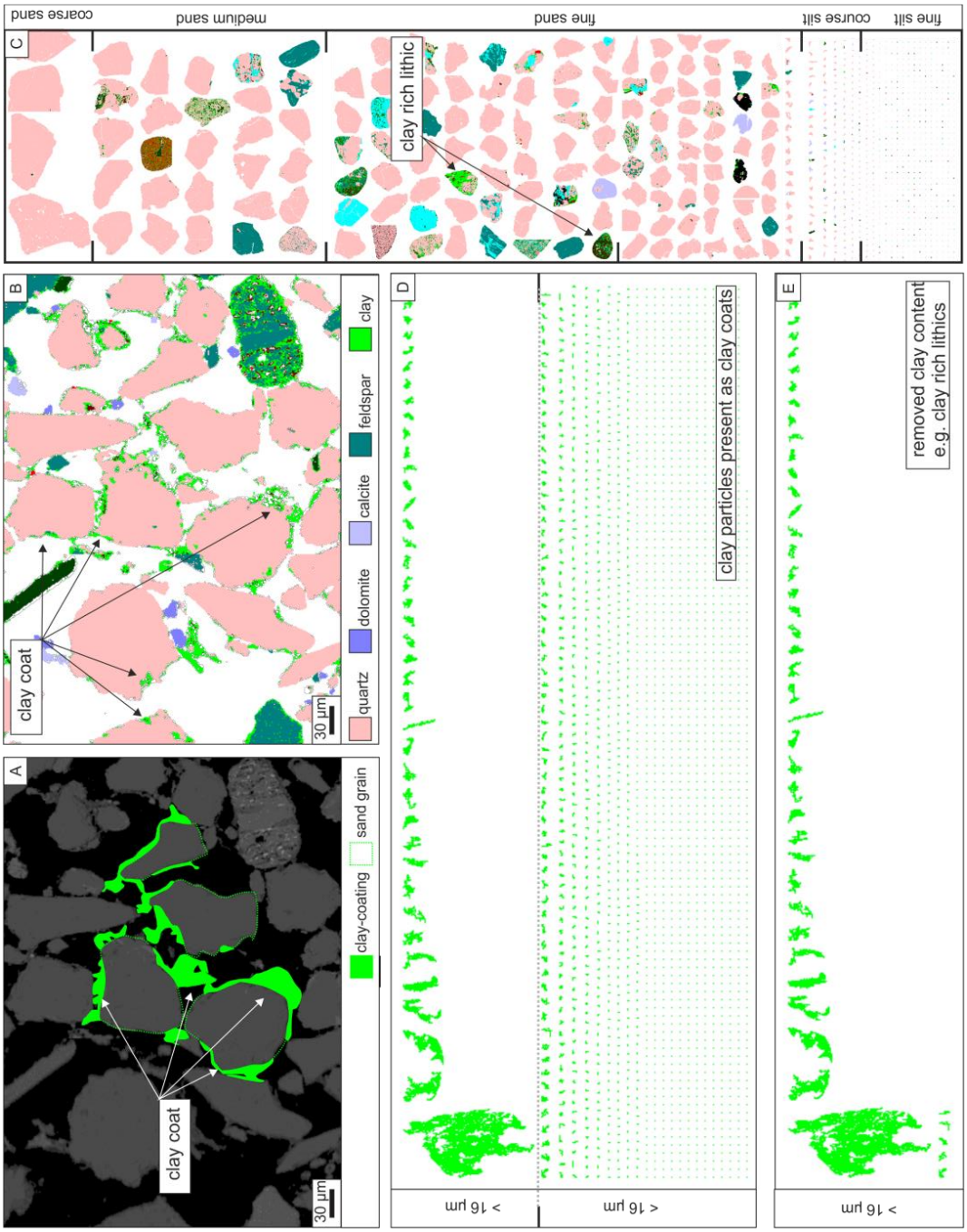

Figure 6-4 Scanning electron microscope–energy dispersive spectrometry (SEM-EDS) images of an estuarine tidal-flat sediment sample showing the SEM-EDS method of calculating clay-coat volume. (A) Backscattered electron image. (B) SEM-EDS image of the bulk mineralogy. (C) SEM-EDS image of the mineralogical mapped and digitally sieved component particles of the whole sample. (D) SEM-EDS image of chlorite clay minerals present within the whole sample organized on particle size (long axis). (E) SEM-EDS image of the component chlorite mineral particles that are > 16 µm and thus removed from clay coat calculations.

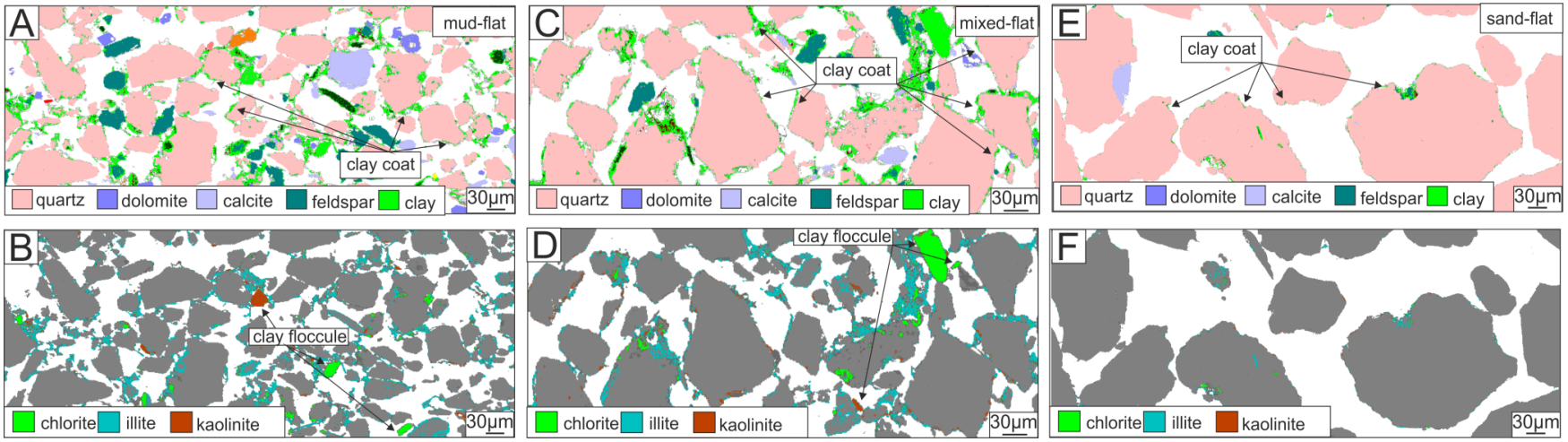

Figure 6-5 Scanning electron microscope energy dispersive spectrometry (SEM-EDS) images of clay-coat mineralogy from surface mud- flat (A, B), mixed-flat (C, D), and sand-flat (E, F) depositional environments. Numbers (1, 2, and 3) on Figure 6.1B show sample locations (e.g. mud-flat images A and B were taken of samples from Figure 6.1B)

6.5. Results

Clay coats in these modern estuarine sediments consist of clay minerals, clay- to silt- sized lithics, and organics, forming discontinuous accumulations of predominantly clay minerals attached to grain surfaces (Figs. 6.1 and 6.5). Strands of clay material extend into the pore from the grain and link framework grains via a bridge to produce a webbed texture that is consistent with previously reported marginal-marine clay coat characteristics (Dowey 2013; Dowey et al. 2017) (Fig. 6.1 C-I). Important observations are that clay coats are heterogeneous across marginal-marine sediments (Fig. 6.6) and that clay coats in the sand-dominated, inner-and outer-outer estuarine, depositional environments (e.g. tidal-flat, tidal-bars, and foreshore) exist as thin, discontinuous accumulations, found preferentially in grain indentions (e.g. Fig. 6.1D-I).

6.5.1. Clay coat distribution patterns in the modern Ravenglass Estuary

Figure 6.6 represents the spatial distribution trends of clay-coat grain coverage across the Ravenglass Estuary as defined by: (i) qualitative (Fig. 6.6A), (ii) quantitative clay-coat coverage (Fig. 6.6B), and (iii) quantitative volume of clay coats (Fig. 6.6C).

Qualitative characterisation of clay coats reveals outer-estuary sediment contains no more than minor quantities of attached clay coats and an overarching trend of increasing coverage with distance from the open ocean (i.e. towards the tidal limit) and with distance from the main ebb channel (Fig. 6.6A).

The quantitative clay coat method (Petrog) revealed a strong heterogeneity in clay-coat coverage within inner estuarine depositional environments ranging from < 1 % to > 50 % with values increasing upstream towards the tidal limits (Fig. 6.6B, Table 6.1). Outer-estuarine sediments display a more homogenous distribution ranging from 4.3 % to < 1 %

with most grains exhibiting partial attached clay coats, increasing with proximately to the tidal inlet (Fig. 6.6B, Table 6.1).

The quantitative clay coat method using SEM-EDS to determine the volume of clay coats also revealed a strong heterogeneity ranging from 2 to 18 % with values increasing with distance away from the open ocean and towards the tidal limit (Fig. 6.6C, Table 6.1). Sediment with clay coat volumes > 5 % are confined to inner estuarine depositional environments (Fig. 6.6C). Sediment samples with clay coat volumes > 7 % are confined to mixed- and mud-tidal flats and tidal-bar depositional environments of the inner estuary (e.g. compare Fig 6.1B to 6.6C, Table 6.1). The central estuarine zone sediments display a progressive increase in clay-coat volume across the tidal-flat succession from < 3 %, in the outer most sand-flat, to 18 % in the upper mud-flat (compare Fig. 6.6C to 6.1B). The marine end of the estuary (i.e. foreshore, pro-ebb delta, and tidal inlet) showed a more homogeneous distribution with values ranging from 2.2 to 4.4 %. The data set presents an incremental decrease in the volume of clay-coating, clay minerals from the inner- to the outer- estuary (Fig. 6.6C). Values are summarized in Table 6.1.

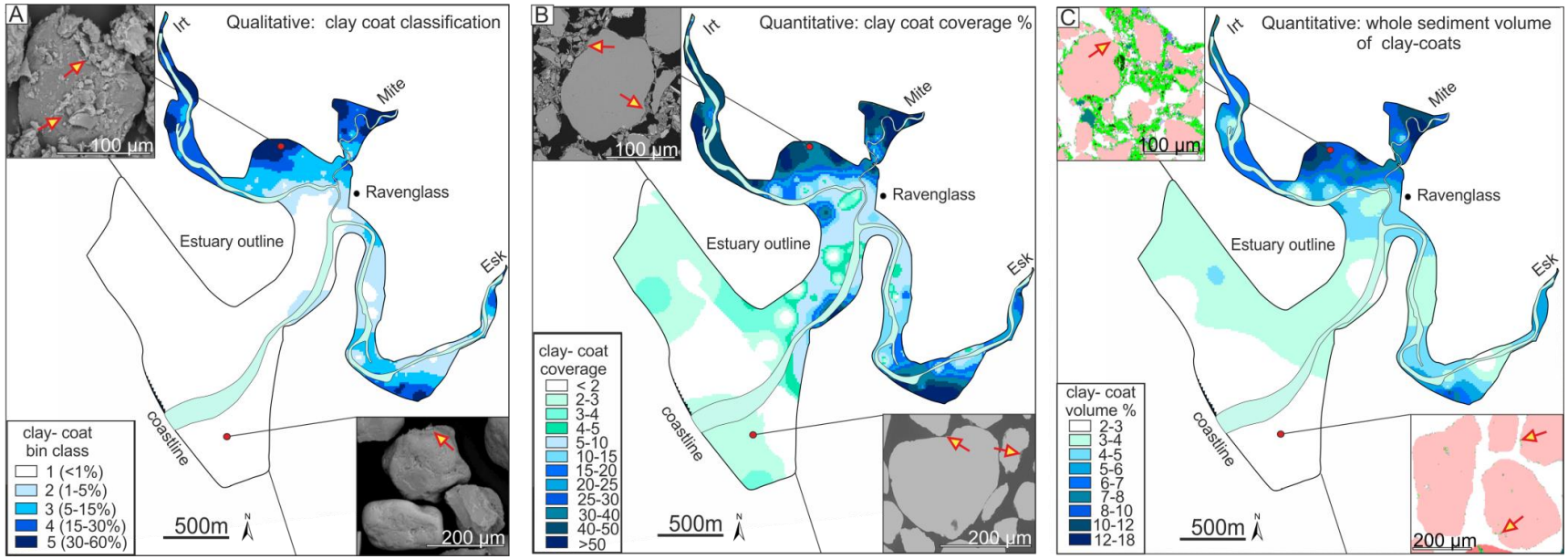

Figure 6-6 Distribution maps of clay-coat coverage across the Ravenglass marginal marine system. (A) Map of clay-coat coverage (quantitative characterisations). (B) Quantitative map clay-coat coverage (Petrog method). (C) Quantitative map of clay-coat volume (SEM-EDS method).

Depositional environment	Quantitative						Qualitative		
	clay-coat coverage %			volume of clay coats %			bin class		
	average	range		average	range		modal class	range	
		max	min		max	min		max	min
Mud-flat	63.74	80.75	53.72	13.32	17.85	8.73	5	5	4
Mixed-flat	30.08	69.35	3.48	8.45	13.78	3.83	3	5	2
Sand-flat	5.17	13.00	0.941	3.24	4.72	2.08	1	3	1
Tidal-bar	4.93	12.25	1.33	3.85	8.07	2.47	1	2	1
Tidal-bar vegetated	9.60	41.63	9.60	4.61	6.63	3.27	_	4	1
Pro-ebb delta	1.89	2.85	0.92	2.52	3.05	2.25	1	1	1
Foreshore	2.43	4.28	1.23	3.02	4.41	2.24	1	1	1

Table 6-1 Clay coat heterogeneity of the Ravenglass Estuarine system.

6.5.2. Effect of qualitative and quantitative classification procedures on the distribution trends of clay-coated sand-grains in the Ravenglass Estuary

The overall distribution trends of the extent (coverage and volume) of detrital-clay-coated grains for the qualitative and quantitative methodologies are similar (Fig. 6.6). All methods depict reduced or absent clay-coat coverage in the high energy foreshore, tidal inlet, sand-flats, and tidal-bar depositional environments (compare Fig. 6.6 to 6.1B). These figures indicate that each technique is capable of differentiating the relative extent of clay coats across marginal-marine sediments.

The two quantitative methods display detailed patterns of variability in the extent of clay-coat coverage in the sand-dominated, high energy settings (i.e. foreshore, tidal inlet, sand-flats, and tidal-bars; Figs 6.6B and C). An incremental increase is present in the abundance of clay-coat coverage from the pro-ebb delta to the inner estuary (Fig. 6.6B and 6.6C).

Where the percentage of clay-coat coverage is greater than 50 % (Fig. 6B) this equates to 12-18 % clay-coat volume (Fig. 6.6C). Also, samples with < 30 % clay-coat coverage have a clay-coat volume corresponding to < 6 %. Overall, this indicates a reduced clay-coat volume (thickness) equates to a reduced clay-coat coverage (Fig. 6.1 C-I).

In the coarser grained sediments that tend to have less well-developed clay coats, the qualitative technique does not adequately discriminate the variability of clay-coat coverage detailed by the quantitative approaches (compare Fig 6.6A to 6.6B and 6.6C). For example, bin class 1 (defined as < 1 %) encompasses a range of samples that contain up to 10 % clay-coat coverage as determined by the quantitative clay-coat coverage method (Petrog) (Fig. 6.7A).

It is apparent that many of these marginal marine sediments have < 10 % clay coverage (Fig. 6.7C). The exceptions tend to be mud- and mixed-tidal flat samples (compare Fig. 6.1

to 6.6) which have > 10 % clay-coat coverage and > 5 % clay-coat volume (Fig. 6.7C). The volume of clay coat material correlates broadly with increased grain coverage (Fig. 6.7C). Figures 6.7A and B illustrate that qualitative (bin class) classification of clay coats are unable to differentiate between low degrees of clay-coat coverage.

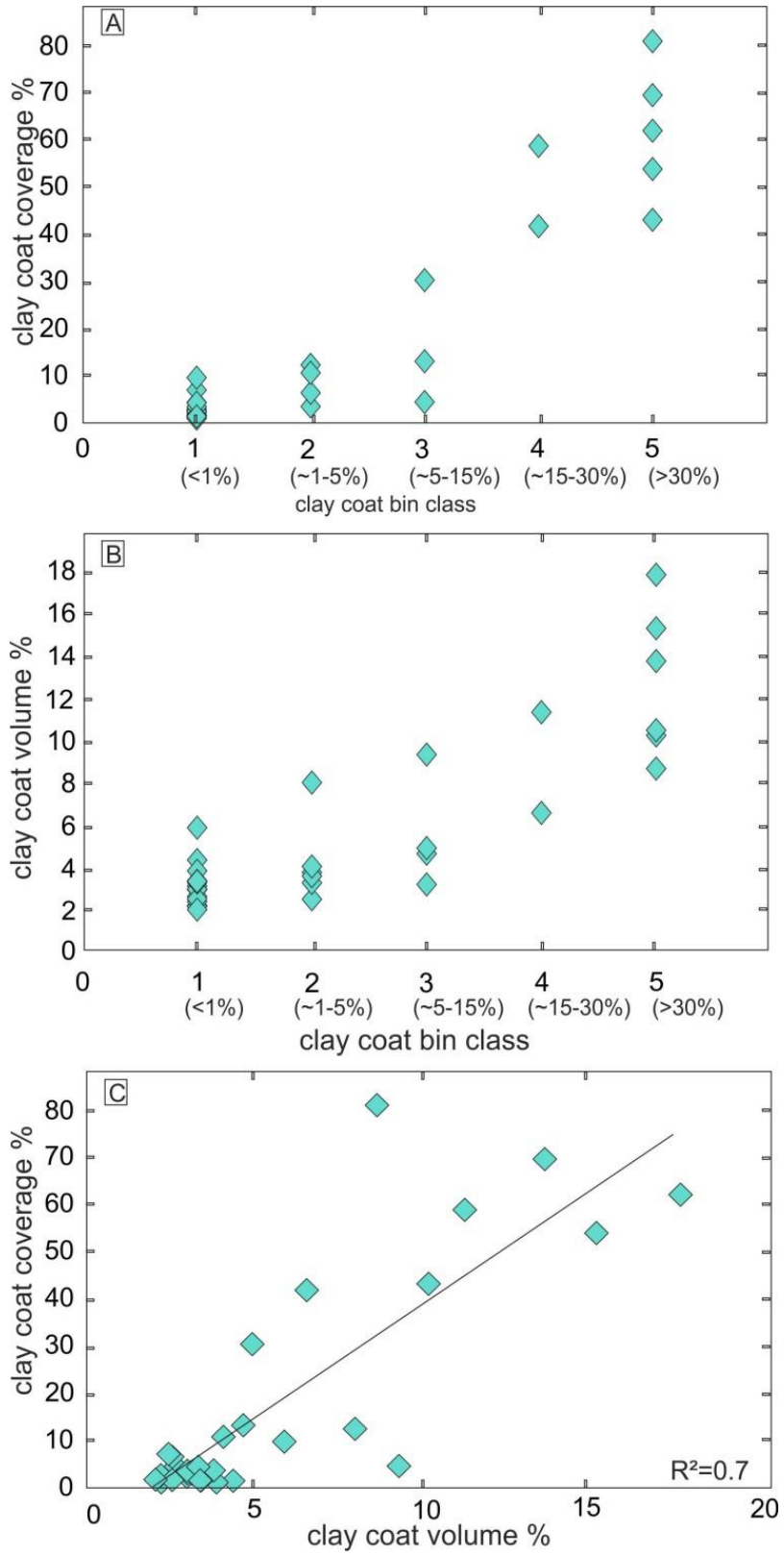

Figure 6-7 Cross-plots of clay coat characteristics as determined via different quantification methods. (A) Plot of qualitative clay-coat coverage (bin classes), against, quantitative clay-coat coverage (Petrog method). (B) Plot of qualitative clay-coat coverage (bin classes), against, quantitative volume of coating clay (SEM-EDS method). (C) Plot of quantitative clay-coat coverage, against, quantitative volume of coating clay.

6.5.3. Application of quantitative classification procedures to Lower Jurassic chlorite cemented sandstones

A high resolution SEM-EDS image (step size of 1 μm), with an area of 4 mm^2, was generated from a polished thin section of a Lower Jurassic, chlorite-cemented, marginal marine sandstone in order to illustrate the applicability of the techniques developed for modern sediments to reservoir samples.

Petrog was used to define the average clay-coat coverage for the entire 4 mm^2 area of the SEM-EDS image (Fig. 6.8) producing data analogous to Figure 6.6B from the modern sediments. The sample contained an average of 12 % clay-coat coverage.

The digital sieving tool in the software suite iDiscover (available to QEMSCAN-users) was then applied to the same 4 mm^2 area (Fig. 6.9). A significant proportion of the clay present in this sample was not grain-coating. Figures 6.9C, D and E detail the distributions of chlorite, kaolinite and illite illustrating the SEM-EDS's capability for resolving grain-coating clay, clay-rich clasts, grain-replacive clay, and detrital phyllosilicates. In this sample, the digital sieve limit for monomineralic clay coat entities was set to < 32 μm (long axis) (Fig. 6.6). Clay entities > 32 μm were not classed as grain-coating. Note that this clay size will probably vary between different petroleum reservoirs thus requiring petrographic analysis ahead of SEM-EDS data processing. The sample contained an average of 7 % clay coat volume.

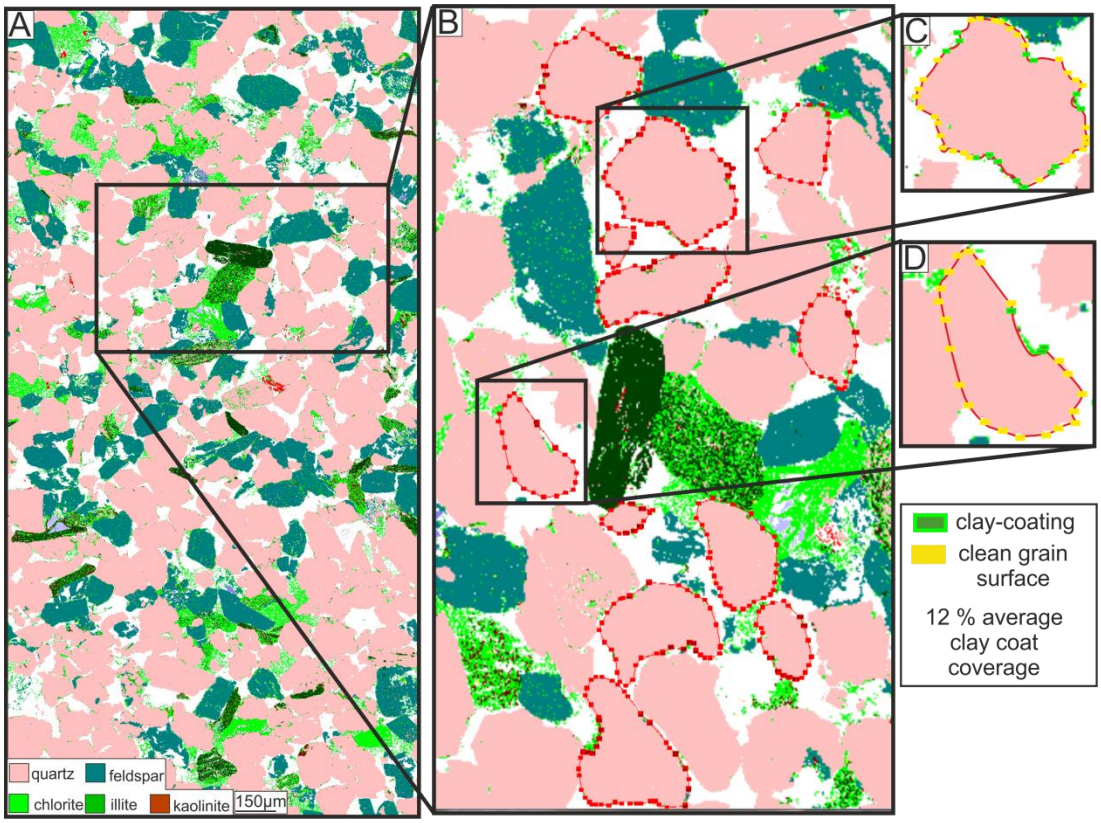

Figure 6-8 (A) Scanning electron microscope–energy dispersive spectrometry (SEM-EDS) of a Lower Jurassic, chlorite cemented sandstone, North Sea reservoir, showing the cross sectional perimeter length method (Petrog). (B) Image illustrating, step 1 of the method; defining the perimeter length of each grain. (C) Image illustrating the technique of clay-coat coverage characterisation (yellow nodes; grain outline; green nodes: location of attached clay coats).

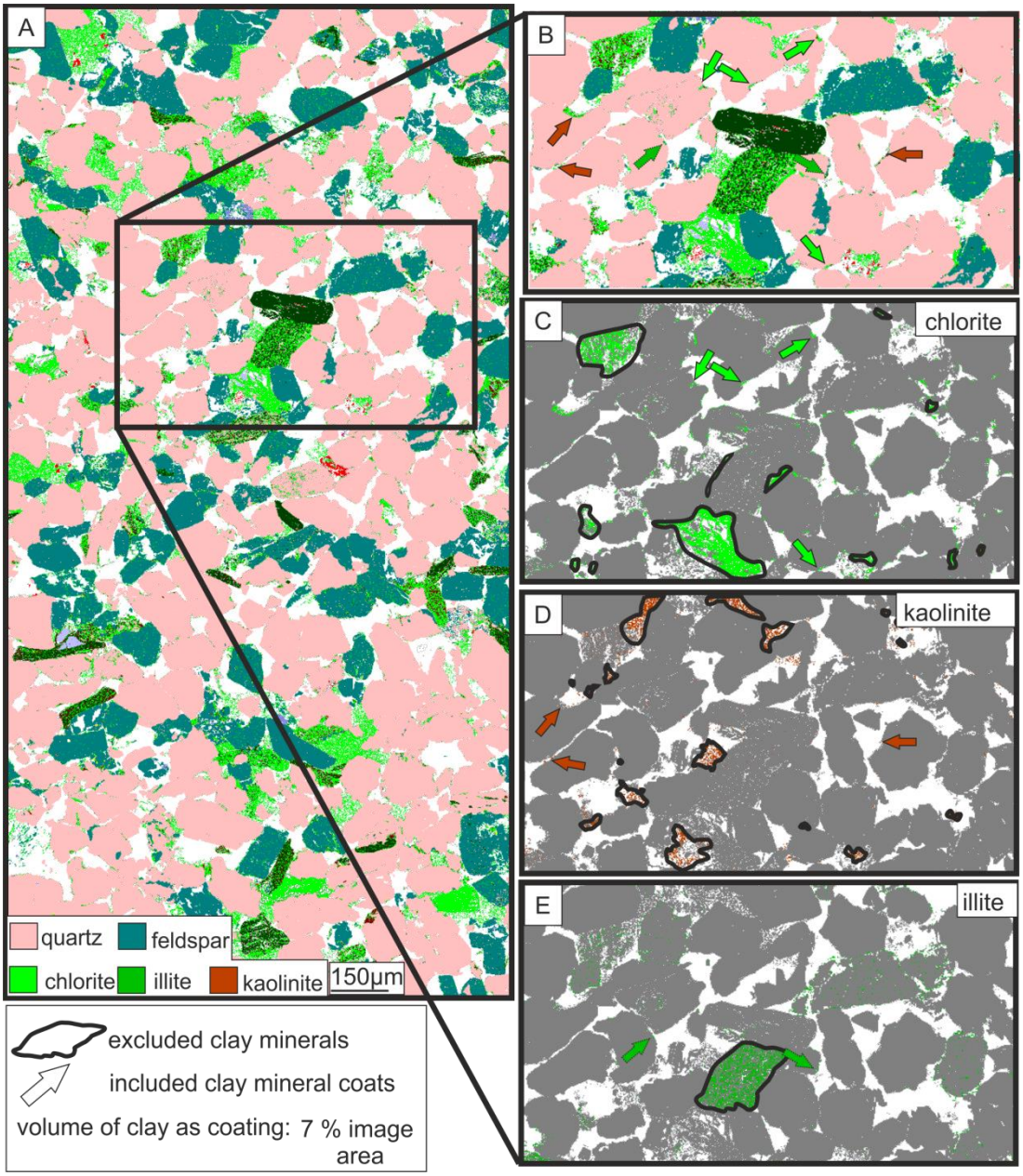

Figure 6-9 (A) Images of scanning electron microscope–energy dispersive spectrometry (SEM-EDS) of a Lower Jurassic, chlorite cemented sandstone, North Sea reservoir, showing the SEM-EDS method for calculating clay-coat volume. (B) Enlarged SEM-EDS image identifying the presence of clay-coat coverage. (C, D, and E) are images depicting the internal distribution of the component clay mineral assemblage (e.g. clay coats, pore-filling, or grain replacing chlorite, kaolinite, and illite).

6.6. Discussion

This comparative study of clay coat characterisation techniques illustrates that, despite the broadly comparable distribution trends between qualitative and quantitative methodologies, there is a need to apply quantitative analytical techniques to accurately resolve the distribution of clay coated sand-grains in marginal-marine, sand-dominated sediments. Qualitative methodologies poorly resolve clay coats with < 10 % average grain coverage (i.e. outer estuarine sediments).

The discrepancy in the distribution of clay coated sand-grains between the two quantitative techniques (compare Fig. 6.6B to 6.6C) in the foreshore samples, potentially results from the challenge presented in manually resolving thin and discontinuous coats using backscattered SEM images (Fig. 6.1C-I). The ability to constrain such thin, discontinuous coats is fundamental because, as noted by Bloch et al. (2000), minor amounts of clay (as little as 1 to 2 % of the rock volume) can coat a relatively large surface areas of sandstone grains and are potentially capable of inhibiting quartz cementation (Bloch et al. 2002; Ehrenberg 1993).

Previous schemes for predicting the characteristics of clay coats in the subsurface have been exclusively based on qualitative methodologies (Dowey 2013; Dowey et al. 2017; Wooldridge et al. 2017b). The work presented here affirms the potential usefulness of such qualitative schemes in predicting large scale trends in clay coat extent (coverage and volume), due to the overall correlation between qualitative and quantitative techniques (Figs. 6.6 and 6.7).

The clay coat distribution trend in the Ravenglass Estuary (Fig. 6.6), is not unique and is broadly comparable to distribution patterns reported for the Anllóns Estuary, NW Spain, and the Leirávogur Estuary, Iceland (Dowey 2013; Dowey et al. 2017) as determined by qualitative characterisation.

The applicability of the two quantitative methods means that they can be applied to calculate clay-coat coverage and the volume of coating clay from ancient sediments, as illustrated from a North Sea, reservoir sandstone in Figures 6.8 and 6.9. An advantage of these quantitative techniques is that they produce data sets of clay coat distribution that are directly comparable between modern analogue and subsurface core-based investigations.

6.7. Implication for future hydrocarbon exploration

The clay coats characterised in this study are characteristic of detrital-clay coats (Wooldridge et al. 2017b) which have been reported to be potential precursors to the clay coats that are present in numerous, deeply-buried, sandstones (Ajdukiewicz and Larese 2012; Bloch et al. 2002; Wise et al. 2001; Worden and Morad 2003). Diagenetic clay coats have been interpreted to derive from the recrystallization of clay-coats that formed during deposition (i.e. detrital-clay coats) (Ajdukiewicz and Larese 2012; Bloch et al. 2002). The ability to produce fully quantitative analogue data sets of clay coat distribution across modern systems will lead to models that are potentially capable of being used to predict reservoir quality in sandstones.

The ability to constrain the volume of clay coat material is of significance because, as shown by Aagaard et al. (2000) in experiments replicating burial diagenesis, discontinuous detrital-clay coats transform (neoform) into complete diagenetic-grain coats. The implication of this is that even with discontinuous (detrital) clay coats, it would require only a minor amount of clay material (1 to 2 % of the rock volume) to transform and completely coat a relatively large surface area of sandstone capable of inhibiting quartz cementation (Bloch et al. 2002). The ability to measure the volume of clay-coat material (Fig. 6.6C) and detrital-clay-coat coverage (Fig. 6.6B) thus permits an enhanced understanding of the

potential post-diagenetic extent (thickness and grain coverage) of clay coats in deeply-buried sandstones.

This study constrained the distribution of clay coated sand-grains across a modern marginal-marine system, an environment of deposition comparable to many notable ancient, clay-coated sandstones, such as the Tilje Formation, Norway (Ehrenberg 1993), the Garn Formation, Norway (Storvoll et al. 2002) and the lower Cook Formation, Knarr Field, Norway (Skarpeid et al. 2017). Sandstones originally deposited in marginal marine settings represent a potential 54 % of all reported chlorite coated sandstone reservoirs (Dowey et al. 2012) so that our novel quantitative maps of clay-coat volume (Fig. 6.6C) can be applied, by analogy, to aid the prediction of best reservoir quality, in deeply-buried, marginal marine sandstones. It is noteworthy that the qualitative methodology for measuring clay-coat coverage cannot resolve clay coats with less than 10 % coverage (Fig. 6.6A and 6.7A) so that quantitative techniques should be employed for both modern sediment and ancient deeply-buried sandstone reservoirs.

6.8. Conclusion

1. Clay coat distribution trends, obtained via qualitative and quantitative methodologies, have been compiled to produce the most complete view of clay coat heterogeneity across a marginal marine system.
2. Quantified data sets for the spatial distribution of the clay-coat volume (indication of thickness) revealed an increase in a landward direction with the greatest volumes of grain coating clay minerals in the inner estuarine tidal-bar and tidal-flat depositional environments.
3. The greatest volumes of grain coating clay minerals occur in the mud-flat samples (< 18 %) with up to 4 % in foreshore sediment assemblages.

4. Qualitative and quantitative methodologies produced broadly comparable clay coat distribution trends. However, qualitative techniques inadequately characterised clay-coat variability in the sand-dominated sediments with < 10 % average grain coverage (e.g. sand-flat, tidal-bars, foreshore, and pro-ebb delta).
5. These techniques developed for modern sediments, have here been shown to work for ancient, deeply-buried sandstone reservoir samples.
6. Current predictive models for the distribution of clay coats in deeply-buried sandstones, based exclusively on qualitative data sets, potentially underestimate the distribution area and extent of clay-coat grain coverage.

7. The origin and distribution of clay-coat mineralogy

7.1. Abstract

The mineralogy of clay minerals attached as clay coats (rims) to grain surfaces has been shown to excerpt a fundamental control on the ability of the clay coat to inhibit quartz cementation during prolonged burial and heating. How and why clay-coat mineralogy varies across marginal systems, remains unconstrained despite clay mineralogy controlling cement growth–interference textures and ultimately the volume of porosity occluding quartz cements. Thus, the ability to predict the distribution of clay-coat mineralogy is crucial in locating good reservoir quality in deeply-buried sandstones.

A moderate amount of clay minerals has been shown to be advantageous for reservoir quality in deeply-buried sandstones, if present as clay coats. Clay minerals have been reported to occur principally as flocculated mud clasts (salinity or biologically facilitated), mud intraclasts (autochthonous grains composed of aggregated clay), and clay-rich rock fragments (allochthonous clay-rich sand-grains) concentrated as laminations, or, dispersed throughout marginal marine sediments. However, the properties of clay mineral volume and internal distribution patterns remain unconstrained, despite being of paramount importance for subsequent diagenetic sandstone properties.

This study focused on the Ravenglass Estuary, UK. The application of a novel methodology utilising scanning electron microscope-energy dispersive spectrometry, enabled for the first time, the ability to differentiate the clay-coat mineral signature from that of the whole sediment and the internal distribution of clay minerals in the sediment.

Clay coats present a mixed mineralogy which is shown to be spatially heterogeneous across marginal-marine depositional environments. The study showed that clay-coat mineralogy is governed, firstly, by the hydrologically controlled feactionation of the clay mineral

assemblage within inner estuarine depositional environments and secondly, by the selective abrasive removal of specific clay mineral classes on reworking and transport. The highest relative abundance of clay-coating chlorite occurred in sand-flat and tidal-bar depositional environments. Marginal marine sediments are shown to have a clay mineral assemblage distributed, principally (81 % average) as clay coats. The availability of an analogue data set and an understanding of the controlling processes of clay-coat mineralogy offer a crucial step in building a predictive capability for clay coat derived elevated reservoir quality in deeply-buried sandstones.

7.2. Introduction

The principal factor controlling the effectiveness of clay coats (chlorite, illite, and mixed mineralogy) to inhibit the typical porosity-occluding, authigenic quartz cement and thus preserve elevated primary porosity in deeply-buried sandstones, is the completeness of grain coverage (Ajdukiewicz and Larese 2012; Bloch et al. 2002; Skarpeid et al. 2017). Clay coat presence is thus the primary control on clay coat-effectiveness to inhibit quartz cement growth (Ehrenberg 1993). Clay-coat mineralogy is an important secondary control on quartz cement growth since there are morphological differences between coats composed of different clay minerals (Ajdukiewicz and Larese 2012).

Detrital-clay coated sand-grains form at, or near, the surface of the sediment in the eodiagenetic realm and form the focus of this study (Ajdukiewicz and Larese 2012; Dowey et al. 2017; Wooldridge et al. 2017b; Worden and Morad 2003). Numerous authors have concluded that diagenetic clay coats (those found in many ancient and deeply-buried sandstone reservoirs) form via: (i) the thermally-driven recrystallization of attached detrital-clay-coat material and (ii) authigenic *in-situ* precipitative growth (accretion) through diagenetic mineral interactions (i.e. grain dissolution and re-precipitation) with pore fluids. Authigenic coats are most commonly reported to have nucleated on an existing detrital-clay mineral root (Ajdukiewicz and Larese 2012; Bloch et al. 2002; Gould et al. 2010; Stricker and Jones 2016; Worden and Morad 2003).

To constrain the fundamental role of clay mineralogy in governing the elevated preservation of primary porosity (through the inhibition of quartz cement), it is worth reviewing the process of quartz cementation and the mechanism of clay coat-derived inhibition. The quantity of the typically-dominant quartz cement (Lander et al. 2008; Worden and Morad 2000) is the main control, after-compaction, on porosity in many deeply-buried sandstones (Worden and Morad 2000). Quartz cementation occurs initially

as scattered “blob”-like anhedral crystallites on isolated sites across a quartz grain surface (Ajdukiewicz and Larese 2012; Lander et al. 2008; Pittman 1972). Epitaxial growth of the anhedral quartz crystallites causes the lateral spreading of the cement across the grain surface until they mutually contact and so coalesce with other originally isolated overgrowths (Ajdukiewicz and Larese 2012; Lander et al. 2008). Continued growths of the coalesced crystallites produces the characteristic euhedral termination associated with authigenic quartz cements (Lander et al. 2008).

Clay coats are reported to inhibit quartz cementation via a two-step process: (1) At moderate temperatures (approximately 115 °C), the coats (if complete) physically isolate the grain surface from silica saturated pore fluids, thus retarding initial quartz cement nucleation (thus known as nucleation inhibition). (2) At high temperatures (115 to > 160 °C), isolated nanocrystals of quartz cement begin to nucleate between the clay mineral particles of the coat (growth inhibition). At these high temperatures, clay particles in the coat act as barriers (discontinuities) which prevent (kinetic or diffusion barrier) the epitaxial quartz growth and subsequent coalescence (Ajdukiewicz and Larese 2012; Billault et al. 2003; Lander et al. 2008). The result is a reduced cement growth rate and isolated quartz nanocrystals between the clay mineral constituents of the coat (Ajdukiewicz and Larese 2012; Billault et al. 2003; Lander et al. 2008). Isolated nano-quartz cement crystallites between clay coat minerals have been reported in the Jurassic, Haltenbanken reservoirs, Norway (Billault et al. 2003) and the Triassic, Skagerrak reservoirs, Central Graben, UK (Stricker and Jones 2016). The clay particle constituents in the coats inhibit the coalescence and formation of euhedral quartz overgrowth terminations, resulting in a reduced net volume of quartz cement (Lander et al. 2008). Clay coat discontinuities on grain surfaces, inhibit the total volume of quartz (i.e. Isolated nano-quartz cement crystallites instead of euhedral, pore-filling, quartz overgrowth terminations) cement until a time whereby the quartz crystallites, isolated by clay coats, grow around the coating clay

particles and form euhedral terminations (Lander et al. 2008); this is typically associated with elevated temperatures, (e.g. > 160 °C) (Ajdukiewicz and Larese 2012).

The ability of the attached clay coats to inhibit epitaxial cement growth is thus a function of clay coat morphology, which is, in turn, controlled by clay mineralogy (Ajdukiewicz and Larese 2012): (i) chlorite (platy to curly crystals) and (ii) illite (fibrous hair like) in deeply-buried sandstones. It is apparent that it is the morphology of the coat that directly controls quartz cement inhibition. Chlorite has been reported to better inhibit quartz cement than illite, due to the typical morphology of chlorite (Ajdukiewicz and Larese 2012; Bloch et al. 2002).

Elevated porosity in deeply-buried sandstones has been commonly associated with chlorite clay coats (Dowey et al. 2012), however illite, and mixed mineralogy (e.g. illite-chlorite-smectite) coats have been reported (Table 7.1). Mixed mineralogy coats occur in sandstones deposited in marginal marine settings (Table 7.1) and have significantly enhanced reservoir quality in several notable marginal marine sandstone reservoirs from the Norwegian Continental Shelf (Martinius et al. 2005; Storvoll et al. 2002), the Ordos Basin, China (Luo et al. 2009), and the Ghawar Field, Saudi Arabia (Al-Ramadan et al. 2004).

Age	Formation	Location	Region	Environment	Mineralogy	Reference	Reservoir quality effect
Middle Jurassic	Garn Formation	Haltenbanken area	Norway	Upper shoreface to foreshore facies	Illite and chlorite	(Storvoll et al. 2002)	Positive
Lower Jurassic	Åre, Tilje, Ile, Tofte, Garn	Halten Terrace	Norway	Deltaic and esturine	Mixed illite-chlorite	(Martinius et al. 2005)	Positive
Jurassic and Triassic	-	Ordos Basin	China	Fluvial and lacustrine-deltaic	Illite and chlorite	(Luo et al. 2009)	Positive
Devonian	Jauf Formation	Ghawar Field	Saudi Arabia	Tidal, fluvial or deltaic channels	Illite, chlorite, and minor kaolinite	(Al-Ramadan et al. 2004)	Positive
Miocene, Neogene	-	Vienna Basin	Austria	Lacustrine to fluvial	Mixed chlorite-illite-smectitie	(Gier et al. 2008)	-
Lower Cretaceous	Pendencia sandstones	Potiguar Basin,	Brazil	Fan delta and fluvial	Mixed illite-smecitre and chlorite-smectitie	(Anjos et al. 2000)	-
Cretaceous-Tertiary	-	Shetland-Faroes Basin	British continental shelf	Turbidites	Illite and chlorite	(Mansurbeg et al. 2008)	Positive
Upper Cretaceous	Mesaverde Group	Piceance Basin	USA	Fluvial	Chlorite and illite	(Stroker et al. 2013)	Positive
Late Cretaceous	Williams Fork Formation	Piceance Basin	USA	Fluvial facies channel and splay sands - marine	Chlorite and illite	(Ozkan et al. 2011)	Positive
Triassic	Skagerrak Formation	Central Graben, North Sea	UK	Braided and meandering fluvial systems	Chlorite, illite, and mixed-layer chlorite/illite–smectite	(Stricker and Jones 2016)	Positive
Devonian-Carboniferous	Clair Group	Clair Basin, North Sea	UK	Fluvial, aeolian, and lacustrine	Chlorite, illite, and mixed mineralogy illite/chlorite-smectite, and chlorite-corrensite	(Pay et al. 2000)	-

Table 7-1 Examples of mixed mineralogy clay coated sandstone reservoirs

Modern detrital-clay coats have been shown to consist of a diverse mixture of phyllosilicates (chlorite, illite, kaolinite, berthierine, smectite, and odinite) that are bound to framework sand-grain surfaces (Daneshvar 2011; Dowey et al. 2017; Ehrenberg 1993; Wooldridge et al. 2017b). Detrital-clay coats are composed of aggregates of clay minerals, silt- to clay-sized lithics, and organics (diatoms) which form discontinuous accumulations attached to sand-grain surfaces (Dowey et al. 2017; Wooldridge et al. 2017a; Wooldridge et al. 2017b).

The initial mineralogy of the detrital-clay coat is the principal control on the mineralogy of the final diagenetic coats present in deeply-buried sandstones (Worden and Morad 2003) and thus influence the potential inhibitory-effectiveness of quartz cementation. There is growing awareness of the distribution of clay coats in modern systems (Wooldridge et al. 2017a; Wooldridge et al. 2017b). However, there is relatively sparse knowledge about the spatial distribution of clay-coat mineralogy in marginal-marine sediments. This represents a shortfall in our ability to develop a credible capability to predict reservoir quality as a function of clay coat-presence and clay-coat mineralogy.

The goal of this study was therefore to document clay-coat mineralogy across a marginal-marine system using an automated scanning electron microscope-energy dispersive spectrometry (SEM-EDS) methodology. This approach has allowed us to develop a novel ability to differentiate the clay-coat mineralogy from that of the whole sediment. The study addresses the following questions, focused on the Ravenglass Estuary, UK (Fig. 7.1).

1. How variable is clay-coat mineralogy in a modern marginal-marine system?
2. What controls the distribution of clay-coat mineralogy across a marginal-marine system?
3. Are trends in clay-coat mineralogy comparable to other modern or ancient and deeply-buried examples?

4. Can clay-coat mineralogy by predicted in modern and ancient and deeply-buried marginal marine sandstones?

7.3. Methods

7.3.1. Study site

The aim of the study was to establish the origin and distribution of clay-coat mineralogy in ancient deeply-buried sandstones by studying, at high resolution, a modern sedimentary analogue. The Ravenglass Estuary is a 5.6 km² area, macro-tidal (tidal range < 7.55 m) system, composed of three rivers that merge in a central estuarine basin: the Esk, the Mite, and the Irt, located in Cumbria, UK (SD 07608 96761) (Bousher 1999; Lloyd et al. 2013; Wooldridge et al. 2017b). A previous study of the estuary constrained the depositional environment and sedimentary framework which is utilized in this study (Fig. 7.1B) (Wooldridge et al. 2017b). The inner estuarine depositional environments of tidal-flats (mud, mixed, and sand) and tidal-bars (vegetated and non-vegetated) are consistent with a back-barrier, tidal-dominated hydrodynamic regime (Wooldridge et al. 2017b). The outer estuary (seaward of the dune topped barrier spits) is characterised by wave-dominated foreshore and pro-ebb delta depositional environments (Fig. 7.1B).

The Ravenglass Estuary has an overall clay mineral assemblage composed of illite, chlorite, and kaolinite, reported to have been derived principally from a suspended fluvial sediment source (Daneshvar 2011; Daneshvar and Worden 2016). Previous studies of the estuary have identified a heterogeneous distribution of clay-coated sand-grains (Wooldridge et al. 2017b) (Fig. 7.1C) across the full range of marginal-marine depositional environments.

Many ancient and deeply-buried, chlorite, illite, and mixed mineralogy clay coated sandstone were deposited in estuarine-marginal marine environments so that studying modern estuaries may unlock the ability to predict clay coat distribution in reservoir

sandstones (Dowey et al. 2012; Ehrenberg 1993; Skarpeid et al. 2017; Wooldridge et al. 2017b). The study area thus offered the ability to: (i) explore the spatial distribution of clay-coat mineralogy and (ii) constrain the controlling mechanisms, to aid prediction and understanding of clay coat derived reservoir quality in ancient and deeply-buried sandstones.

The fluvial-derived clay mineral assemblage originates principally from the incision and weathering of the hinterland Palaeozoic Eskdale Granite, the Triassic Sherwood Sandstone Group, the Borrowdale Volcanic Group geology, and outcropping glacial units (Moseley 1978). The chloritized Eskdale Granite (Moseley 1978) and chloritized pyroxenes in the Borrowdale Volcanic Group have been suggested by Griffiths (2017) to be the source of detrital-chlorite, with mica-bearing rocks in the hinterland providing the source for illite, and kaolinite derived as an alteration product of feldspar minerals or other aluminous silicate minerals.

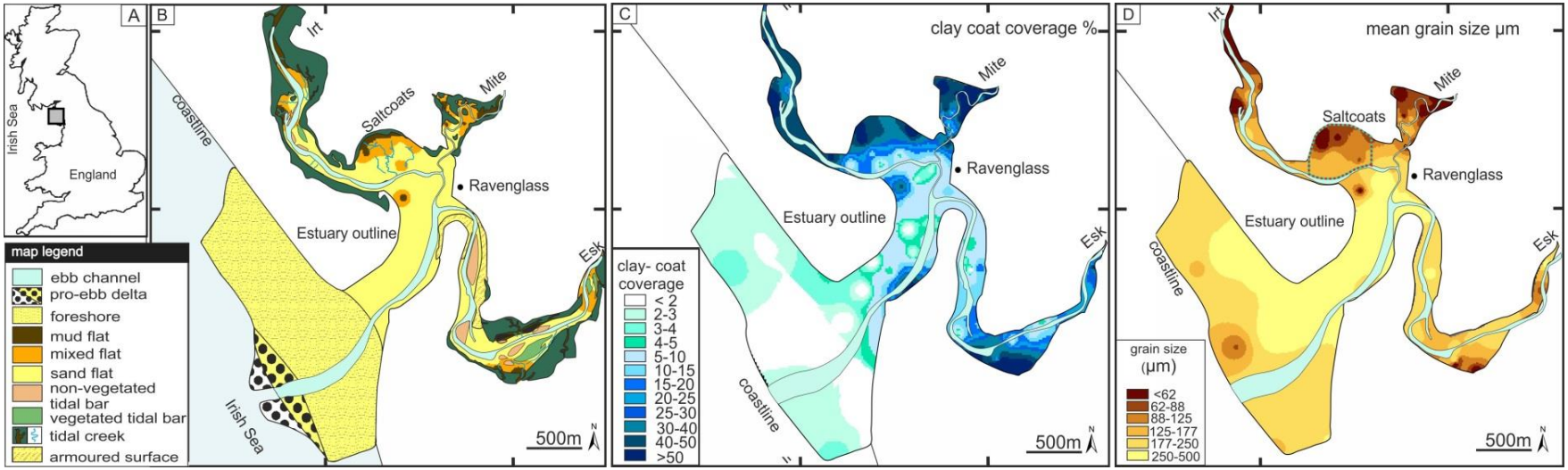

Figure 7-1 Location, depositional environment, clay-coat coverage and mean grain size maps of the Ravenglass Estuary. (A) The Ravenglass Estuary, in relation to the UK. (B) Geomorphological map of depositional environments. (C) Map illustrating the distribution of clay coated sand-grains. (D) Map of mean surface sediment grain size.

7.3.2. Sample suite and methodology

The study focused on a suite of 38 surface sediment samples (i.e. collected from the top < 2 cm of sediment) from which polished thin sections were constructed as grain mounts. Samples encompassed the range of intertidal depositional environments to produce a complete fluvial to marine transect of clay-coat mineralogy. Spatial distribution maps were plotted using the interpolation function in ArcGIS (https://www.arcgis.com). Clay mineralogy is here reported as index maps (e.g. illite/(illite + chlorite + kaolinite)) to constrain any relative distribution trends or spatial patterns. Pearson's correlation coefficient was used to determine the statistical significance between clay-coat mineralogy, clay-coat coverage, and sediment grain size.

Quantification of clay-coat mineralogy was undertaken via scanning electron microscope-energy dispersive spectrometry (SEM-EDS), using a QEMSCAN® system (Armitage et al. 2010; Armitage et al. 2016; Wooldridge et al. 2017b). This methodology permitted the *in-situ* mineralogical imaging and quantification of the sediment (e.g. framework grains and clay mineral assemblage) to a resolution of ~ 1 µm. The SEM-EDS, QEMSCAN® system digitizes the thin sectioned sediment by undertaking chemical mapping via two fast energy dispersive spectrometers (EDS detectors) with each analysed point (1 µm) compared to a library of spectra and assigned to a specific mineral (Armitage et al. 2010). Mineral mapping also produces a backscatter electron image and quantitative digital maps of clay mineralogy (image-area percentage and imaged area mass).

The granulometry function in the QEMSCAN® system permits the ability to digitally sieve component sediment minerals (e.g. chlorite and illite) based on particle size (long axis) (Fig. 7.2). The QEMSCAN® technique thus enables the digital-disaggregation of all the clay mineral components of a sample based on particle size (Fig. 7.2C).

Previous clay coat analysis of the Ravenglass Estuary defined the following typical maximum dimension of monomineralic clay mineral accumulations (illite < 32 µm, chlorite < 16 µm, and kaolinite < 16 µm) that are present in clay coats (Wooldridge et al. 2017b). The size of the clay minerals present in the coats defines them as silt-grade material, based on a particle size classification. However, for consistency with literature, clay coat terminology has here been applied. For a summary of the definitions of clay coat terminology see Dowey et al. (2017).

A fundamental assumption behind the methodology is that any monomineralic clay particle in excess of our user-defined clay coat maximum size, is present as either; (i) clay-rich lithic fragments, (ii) large clumps of clay material that potentially resulted from flocculation, or (iii) clay-rich intraclasts in the sediment and not as components of clay coats (Worden and Morad 2003). The ability to size-sieve minerals and separate out large clay-rich grains from clay coats (Fig. 7.2C) thus allowed us to quantify the clay mineralogy of grain coats.

Note that previous studies of clay-coat mineralogy used X-ray diffraction analysis (XRD) of separated fine and coarse sediment fractions of the whole sediment (Dowey 2013; Dowey et al. 2017; Wooldridge et al. 2017b). The methodology adopted here provides us with the novel ability to constrain the clay-coat mineralogy and differentiate it from the clay mineralogy of the whole sediment with one analysis followed by computational size-sieving.

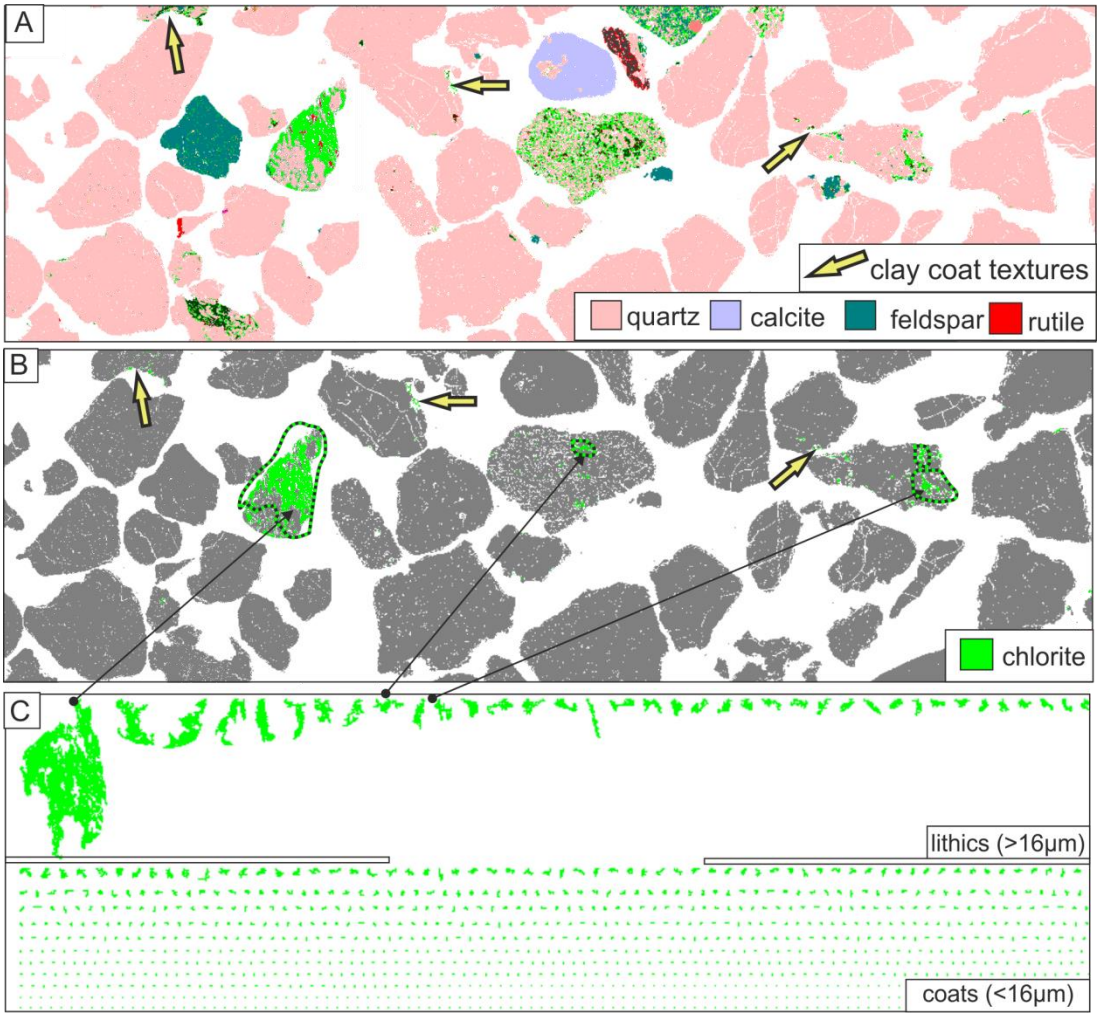

Figure 7-2 Methodology used for the quantification of clay-coat mineralogy via scanning electron microscope–energy dispersive spectrometry (SEM-EDS). (A) SEM-EDS image of the whole sediment. (B) SEM-EDS image of component chlorite mineral particles. (C) SEM-EDS image of the organised (based on long axis particle size) chlorite mineral particles. The line separates the component chlorite minerals based on size (long axis) (i.e. < 16 µm) which typically form components of clay coats opposed to (> 16 µm) which occur in clay rich lithics.

7.4. Results

7.4.1. Distribution of clay minerals in marginal-marine sediments

The whole sediment, clay mineral abundance map (Fig. 7.3A) shows an overall trend of increasing clay mineral content with increasing distance from the open ocean (i.e. towards the tidal limit). Values of sediment clay mineral percentages are summarised in Table 7.2. Note that there is no visible grain-supporting, clay matrix in any of the imaged samples (Fig. 7.3C to F).

Samples which contain a clay mineral content > 4 % are found predominantly in inner estuarine environments (compare Fig. 7.3A to 1B). Clay mineral abundance is heterogeneously distributed in the inner estuary, ranging from ~ 18 % to 2 %, with a higher average clay mineral percentage in samples from the northerly Irt arm of the estuary than the southerly Esk arm of the estuary (compare Fig. 7.3A to 1B). Inner estuarine samples that contain < 4 % average clay minerals occur principally in deposits from non-vegetated tidal-bars and sand-flats (compare Fig. 7.1B to 7.3A). Mud-flat samples contain the highest average sediment clay mineral abundance (12.7 %). The outer estuarine depositional environments (foreshore and pro-ebb delta) have a fairly homogenous distribution of total clay minerals, ranging from 4.4 % to 2.2 %.

The internal distribution and textural characteristics of clay minerals in estuarine sediment are documented in Figures 7.3C to 7.3F. Clay minerals in the marginal marine sediments studied here, occur predominantly as: (i) coats on and between framework grains, (ii) clay-rich lithic clasts (allochthonous clay-rich sand-grains), (iii) clasts (floccules) composed predominantly of clay minerals, and (iv) in association with feldspars (Fig. 7.3C). Clay-rich rock fragments enter the systems (Fig. 7.3F) in the fluvial arms. Inner estuary sediment contains abundant clay mineral linkages (bridging structures) between grains (Fig. 7.3C) whereas the outer estuary sediment contains no linkages (Fig.7.3F).

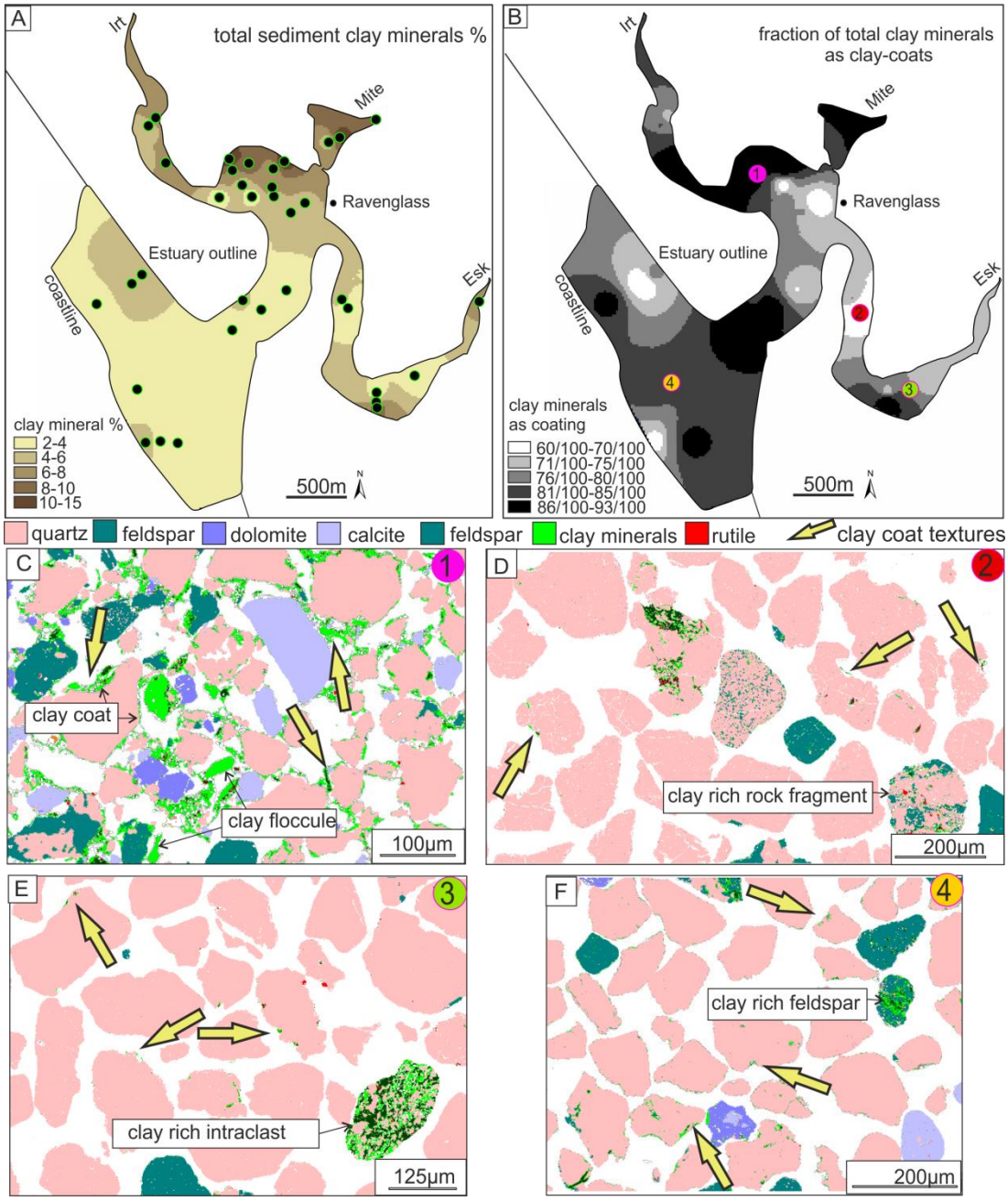

Figure 7-3 Maps of total clay mineral percentage and the fraction of the total clay minerals present as clay coats. (A) Map of total clay mineral percentage. Filled circles on map A indicate sample locations. (B) Map of clay mineral content present as clay coats. (C, E, F, G) SEM-EDS images of sediment bulk mineralogy, showing the progression in the abundance and distribution styles (e.g. coats or floccules) of clay minerals.

		Clay minerals in sediment %	Fraction of clay minerals as clay coats	SEM-EDS whole sediment clay mineralogy (image area)			SEM-EDS clay coating, clay mineralogy (image area)		
				total sediment-illite	total sediment-kaolinite	total sediment-chlorite	clay coating-illite	clay coating-kaolinite	clay coating-chlorite
Pro-ebb delta	Average	2.5	76/100	1.34	0.22	0.81	1.29	0.19	0.26
	Maximum	3	83/100	1.38	0.25	1.27	1.38	0.24	0.3
	Minimum	2.2	66/100	1.28	0.20	0.56	1.19	0.17	0.23
Foreshore	Average	3	79/100	1.47	0.42	1.00	1.45	0.39	0.37
	Maximum	4.4	89/100	1.78	0.51	2.17	1.75	0.5	0.59
	Minimum	2.2	62/100	1.17	0.28	0.44	1.14	0.28	0.26
Tidal-bar vegetated	Average	6.2	82/100	4.46	0.33	0.87	3.94	0.31	0.39
	Maximum	6.6	89/100	4.49	0.51	0.89	4.32	0.48	0.42
	Minimum	5.9	75/100	4.42	0.15	0.85	3.55	0.14	0.36
Tidal-bar	Average	3.9	75/100	2.02	0.39	1.19	1.96	0.25	0.44
	Maximum	8	89/100	3.96	0.74	2.93	3.93	0.64	0.97
	Minimum	2.4	61/100	1.05	0.08	0.41	1.04	0.07	0.2
Mud-flat	Average	12.7	89/100	9.33	1.25	1.68	8.25	1.02	1.23
	Maximum	17.8	93/100	13.20	1.68	2.63	11.94	1.48	2.26
	Minimum	8.7	85/100	4.80	0.81	1.27	4.78	0.67	0.64
Mixed-flat	Average	8.4	84/100	5.52	0.59	1.62	5.29	0.53	0.61
	Maximum	13.7	92/100	10.24	1.22	4.56	9.56	1.12	1.24
	Minimum	3.8	63/100	2.51	0.23	0.71	2.44	0.21	0.37
Sand-flat	Average	3.2	78/100	1.82	0.36	0.98	1.69	0.3	0.38
	Maximum	4.7	89/100	2.58	0.82	1.54	2.53	0.82	0.49
	Minimum	2	61/100	0.92	0.06	0.43	0.87	0.05	0.25
Tidal (Inlet) bar	Average	3.4	90/100	2.15	0.26	0.60	2.1	0.2	0.37
	Maximum	3.5	92/100	2.21	0.28	0.69	2.14	0.2	0.5
	Minimum	3.3	87/100	2.08	0.23	0.51	2.05	0.2	0.24

Table 7-2 Summary information for the scanning electron microscope-energy dispersive spectrometry (SEM-EDS) derived: (i) sediment clay mineral percentages, (ii) total clay minerals present as clay coats, and (iii) clay coat mineralogy.

7.4.2. The fraction of clay mineral abundance present as clay coats and its distribution

In order to avoid confusing the use of percentages of total clay and percentages of clay that occurs as coats, the latter has been expressed as a fraction of 100 to emphasise this different feature that has been quantified. The amount of the total clay mineral abundance that is present as clay coats varied from 93/100 to 61/100 across the estuary, with defined heterogeneity (Fig. 7.3B, Table 7.2). There is a systematic increase in the fraction of clay mineral abundance present as clay coats from the inner to outer estuarine depositional environments and towards the tidal limit (Fig. 7.3B, Table 7.2).

The spatial distribution reveals that, on average, 81/100 of the total estuarine sediment clay mineral content is present as clay coats, rising to 89/100 and 90/100 in the deposits consisting of mud-flat and tidal inlet depositional environments, respectively (Table. 7.2). Tidal-bars (non-vegetated) have the lowest average fraction of clay mineral abundance present as clay coats (75/100) (Table. 7.2). The tidal bar complex located in the lower Esk arm of the estuary represents a depositional environment in close spatial correspondence to a surface armoured by pebbles (compare Fig. 7.1B to 7.3B). The sediment assemblage consists of an elevated proportion of clay-rich lithic fragments (Fig. 7.3E).

Figure 7.3B documents the internal distribution (e.g. coats or lithic grains) of clay minerals within marginal marine sediments. For example, regions with a high fraction of the total clay mineral abundance that is present in clay-rich lithics or as clay floccules, has a reduced fraction of clay mineral abundance present as clay coats (i.e. Fig. 7.3E).

7.4.3. The spatial distribution of whole sediment clay mineralogy

The overall clay mineral assemblage of the Ravenglass Estuary is dominated by illite which contributes a minimum 47 % of the clay material across the estuary, with chlorite (7 % to

48 %) and kaolinite (2 % to 22 %) contributing smaller proportions (Fig. 7.4). Whole sediment clay mineralogy is highly heterogeneous across the marginal-marine sediments of the Ravenglass Estuary (Fig. 7.4).

Illite is the principal component of the clay mineral assemblage (illite index 47 % to 87 %) with the highest relative abundance present in the mud-and mixed-tidal-flat sediments of the Irt and Mite arms of the estuary, and the southern foreshore (compare Fig. 7.4A to 7.1B). Inner estuarine whole sediment has a higher illite proportion compared to outer estuarine depositional environments (e.g. foreshore and pro-ebb delta) although local variability occurs.

Kaolinite clay mineral content of the whole sediment has a bimodal distribution with sediments containing > 10 % restricted to either the inner-central estuarine tidal-flats and tidal-bars, or the outer foreshore and pro-ebb delta depositional environments. Sediments that contain high proportions of kaolinite (i.e. > 12 %) are restricted to the tidal-bars and sand-flats of the River Esk arm of the Estuary (compare Fig. 7.1B to 7.4C); imaged in Figure 7.3D and E.

Highest relative, whole sediment chlorite content occurs in the inner-central and Esk arm of the estuary, corresponding to tidal-bar and tidal-flat (mixed and sand) depositional environments (Fig. 7.4B). Elevated relative chlorite abundance occurs in the tidal inlet and northern foreshore sediments. Chlorite is relatively depleted in the sediments from the tidal-flats (mud and mixed) of the Irt and Mite arms of the estuary.

Focussing on the tidal flat environment (Fig. 7.1B) of the inner-central estuary reveals the local variability in clay mineralogy across mud-, mixed-, and sand-flats with most chlorite in the sand-flats and most illite and kaolinite in the mud- and mixed-flats (Fig. 7.4). Clay

mineral proportion of illite from Ravenglass is highest in low energy settings. Chlorite abundance from Ravenglass is relatively highest in high energy settings.

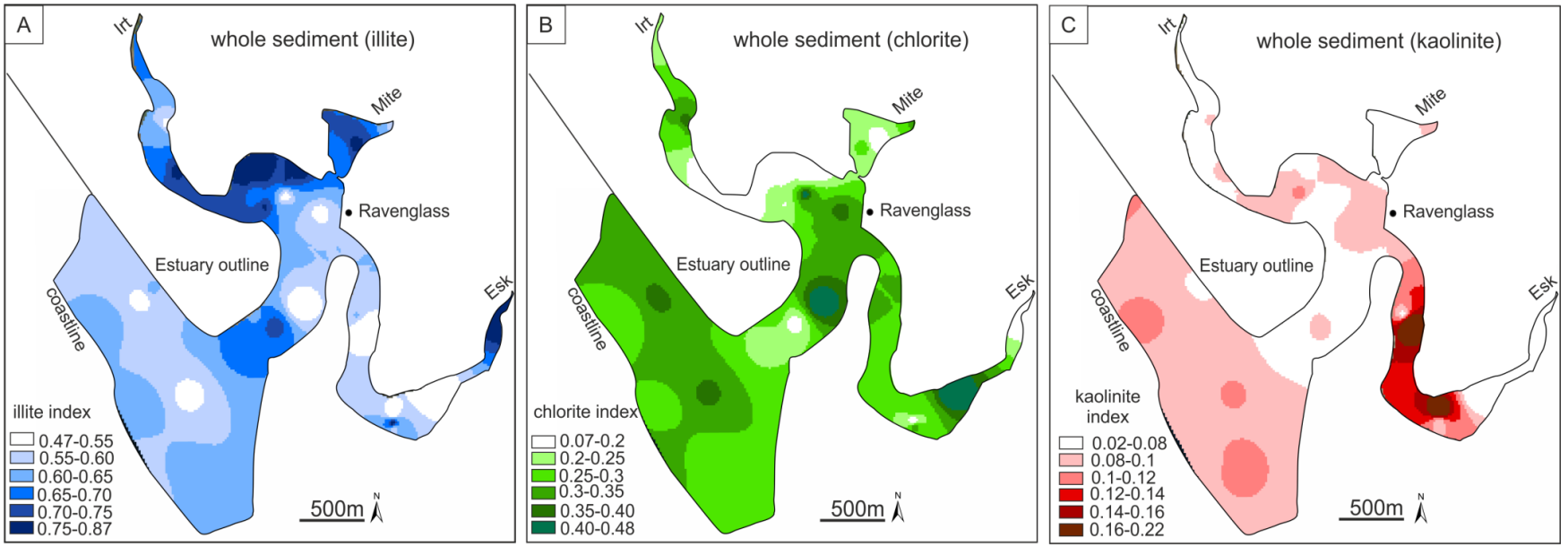

Figure 7-4. Whole sediment clay mineral index maps. (A) Distribution of relative total sediment illite content. (B) Distribution of relative total sediment chlorite content. (C) Distribution of relative total sediment kaolinite content.

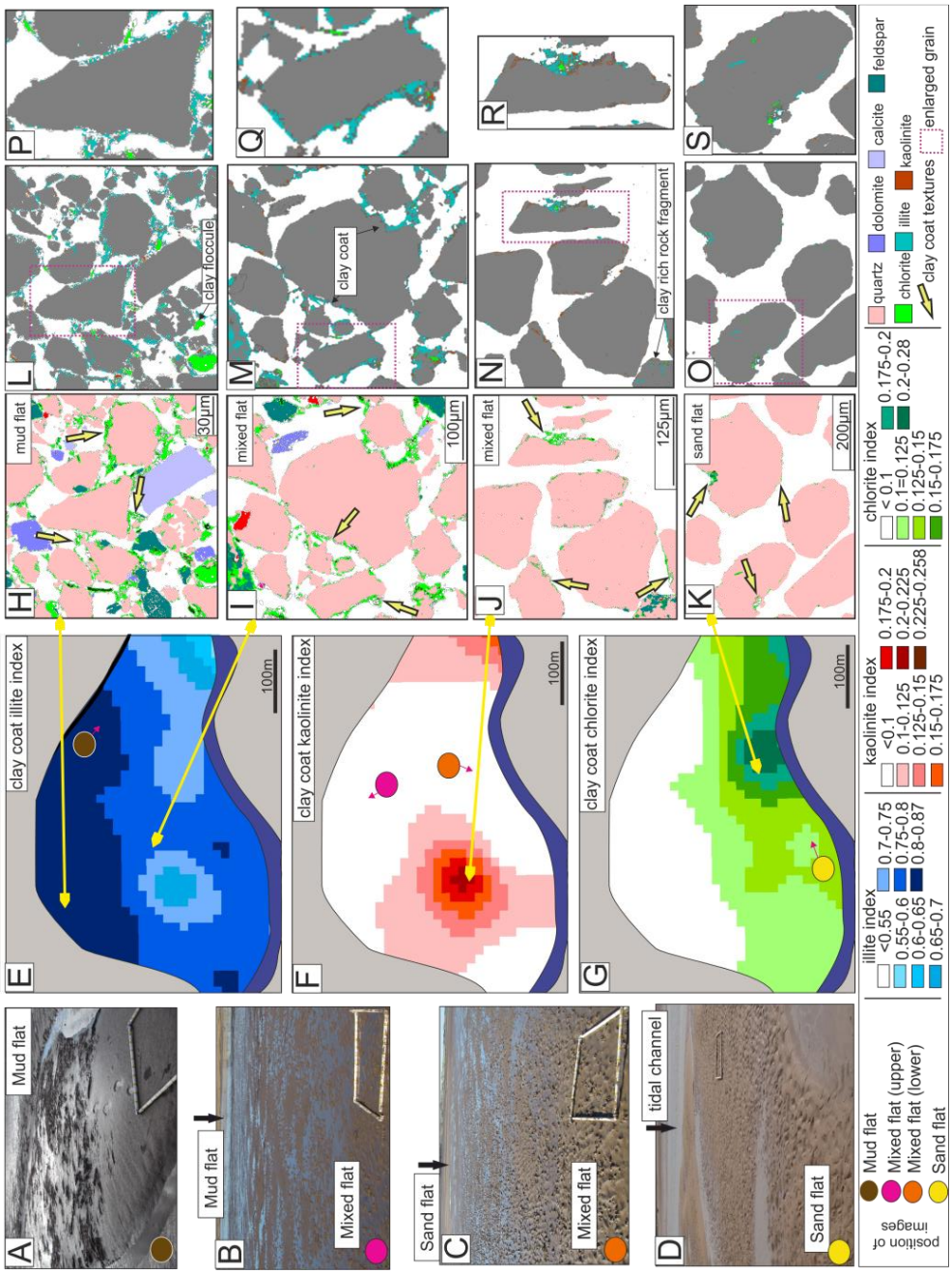

Figure 7-5 Photographs, clay-coat mineralogy index maps, and SEM-EDS images of tidal-flat sediments. (A, B, C) Photographs of illustrating the surface sediment features and environments (quadrant 1 m^2). Arrows on E, F, G, indicate the direction of images in (A, B, D). (E, F, G) Clay mineral index maps of relative clay-coat mineralogy. For location of the Saltcoats tidal-flat see Figure 7.1A. (H, I, J, K) SEM-EDS images of bulk sediment mineralogy. (L, M, N, O) SEM-EDS images of clay mineralogy. (P, Q, R, S) enlarged SEM-EDS images of clay mineralogy. Purple rectangles on (L, M, N, O) indicate the location of images in the larger sample. Arrows on (E-H and I, F-J, and G-K) indicate the relative position of the imaged samples. (H, L, P) Mud-flat. (I, M, Q) Mixed-flat upper. (J, N, R) Mixed-flat lower. (K, O, S) Sand-flat.

7.4.4. The spatial distribution of clay-coat mineralogy

Clay coats are dominated by illite which contributes a minimum 50 % of the attached clay coat material across the estuary, with less chlorite (< 5 % to 25 %) and kaolinite (< 4 % to 25 %) (Fig. 7.6).

The illite component occurs typically as irregular accumulations of crystals forming both clay mineral accumulations on grain surfaces and bridging structures between grains (Fig. 7.5). Chlorite principally occurs with a "flake like" morphology occurring as prominent projections away from the grain. Kaolinite is present both as larger isolated clasts and in irregular accumulations associated with illite (Fig. 7.5).

Clay-coat mineralogy is heterogeneously distributed across the marginal-marine environments of the Ravenglass Estuary (Fig. 7.6). The illite proportion in clay coats increases from the inner (> 50 % of coat mineralogy) to the outer estuarine depositional environments (> 70 %) (Fig. 7.6A). Clay coats have an elevated illite percentage in the tidal-flats (mixed and mud) and tidal-bar depositional environments from the Rivers Irt and Mite compared to the River Esk arm of the estuary (compare Fig. 7.1 to 7.6A). Focussing on the tidal-flat environment (Fig. 7.1B), reveals the local variability in clay-coat mineralogy across mud-, mixed-, and sand-flats with most illite in the mud-flats and least illite in the sand-flats (Fig. 7.6A and 7.5).

Kaolinite clay coat content has a bimodal distribution with clay coats containing > 16 % kaolinite restricted to either the inner-central estuarine tidal-flats, tidal-bars, or the outer foreshore and pro-ebb delta depositional environments (Fig. 7.6C).

Clay coats have decreasing chlorite content from the inner-central (20-28 %) to the outer estuary (pro-ebb delta) (< 17 %) (Fig. 7.6B). Clay coats with the highest chlorite content

occur in the inner-central and Esk arm of the estuary, corresponding to tidal-bar and tidal-flat (mixed and sand) depositional environments (compare Fig. 7.1B to 7.6B).

A key conclusion is that clay-coat mineralogy is heterogeneously distributed across the marginal-marine sediments at Ravenglass. Clay coats are dominated by illite with an increasingly mixed mineralogy (chlorite and kaolinite) at inner estuarine sites in the higher energy settings, representing sand-flat and tidal-bar (non-vegetated) depositional environments (Fig. 7.6). Clay coats in outer estuary settings have a low chlorite content and are relatively enriched in illite and kaolinite (Fig. 7.6).

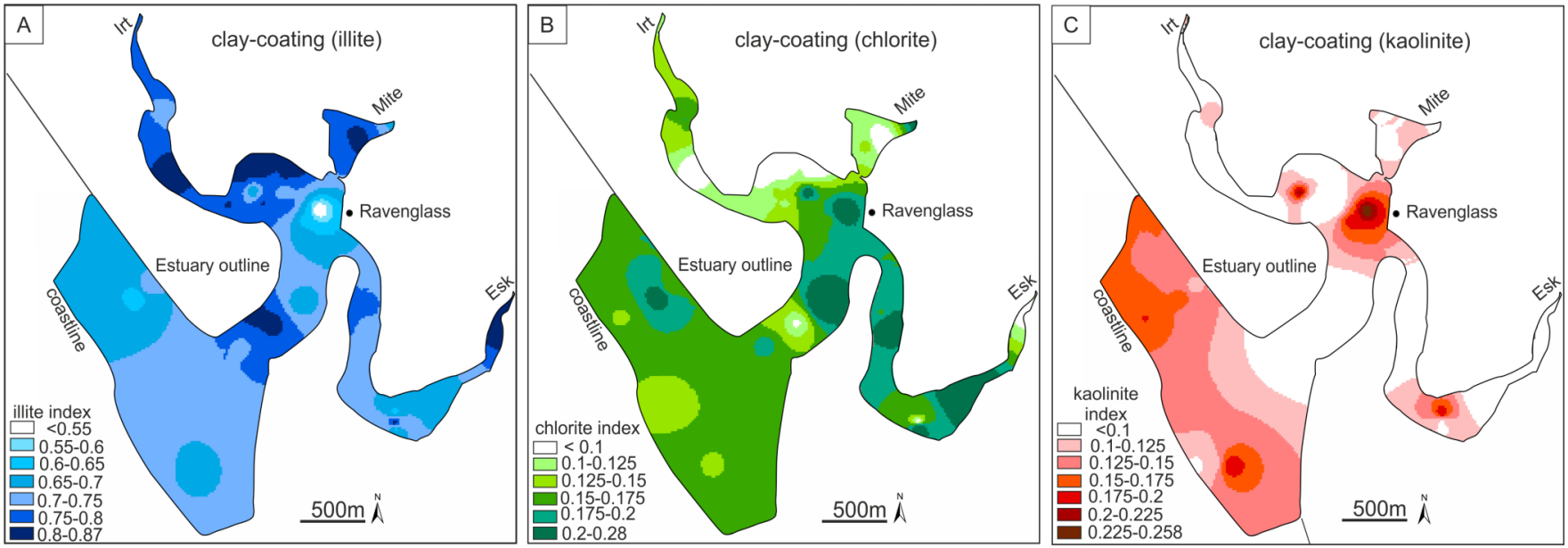

Figure 7-6 Clay-coat mineral index maps. (A) Distribution of relative illite clay coat content. (B) Distribution of relative chlorite clay coat content. (C) Distribution of relative kaolinite clay coat content.

7.4.5. Correlation between whole sediment and clay-coat mineralogy

The relative difference in clay mineral abundance (illite, chlorite, and kaolinite) present in the sediment (i.e. inclusive of clay coats and clay rich lithics) compared to the abundance of clay minerals distributed exclusively as clay coats is documented in Figure 7.7.

The close correlation between total sediment and clay coating illite abundance in marginal marine sediments (compare Fig. 7.4A to 7.7A) suggests that illite principally occurs as clay coats, especially in outer estuarine sediments (e.g. foreshore and pro-ebb delta). In mud-flat sediments, an additional ~10 % illite is present not as clay coats but as clumps that potentially resulted from flocculation (Figs. 7.3C, 5H, 7.5L, 7.5P).

Kaolinite principally occurs as components of clay coats especially for outer estuarine environments in which ~92 % (foreshore) and ~86 % (pro-ebb delta) of the total kaolinite is present as clay coats (Fig. 7.7). Tidal-bar sediments have only ~64 % of the total kaolinite content present as clay coats. Tidal-bar (non-vegetated) sediments are enriched (relative to other inner-estuarine sediments) in clay rich lithics (Fig. 7.3D).

Chlorite in tidal-flat sediments are show as clumps that potentially resulted from flocculation (Fig. 7.5L), in clay rich lithics (Fig. 7.5N), and as components of clay coats (Fig. 7.5O and S) with approximately 50 % of the total chlorite across the estuary present as clay coats. In samples from tidal-bar, foreshore, and pro-ebb delta depositional environments ~63 %, ~63 %, and ~68 %, respectively (Table 7.2) of the chlorite derives from clay-rich lithics (Fig. 7.3 D, F) and not as clay coats.

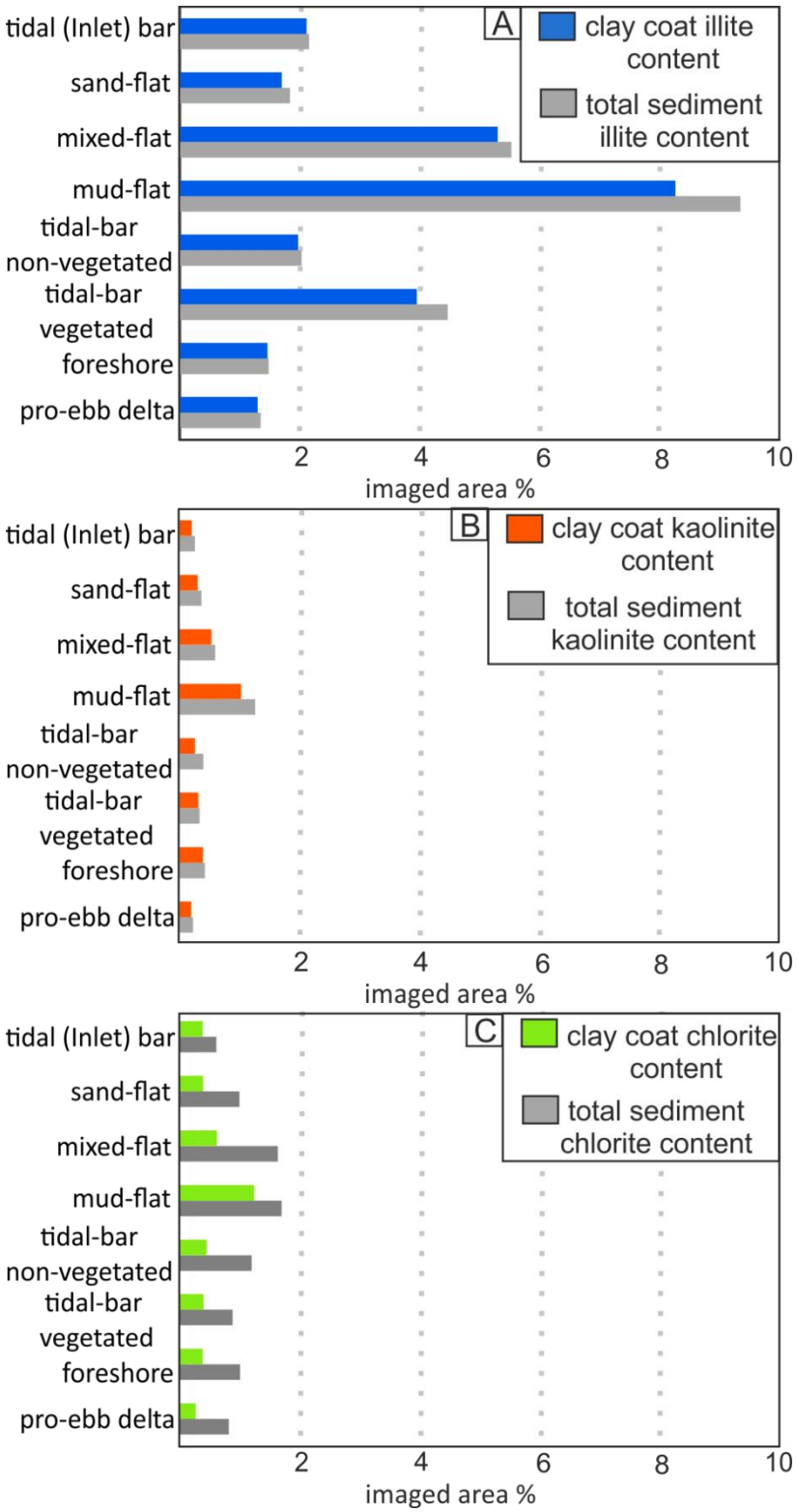

Figure 7-7 Plots comparing total sediment clay mineral abundance against clay coat, clay mineral abundance. (A) Illite. (B) Kaolinite. (C) Chlorite.

7.4.6. Sedimentary environments and clay-coat mineralogy

Clay-coat mineralogy of the Ravenglass sediments has here been differentiated by depositional environment (Fig. 7.8A) to allow comparison between modern and ancient marginal marine sediments (Table 7.2). Clay coats with the highest chlorite content occur in sediments from sand-flat and non-vegetated tidal-bar depositional environments (Fig. 7.8A). The lowest chlorite content (typically < 15 %) is present in clay coats in vegetated tidal-bar sediments (Table 7.2). Clay coats with the highest illite content occur in samples from vegetated tidal-bars and mud- and mixed-tidal-flats. The highest values of clay coating kaolinite occur in sand-flat and foreshore depositional environments (Fig. 7.8A).

There is no simple graphical or statistical relationship between clay-coat mineralogy and clay-coat coverage (Fig. 7.8B and Table 7.3). There is a minor relative increase in chlorite with increasing grain size (which is a proxy for energy regime) (Fig. 7.8C); this is broadly consistent with spatial distribution patterns of clay-coat mineralogy (Fig. 7.6) and grain size (Fig. 7.1D). Overall, lower energy settings tend to have higher degrees of clay-coat coverage and tend to have a greater quantity of illite (Figs. 7.1C, 7.6).

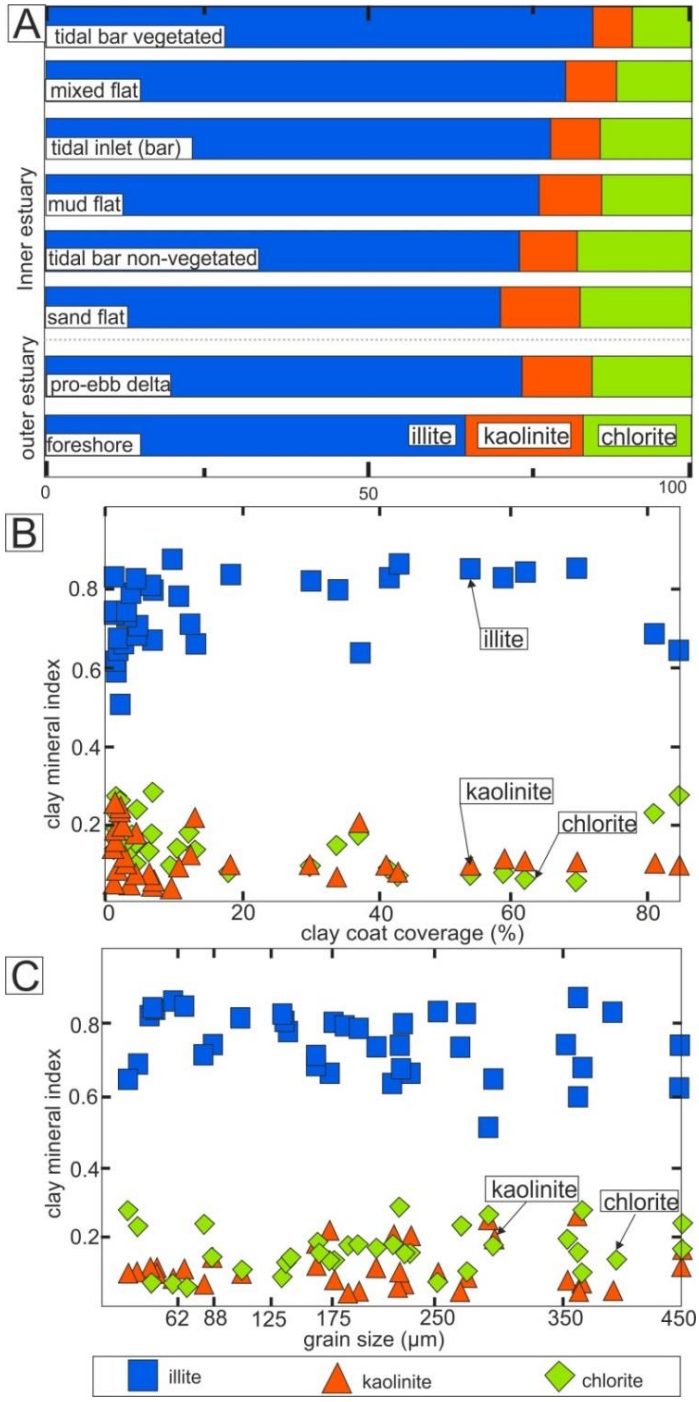

Figure 7-8 Plots comparing total clay-coat mineralogy against depositional environment, clay-coat coverage, and grain size. (A) Plot of normalized indexed clay-coat mineralogy, segregated by depositional environments. (B) Cross plot of indexed clay-coat mineralogy and clay-coat coverage. (C) Cross plot of clay-coat mineralogy and mean sediment grain size.

	total clay minerals	percentage of clay minerals as coatings	clay coating-illite	clay coating-kaolinite	clay coating-chlorite	clay coating index-illite	clay coating index-kaolinite	clay coating index-chlorite	clay-coat coverage	mean grain size
total clay minerals		*0.029	***0.000	***0.000	***0.000	**0.022	0.419	*0.014	***0.000	***0.000
Percentage of clay minerals as coatings	0.36		**0.002	*0.011	0.784	***0.000	0.684	***0.000	**0.003	**0.005
clay coating-illite	0.98	0.48		***0.000	**0.006	**0.002	0.339	***0.000	***0.000	***0.000
clay coating-kaolinite	0.88	0.41	0.87		**0.003	0.571	0.076	*0.012	***0.000	***0.000
clay coating-chlorite	0.58	0.05	0.44	0.47		0.271	0.643	*0.045	***0.000	0.002
index-illite	0.37	0.54	0.49	0.10	-0.19		***0.000	***0.000	0.138	0.067
index-kaolinite	-0.14	-0.07	-0.16	0.30	-0.08	-0.70		0.739	0.616	0.418
index-chlorite	-0.40	-0.69	-0.54	-0.40	0.33	-0.75	0.06		0.109	0.073
clay-coat coverage	0.78	0.47	0.77	0.74	0.65	0.25	-0.09	-0.27		***0.000
mean grain size	-0.64	-0.45	-0.64	-0.57	-0.49	-0.30	0.14	0.30	-0.69	

Table 7-3 Pearson's Correlation Coefficient matrix illustrating the statistical significance between (i) clay mineral abundance and mineralogy, (ii) mean grain size, and (iii) clay coat data. For P-values < 0.05*, the correlation is statistically significant. P values of (P < 0.01) and (p< 0.001)*** represent very and extremely significant correlations, respectively.**

7.5. Discussion

7.5.1. Origin of sediment clay minerals

This study has revealed that the majority of the sediment clay mineral volume, in excesses of 61/100, is present as clay coats in the Ravenglass sediment. This fraction is highest in the sand-dominated assemblages of the mixed-tidal-flats (84/100), sand-tidal-flats (78/100), tidal-bars (non-vegetated) (75/100), tidal inlet (90/100), and foreshore (79/100) depositional environments (Table 7.2).

The origin of the additional clay minerals (i.e. not present as clay coats) occur principally as: (i) floccules of clay (salinity and biologically mediated) (Fig. 7.6I) in sediment from reduced energy conditions (Fig. 7.9A), (ii) clay-rich rock fragments (Fig. 7.9F), and (iii) in association with feldspars, which can develop via the rapid early diagenetic alteration to illite and kaolinite clay minerals (Daneshvar and Worden 2016) (Fig. 7.9B).

The predominant role of grain-coating clay in the overall clay mineral budget in the sediments studied here highlights the fundamental role of clay coat-forming processes in influencing sediment variability (Wilson 1992; Wooldridge et al. 2017b; Worden et al. 2006).

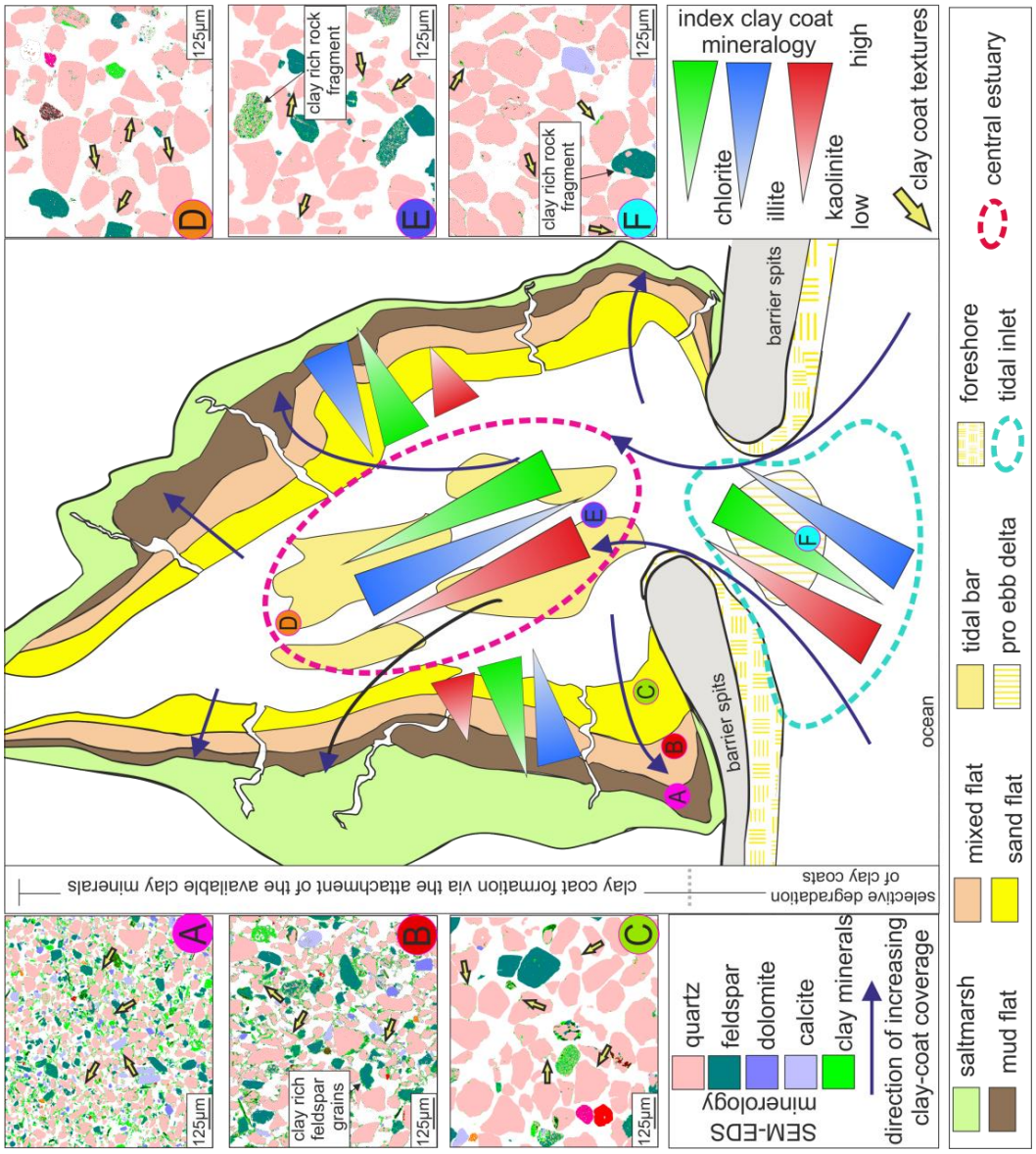

Figure 7-9 Schematic model showing relative trends in clay-coat mineralogy and clay-coat coverage across a typical marginal marine transect of depositional environments , after Dalrymple et al. (1992). (A) Mud-flat. (B) Mixed-flat. (C) Sand-flat. (D) Distal (from ocean or vegetated) tidal-bar. (E) Proximal (to ocean) tidal-bar. (F) Pro-ebb delta. Yellow arrows indicate the location of attached clay coats.

7.5.2. Origin of minerals in clay coats

7.5.2.1. Comparison of fine fraction and whole sediment SEM-EDS clay mineral patterns

The mineralogy of estuarine clay minerals is mainly governed by the geology of the hinterland, climate, relief, and the length of the fluvial transport system (Daneshvar and Worden 2016; Wooldridge et al. 2017b; Worden and Morad 2003). The similar mineralogy and spatial patterns between the total sediment clay mineral and clay-coat mineralogy for inner-estuarine sediments implies that coat mineralogy is principally a function of the fluvial inputted clay mineral assemblage.

A key conclusion of the comparison between whole sediment clay mineralogy (Fig. 7.4) and clay-coat mineralogy (Fig. 7.6) is that spatial patterns in the illite and chlorite are broadly similar especially for inner estuarine sediments. Discrepancies between the whole sediment clay mineral assemblage and clay-coat mineralogy (e.g., kaolinite content in the River Esk) (compare Fig. 7.4C to 7.6C), result from the inclusion of clay minerals present in clay-rich lithics (e.g. Fig. 7.3D) in the calculations of whole sediment clay mineralogy. The identified consistent trend between whole sediment clay mineralogy and clay-coat mineralogy for illite and chlorite in the Ravenglass Estuary suggests that clay coats were formed in the inner estuary via the attachment of the hydrodynamically-fractionated clay mineral assemblage thus explaining the cause of the similarity of the whole sediment and clay coat mineral trends (Fig. 7.4 and 7.6). The correlation between whole sediment and clay-coat mineralogy suggests that clay-coat mineralogy is principally governed by processes which control the depositional fractionation of clay minerals supplied to the estuary (see later).

The difference between the whole sediment clay mineral abundance (Fig. 7.4) and the proportion of clay-coating minerals (Fig. 7.7) suggests that techniques which quantify the total sediment (e.g. identified by XRD) may potentially over-predict the abundance and

mineralogy of clay coats (e.g. chlorite, Fig. 7.7C). In summary therefore, it appears to be beneficial to look at clay-coat mineralogy as well as whole sediment composition.

7.5.2.2. Origin of inner estuarine clay-coat mineralogy heterogeneity

Previous work on the Ravenglass Estuary Wooldridge et al. (2017b), concluded that there was a "clay coat factory" in the inner estuary. Griffiths (2017) reviewed the potential processes that govern the fractionation of the fluvial-derived clay minerals and concluded that the heterogeneity of illite and chlorite in inner estuarine sediment partly derive from differential settling rates (governed by particles size) (Fig. 7.5) (Whitehouse et al. 1960).

In the Ravenglass Estuary, chlorite typically sits in coarser sediments than illite (Fig. 7.4) and therefore must have dropped out of suspension closer to the main ebb channel. Differential settling rates could explain the systematic variations of chlorite and illite abundance across the tidal-flat sequences (Fig. 7.4) with chlorite typically present as larger "flakes" (compared to illite) in clay coats (Fig. 7.5).

The mineralogy of inner estuarine clay coats are thus governed, firstly, but the fluvial inputted clay mineral assemblage (heterogeneous between the fluvial arms, Fig. 7.4) and, secondly, by the differential settling rates of the predominantly fluvial derived clay mineral assemblage with chlorite deposited closer to the ebb tidal channels (e.g. clay coats enriched in chlorite in sand-flats). The ability to constrain if trends in clay-coat mineralogy are applicable to other marginal-marine systems is hampered by the absence of comparable high-resolution data sets.

7.5.2.3. Origin of outer estuarine patterns of clay coat mineralogy

In natural systems, multiple processes occur simultaneously, such as the formation of clay coated sand-grains (limited to inner estuary depositional environments) along with continued erosion, transport and deposition of clay coated sand-grains. Evidence for the

transport of clay coated sand-grain in the Ravenglass Estuary from the inner to outer estuary include: (i) the presence of partial clay coats in samples from the pro-ebb delta, (ii) the systematic decrease in the extent of clay-coat coverage from inner to outer estuarine sediments (Fig. 7.1C) and (iii) clay coats from sand-flats, tidal-bars, and the outer estuarine sediments (Fig. 7.3D-G) display textural characteristics consistent with abrasive transport (grain to grain collision) (Wilson 1992). Clay coats from foreshore and pro-ebb delta samples display the greatest coat thickness in grain indentations, a lack of clay coat projections, and elevated clay coat grain coverage on the finer grain size sediment components (Fig. 7.9F). Abrasive transport (remobilisation of the sediment) would remove grain projections and such, preserve the greatest clay-coat thickness in grain indentations, with coats preferentially retained on the finer grain size sediment components due to a reduced abrasive effect (Wilson 1992).

Abrasive transport of inner-estuary, clay-coated grains may explain the evolution in clay-coat mineralogy from the inner to outer estuarine sediments. The larger "flakes" of chlorite in clay coats (Fig. 7.5) typically form prominent perpendicular projections which, upon grain-to-grain collisions (during transport), would experience preferential early detachment compared to more tangential and finer-grained illite and kaolinite. The overall result of preferential early detachment with transport out of the inner estuary is that chlorite coat constituents will be removed (note the ~ 10 % decrease in clay coating chlorite from inner to outer estuarine depositional environments) (Fig. 7.6B) resulting in the increased relative illite content of the remaining attached coat material (Fig. 7.6A).

7.5.3. Comparison of clay-coat mineralogy to the Anllóns Estuary, Spain

There are few high resolution published studies of clay mineralogy in estuaries (Algan et al. 1994; Brockamp and Clauer 2012; Dowey 2013). The most detailed study was by Dowey (2013) of the Anllóns Estuary, Spain, using XRD techniques on clay fraction separates

although details of clay-coat mineralogy were not reported. The Anllóns study has a clay mineral assemblage dominated by kaolinite, illite, and chlorite (Dowey 2013). Illite is dominant in the inner estuary with kaolinite content increasing towards the marine end of the system. Chlorite concentration is highest in sediment from the central estuary, close to the main ebb channel, in sand-flat depositional environments. Kaolinite concentration are lowest in the open marine-influenced shoreface and sand-flat areas of the estuary (Dowey 2013).

The elevated chlorite, clay coat content in inner estuarine sand-flat and tidal-bar depositional settings (e.g. high energy settings) reported here for the Ravenglass Estuary are similar to the whole sediment trends reported for the Anllóns, Estuary (Dowey 2013). The relative increase in the kaolinite clay coat content in outer estuarine sediments in the Ravenglass system reported here is not consistent with the clay mineral distribution trends (clay fraction separates) of the Anllóns Estuary (Dowey 2013).

A key conclusion from this comparison is that spatial trends in clay-coat mineralogy from Ravenglass are broadly consistent (i.e. for illite and chlorite) with those reported for the bulk inner-estuarine sediment clay mineral assemblage of the Anllóns Estuary (Dowey 2013). Differences between the relative bulk sediment clay fraction and clay-coat mineralogy (i.e. kaolinite content), potentially result from the different methodologies adopted; SEM-EDS analysis and computational size sieving data from Ravenglass is unlikely to provide exactly comparable data as physical separation and XRD analysis.

7.6. Reservoir quality implications and prediction of clay-coat mineralogy

Mixed mineralogy clay coats have been reported in sandstones that were deposited in marginal-marine environments (Table 7.1). Most clay coats seem to contain chlorite and a mixture of other clay minerals.

Detrital-clay coated sand-grains form via the attachment of the locally available clay minerals, mainly in the inner-estuarine tidal-flat and tidal-bar depositional environments (Wooldridge et al. 2017b). It has been suggested that modern-clay coats (detrital-clay coats) represent precursors to those found in some deeply-buried sandstones (Ajdukiewicz and Larese 2012; Bloch et al. 2002; Wooldridge et al. 2017b). The precursor detrital-coat material exerts a fundamental control on the diagenetic pathway and final mineralogy of clay coats in deeply-buried sandstones (diagenetic clay coat) (Worden and Morad 2003). In turn diagenetic clay coats directly influence the effectiveness of quartz cement inhibition (Ajdukiewicz and Larese 2012). If, as reported (Aagaard et al. 2000; Ajdukiewicz and Larese 2012; Bloch et al. 2002; Worden and Morad 2003) diagenetic clay-coats form via the recrystallization of a precursor detrital-clay-coat, then an analogue data set of detrital-clay-coat mineralogy will aid in the prediction of reservoir quality in deeply-buried marginal-marine sandstones.

This study reveals that the clay-coat mineralogy reflects that of the bulk clay mineral assemblage (Table 7.2). Pre-drill predictions of clay-coat mineralogy (whether chlorite, illite, or mixed) should consider the initial clay assemblage at the time of deposition (which in turn is influenced by paleo-climate and source hinterland geology).

The results here suggest that facies deposited in sand-flat and tidal-bar environments in the inner estuary will have clay coats that are relatively enriched in chlorite (Fig. 7.6B). Facies deposited from tidal-flat (mixed and mud) environments are relatively enriched in illite (Fig. 7.6A). Foreshore facies have the greatest relative enrichment in kaolinite (Fig. 7.6C). Figure 7.9 is a schematic diagram illustrating, the identified spatial trends in clay-coat mineralogy and coat grain coverage (area of grain covered by attached clay material) (Wooldridge et al. 2017a; Wooldridge et al. 2017b) across a typical marginal-marine transect of depositional environments (Dalrymple et al. 1992).

The effect of the specific clay-coat mineralogy (i.e. ratio between illite and chlorite) on quartz cement inhibition remains unresolved in the literature. On the assumption that increasing chlorite content, in the mixed mineralogy coats from Ravenglass, will be advantageous for quartz cement inhibition, this work suggests that, in deeply-buried marginal marine sandstones, the best porosity should be found in the inner estuarine sand-flat and tidal-bar depositional elements.

The ability to test the applicability of such an analogue model in predicting clay-coat mineralogy in the subsurface is hampered by the absence of high-resolution, core based studies on the distribution of diagenetic-clay-coat mineralogy, owing to the typically poor spatial and stratigraphic coverage of core intervals (Wooldridge et al. 2017b). The study by Skarpeid et al. (2017) on the Cook Formation, Knarr Field, Norway, reported a total sediment chlorite abundance and mean grain coat coverage are greatest in estuarine facies compared to fully marine facies. There is therefore concurrence between the modern Ravenglass Estuary and the Jurassic Cook Formation (Churchill et al. 2016; Skarpeid et al. 2017).

7.7. Conclusions

1. The clay mineral assemblage occurs principally as clay coats on sand gain surfaces (61/100 to 93/100 of the total sediment clay mineral abundance).
2. On average, 81/100 of the total sediment clay mineral assemblage is present as clay coats, revealing the master-control of clay coat-forming processes in determining primary depositional sediment properties.
3. The mineralogy of clay coats are spatially heterogeneous across marginal marine depositional environments.
4. Clay-coat mineralogy across the Ravenglass Estuary is dominated by illite (> 50 %). Compared to the low energy environments, inner estuarine clay coats have a more

mixed mineralogy (i.e. increased chlorite and kaolinite) in the high energy sediment assemblages of the sand-flat and tidal-bar depositional environments.

5. With distance away from the inner estuary, the clay coats in outer estuarine sediments (pro-ebb delta and foreshore) are increasingly chlorite-deficient and illite-enriched.
6. Clay-coat mineralogy reflects that of the whole sediment clay mineral assemblage. This indicates that clay mineralogy is principally governed by the geology and weathering regime of the hinterland drainage area.
7. Spatial trends in clay-coat mineralogy are governed, first, by differential settling rates of the predominantly fluvial-derived clay mineral assemblage and, second by the selective abrasive removal of specific clay mineral types (e.g. chlorite) during reworking and transport.
8. Based on the distribution of clay-coating chlorite, this study suggests that in deeply-buried marginal-marine sandstones the best prospects for elevated clay coat derived reservoir quality (i.e. with inhibited growth of quartz cement) should most likely be sought in the typically coarse, relatively clean, sand-flat and tidal-bar facies.

8. Discussion and overall summary of results

This chapter discusses the results and summarises the main conclusions of this bio-sedimentary investigation into the origin, characteristics, and distribution, of clay-coated sand-grains in the Ravenglass Estuary. The results of the previous chapters are presented as answers to the research questions posed in chapter 1. Questions have here been divided into five main themes: (1) the characterisation and distribution of detrital-clay coats, (2) controls on the formation and distribution of detrital-clay coats, (3) sedimentological and biological heterogeneity across a marginal marine system, (4) the biofilm influence on the diagenetic properties of marginal marine sediments, and (5) reservoir quality predictions.

8.1. The characteristics and distribution of clay coats

Textural and mineralogical characterisation of clay-coated sand-grains was undertaken on clay coats in dehydrated (Fig. 4.4) and hydrated form (Fig. 3.1), from semi-consolidated (Fig. 4.7) and unconsolidated sediment (Fig. 2.5) via a range of scanning electron microscope petrography (SEM, ESEM, SEM-EDS).

To allow mapping of clay coat heterogeneity across the Ravenglass Estuary, this study applied qualitative (Chapter 2) and two quantitative methods (Chapter 6, Fig. 6.6). The qualitative method used categorical bin classes, based on SEM images, of whole sediment. The quantitative methods measured: (1) the fraction of the perimeter of a grain that is covered by attached clay (Fig. 3.3) and (2) the volume of clay present as clay coats (Fig. 6.6) via SEM and SEM-EDS imaging of thin sections (Chapter 6). Figures 3.3, 4.6, 5.3, and 6.6 represent the first, fully quantitative, maps and plots of clay coat distribution in marginal marine sediment (surface and near-surface).

Quantifying clay-coat mineralogy involved developing the ability to constrain clay-coat mineralogy and differentiate it from the clay mineralogy of the whole sediment (Chapter 7). The maps presented in Figure 7.6 thus offer a unique view of the heterogeneity of clay-coat mineralogy across a fluvial to marginal marine transect of depositional environments.

8.1.1. Questions: 1. what are the textural and mineralogical characteristics of clay coats?

The morphology of detrital-clay coats has been illustrated in Figures 2.5, 2.6, 2.7, 3.1, 4.4, 4.5, 4.7, 5.3, 5.5, 5.6, 6.1, 6.5, and 7.5. This multi-technique approach has permitted an advancement in the textural understanding of clay-coat morphology from the traditional ridged, bridged, and clumped textural classification schemes (Wilson 1992). This approach captured fully the morphological variability across a fluvial to marginal marine transect of depositional environments (summarised in Figs. 5.3, 5.15, 6.1, and 7.3).

Marginal marine detrital-clay coats from the Ravenglass Estuary can be collectively described as discontinuous, micron scale accumulations of clay minerals and clay-to silt-sized material (i.e. clay particles, organics, and lithics) typically presenting as either clumps, tangentially attached coats, or bridging strands of clay material between grains (Figs. 2.5, 2.6, 4.4, 4.7, and 6.5) thus creating a diverse mixture of phyllosilicates (Figs. 2.7, 4.3, 6.5, and 7.5). In dehydrated form detrital-clay coats can be segregated into two morphological classes.

(1) Clay coats from tidal-flat (mud and mixed), tidal creeks, and tidal-bar (vegetated) samples consist of a network of partial grain-coating and grain-bridging, fibrous filaments composed of clay minerals and clay- to silt-sized material (organics, lithics, and clay minerals) capable of coating up to 86 % of grain surfaces (Figs. 4.4 and 6.6).

(2) Clay coats in sand-flat, tidal-bars (non-vegetated), pro-ebb delta, and foreshore samples occur as discontinuous (typically < 10 % average grain coverage) thin coats with greatest thickness of attached clay minerals in grain indentations. These are composed principally of clay minerals (Figs. 4.5, 5.3, and 6.5). There is an absence of grain-bridging clay mineral linkages between grains in samples from such high energy depositional environments (Figs. 4.5 and 5.3).

Chapter 4 revealed no apparent differences in the textural characteristics of surface and near-surface clay coats (compare Fig. 4.4 to 4.7). Clay coats are present on all component framework grains in the sediment (i.e. clay-coated bioclasts, feldspars, lithic grains, and quartz) (Figs. 2.7, 4.5, 5.3, and 6.5). Quantification of clay-coat coverage and clay-coat volume (Fig. 6.6) in Chapter 6 identified that a reduced clay-coat volume (thickness) equates to a reduced clay-coat coverage (Fig. 6.7). Thus where the percentage of clay-coat coverage is most complete (e.g. mud-flat, 63 % average) also equates to the greatest average clay-coat volume (e.g. 13.3 % of the total sediment) (Fig .6.6).

Hydrated clay coats from a mixed tidal-flat occur as discontinuous, tangentially orientated (sub-parallel to grain) coats with limited bridging structures between the framework coated grains, lacking any supporting clay matrix material (Figs. 3.1, 5.5, and 5.6). Attached clay material occurred in close association with biofilm coatings and diatoms, with fine-grained, clay- to silt-size material stuck on the part of the grain covered with biofilm but not on the biofilm-free parts of sand-grains (Figs. 3.1, and 5.5).

Clay coats from the Ravenglass Estuary consist of a diverse mixture of interlocking, heterogeneous phyllosilicates (Figs. 2.7, 4.3, 5.3, 6.5, and 7.5). Clay-coat mineralogy is dominated by illite which contributes a minimum 50 % of the attached clay coat material across the estuary, with less chlorite (5 % to 25 %) and kaolinite (4 % to 25 %) (Fig. 7.6).

Texturally, the illite components of clay coats occurred as irregular accumulations of crystals as coats on grain surfaces and bridging structures between grains (Fig. 7.5). Clay-coating chlorite principally occurred with a larger (compared to illite) "flake like" morphology forming prominent projections away from the grain. Kaolinite is present as both larger isolated clasts and in irregular accumulations associated with illite (Fig. 7.5). Figures 2.7, 4.5, 5.3, and 7.5, showed no difference in clay-coat mineralogy between clay coat textural types (e.g. coating- vs bridging-structures) or framework grains (e.g. bioclasts, quartz, or feldspars).

8.1.2. Question 2. How are clay-coated sand-grains distributed across marginal-marine sediments?

Clay-coat coverage in the surface sediment of the Ravenglass Estuary showed a high degree of variability ranging from < 1 % to 87 % (Figs. 2.8, 3.3, 4.6, 4.9, 5.8, and 6.6). Clay-coat coverage maps (Fig. 6.6) show an overall trend of increasing clay-coat coverage with increasing distance from the open ocean (i.e. towards the tidal limit).

Samples which contain > 10 % clay-coat coverage occur in inner estuarine tidal-flat (mud-, mixed-, and sand-flats) and tidal-bar (vegetated and non-vegetated) depositional environments (Fig. 5.9, Table 5.1). There is strong heterogeneity in clay-coat coverage in inner estuarine sediments ranging from < 1 % to 87 % (Figs. 5.8 and 6.6). Maximum average clay-coat coverage occurred in sediment samples from the mud-tidal-flat (60 %) and tidal-creek (73 %) depositional environments (Fig. 5.9). Chapter 4 documents clay-coat coverage across the Saltcoats tidal-flat and identified heterogeneity in the proportion (percentage of measured grains) of surface grains devoid of clay-coats; sand-flats have 43 % of grains with no coats, mixed-flats have 6 % of grains with no coats, and mud-flats have 1 % of grains devoid of clay-coats.

Outer estuarine sediments expressed a more homogenous distribution in clay-coat coverage ranging from < 1 % to 4.4 % with most grains exhibiting at least partial coatings (Figs. 5.3 and 6.6). Samples from the pro-ebb delta and foreshore depositional environments have clay-coat coverage values of 1.9 % and 2.4 %, respectively. The extent of clay-coat coverage in outer estuarine sediment broadly increases with proximity of the sample to the tidal inlet with a systematic reduction with distance away from the inner estuary (Figs. 5.8 and 6.6).

Qualitative and quantitative methods of clay coat quantification revealed variable but broadly comparable distribution trend in clay-coat coverage (Fig. 6.6). It is apparent that a large portion of marginal marine depositional environments have < 10 % clay-coat coverage (Figs. 6.6 and 6.7) with sediment samples containing extensive (defined as > 50 % average grain clay-coat coverage) restricted to the mud-and mixed-tidal-flats, tidal-bars, and tidal creek depositional environments (Fig. 5.9).

The near-surface distribution of clay-coated sand-grains in a tidal-flat sedimentary package was investigated in Chapter 4. Clay-coat coverage displayed a heterogeneous distribution (Fig. 4.6). Clay-coat coverage increased in more heterolithic intervals with surface trends reflected in samples from the near-surface. Namely, mud-flats have the highest clay-coat coverage (surface, 61.7 %; near subsurface, 61.9 %), while sand-flats have the least coverage (surface, 3.9 %; near subsurface, 15.7 %). The study showed primary (surface) depositional clay-coat coverage patterns are reflected in near-surface sediment.

Figures 5.10 (surface) and 4.11 (surface and near-surface) plotted clay-coat coverage as a function of sediment heterogeneity (grain size and clay fraction content) and revealed that to create extensive (> 50 %) clay-coat grain coverage in marginal marine sediments, the sediment must be very fine sand, with > 7 % clay-grade material. However, in surface sediments, clay-coat coverage can reach 70 % in sand-dominated assemblages (e.g. very

fine sand) with 55 % and 20 % clay-coat coverage possible in fine sand and medium sand sized sediments, respectively (Fig. 5.10).

Trends in surface clay-coat coverage from the Ravenglass Estuary are represented schematically in Figure 8.1 across a typical fluvial to marginal marine transect of depositional environments.

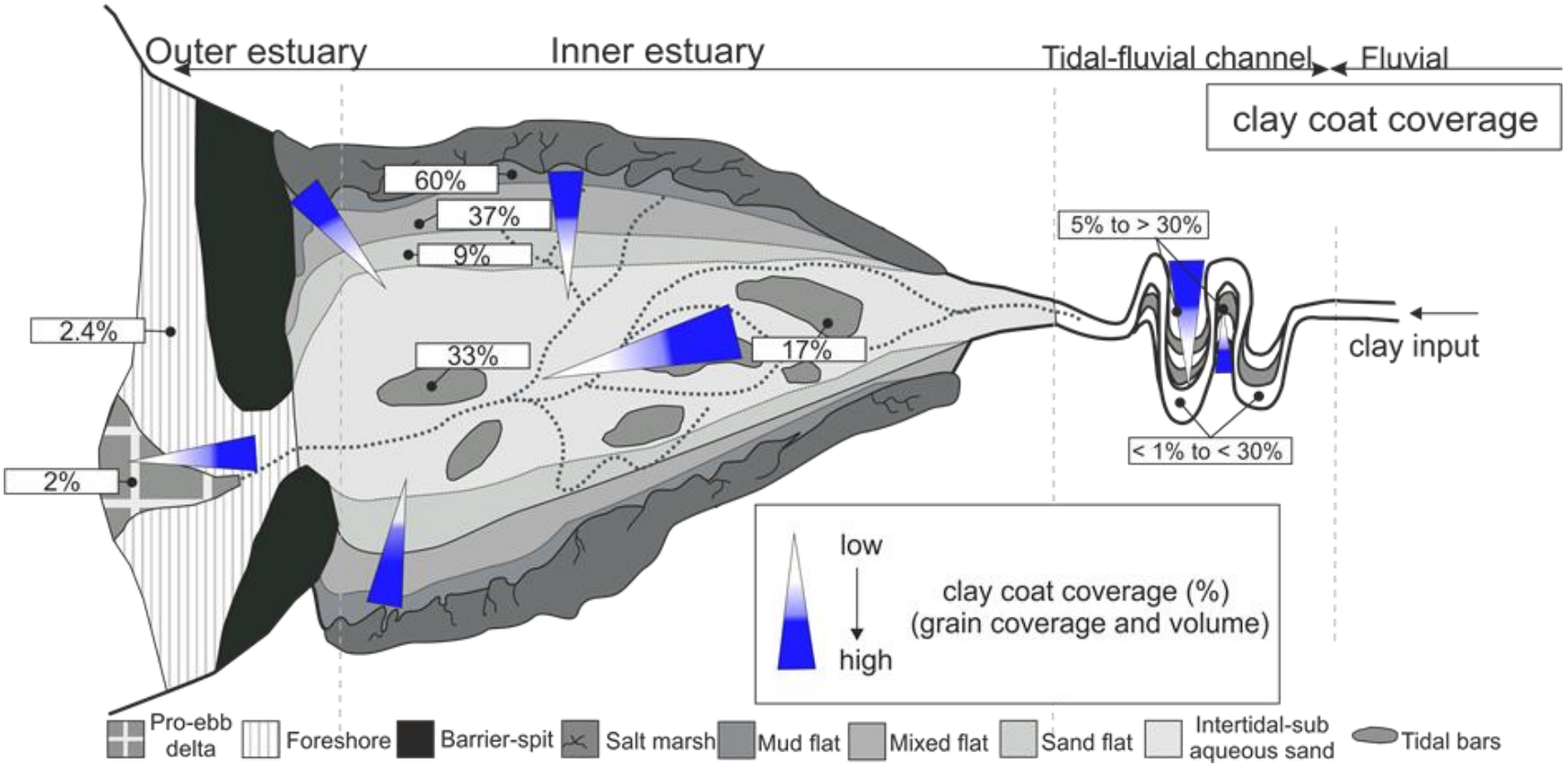

Figure 8-1 Schematic model demonstrating the likely trends in clay-coat coverage across a fluvial to marginal marine transect of depositional environments; after Dalrymple et al. (1992). Reported values are averages or where applicable ranges determined from comparable depositional environments in the Ravenglass Estuary.

8.1.3. Question 3. Does the mineralogy of clay-coated sand-grains vary in marginal marine sediments?

The mineralogy of clay coats (i.e. the ratio between illite and chlorite) are spatially heterogeneous across marginal marine depositional environments (Fig. 7.6). Clay coats have an elevated illite percentage in the tidal-flats (mixed and mud) and tidal-bar depositional environments from the Rivers Irt and Mite compared to the River Esk arm of the estuary (compare Fig. 7.1 to 7.6). The illite proportion in clay coats increases from the inner (50 % of coat mineralogy) to the outer estuarine depositional environments (> 70 % coat mineralogy; Fig.7.6).

Clay coats with the highest chlorite content occur in the inner-central and Esk arm of the estuary, corresponding to tidal-bar and tidal-flat (mixed and sand) depositional environments (compare Fig. 7.1 to 7.6). Clay coats have decreasing chlorite content from inner-central (20-28 %) to the outer (< 17 %) estuary sediments (Fig. 7.6).

Kaolinite clay-coat content has a bimodal distribution. Most environments typically have < 12.5 % kaolinite (Fig. 7.6). Clay coats containing > 15 % kaolinite are restricted to either the inner-central estuarine tidal-flats, tidal-bars, or the outer foreshore and pro-ebb delta depositional environments (Fig. 7.6).

In low energy environments that are characteristic of mud-and mixed-tidal-flats, clay coats are illite-enriched compared to clay coats, from sand-flat and tidal-bar depositional environments (high energy sediment assemblages) which have a more mixed mineralogy (i.e. chlorite and kaolinite). Clay coats in outer estuarine sediments (pro-ebb delta and foreshore) are progressively chlorite-deficient and illite-enriched with distance away from the inner estuary (i.e. tidal inlet) (Fig. 7.6).

Chapter 4 employed the assumption that the majority of the sediment clay mineral content was present as clay coats (Figs. 4.9 and 4.10) and allowed mapping of clay-coat mineralogy across a tidal-flat environment. Figure 4.9 and 4.10 revealed the local variability in clay-coat mineralogy across mud-, mixed-, and sand-flats with illite most abundant in the mud-flats and chlorite and kaolinite most abundant in the sand-flats. Chapter 4 compared clay-coat mineralogy from surface and near-surface tidal-flat sediments which identified that near-surface clay-coat mineralogy showed trends identical to surface sediment clay coats with no systematic variation or regular variability with depth (compare Fig. 4.10 to 4.9).

8.1.4. Key conclusions:

- Detrital-clay-coated grains consist of discontinuous coats and bridging structures between sand-grains. Clay-coats are composed of clay minerals, silt- to clay-sized lithics, and organics (diatoms and biofilms).
- Clay-coat mineralogy is dominated by illite which contributes a minimum 50 % of the attached clay coat material across the estuary, with less chlorite (< 10 % to 28 %) and kaolinite (< 10 % to 26 %).
- Detrital-clay coats are heterogeneously distribution across marginal marine sediments ranging from < 1 % to 87 % grain coverage. Clay coats are most extensive (grain coverage) in inner estuarine tidal-flat and tidal-bar depositional environments. There is a systematic decrease in the extent of clay-coat coverage from inner to outer estuarine sediments.
- Clay-coat coverage does not increase with increasing depth below the sediment surface. The distribution of clay-coat coverage in the near-surface is principally controlled by surface-based processes local to the site of deposition.
- In marginal marine sediments (surface and near-surface), an assemblage composed of a very fine sand, that contains > 7 % clay-grade material is required to create

extensive (> 50 %) clay-coat grain coverage. These conditions are met in the mixed- and mud-flat environments.

- The mineralogy of clay coats are spatially heterogeneous across marginal marine depositional environments.
- Compared to the low energy environments (illite enriched), inner estuarine clay coats have a more mixed mineralogy (i.e. increased chlorite and kaolinite) in the high energy sediment assemblages of the sand-flat and tidal-bar depositional environments.
- With distance away from the inner estuary, the clay coats in outer estuarine sediments (pro-ebb delta and foreshore) are increasingly chlorite-deficient and relatively illite-enriched.
- In tidal-flat sediments there is a comparable pattern of clay-coat mineralogy between samples from the surface and near-surface.

8.2. Controls on the formation and distribution of clay coats

8.2.1. Question 4. What controls the formation of clay-coated sand-grains in marginal marine sediments?

The ability to understand the mechanisms which govern the formation (i.e. attachment of clay minerals to grain surface) of clay coats in marginal marine sediments elevates this investigation from a series of high resolution analogue data sets, to a credible transposable framework able to aid prediction in modern and ancient marginal marine sediments. Detrital-clay coats in sand-dominated sediments have been reported to form via the sedimentological processes of inheritance, mechanical infiltration, and drying adhesion (Dowey et al. 2017; Matlack et al. 1989; Wilson 1992). Clay coat formation has also been reported to result from the biological-sediment interactions of sediment mixing and macro-

and micro-organism produced biofilm coatings on grain surfaces (McIlroy et al. 2003; Needham et al. 2005; Wooldridge et al. 2017a; Worden et al. 2006).

In Chapter 3 the research identified textural (Fig. 3.1), chemical (Fig. 3.2), and statistically significant, spatial distribution trends (Figs. 3.3 and 3.4) supporting a diatom-produced, biofilm mediated origin of clay coats in surface sediments of the Ravenglass Estuary.

Clay coats in near-surface tidal-flat sediments (Chapter 4) were shown to have: (i) a comparable statistical correlation (Table 4.4 and Fig. 4.10) between detrital-clay-coat coverage and biofilm abundance with that of surface sediment (compare Fig. 4.14 to 3.4), (ii) consistent biologically-mediated (biofilm) textures as reported in Chapter 3 (compare Fig. 4.7 to 3.1), and (iii) an absence of a pervasive post-depositional increase in the extent of clay-coat coverage (Figs. 4.6 and 4.11). Therefore the formation of near-surface clay-coated sand-grains is principally controlled by surface-based, biological (biofilm) processes local to the site of deposition. The post-depositional processes of infiltration and bioturbation may have a possible secondary role in increasing clay-coat coverage but do not significantly alter primary depositional (surface) clay-coat coverage patterns (i.e. limited influence in the formation of marginal marine clay coats).

Although, the macro-organism (lugworm, *Arenicola marina,* Fig. 5.4) formation of clay coats has been experimentally proven (Needham et al. 2005; Worden et al. 2006), the discordance in distribution between lugworm population density and clay-coat coverage (Fig. 2.10 and compare Fig. 5.4 to 5.8), shows that this is not the principal control on clay coat formation in the Ravenglass Estuary. The presence of clay-coated autochthonous grains (e.g. bioclasts) (Fig. 5.3) and the absence of a systematic reduction in clay-coat coverage from the source of fluvial input (Fig. 6.6) confirms that clay coats principally developed in the inner estuarine (hence: “clay coat factory”). Inheritance (from the

hinterland) is thus not a dominant source of clay coats in the sediments of the Ravenglass Estuary.

The study has identified a positive statistical correlation between clay-coat coverage and biofilm abundance for both surface (chlorophyll-a) (Fig. 3.4) and near-surface (total carbohydrate fraction) sediment (Fig. 4.14), the occurrence of diatoms and biofilms on sand-grain surfaces and in clay-coats (Fig.4.4), and the consistent spatial distribution between clay-coat coverage and biofilm abundance (surface and near-surface) (Figs. 3.4 and 4.11), all strongly suggest a dominant biological control on clay mineral attachment to grain surfaces in the Ravenglass Estuary.

It has been noted that biofilm-producing diatoms are associated with texturally comparable detrital-clay-coated grains (to this study) in the Anllóns Estuary, Spain (Dowey 2013), the Mandovi Estuary, India (Kessarkar et al. 2010), and reported in association with the Gironde Estuary, France (Virolle et al. 2016). The consistent co-occurrence of diatoms and clay coats thus reveal that clay mineral attachment to sand-grain surfaces in other modern marginal marine sediments probably has a biological biofilm mediated origin. Jones (2017) noted that biofilm-sediment interactions have been reported in sediment from just about all geological time periods (Noffke et al. 2006) indicating that highly evolved microbial activity occurred early in Earth's history. Further work is needed to constrain the link between sediment biofilm material and clay coats in marginal marine sandstones; however, this biological interaction potentially revolutionizes the understanding as to the origin of clay-coated sand-grains in ancient, deeply-buried sandstones.

8.2.2. Question 5. What processes govern the distribution of clay-coated sand-grains?

The distribution of clay-coated sand-grains across marginal marine systems (Figs. 5.8 and 6.6) can be explained, firstly, by an inner estuarine zone of active formation "clay coat

factory" governed by sediment biofilm abundance (formation mechanism) and, secondly, by transport-related abrasive clay-coat degradation due to grain-to-grain collisions (Chapter 5).

The attachment of clay minerals to sand-grain surfaces was shown to be mediated by biofilms (Chapter 3), the abundance of which is controlled by the environmental niche of EPS secreting organisms (diatoms) (Stal 2003) which are confined principally to the reduced energy conditions of the inner estuarine tidal-flat and tidal-bar depositional environments (Figs. 3.3 and 4.3). The result is that the distribution pattern of clay coats in inner estuarine sediments is principally a function of variability in formation rate (i.e. availability of adhesive biofilm material coats on grains).

There are progressive changes in clay coat textures and extent (grain coverage and volume) across inner estuarine sediments (Figs. 5.3, 5.15, and 6.1). For example, from mud-to sand-flats clay coats undergo removal of grain-bridging structures and a reduction in coat thickness (volume) (Figs. 2.7, 4.3, and 7.5). This distribution of textures is replicated on a larger scale, e.g. between inner and outer estuarine sediments (Figs. 5.3, 5.15, and 6.1). This evolution in clay coat texture and coating extent may represent transportation of clay-coated grains from the site of greatest biofilm concentration in the inner estuary (i.e. the "clay-coat factory") out of the estuary via the main channel accompanied by a degree of abrasive clay coat degradation due to sediment re-suspension and grain to grain collision. The implication of this is that, for outer estuarine sediments, clay-coat coverage and volume is a function of distance from the inner estuarine clay coat factory (Fig. 5.8).

The distribution of clay-coat coverage in the near-surface sediments of a tidal-flat (Fig. 4.6) showed similar patterns as surface clay-coat coverage (compare Fig. 4.6 to Fig 4.9). The similarity suggests that the distribution of clay-coated sand-grains is principally controlled by surface-based processes local to the site of deposition (i.e. biofilm abundance, Chapter

3). The post-depositional processes of infiltration and bioturbation have a possible secondary role in increasing clay-coat coverage but do not significantly alter primary depositional (surface) clay-coat coverage patterns. The bioturbation intensity recorded in near-surface sediment (Fig. 4.13) showed no correlation to the extent of clay-coat coverage.

The distribution of clay-coated sand-grains across sediments in the Ravenglass Estuary (Fig. 6.6) thus results from the interplay between active formation (biofilm mediated in the inner estuary) and transport of inner estuarine formed clay-coated sand-grains into higher energy environments (Fig. 5.15).

8.2.3. Question 6. What processes control the mineralogy of surface and near-surface clay-coated sand-grains?

Clay coats present a mixed mineralogy (Fig. 7.5) which is shown to be spatially heterogeneous across marginal-marine depositional environments (Fig. 7.6). Detrital-clay-coated sand-grains form via the attachment of the locally-available clay mineral assemblage in inner estuarine depositional environments (Chapter 4).

The origin of heterogeneity in clay-coat mineralogy is investigated in Chapter 7. Clay-coat mineralogy is governed principally by the hydrological controlled fractionation of the fluvial-inputted clay minerals. Clay-coat mineralogy is thus controlled by differential settling rates, with the typically larger chlorite minerals deposited out of suspension closer to the main ebb channel compared to illite (Fig. 7.5).

A secondary control on clay-coat mineralogy is the transport of clay-coated grains from the site of greatest biofilm concentration in the inner estuary (i.e. the “clay coat factory") out of the estuary via the main channel accompanied by a degree of abrasive clay coat degradation due to grain collisions (Fig. 7.9). The chlorite clay-coat component, typically

form prominent projections (Fig. 7.5) which, with grain to grain collisions (transport), experience preferential and early detachment compared to illite and kaolinite clay coat constituents. The result is the relative decrease (10 %) in clay coat chlorite content from inner to outer estuarine sediments (Fig. 7.6).

Inner estuarine clay-coat mineralogy is controlled by the deposited clay minerals with relative enrichment of clay-coating chlorite in the inner-estuarine sand-tidal-flat and tidal-bar depositional environments (Fig. 7.6). Outer estuarine clay-coat mineralogy results from the abrasive removal of specific clay mineral types (e.g. chlorite) with transport of inner estuarine formed clay coats, with sediment clay coats increasingly chlorite deficient and illite dominated, with distance away from the inner estuary (Figs. 7.6 and 7.9).

In Chapters 2, 4, 5, and 7 clay-coat mineralogy is shown to consist of illite, chlorite, and kaolinite, and reflect the fluvial clay mineral assemblage derived from the incision and weathering of the hinterland Palaeozoic Eskdale Granite, the Triassic Sherwood Sandstone Group, the Borrowdale Volcanic Group geology, and outcropping glacial units (Moseley 1978) (Chapter 1). The implication is that the pre-drill prediction of bulk clay-coat mineralogy requires consideration of the initial clay assemblage at the time of deposition, governed by paleo-climate and source hinterland geology.

Near-surface clay-coat mineralogy was shown to be similar to surface clay-coat mineralogy in tidal-flat sediments (compare Fig. 4.9 to 4.10) with chlorite most enriched in the sand-flat sediments and illite most enriched in mud-flat sediments. The similarity of surface and near-surface trends in clay-coat mineralogy suggests an absence of large-scale, post-depositional infiltration of clay minerals. If large-scale, post-depositional infiltration of clay minerals had occurred, then a more regular signature (i.e. over-printing the fractionated primary depositional clay assemblage, Fig. 4.11) would be expected.

8.2.4. Key conclusions:

- The origin and distribution of clay-coated sand-grains in inner estuarine sediment is primarily controlled by diatom-produced biofilms. A secondary control is the transport of clay-coated grains from the site of greatest biofilm concentration in the inner estuary (i.e. the “clay coat factory") out of the estuary via the main channel accompanied by abrasive degradation of the attached clay coat.
- Clay-coat coverage does not increase with increasing depth below the sediment surface. Therefore the generation and distribution of clay-coated sand-grains is principally controlled by surface-based processes local to the site of deposition. The post- depositional processes of infiltration and bioturbation have a possible secondary role in increasing clay-coat coverage but do not significantly alter primary depositional (surface) clay-coat coverage patterns.
- Spatial trends in clay-coat mineralogy are governed, first, by differential settling rates of the predominantly fluvial-derived clay mineral assemblage and, second by the selective abrasive removal of specific clay mineral types (e.g. chlorite) during reworking and transport.
- Mineralogy of inner estuarine clay coats is controlled by the suspension-controlled segregation of the fluvial-derived clay mineral assemblage with chlorite (larger detrital flakes) preferentially deposited in close proximity to the ebb-tidal channel (i.e. sand flats).
- Patterns in clay-coat mineralogy are consistent between surface and near-subsurface tidal-flat sediments with mud-flat facies richer in illite and poorer in chlorite than clay coats from sand-flat facies.

8.3. Sedimentological and biological heterogeneity across a marginal marine system

8.3.1. Question 7. What are the sediment and biological characteristics of a macro-tidal estuarine system?

8.3.1.1. Sedimentological heterogeneity across macro-tidal estuarine system

The Ravenglass Estuary has a grain size range from silt to medium sand, a clay fraction content which varies from < 1 % to < 16 %, and sediment sorting values from well sorted to very poorly sorted (Fig. 5.2 and Table 5.1).

The coarsest grain size in the estuary, medium sand sized sediment, is located in deposits from the tidal-inlet and foreshore (compare Fig. 5.1 to 5.2). The outer estuary has a broadly homogeneous grain size distribution, dominated by an upper fine to medium sand (Fig. 5.2, Table 5.1). Inner estuary sediments express a heterogeneous distribution of grains sizes and sorting ranging from silt to medium sand, and well sorted to very poorly sorted.

The estuary shows an overall trend of decreasing grain size and sorting away from the ocean (i.e. towards the tidal limit) and a smaller inner estuarine pattern of decreasing grain size and sorting with distance from the main ebb channel (Fig. 2.3, and 5.2). There was no systematic increase in the proportion of sediment clay fraction with depth (Fig. 4.6) in tidal-flat sediments with surface sediment trends broadly replicated in the sediment cores (compare Fig. 4.6 to 4.3). Namely, the greatest abundance of clay fraction occurred in mud-flat samples (surface, 8.6 %; near subsurface, 10 %) and least in sand-flat samples (surface, 1.2 %; near subsurface, 1.7 %). The correlation between clay fraction content and the environment of deposition across tidal-flat sediments (surface Fig. 4.3 and near-surface, Fig. 4.11) indicates that sediment heterogeneity is controlled, principally, by clay particle entrapment at the site of deposition.

Chapter 7 revealed that the majority of the sediment clay mineral volume that is present as clay coats is in excess of 61/100 (Fig. 7.3). This fraction is highest in the sand-dominated assemblages of the mixed-tidal flat (84/100), sand-tidal-flats (78/100), tidal-bars (non-vegetated) (75/100), tidal inlet (90/100), and foreshore (79/100) depositional environments (Table 7.2). The predominant role of grain-coating clay in the overall clay mineral budget highlights the fundamental role of clay coat-forming processes (Chapters 3 and 5) in influencing sediment clay fraction content variability. The remaining (non-attached) part of the whole sediment clay mineral assemblage occurs as inclusions in clay-rich lithics or as clumps that potentially resulted from flocculation (Figs. 7.3 and 7.5). Clay coat forming processes (i.e. biofilms) thus explain a mechanism in which clay-grade material overcome hydrodynamic segregation and persist in high energy, sand-dominated sediments (e.g. tidal bars and foreshore).

There is a difference in the distribution between clay minerals in the estuarine sediment (i.e. whether a clay mineral is predominantly grain coatings or in clay-rich lithics) (Fig. 7.7). Illite is present mostly as clay coats, especially in outer estuarine sediments (e.g. foreshore and pro-ebb delta). Approximately 50 % of the whole sediment chlorite abundance is present as clay coats (Fig. 7.7). Kaolinite predominantly occurs as components of clay coats especially for outer estuarine environments (e.g. 92 % foreshore and 86 % pro-ebb delta) (Fig. 7.7).

Trends in surface sediment characteristics (e.g. grain size and clay fraction content) are represented schematically across a typical fluvial to marginal marine transect of depositional environments) in Figure 8.2.

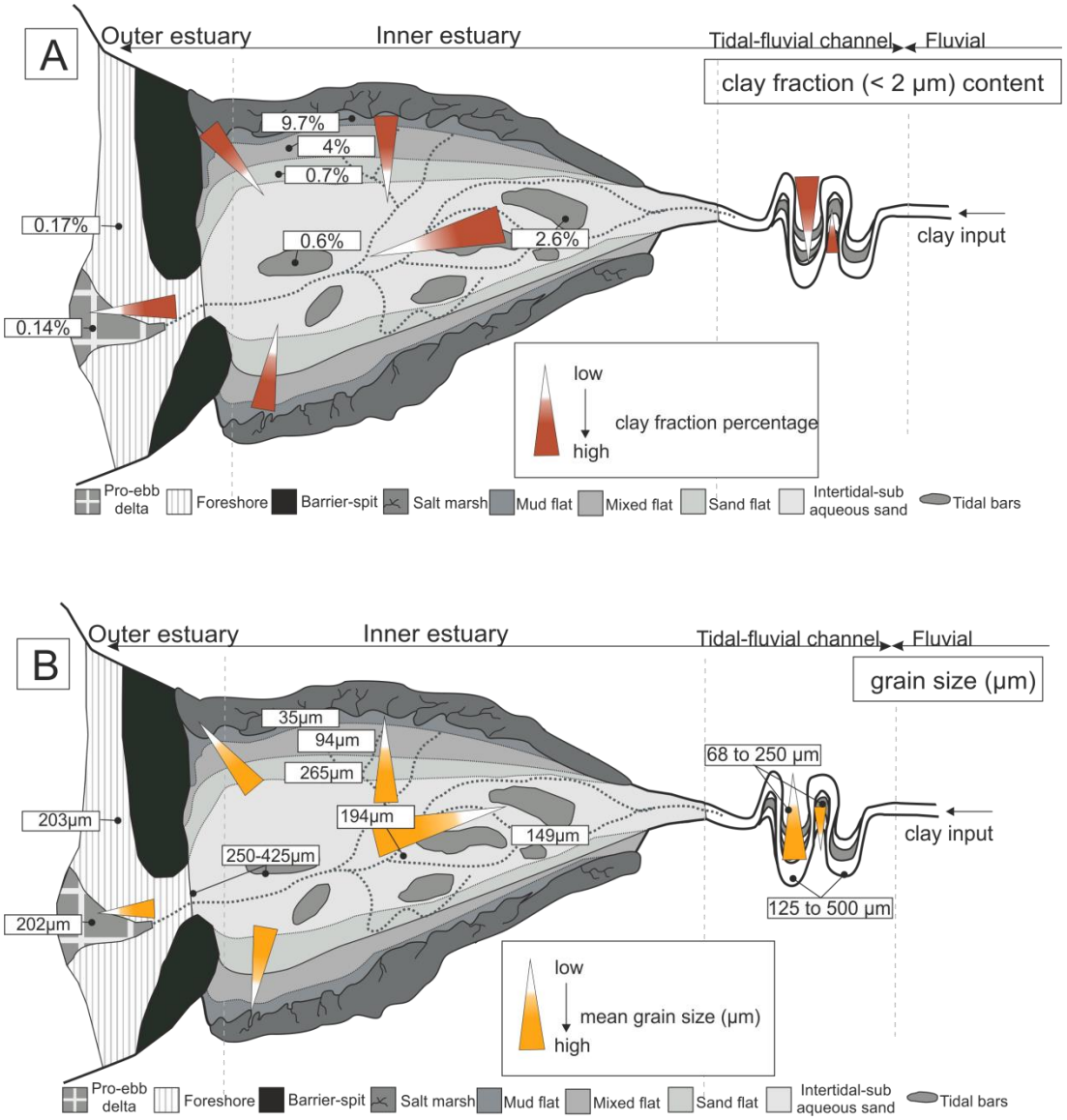

Figure 8-2 Schematic model demonstrating the likely trends in sediment heterogeneity (clay fraction content and mean grain size) across a fluvial to marginal marine transect of depositional environments; after Dalrymple et al. (1992). (A) Distribution map of sediment clay fraction content. (B) Distribution map of mean grain size. Reported values are averages or where applicable ranges determined from comparable depositional environments in the Ravenglass Estuary.

8.3.1.2. Biological heterogeneity across macro-tidal estuarine system

The surface distribution of chlorophyll-a (biofilm proxy) revealed (1) a heterogeneous distribution pattern and (2) the presence of biofilm-producing diatoms (MPB) within all inner-estuarine environments but at different population densities (Figs. 3.3 and 5.7). Chlorophyll-a increases in concentration in a landward direction, and is most extensive within the mid to upper estuarine tidal-flats (e.g. mud- and mixed-tidal-flats). Biofilm abundance increased with a decreasing grain size and increasing clay fraction content which are characteristic of low energy environments (Table 4.4 and 5.2). Trends in surface sediment biofilm abundance are represented schematically across a typical fluvial to marginal marine transect of depositional environments in Figure 8.3.

Biofilm abundance in near-surface, tidal-flat sediment (total carbohydrate fraction) (Fig. 4.8) showed a heterogeneous distribution with elevated sediment biofilm abundance in finer grained sediment samples from mud-and mixed-tidal-flats and lack a systematic pattern with depth (Fig. 4.10). The consistent trends between surface and near-surface biofilm abundance indicates a distribution trend directly inherited from surface processes (Figs. 4.3 and 4.10).

Macro-faunal bioturbation in the biotic zone of estuarine sediments was measured via the spatial density counts of faecal casts of the lugworm, *Arenicola marina* (Chapters 2 and 5). Lugworm faecal counts present a heterogeneous distribution across the estuary (Figs. 2.3 and 5.4) with highest density in the mixed-flat and tidal-bar (non-vegetated) (> 50 per m^2) depositional environments (Fig. 2.3). Lugworm populations are predominantly absent in the mud-flat and outer estuarine depositional environments (compare Fig. 5.1 to 5.4).

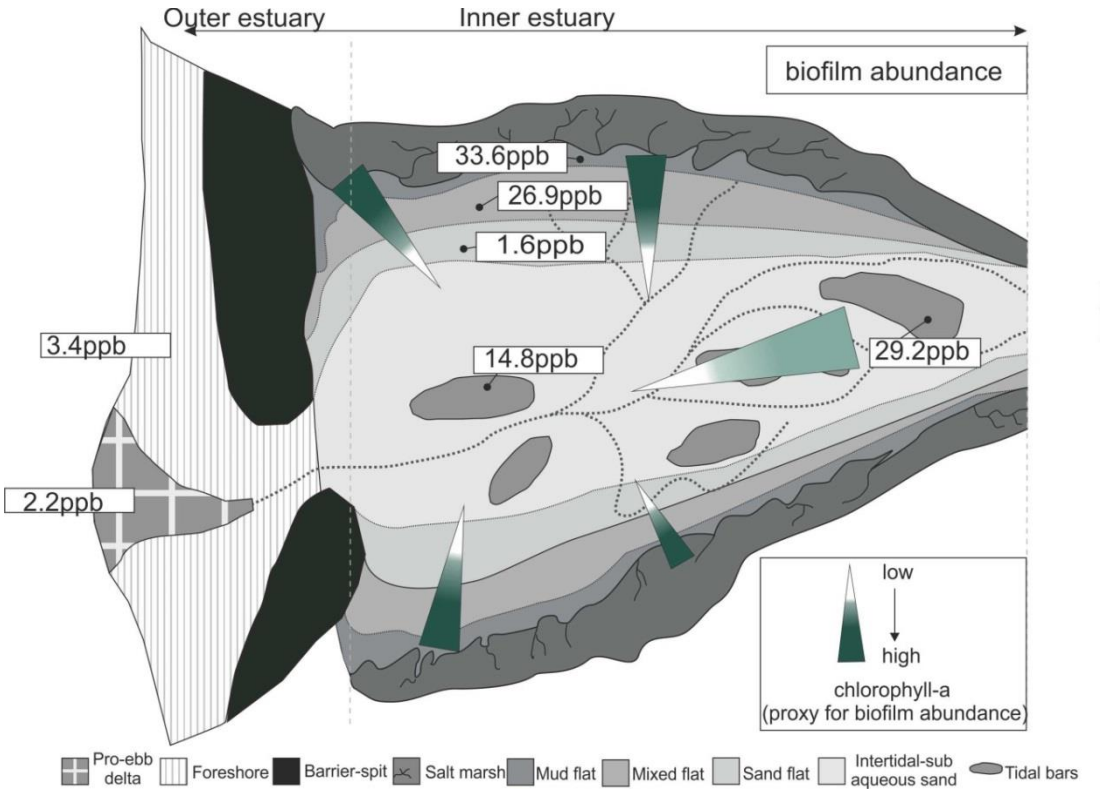

Figure 8-3 Schematic model demonstrating the likely trends in sediment biofilm abundance (chlorophyll-a proxy) across a fluvial to marginal marine transect of depositional environments; after Dalrymple et al. (1992). Reported values are averages from comparable depositional environments (chlorophyll-a concentrations) in the Ravenglass Estuary.

8.3.2. Key conclusions

- Marginal marine grain size varies from silt to medium sand, the clay fraction varies from < 1 % to 16 %, and sorting from well sorted to very poorly sorted.
- The clay-fraction in estuarine sediments occurs principally (average 81 % of the total clay mineral abundance) as clay coats and bridging structures between sand-grains.
- Biofilms are pervasive but heterogeneously distributed in all inner estuarine sediments. Biofilm abundance increases in a landward direction, and is most extensive within the mid to upper estuarine tidal-flats.
- Tidal-flat biofilm abundance of the near-surface shows comparable trends as surface sediment with the greatest biofilm content in mud-flat facies and least in sand-flat facies.

8.4. The biofilm influence on the diagenetic properties of marginal marine sediments

8.4.1. Question 8. How do sediment biofilms influence the diagenetic properties of marginal marine sediments?

The marginal marine sediments of the Ravenglass Estuary have, on average, 81 % of the total sediment clay mineral abundance that is present as clay coats (Fig. 7.3, Table 7.2). Clay coats in Chapter 3 were shown to derive principally from the adhesive properties of biofilms produced by micro-organisms (diatoms). The implication is that biofilm-formed clay coats are the principal mechanism explaining how clay size particles overcome hydrodynamic segregation and co-deposit in sand-dominated estuarine sediments (Figs. 6.1, 5.3, and 5.15).

The biofilm entrapment of silt- and clay-sized material as coats has resulted in a reduced mean grain size and produced the remarkably similar correlation between mean grain size,

clay fraction content, and biofilm abundance (chlorophyll-a) (Figs. 4.3, 4.11 and compare Fig. 5.2 to 5.7). The correlation between grain size (and clay fraction) and biofilm abundance at Ravenglass is consistent with a study of the Minas Basin, Bay of Fundy, Canada (Garwood et al. 2015).

Biofilm production is restricted to the top few centimetres of the sediment (where light penetrates) (Stal 2003) so that active, biofilm-mediated entrapment of clay minerals (i.e. clay coat formation) is restricted to the sediment surface, potentially, explaining the strong correlation in clay-coat mineralogy and clay-coat coverage between surface and near-surface tidal-flat sediments (compare Figs. 4.6, 4.9, and 4.10, Table 4.4). The implication is that biofilms influence the primary depositional characteristics of marginal marine sediment (e.g. grain size, sorting, and clay content) and mediate the formation and distribution of detrital clay-coated sand-grains in the Ravenglass Estuary (Chapters 3, 4, and 5).

Reservoir quality in deeply-buried sandstones is mainly controlled by three factors; (1) the primary depositional characteristics of the sediment (e.g. grain size, sorting, clay content, clay mineralogy, and bulk assemblage mineralogy), (2) the extent of mechanical and chemical compaction, and (3) the volume and type of pore-filling cement (Worden and Morad 2003). Biofilms (diatom produced) thus exert a fundament control on the diagenetic properties of marginal marine systems by: (1) mediating the creation of clay coats (precursors to quartz cement inhibiting diagenetic-clay coats) and (2) exacerbating the entrapment of fine (clay to silt) particles (i.e. altering sediment characteristics).

8.5. Reservoir quality predictions

8.5.1. Question 9. What are the target reservoir quality prospects of marginal marine sediments?

At depths > 3 km (temperatures > 90 °C) pervasive authigenic quartz cement typically starts to become a dominant, porosity-occluding cement in sandstones (Bloch et al. 2002; Worden and Morad 2000). The principal factor controlling the effectiveness of clay coats (chlorite, illite, and mixed mineralogy) in inhibiting quartz cement (and thus preserving elevated porosity in deeply-buried sandstones) is the completeness of grain coat coverage (Ajdukiewicz and Larese 2012; Bloch et al. 2002; Ehrenberg 1993). Sandstones with absent, or partially developed, clay coats thus risk becoming extensively quartz cemented when deeply-buried. Clay-coat mineralogy is an important secondary control on quartz cement growth since there are morphological differences between coats composed of different clay minerals (Ajdukiewicz and Larese 2012), with chlorite reported to better inhibit quartz cement (i.e. inhibition of epitaxial growth, Fig. 1.2) than illite, due to the typical morphology of chlorite coatings (Ajdukiewicz and Larese 2012).

Figure 8.4 shows the surface distribution patterns of clay-coating chlorite and clay-coat volume across the depositional environments of the Ravenglass Estuary. On the assumption that increasing the chlorite content, in the mixed mineralogy coats and increasing clay-coat volume (i.e. more likely to produce complete diagenetic-clay coats), would preferentially inhibit quartz cement, this work suggests that, in deeply-buried marginal marine sandstones, the best porosity would be found in the inner estuarine sand-flat and tidal-bar depositional facies.

The limited clay-coat coverage and volume of outer estuarine sediments (Figs. 6.6 and 8.4), irrespective of chlorite content, would more likely (compared to inner estuarine sediment)

produce discontinuous to absent diagenetic-clay coats and thus experience pervasive quartz cementation.

The results of this study suggest, against common convention, that in deeply-buried prospects, the best porosity might be found in finer-grained, more clay-rich inner estuarine tidal-flat-and tidal-bar facies. Thus a moderate amount of clay that is distributed in sandstones as grain coats is potentially good for reservoir quality in deeply-buried sandstones.

Clay-coat coverage plotted as a function of surface (Fig. 5.10) and near-surface (Fig. 4.11) sediment characteristics show that, for inner estuarine sediment (zone of active clay coat formation), clay-coat coverage increases in a linear trend with a decreasing grain size and sorting and increasing clay fraction content. In summary, for extensive clay coat grain coverage (> 50 % average) sediment must be very fine sand, with > 7 % clay fraction. These conditions are met in mud- and mixed-tidal-flats and tidal-bar depositional environments (Figs 5.10 and 4.11). For outer estuarine sediments (Fig. 5.3), the extent of clay-coat coverage increases and thus the possibility of forming complete diagenetic-clay coats (on burial) potentially capable of inhibiting quartz cement, increases on proximity to the inner estuary (Figs. 5.8 and 6.6).

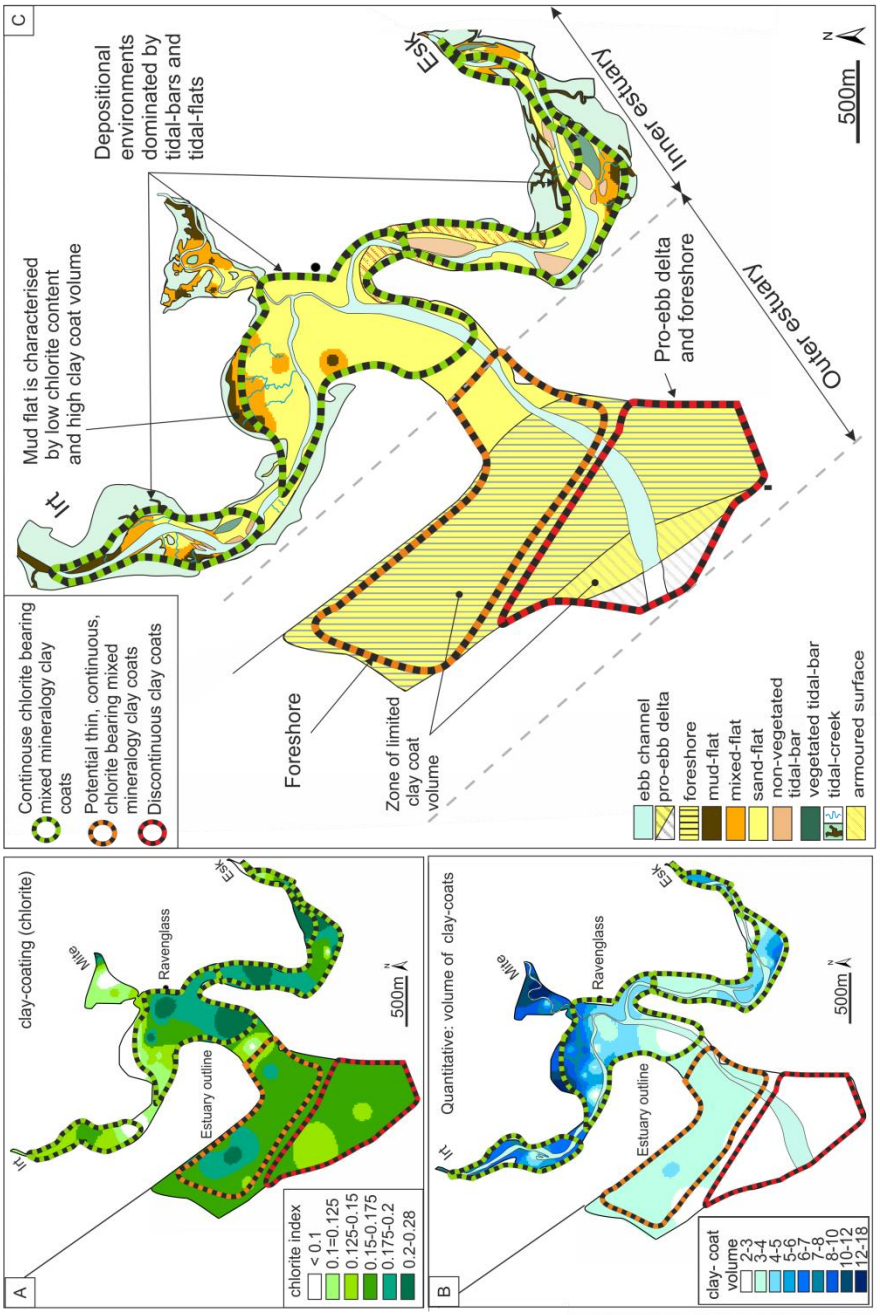

Figure 8-4 Schematic model for the likely distribution of clay coat derived enhanced reservoir quality on deep burial and heating. (A) Map of relative clay coating chlorite abundance. (B) Map showing the distribution of clay-coat volume. (C) Distribution map of depositional environments indicating zones of potential relative degrees of clay coat characteristics (i.e. based on chlorite content and grain coat coverage). Green lines outline the zone of potential advantageous clay coats (i.e. sufficient to completely coat grains to inhibit quartz cement but not enough to block pore throats). Orange line outlines the region of limited clay coating clay minerals which would potentially result in chlorite enriched but discontinuous (in respect of grain coverage) diagenetic coats. Red lines outline zones of minor to absent clay-coat coverage which would potentially result, with diagenetic transformation, in discontinuous clay coats and thus experience pervasive quartz cementation with deep burial and heating.

8.6. Concluding remarks

The importance of biofilms in marginal marine systems has been undervalued and represents an area of clastic sedimentology that requires further investigation. The data sets collected in this study have begun to reveal the fundamental role played by biofilms in governing the diagenetic characteristics of marginal marine sediments via influencing the primary depositional characteristics of the sediment (e.g. grain size, sorting, and clay content) and mediating the formation of detrital clay-coated sand-grains. The identified novel biological, biofilm, origin of modern clay-coated sand-grains which represent the precursor material to quartz cement, inhibiting, diagenetic clay coats represents a new mechanism in which to appraise the distribution of clay coat derived reservoir quality in ancient, deeply-buried sandstones.

9. Further Work

The ideas introduced below offer the opportunity to expand the work reported in this thesis to other sedimentary systems and constrain with greater certainty the link between the modern (detrital) clay coats of this study and those present in ancient (diagenetic) deeply-buried sandstones.

9.1. Experimental approaches: replicating diagenesis

9.1.1. Replicating burial diagenesis of detrital-clay coats (bridging the gap)

The work by Aagaard et al. (2000) showed, in hydrothermal experiments that replicated burial diagenesis at 90 °C, that partial detrital-clay-coats can undergo recrystallization to produce a complete grain-coating with textural and mineralogical characteristics consistent with naturally occurring clay coats in deeply-buried sandstones. The work reported by Aagaard et al. (2000) lacked a detailed description of pre- and post-experimental clay coat textures.

The stratigraphy of deeply-buried diagenetic-clay coats consists of; (1) an inner chaotic, tangentially oriented (to grain) lower root structure, and (2) an outer rim (perpendicular to grain) composed of euhedral clay minerals, typically growing pore-ward from a lower unstructured clay coat root (Bloch et al. 2002). The inner clay coat stratigraphy has been reported to represent a detrital or very early diagenetic clay-coat (diagenetic-recrystallized coat) which acts as a seed for later precipitation from pore fluids (diagenetic-authigenic coat) (Billault et al. 2003; Bloch et al. 2002; Ehrenberg 1993; Gould et al. 2010).

A new series of hydrothermal bomb experiments replicating diagenesis would test such a conclusion and permit an enhanced understanding of the evolutionary stages between detrital-and diagenetic-clay coats (Fig. 1.2), in terms of texture and mineralogy.

The advantages of undertaking hydrothermal bomb experiments similar to Aagaard et al. (2000) are that: (i) the results would test if detrital-clay coats are, in fact, direct precursors to diagenetic-clay coats, (ii) identify the volume of detrital-clay coat material that is needed to form continuous diagenetic-clay coats that are capable of inhibiting quartz cement, and (iii) constrain the role played by detrital coats (e.g. mineralogy) in governing the morphology of the resulting diagenetic-clay coat.

9.1.2. Testing the cement inhibition effectiveness of different mineralogy clay coats

Ajdukiewicz and Larese (2012) undertook hydrothermal experiments to investigate the role of clay-coat mineralogy in governing quartz cement inhibition. Their study focused on pure illite and pure chlorite clay coats. However, as noted in Chapter 7 mixed mineralogy coats are common in marginal marine systems. A key gap in current understanding is thus the effect of mixed mineralogy coats (e.g. illite, chlorite, and kaolinite) on quartz cement inhibition.

A series of hydrothermal bomb experiments involving mixed mineralogy coats of differing compositions (i.e. ratio of illite vs chlorite) would, potentially, lead to a novel understanding of the specific role of chlorite-illite ratios on quartz cement inhibition in deeply-buried sandstones.

9.2. Experimental approaches: replicating modern biofilm-sediment interactions

9.2.1. Experimental production of clay coats

A key outcome of this study has been the identification of a biological origin of detrital-clay-coated sand-grains via the biofilm (“bio-glue”) mediated attachment of clay minerals to sand-grain surfaces. In natural systems there are typically multiple processes occurring simultaneously (e.g. active formation of clay coats with continued erosion and transport)

thus a potential advancement would be the ability to replicate individual biofilm-sediment interactions (e.g. biofilm formation and clay mineral attachment) via a series of experiments involving laboratory-grown biofilms.

The advantages of such a lab-based methodology are: (i) the ability to constrain the abundance of biofilm (EPS) material necessary for clay-coat formation and (ii) identify other potential sources (e.g. instead of diatoms and lugworms) of EPS material capable of coating sand-grain surfaces.

Sediment biofilms are produced by microphytobenthic (MPB) communities that are composed of algae (diatoms, euglenids, crysophyceans, dinoflagelates), cyanobacteria and other photosynthetic bacteria (Jesus et al. 2009). In the Ravenglass Estuary, diatoms form the dominant biofilm producing micro-organism, however, in other marginal marine, fluvial or terrestrial settings; biofilm coatings (potentially capable of gluing clay to sand-grains) will derive from other organisms. The ability of the above series of experiments to test the validity of biofilm coats (e.g. produced by cyanobacteria) could potentially, revolutionise the understanding of clay coats in modern sedimentary systems.

9.2.2. Experimental degradation of clay coats

Experimentally-produced, biofilm-mediated clay-coats (see above) would facilitate with the subsequent use of flume tank experiments the ability to: (i) constrain the rate and style of clay coat degradation (strength of attachment) with grain transport and (ii) confirm whether a degree of abrasive clay-coat degradation during transport partly controls clay coat morphology in outer estuarine sediments.

A flume tank data set would also test the validity of the reported inner estuarine “clay coat factory” origin (erosion and transport) of clay coats in some sandstones deposited further

down the system in continental shelf, continental slope, and basin floor settings (Bloch et al. 2002; Houseknecht and Ross Jr 1992).

9.3. The origin of clay-coated sand-grain in other modern depositional environments

Diatom-produced biofilms have been shown in Chapter 3 to facilitate the formation of detrital-clay-coated sand-grains in marginal marine sediments of the Ravenglass Estuary. Clay-coats have been reported extensively in other non-estuarine marginal marine settings, such as deltas, lagoons, and clastic shoreface sandstones (Dowey et al. 2012). Data sets including biological content, clay-coat coverage, and sediment heterogeneity from a range of marginal marine systems would provide further insights into the distribution and controlling mechanisms of clay-coated sand-grains.

Biofilms have been shown to have a fundamental control on terrestrial and fluvial (Belnap and Weber 2013; Gerbersdorf et al. 2008) depositional settings; environments estimated by Dowey et al. (2012) to represent a third of all reported clay-coated sandstones. However, to the author's knowledge there remains no high resolution attempt to constrain the presence, distribution, or origin, of clay coats in such depositional settings.

The application of the sedimentological, mineralogical, and biological approaches, used and developed in this study, to other sedimentary settings would: (i) produce a predictive framework of clay coat distribution encompassing all sedimentary systems and (ii) identify if the biological (biofilm) control on clay coat formation (Chapter 3) is applicable to other systems (e.g. deltas).

9.4. High resolution core based analysis

The ability to test if the clay-coat distribution data sets reported in this study are applicable for aiding prediction in deeply-buried sandstones is hindered by the absence of

quantitative, high-resolution, core based studies on the distribution, textures, and mineralogy of diagenetic clay-coats.

Despite the poor spatial and poor stratigraphic coverage of oil-field core-based studies of grain coating (Wooldridge et al. 2017b), multiple core-based studies could quantify trends in: (i) clay-coat mineralogy, (ii) changes in mineralogy across clay coat stratigraphy (e.g. diagenetic-recrystallized coat vs. diagenetic-authigenic coat components), and (iii) constrain the distribution of clay coated sand-grains.

10. References

AAGAARD, P., JAHREN, J.S., HARSTAD, A.O., NILSEN, O., AND RAMM, M., 2000, Formation of grain-coating chlorite in sandstones. Laboratory synthesized vs. natural occurrences: Clay Minerals, v. 35, p. 261-269.

AGOGUÉ, H., MALLET, C., ORVAIN, F., DE CRIGNIS, M., MORNET, F., AND DUPUY, C., 2014, Bacterial dynamics in a microphytobenthic biofilm: a tidal mesocosm approach: Journal of Sea Research, v. 92, p. 36-45.

AINSWORTH, R.B., VAKARELOV, B.K., AND NANSON, R.A., 2011, Dynamic spatial and temporal prediction of changes in depositional processes on clastic shorelines: toward improved subsurface uncertainty reduction and management: AAPG bulletin, v. 95, p. 267-297.

AJDUKIEWICZ, J.M., AND LARESE, R.E., 2012, How clay grain coats inhibit quartz cement and preserve porosity in deeply buried sandstones: Observations and experiments: American Association of Petroleum Geologists Bulletin, v. 96, p. 2091-2119.

AL-RAMADAN, K.A., HUSSAIN, M., IMAM, B., AND SANER, S., 2004, Lithologic characteristics and diagenesis of the Devonian Jauf sandstone at Ghawar Field, eastern Saudi Arabia: Marine and Petroleum Geology, v. 21, p. 1221-1234.

ALGAN, O., CLAYTON, T., TRANTER, M., AND COLLINS, M.B., 1994, Estuarine mixing of clay minerals in the Solent region, southern England: Sedimentary Geology, v. 92, p. 241-255.

AMOS, C.L., 1995, Siliciclastic tidal flats: Developments in Sedimentology, v. 53, p. 273-306.

ANJOS, S.M.C., DE ROS, L.F., DE SOUZA, R.S., SILVA, C.M.D., AND SOMBRA, C.L., 2000, Depositional and diagenetic controls on the reservoir quality of Lower Cretaceous Pendencia sandstones, Potiguar rift basin, Brazil: American Association of Petroleum Geologists Bulletin, v. 84, p. 1719-1742.

APPERT, O., 1998, Editorial: Revue de l'Institut Français du Pétrole, v. 53, p. 243-252.

ARMITAGE, P.J., WORDEN, R.H., FAULKNER, D.R., APLIN, A.C., BUTCHER, A.R., AND ILIFFE, J., 2010, Diagenetic and sedimentary controls on porosity in Lower Carboniferous fine-grained lithologies, Krechba field, Algeria: A petrological study of a caprock to a carbon capture site: Marine and Petroleum Geology, v. 27, p. 1395-1410.

ARMITAGE, P.J., WORDEN, R.H., FAULKNER, D.R., BUTCHER, A.R., AND ESPIE, A.A., 2016, Permeability of the Mercia Mudstone: suitability as caprock to carbon capture and storage sites: Geofluids, v. 16, p. 26-42.

BARRIE, G.M., WORDEN, R.H., BARRIE, C.D., AND BOYCE, A.J., 2015, Extensive evaporation in a modern temperate estuary: Stable isotopic and compositional evidence: Limnology and Oceanography, v. 60, p. 1241-1250.

BELNAP, J., AND WEBER, B., 2013, Biological soil crusts as an integral component of desert environments: Ecological Processes, v. 2, p. 11.

BILLAULT, V., BEAUFORT, D., BARONNET, A., AND LACHARPAGNE, J.C., 2003, A nanopetrographic and textural study of grain-coating chlorites in sandstone reservoirs: Clay Minerals, v. 38, p. 315-328.

BLOCH, S., LANDER, R.H., AND BONNELL, L., 2002, Anomalously high porosity and permeability in deeply buried sandstone reservoirs: Origin and predictability: American Association of Petroleum Geologists Bulletin, v. 86, p. 301-328.

BOUSHER, A., 1999, Ravenglass Estuary: Basic characteristics and evaluation of restoration options: RESTRAT Technical Deliverable TD, v. 12.

BROCKAMP, O., AND CLAUER, N., 2012, Clay mineral provinces in tidal mud flats at Germany's North Sea coast with illite K-Ar ages potentially modified by biodegradation: Estuarine Coastal and Shelf Science, v. 107, p. 32-45.

BROCKAMP, O., AND ZUTHER, M., 2004, Changes in clay mineral content of tidal flat sediments resulting from dike construction along the Lower Saxony coast of the North Sea, Germany: Sedimentology, v. 51, p. 591-600.

BUURMAN, P., JONGMANS, A., AND PIPUJOL, M., 1998, Clay illuviation and mechanical clay infiltration—Is there a difference?: Quaternary International, v. 51, p. 66-69.

CHAKRABARTI, A., 2005, Sedimentary structures of tidal flats: a journey from coast to inner estuarine region of eastern India: Journal of earth system science, v. 114, p. 353-368.

CHANG, J., AND CHOI, J., 2001, Tidal-flat sequence controlled by Holocene sea-level rise in Gomso Bay, west coast of Korea: Estuarine, Coastal and Shelf Science, v. 52, p. 391-399.

CHURCHILL, J.M., POOLE, M.T., SKARPEID, S.S., AND WAKEFIELD, M.I., 2016, Stratigraphic architecture of the Knarr Field, Norwegian North Sea: sedimentology and biostratigraphy of an evolving tide-to wave-dominated shoreline system: Geological Society, London, Special Publications, v. 444, p. SP444. 4.

COCKER, J., KNOX, W., LOTT, G., AND MILODOWSKI, A., 2003, Petrologic controls on reservoir quality in the Devonian Jauf Formation sandstones of Saudi Arabia: Geofrontier, v. 1, p. 6-11.

CRONE, A.J., 1975, Laboratory and field studies of mechanically infiltrated matrix clay in arid fluvial sediments: University of Colorado, [Ph.D. thesis], 162 p.

DALRYMPLE, R.W., ZAITLIN, B.A., AND BOYD, R., 1992, Estuarine facies models - conceptual models and stratigraphic implications: Journal of Sedimentary Petrology, v. 62, p. 1130-1146.

DANESHVAR, E., 2011, Role of provenance on clay minerals and their distribution in modern estuaries: University of Liverpool, [Ph.D. thesis], 236 p.

DANESHVAR, E., AND WORDEN, R.H., 2016, Feldspar alteration and Fe minerals: origin, distribution and implications for sandstone reservoir quality in estuarine sediments. In: Armitage, P. J., Butcher, A. R., Churchill, J. M., Csoma, A. E., Hollis, C., Lander, R. H., Omma, J. E. & Worden, R. H. (eds) 2016. Reservoir Quality of Clastic and Carbonate Rocks: Analysis, Modelling and Prediction. .

DE BROUWER, J., DE DECKERE, E., AND STAL, L., 2003, Distribution of extracellular carbohydrates in three intertidal mudflats in Western Europe: Estuarine, Coastal and Shelf Science, v. 56, p. 313-324.

DE WINDER, B., STAATS, N., STAL, L., AND PATERSON, D., 1999, Carbohydrate secretion by phototrophic communities in tidal sediments: Journal of Sea Research, v. 42, p. 131-146.

DECHO, A.W., 1990, Microbial exopolymer secretions in ocean environments: their role (s) in food webs and marine processes: Oceanogr. Mar. Biol. Annu. Rev, v. 28, p. 73-153.

DECHO, A.W., 2000, Microbial biofilms in intertidal systems: an overview: Continental Shelf Research, v. 20, p. 1257-1273.

DELGADO, M., 1989, Abundance and distribution of microphytobenthos in the bays of Ebro Delta (Spain): Estuarine, Coastal and Shelf Science, v. 29, p. 183-194.

DELGADO, M., DE JONGE, V., AND PELETIER, H., 1991, Effect of sand movement on the growth of benthic diatoms: Journal of Experimental Marine Biology and Ecology, v. 145, p. 221-231.

DOWEY, P.J., 2013, Prediction of clay minerals and grain coatings in sandstone reservoirs utilising ancient examples and modern analogue studies: University of Liverpool, [Ph.D. thesis], 390 p.

DOWEY, P.J., HODGSON, D.M., AND WORDEN, R.H., 2012, Pre-requisites, processes, and prediction of chlorite grain coatings in petroleum reservoirs: A review of subsurface examples: Marine and Petroleum Geology, v. 32, p. 63-75.

DOWEY, P.J., WORDEN, R.H., UTLEY, J., AND HODGSON, D.M., 2017, Sedimentary controls on modern sand grain coat formation: Sedimentary Geology.

DUTTON, S.P., LOUCKS, R.G., AND DAY-STIRRAT, R.J., 2012, Impact of regional variation in detrital mineral composition on reservoir quality in deep to ultradeep lower Miocene sandstones, western Gulf of Mexico: Marine and Petroleum Geology, v. 35, p. 139-153.

DYER, K.R., 1979, Estuarine hydrography and sedimentation: a handbook, v. 2: Cambridge, Cambridge University Press Cambridge, 230 p.

EHRENBERG, S.N., 1993, Preservation of anomalously high-porosity in deeply buried sandstones by grain coating chlorite - examples from the Norwegian continental shelf: American Association of Petroleum Geologists Bulletin, v. 77, p. 1260-1286.

EHRENBERG, S.N., 1997, Influence of depositional sand quality and diagenesis on porosity and permeability: Examples from Brent Group Reservoirs, northern North Sea (vol 67, pg 202, 1997): Journal of Sedimentary Research, v. 67, p. 618-618.

EMERY, D., AND ROBINSON, A.G., 1993, Inorganic geochemistry: application to petroleum geology: Oxford, Blackwell, 254 p.

FAAS, R.W., CHRISTIAN, H.A., DABORN, G.R., AND BRYLINSKY, M., 1993, Biological control of mass properties of surficial sediments: an example from Starr's Point tidal flat, Minas Basin, Bay of Fundy: Nearshore and estuarine cohesive sediment transport, p. 360-377.

FLEMMING, B.W., 2012, Siliciclastic back-barrier tidal flats, Principles of Tidal Sedimentology: Netherlands, Springer, p. 231-267.

FOLK, R.L., AND WARD, W.C., 1957, Brazos river bar. A study in the significance of grain size parameters: Journal of Sedimentary Petrology, v. 27, p. 3-26.

GARWOOD, J.C., HILL, P.S., MACINTYRE, H.L., AND LAW, B.A., 2015, Grain sizes retained by diatom biofilms during erosion on tidal flats linked to bed sediment texture: Continental Shelf Research, v. 104, p. 37-44.

GAUPP, R., AND OKKERMAN, J.A., 2011, Diagenesis and reservoir quality of Rotliegend Sandstones in the Northern Netherlands - A review, *in* Grotsch, J., and Gaupp, R., eds., Permian Rotliegend of the Netherlands: Society for Sedimentary Geology Special Publication, p. 193-226.

GERBERSDORF, S.U., JANCKE, T., WESTRICH, B., AND PATERSON, D.M., 2008, Microbial stabilization of riverine sediments by extracellular polymeric substances: Geobiology, v. 6, p. 57-69.

GIER, S., WORDEN, R.H., JOHNS, W.D., AND KURZWEIL, H., 2008, Diagenesis and reservoir quality of Miocene sandstones in the Vienna Basin, Austria: Marine and Petroleum Geology, v. 25, p. 681-695.

GLASMANN, J., LUNDEGARD, P.D., CLARK, R., PENNY, B., AND COLLINS, I., 1989, Geochemical evidence for the history of diagenesis and fluid migration: Brent sandstone, Heather Field, North Sea: Clay Minerals, v. 24, p. 255-284.

GOULD, K., PE-PIPER, G., AND PIPER, D.J.W., 2010, Relationship of diagenetic chlorite rims to depositional facies in Lower Cretaceous reservoir sandstones of the Scotian Basin: Sedimentology, v. 57, p. 587-610.

GRIFFITHS, J., 2017, Compositional and textural variation in modern estuarine sands: Implications for sandstone reservoir quality: University of Liverpool, [Ph.D. thesis], 300 p.

GRIGSBY, J.D., 2001, Origin and growth mechanism of authigenic chlorite in sandstones of the lower Vicksburg Formation, south Texas: Journal of Sedimentary Research, v. 71, p. 27-36.

HEALD, M.T., AND BAKER, G.F., 1977, Diagenesis of Mt Simon and Rose Run Sandstones in western West Virginia and southern Ohio: Journal of Sedimentary Petrology, v. 47, p. 66-77.

HEALD, M.T., AND LARESE, R.E., 1974, Influence of coatings on quartz cementation: Journal of Sedimentary Petrology, v. 44, p. 1269-1274.

HERLORY, O., GUARINI, J.-M., RICHARD, P., AND BLANCHARD, G., 2004, Microstructure of microphytobenthic biofilm and its spatio-temporal dynamics in an intertidal mudflat (Aiguillon Bay, France): Marine Ecology Progress Series, v. 282, p. 33-44.

HIGGINS, M.J., MOLINO, P., MULVANEY, P., AND WETHERBEE, R., 2003, The structure and nanomechanical properties of the adhesive mucilage that mediates diatom-substratum adhesion and motility: Journal of Phycology, v. 39, p. 1181-1193.

HIGGS, R., SHANMUGAM, G., AND POFFENBERGER, M., 2002, Tide-dominated estuarine facies in the Hollin and Napo (T and U) formations (Cretaceous), Sacha field, Oriente Basin, Ecuador: Discussion: AAPG Bulletin, v. 86, p. 329-334.

HOAGLAND, K.D., ROSOWSKI, J.R., GRETZ, M.R., AND ROEMER, S.C., 1993, Diatom extracellular polymeric substances: function, fine structure, chemistry, and physiology: Journal of Phycology, v. 29, p. 537-566.

HOUSEKNECHT, D.W., AND ROSS JR, L.M., 1992, Clay minerals in Atokan deep-water sandstone facies, Arkoma basin: origins and influence on diagenesis and reservoir quality, *in* Houseknecht, D.W., and Pittman, E.D., eds., Origin, diagenesis, and petrophysics of clay minerals in sandstones, SEPM Special Publication, p. 227-240.

IVLEVA, N.P., WAGNER, M., HORN, H., NIESSNER, R., AND HAISCH, C., 2009, Towards a nondestructive chemical characterization of biofilm matrix by Raman microscopy: Analytical and bioanalytical chemistry, v. 393, p. 197-206.

JERNIGAN, D.L., AND MCATEE, J.L., 1975, Critical point drying of electron microscope samples of clay minerals: Clays and Clay Minerals, v. 23, p. 161-162.

JESUS, B., BROTAS, V., RIBEIRO, L., MENDES, C., CARTAXANA, P., AND PATERSON, D., 2009, Adaptations of microphytobenthos assemblages to sediment type and tidal position: Continental Shelf Research, v. 29, p. 1624-1634.

JIMÉNEZ, A., ELNER, R.W., FAVARO, C., RICKARDS, K., AND YDENBERG, R.C., 2015, Intertidal biofilm distribution underpins differential tide-following behavior of two sandpiper species (Calidris mauri and Calidris alpina) during northward migration: Estuarine, Coastal and Shelf Science, v. 155, p. 8-16.

JONES, S., 2017, Goo, glue, and grain binding: Importance of biofilms for diagenesis in sandstones: Geology, v. 45, p. 959-960.

KELLY, M., EMPTAGE, M., MUDGE, S., BRADSHAW, K., AND HAMILTON-TAYLOR, J., 1991, The relationship between sediment and plutonium budgets in a small macrotidal estuary - Esk Estuary, Cumbria, UK: Journal of Environmental Radioactivity, v. 13, p. 55-74.

KESSARKAR, P.M., PURNACHANDRA RAO, V., SHYNU, R., MEHRA, P., AND VIEGAS, B.E., 2010, The nature and distribution of particulate matter in the Mandovi estuary, central west coast of India: Estuaries and coasts, v. 33, p. 30-44.

KOPPEL, J., HERMAN, P.M., THOOLEN, P., AND HEIP, C.H., 2001, Do alternate stable states occur in natural ecosystems? Evidence from a tidal flat: Ecology, v. 82, p. 3449-3461.

LANDER, R.H., LARESE, R.E., AND BONNELL, L.M., 2008, Toward more accurate quartz cement models: The importance of euhedral versus noneuhedral growth rates: American Association of Petroleum Geologists Bulletin, v. 92, p. 1537-1563.

LLOYD, J.M., ZONG, Y., FISH, P., AND INNES, J.B., 2013, Holocene and Lateglacial relative sea-level change in north-west England: implications for glacial isostatic adjustment models: Journal of Quaternary Science, v. 28, p. 59-70.

LUO, J.L., MORAD, S., SALEM, A., KETZER, J.M., LEI, X.L., GUO, D.Y., AND HLAL, O., 2009, Impact of diagenesis on reservoir quality evolution in fluvial and lacustrine-deltaic sandstones: evidence from Jurassic and Triassic sandstones from the Ordos Basin, China: Journal of Petroleum Geology, v. 32, p. 79-102.

MALARKEY, J., BAAS, J.H., HOPE, J.A., ASPDEN, R.J., PARSONS, D.R., PEAKALL, J., PATERSON, D.M., SCHINDLER, R.J., YE, L., AND LICHTMAN, I.D., 2015, The pervasive role of biological cohesion in bedform development: Nature communications, v. 6.

MANSURBEG, H., MORAD, S., SALEM, A., MARFIL, R., EL-GHALI, M.A.K., NYSTUEN, J.P., CAJA, M.A., AMOROSI, A., GARCIA, D., AND LA IGLESIA, A., 2008, Diagenesis and reservoir quality evolution of palaeocene deep-water, marine sandstones, the Shetland-Faroes Basin, British continental shelf: Marine and Petroleum Geology, v. 25, p. 514-543.

MARTINIUS, A., AND VAN DEN BERG, J., 2011, Atlas of sedimentary structures in estuarine and tidally-influenced river deposits of the Rhine-Meuse-Scheldt system, EAGE, 298 p.

MARTINIUS, A.W., RINGROSE, P.S., BROSTROM, C., ELFENBEIN, C., NAESS, A., AND RINGAS, J.E., 2005, Reservoir challenges of heterolithic tidal sandstone reservoirs in the Halten Terrace, mid-Norway: Petroleum Geoscience, v. 11, p. 3-16.

MATLACK, K.S., HOUSEKNECHT, D.W., AND APPLIN, K.R., 1989, Emplacement of clay into sand by infiltration: Journal of Sedimentary Petrology, v. 59, p. 77-87.

MCILROY, D., WORDEN, R.H., AND NEEDHAM, S.J., 2003, Faeces, clay minerals and reservoir potential: Journal of the Geological Society, v. 160, p. 489-493.

MOORE, D.M., AND REYNOLDS JR., R.C., 1989, X-ray diffraction and the identification and analysis of clay minerals, v. 378: Oxford, Oxford University Press, 155 p.

MORAD, S., AL-RAMADAN, K., KETZER, J.M., AND DE ROS, L.F., 2010, The impact of diagenesis on the heterogeneity of sandstone reservoirs: A review of the role of depositional facies and sequence stratigraphy: American Association of Petroleum Geologists Bulletin, v. 94, p. 1267-1309.

MORAES, M.A.S., AND DE ROS, L.F., 1992, Depositional, infiltrated and authigenic clays in fluvial sandstones of the Jurassic Sergie Formation, Reconcavo Basin, northeastrn Brazil: In: Origin, diagenesis and petrophysics of clay minerals in sandstones (eds. Houseknecht, D.W. and Pittman, E.D.) SEPM Special Publication, v. 47, p. 197-208.

MOSELEY, F., 1978, The Geology of the Lake District, Occoasional Publication: Leeds, Yorkshire Geological Society, p. 284.

MULDER, T., SYVITSKI, J.P., MIGEON, S., FAUGÈRES, J.-C., AND SAVOYE, B., 2003, Marine hyperpycnal flows: initiation, behavior and related deposits. A review: Marine and Petroleum Geology, v. 20, p. 861-882.

NEEDHAM, S.J., WORDEN, R.H., AND CUADROS, J., 2006, Sediment ingestion by worms and the production of bio-clays: a study of macrobiologically enhanced weathering and early diagenetic processes: Sedimentology, v. 53, p. 567-579.

NEEDHAM, S.J., WORDEN, R.H., AND MCILROY, D., 2004, Animal-sediment interactions: the effect of ingestion and excretion by worms on mineralogy: Biogeosciences, v. 1, p. 113-121.

NEEDHAM, S.J., WORDEN, R.H., AND MCILROY, D., 2005, Experimental production of clay rims by macrobiotic sediment ingestion and excretion processes: Journal of Sedimentary Research, v. 75, p. 1028-1037.

NOFFKE, N., BEUKES, N., GUTZMER, J., AND HAZEN, R., 2006, Spatial and temporal distribution of microbially induced sedimentary structures: a case study from siliciclastic storm deposits of the 2.9 Ga Witwatersrand Supergroup, South Africa: Precambrian Research, v. 146, p. 35-44.

NOFFKE, N., GERDES, G., KLENKE, T., AND KRUMBEIN, W.E., 2001, Microbially Induced Sedimentary Structures--A New Category within the Classification of Primary

Sedimentary Structures: PERSPECTIVES: Journal of Sedimentary Research, v. 71, p. 649-656.

O'REILLY, S., MARIOTTI, G., WINTER, A., NEWMAN, S., MATYS, E., MCDERMOTT, F., PRUSS, S., BOSAK, T., SUMMONS, R., AND KLEPAC-CERAJ, V., 2017, Molecular biosignatures reveal common benthic microbial sources of organic matter in ooids and grapestones from Pigeon Cay, The Bahamas: Geobiology, v. 15, p. 112-130.

OZKAN, A., CUMELLA, S.P., MILLIKEN, K.L., AND LAUBACH, S.E., 2011, Prediction of lithofacies and reservoir quality using well logs, Late Cretaceous Williams Fork Formation, Mamm Creek field, Piceance Basin, Colorado: American Association of Petroleum Geologists Bulletin, v. 95, p. 1699-1723.

PANTOPOULOS, G., AND ZELILIDIS, A., 2012, Petrographic and geochemical characteristics of Paleogene turbidite deposits in the southern Aegean (Karpathos Island, SE Greece): Implications for provenance and tectonic setting: Chemie der Erde-Geochemistry, v. 72, p. 153-166.

PARRY, W.T., CHAN, M.A., AND NASH, B.P., 2009, Diagenetic characteristics of the Jurassic Navajo Sandstone in the Covenant oil field, central Utah thrust belt: American Association of Petroleum Geologists Bulletin, v. 93, p. 1039-1061.

PATERSON, D., TOLHURST, T., KELLY, J., HONEYWILL, C., DE DECKERE, E., HUET, V., SHAYLER, S., BLACK, K., DE BROUWER, J., AND DAVIDSON, I., 2000, Variations in sediment properties, Skeffling mudflat, Humber Estuary, UK: Continental Shelf Research, v. 20, p. 1373-1396.

PATERSON, D.M., 1989, Short-term changes in the erodibility of intertidal cohesive sediments related to the migratory behavior of epipelic diatoms: Limnology and Oceanography, v. 34, p. 223-234.

PAY, M., ASTIN, T., AND PARKER, A., 2000, Clay mineral distribution in the Devonian-Carboniferous sandstones of the Clair Field, west of Shetland, and its significance for reservoir quality: Clay Minerals, v. 35, p. 151-151.

PIERCE, J., AND NICHOLS, M.M., 1986, Change of particle composition from fluvial into an estuarine environment: Rappahannock River, Virginia: Journal of coastal research, p. 419-425.

PITTMAN, E.D., 1972, Diagenesis of quartz in sandstones as revealed by scanning electron microscopy: Journal of Sedimentary Research, v. 42, p. 507-519.

PITTMAN, E.D., LARESE, R.E., AND HEALD, M.T., 1992, Clay coats: occurrence and relevance to preservation of porosity in sandstones: In: Origin, diagenesis and petrophysics of clay minerals in sandstones (eds. Houseknecht, D.W. and Pittman, E.D.) SEPM Special Publication, v. 47, p. 241-255.

PITTMAN, E.D., AND LUMSDEN, D.N., 1968, Relationship nbetween chlorite coatings on quartz grains and porosity, Spiro Sand, Oklahoma: Journal of Sedimentary Petrology, v. 38, p. 668-670.

RIDING, R., 2000, Microbial carbonates: the geological record of calcified bacterial–algal mats and biofilms: Sedimentology, v. 47, p. 179-214.

ROSOWSKI, J., HOAGLAND, K., AND ALOI, J., 1986, Structural morphology of diatom-dominated stream biofilm communities under the impact of soil erosion: Studies in Environmental Science, v. 28, p. 247-299.

SAÏAG, J., BRIGAUD, B., PORTIER, É., DESAUBLIAUX, G., BUCHERIE, A., MISKA, S., AND PAGEL, M., 2016, Sedimentological control on the diagenesis and reservoir quality of tidal sandstones of the Upper Cape Hay Formation (Permian, Bonaparte Basin, Australia): Marine and Petroleum Geology, v. 77, p. 597-624.

SANTOS, I.R., EYRE, B.D., AND HUETTEL, M., 2012, The driving forces of porewater and groundwater flow in permeable coastal sediments: A review: Estuarine, Coastal and Shelf Science, v. 98, p. 1-15.

SCHINDLER, R.J., PARSONS, D.R., YE, L., HOPE, J.A., BAAS, J.H., PEAKALL, J., MANNING, A.J., ASPDEN, R.J., MALARKEY, J., AND SIMMONS, S., 2015, Sticky stuff: Redefining bedform prediction in modern and ancient environments: Geology, v. 43, p. 399-402.

SEMENIUK, V., 2005, Tidal Flats, *in* Schwartz, M.L., ed., Encyclopedia of Coastal Science: Dordrecht, Springer Netherlands, p. 965-975.

SHAMMARI, S., FRANKS, S., AND SOLIMAN, O., 2010, Depositional and Facies Controls on Infiltrated/Inherited Clay Coatings: Unayzah Sandstones, Saudi Arabia: GEO 2010.

SKARPEID, S.S., CHURCHILL, J.M., HILTON, J.P., IZATT, C.N., AND POOLE, M.T., 2017, The Knarr Field: a new development at the northern edge of the North Sea: Geological Society, London, Petroleum Geology Conference series, p. PGC8. 23.

SMITH, D.J., AND UNDERWOOD, G.J., 2000, The production of extracellular carbohydrates by estuarine benthic diatoms: the effects of growth phase and light and dark treatment: Journal of Phycology, v. 36, p. 321-333.

STAL, L., AND DE BROUWER, J., 2003, Biofilm formation by benthic diatoms and their influence on the stabilization of intertidal mudflats: Berichte-Forschungszentrum Terramare, v. 12, p. 109-111.

STAL, L.J., 2003, Microphytobenthos, their extracellular polymeric substances, and the morphogenesis of intertidal sediments: Geomicrobiology Journal, v. 20, p. 463-478.

STAL, L.J., 2010, Microphytobenthos as a biogeomorphological force in intertidal sediment stabilization: Ecological Engineering, v. 36, p. 236-245.

STEVENS, V., 1991, The Beatrice Field, Block 11/30a, UK North Sea: Geological Society, London, Memoirs, v. 14, p. 245-252.

STORVOLL, V., BJORLYKKE, K., KARLSEN, D., AND SAIGAL, G., 2002, Porosity preservation in reservoir sandstones due to grain-coating illite: a study of the Jurassic Garn Formation from the Kristin and Lavrans fields, offshore Mid-Norway: Marine and Petroleum Geology, v. 19, p. 767-781.

STRICKER, S., AND JONES, S.J., 2016, Enhanced porosity preservation by pore fluid overpressure and chlorite grain coatings in the Triassic Skagerrak, Central Graben, North Sea, UK: Geological Society, London, Special Publications, v. 435, p. SP435. 4.

STROKER, T.M., HARRIS, N.B., ELLIOTT, W.C., AND WAMPLER, J.M., 2013, Diagenesis of a tight gas sand reservoir: Upper Cretaceous Mesaverde Group, Piceance Basin, Colorado: Marine and Petroleum Geology, v. 40, p. 48-68.

SULLIVAN, M., COOMBES, T., IMBERT, P., AND AHAMDACH-DEMARS, C., 1999, Reservoir quality and petrophysical evaluation of Paleocene sandstones in the West of Shetland area: Geological Society, London, Petroleum Geology Conference series, p. 627-633.

TAYLOR, A., AND GOLDRING, R., 1993, Description and analysis of bioturbation and ichnofabric: Journal of the Geological Society, v. 150, p. 141-148.

TAYLOR, I., AND PATERSON, D., 1998, Microspatial variation in carbohydrate concentrations with depth in the upper millimetres of intertidal cohesive sediments: Estuarine, Coastal and Shelf Science, v. 46, p. 359-370.

TOLHURST, T., JESUS, B., BROTAS, V., AND PATERSON, D., 2003, Diatom migration and sediment armouring—an example from the Tagus Estuary, Portugal, Migrations and Dispersal of Marine Organisms, Springer, p. 183-193.

UNDERWOOD, G., PATERSON, D., AND PARKES, R.J., 1995, The measurement of microbial carbohydrate exopolymers from intertidal sediments: Limnology and Oceanography, v. 40, p. 1243-1253.

UNDERWOOD, G.J., AND PATERSON, D.M., 1993, Seasonal changes in diatom biomass, sediment stability and biogenic stabilization in the Severn Estuary: Journal of the Marine Biological Association of the United Kingdom, v. 73, p. 871-887.

VIGNAGA, E., SLOAN, D.M., LUO, X., HAYNES, H., PHOENIX, V.R., AND SLOAN, W.T., 2013, Erosion of biofilm-bound fluvial sediments: Nature Geoscience, v. 6, p. 770-774.

VIROLLE, M., BOURILLOT, R., FENIES, H., BRIGAUD, B., PORTIER, E., PATRIER, P., AND BEAUFORT, D., 2016, Origin and Spatial Temporal Distribution of Clay Coatings in Shallow Marine Clastic Deposits: Insights From a Modern Estuarine Reservoir Analog (Gironde Estuary, France): AAPG/SEG International Conference & Exhibition.

VOS, P., DE BOER, P., AND MISDORP, R., 1988, Sediment stabilization by benthic diatoms in intertidal sandy shoals; qualitative and quantitative observations, Tide-influenced sedimentary environments and facies, Springer, p. 511-526.

WALDERHAUG, O., 1996, Kinetic modeling of quartz cementation and porosity loss in deeply buried sandstone reservoirs: American Association of Petroleum Geologists Bulletin, v. 80, p. 731-745.

WHITEHOUSE, U.G., JEFFREY, L.M., AND DEBBRECHT, J.D., 1960, Differential settling tendencies of clay minerals in saline waters: Clays and Clay Minerals, v. 7, p. 1-79.

WILSON, M.D., 1992, Inherited grain-rimming clays in sandstones from eolian and shelf environments: their origin and control on reservoir properties: In: Origin, diagenesis and petrophysics of clay minerals in sandstones (eds. Houseknecht, D.W. and Pittman, E.D.) SEPM Special Publication, v. 47, p. 209-225.

WISE, S., SMELLIE, J., AGHIB, F., JARRARD, R., AND KRISSEK, L., 2001, Authigenic smectite clay coats in CRP-3 drillcore, Victoria Land Basin, Antarctica, as a possible indicator of fluid flow: a progress report: Terra Antartica, v. 8, p. 281-298.

WOOLDRIDGE, L.J., WORDEN, R.H., GRIFFITHS, J., THOMPSON, A., AND CHUNG, P., 2017a, Biofilm origin of clay-coated sand grains: Geology, v. 45, p. 875-878.

WOOLDRIDGE, L.J., WORDEN, R.H., GRIFFITHS, J., AND UTLEY, J.E., 2017b, Clay-coated sand grains in petroleum reservoirs: understanding their distribution via a modern analogue: Journal of Sedimentary Research, v. 87, p. 338-352.

WORDEN, R.H., AND BURLEY, S.D., 2003, Sandstone diagenesis: the evolution from sand to stone, *in* Burley, S.D., and Worden, R.H., eds., Sandstone diagenesis, recent and ancient. International Association of Sedimentologists Reprint Series, p. 3-44.

WORDEN, R.H., AND MORAD, S., 2000, Quartz cementation in sandstones: a review of the key controversies In: Quartz cementation in sandstones (eds. Worden, R.H. and Morad, S.) International Association of Sedimentologists Special Publications, p. 1-20.

WORDEN, R.H., AND MORAD, S., 2003, Clay minerals in sandstones: Controls on formation, distribution and evolution: In: Clay mineral cements in sandstones (eds. Worden, R.H. and Morad, S.) International Association of Sedimentologists Special Publications, v. 34, p. 3-41.

WORDEN, R.H., NEEDHAM, S.J., AND CUADROS, J., 2006, The worm gut; a natural clay mineral factory and a possible cause of diagenetic grain coats in sandstones: Journal of Geochemical Exploration, v. 89, p. 428-431.

YANG, B., DALRYMPLE, R., AND CHUN, S., 2005, Sedimentation on a wave-dominated, open-coast tidal flat, south-western Korea: summer tidal flat–winter shoreface: Sedimentology, v. 52, p. 235-252.

YEZERSKI, D.J., AND SHUMAKER, N., 2017, Improving Prediction of Porosity Preservation in Thermally-Stressed Deep Marine Sandstones: A Synthesis of Grain-Coating Chlorite Observations: AAPG Annual Convention and Exhibition.